



THE UNIVERSITY *of* EDINBURGH

This thesis has been submitted in fulfilment of the requirements for a postgraduate degree (e.g. PhD, MPhil, DClinPsychol) at the University of Edinburgh. Please note the following terms and conditions of use:

This work is protected by copyright and other intellectual property rights, which are retained by the thesis author, unless otherwise stated.

A copy can be downloaded for personal non-commercial research or study, without prior permission or charge.

This thesis cannot be reproduced or quoted extensively from without first obtaining permission in writing from the author.

The content must not be changed in any way or sold commercially in any format or medium without the formal permission of the author.

When referring to this work, full bibliographic details including the author, title, awarding institution and date of the thesis must be given.

SCHOOL OF CHEMISTRY
THE UNIVERSITY OF EDINBURGH



**The Synthesis of Novel Polymers of
Intrinsic Microporosity for Potential
Application as Gas Separation
Membranes**

Thesis submitted for the degree of Doctor of Philosophy by:

Sadiq Abdul-Hussain Karim

Supervisor: Neil B. McKeown

2016

Declaration

This work has not been submitted in substance for any other degree or award at this or any other university or place of learning, nor is it being submitted concurrently in candidature for any degree or other award.

Signed (candidate)

Date

Statement 1

This thesis is being submitted in partial fulfilment of the requirements for the degree of Doctor of Philosophy.

Signed (candidate)

Date

Statement 2

This thesis is the result of my own independent work/investigation, except where otherwise stated. Other sources are acknowledged by explicit references. Any views expressed are my own.

Signed (candidate)

Date

Statement 3

I hereby give consent for my thesis, if accepted, to be available for photocopying and for inter-library loan, and for the title and summary to be made available to outside organisations.

Signed (candidate)

Date

Acknowledgments

First of all, I would like to thank my supervisor Professor Neil B. McKeown, for accepting me as a PhD student and for his supervision and great patience. I'd also like to give a special thanks to Dr. Kadhum J. Msayib, for his great support and a friendly relationship.

I am grateful to Dr. Mariolino Carta, Dr. C. Grazia Bezzu and Dr. Richard Maplass-Evans, for the valued support for their help during my study and especially at the thesis writing.

I would like to thank everyone else who has worked with me in lab during this time: Ali, Michael, Ian, Rhodri, Matthew, Rupert, Sabeeha, Sarah, Luke, Richard Kirk and Angelos for making it such a friendly and enjoyable place to work.

I thank Dr. John Jansen and his team at The Institute of Membrane Technology (ITM) CNR (Calabria, Italy) for polymer gas permeability measurements. I would also like to show my appreciation for all of the technical staff at the School of Chemistry, both in Edinburgh and in Cardiff for their expertise and willingness to go out of their way to help me.

Thanks also to my sponsor "Iraqi Ministry of higher Education and Scientific Research".

Finally, I would like to thank all of my family, friends and loved ones for all the love and support they have shown me over this time. Without you, none of this could have been possible.



Abstract

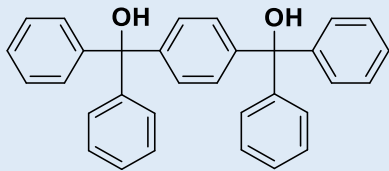
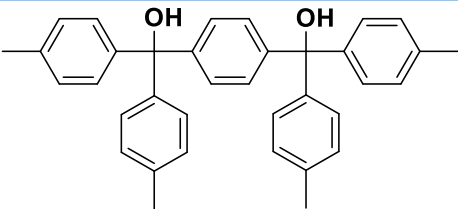
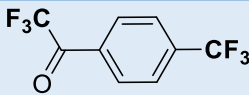
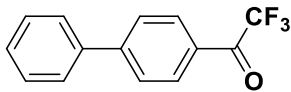
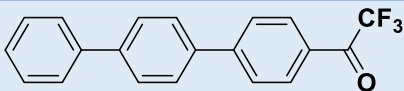
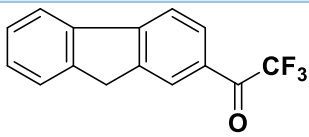
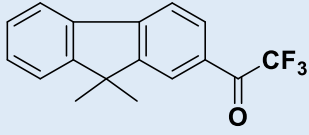
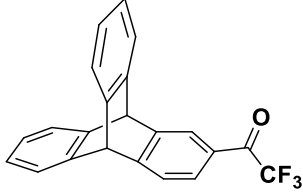
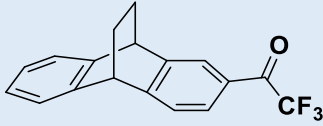
The work reported in this thesis describes the successful preparation of three classes of polymer that were designed to possess intrinsic microporosity from a range of aromatic tetrahydroxy and diamine monomers. The tetrahydroxy family of monomers were used to prepare a number of polybenzodioxane polymers and co-polymers using the chemistry developed for the archetypal PIM-1. Two co-polymers formed films suitable for gas permeability measurements indicating that they transport gases at high selectivity but lower permeability as compared to PIM-1.

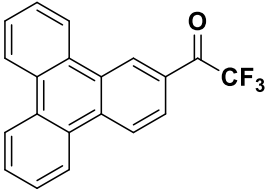
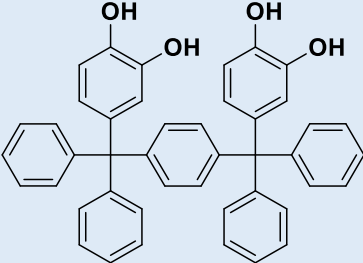
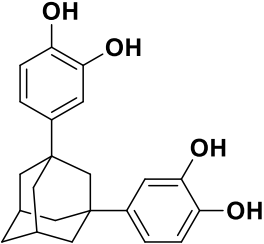
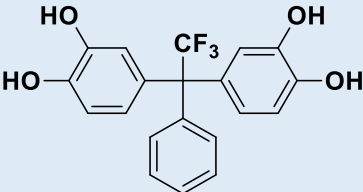
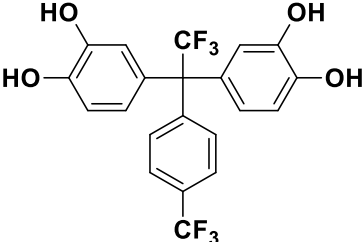
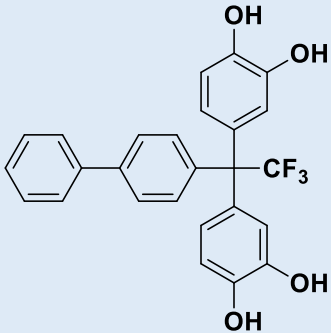
The diamino-containing monomers were used to prepare a number of polyimides (PIM-PIs) using well-established polymerisation chemistry and also some Troger's base polymers (PIM-TBs) using a recently developed polymerisation method. A series of TB-PIMs with different substituents next to the amino group (H and CH₃) and containing various pendant groups were prepared in order to establish structure-property relationships. Some of these polymers proved microporous with surface areas ranging from 22-510 m²/g. Unfortunately, none were suitable for film formation or gas permeation measurements. PIM-PIs were prepared from diamino monomers based on bulky 1,4-ditriptylbenzene (BAB), adamantane (AD) and trifluorodiaminoaryl (TFA) units by reaction with commercial 4,4'-(hexafluoroisopropylidene)diphthalic anhydride (6FDA). Some of these polymers also demonstrated microporosity with surface areas ranging from 8-560 m²/g. Two polymers (PIM-AD5-PI and PIM-AD6-PI), exhibited good solubility, excellent thermal stability and intrinsic microporosity, with the introduction of highly rigid and bulky groups adjacent to the imide group. PIM-AD5-PI and PIM-AD6-PI demonstrate a very good combination of high permeability and good selectivity for CO₂/CH₄, H₂/N₂ and H₂/CH₄ gas pairs with data that lie close to the Robeson 2008 upper bounds, which is the benchmark for the evaluation of the potential of a new polymer for making gas separation membranes. Finally, a series of trifluoromethyl (CF₃) containing PIM-PIs were prepared. Again, it was found that by increasing the rigidity of the polymers by increasing the number of methyl substituents a greater amount of intrinsic microporosity is generated by the polymer. Seven polymers of this series formed robust films suitable for gas permeability measurements and demonstrated good selectivity for CO₂/CH₄, O₂/N₂, H₂/N₂ and H₂/CH₄ gas pairs with data that lie near the 2008 upper bounds.

Abbreviations

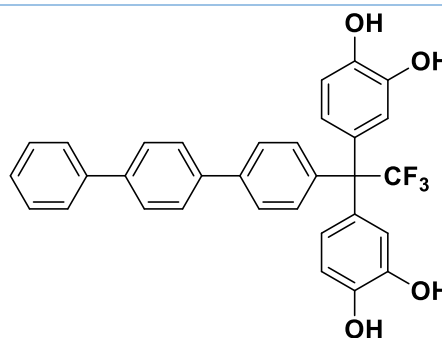
AD2	1,3-bis(3-methyl-4-aminophenyl)adamantane	AD3	1,3-bis(3,5-dimethyl-4-aminophenyl)adamantane
AD4	2,2-bis(4-aminophenyl)adamantane	AD5	2,2-bis(3-methyl-4-aminophenyl)adamantane
AD6	2,2-bis(3,5-methyl-4-aminophenyl)adamantane	BAB1	<i>p</i> -bis-(4-amino-3-methylphenyldiphenylmethyl)benzene
BAB2	<i>p</i> -bis-(4-amino-3,5-dimethylphenyldiphenylmethyl)benzene	BAB3	<i>p</i> -bis-(4-amino-3,5-dimethylphenylditoluoylmethyl)benzene
BAB4	<i>p</i> -bis(3,4-dihydroxyphenyldiphenylmethyl)benzene	BDA	1,3-bis(3,4-dihydroxyphenyl)adamantane
BET	Brunauer, Emmett and Teller	BPDA	4,4'-Biphthalic dianhydride
COF	Covalent Organic Framework	DMN	3,3'-Dimethylnaphthidine
DPD	2,5-Dimethyl-1,4-phenylenediamine	FDT	4,4'-(9-Fluorenylidene)dianiline
Fig	Figure	GPC	Gel Permeation Chromatography
6FDA	4,4'-(Hexafluoroisopropylidene)diphthalic anhydride	HFV	High Free Volume
HFTPS	Heptafluoro- <i>p</i> -tolylphenylsulfone	HCP	Hyper Cross-linked Polymers
IUPAC	International Union of Pure and Applied Chemistry	<i>J</i>	Coupling constants
LRMS	low-resolution mass spectrometric	Mp	Melting Point
MOF	Metal Organic Framework	NMP	1-methyl-2-pyrrolidone
NMR	Nuclear Magnetic Resonance	PI	Polyimide
PAF	Porous Aromatic Frameworks	PALS	Positron Annihilation Lifetime Spectroscopy
PIM	Polymers of Intrinsic Microporosity	PXRD	Powder X-Ray Diffraction
PTMSP	poly[(1-trimethylsilyl)-1-propyne]	PCP	Porous Coordination Polymers
SBFDA	Spirobifluorene-dianhydride	TB	Tröger-base
TEM	Transmission Electron Microscopy	4MPDA	2,3,5,6-Tetramethyl-1,4-phenyldiamine
TFA	Trifluoroacetic acid	TFAA	Trifluoroacetic anhydride
TFSA	Trifluoromethanesulfonic acid	TFTPN	Tetrafluoroterephthalonitrile

Table of Molecules

Chemical Name	Structure	Number
1,4-Bis(diphenylhydroxymethyl) benzene		1
1,4-Bis(di-p-toluenylhydroxymethyl) benzene		2
4-(Trifluoromethyl)-α,α,α-trifluoroacetophenone		3
4-Biphenyl trifluoromethyl ketone		4
4-Terphenyl trifluoromethyl ketone		5
2-Fluorenyl trifluoromethyl ketone		6
2-(9,9-Dimethyl)fluorenyl trifluoromethyl ketone		7
2-Triptyceny trifluoromethyl ketone		8
2-(9,10-Dihydro-9,10-ethanoanthracenyl)trifluoromethyl ketone		9

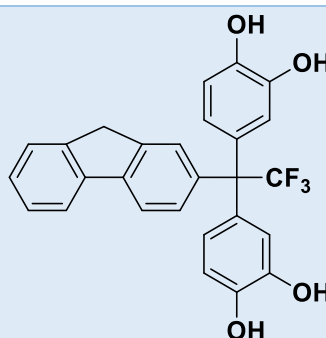
<p>2-Triphenylyl trifluoromethyl ketone</p>		<p>10</p>
<p>p-bis(3,4-dihydroxyphenyldiphenylmethyl) benzene (BAB4)</p>		<p>11</p>
<p>1,3-bis(3,4-dihydroxyphenyl)adamantane (BDA)</p>		<p>12</p>
<p>1,1-Bis(3,4-dihydroxyphenyl)-2,2,2-trifluoro-1-phenylethane (TF1)</p>		<p>13</p>
<p>1,1-Bis(3,4-dihydroxyphenyl)-2,2,2-trifluoro-1-(4-trifluorotoluy)ethane (TF2)</p>		<p>14</p>
<p>1,1-Bis(3,4-dihydroxyphenyl)-2,2,2-trifluoro-1-(4-biphenyl)ethane (TF3)</p>		<p>15</p>

1,1-Bis(3,4-dihydroxyphenyl)-2,2,2-trifluoro-1-(4-terphenyl)ethane (TF4)



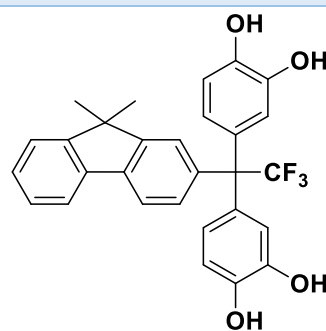
16

1,1-Bis(3,4-dihydroxyphenyl)-2,2,2-trifluoro-1-(2-fluorenyl)ethane (TF5)



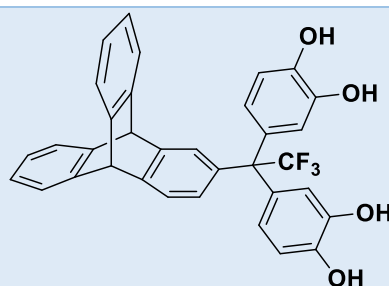
17

1,1-Bis(3,4-dihydroxyphenyl)-2,2,2-trifluoro-1-(9,9-dimethyl-2-fluorenyl)ethane (TF6)



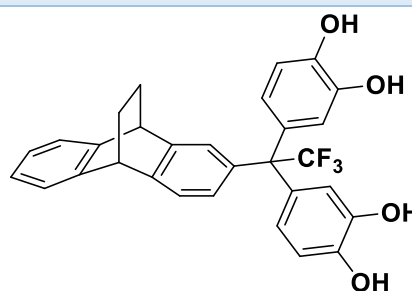
18

1,1-bis(3,4-dihydroxyphenyl)-2,2,2-trifluoro-1-(2-tripticenylyl)ethane (TF7)



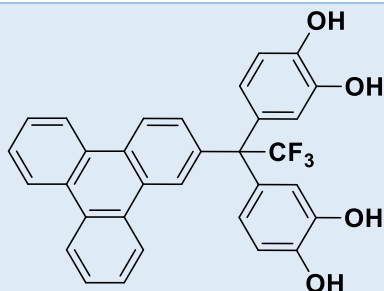
19

1,1-Bis[(3,4-dihydroxyphenyl)-2,2,2-trifluoro-1-(2-(9',10'-dihydro-9',10'-ethanoanthracenyl))]ethane (TF8)



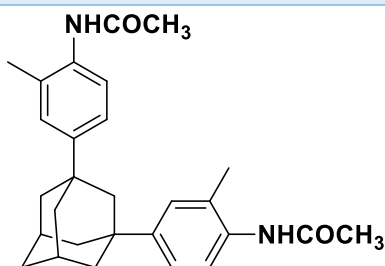
20

1,1-Bis(3,4-dihydroxyphenyl)-2,2,2-trifluoro-1-(2-triphenyl)ethane (TF9)



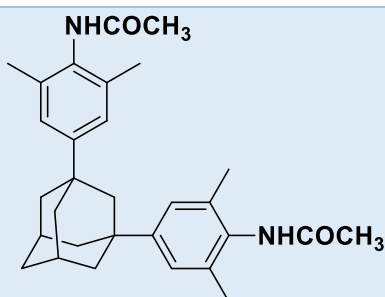
21

1,3-bis(3-methyl-4-acetimidide)adamantane



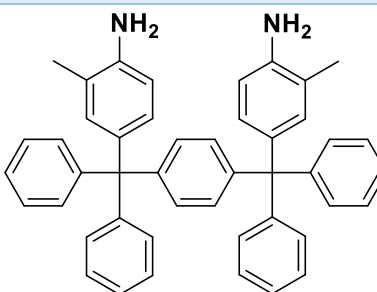
22

1,3-bis(3,5-dimethyl-4-acetimidide)adamantane



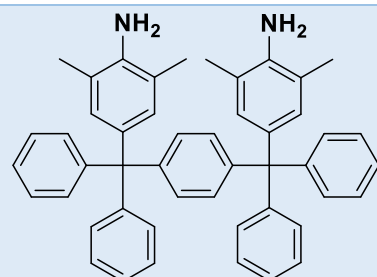
23

p-Bis(4-amino-3-methylphenyldiphenylmethyl)benzene (BAB1)



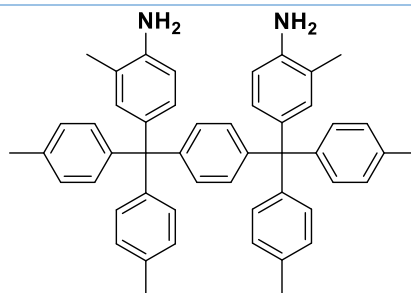
24

p-Bis(4-amino-3,5-dimethylphenyldiphenylmethyl)benzene (BAB2)



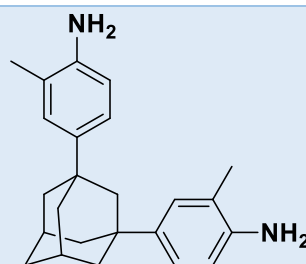
25

p-Bis(4-amino-3-methylphenyldi(p-tolyl)methyl)benzene (BAB3)



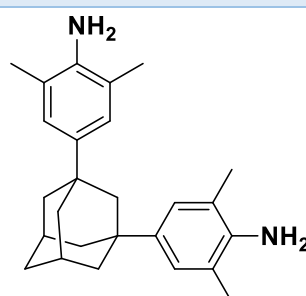
26

1,3-Bis(3-methyl-4-aminophenyl)adamantane (AD2)



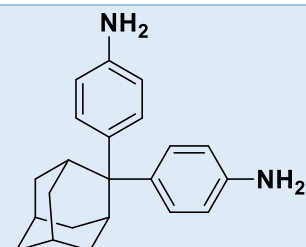
27

1,3-Bis(3,5-dimethyl-4-aminophenyl)adamantane (AD3)



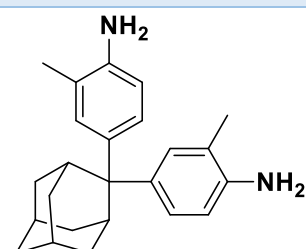
28

2,2-Bis(4-aminophenyl)adamantane (AD4)



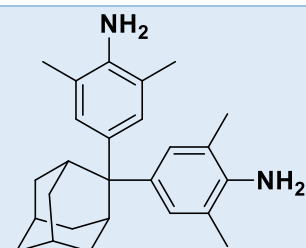
29

2,2-Bis(3-methyl-4-aminophenyl)adamantane (AD5)

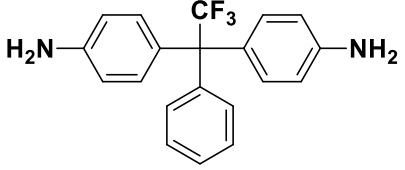
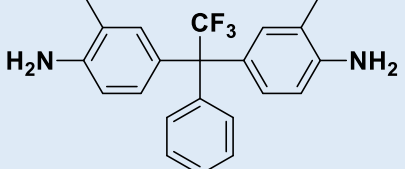
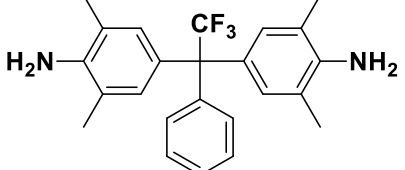
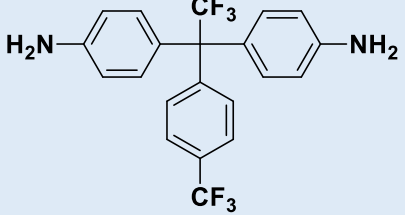
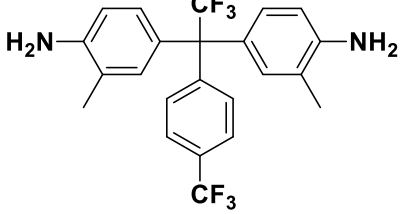
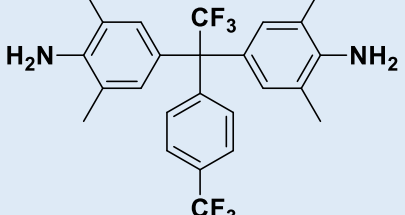
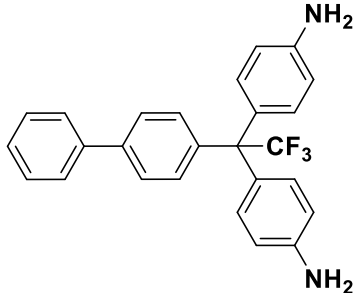


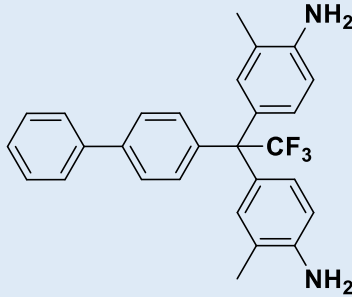
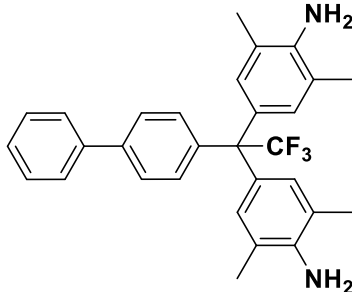
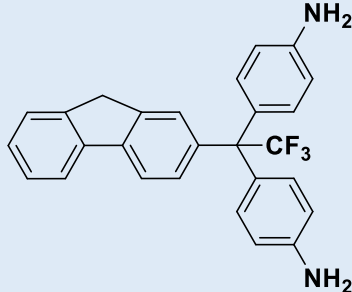
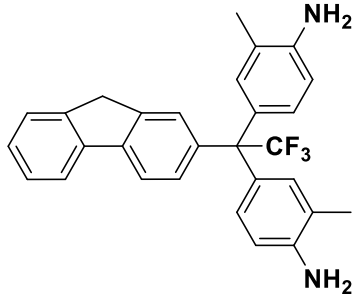
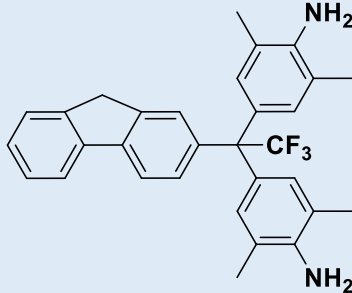
30

2,2-bis(3,5-dimethyl-4-aminophenyl)adamantane (AD6)



31

1,1-Bis(4-aminophenyl)-1-phenyl-2,2,2-trifluoroethane (TFA1)		32
1,1-Bis(3-methyl-4-aminophenyl)-1-phenyl-2,2,2-trifluoroethane (TFA2)		33
1,1-Bis(3,5-dimethyl-4-aminophenyl)-1-phenyl-2,2,2-trifluoro-ethane (TFA3)		34
1,1-Bis(4-aminophenyl)-1-(4-trifluorotoluy)l)-2,2,2-trifluoroethane (TFA4)		35
1,1-bis(3-methyl-4-aminophenyl)-1-(4-trifluorotoluy)l)-2,2,2-trifluoroethane (TFA5)		36
1,1-Bis(3,5-dimethyl-4-aminophenyl)-1-(4-trifluorotoluy)l)-2,2,2-trifluoroethane (TFA6)		37
1,1-bis(4-aminophenyl)-1-(4-biphenylyl)-2,2,2-trifluoroethane (TFA7)		38

<p>1,1-bis(3-methyl-4-aminophenyl)-1-(4-biphenyl)-2,2,2-trifluoroethane (TFA8)</p>	 <p style="text-align: right;">39</p>
<p>1,1-Bis(3,5-dimethyl-4-aminophenyl)-1-(4-biphenyl)-2,2,2-trifluoroethane (TFA9)</p>	 <p style="text-align: right;">40</p>
<p>1,1-bis(4-aminophenyl)-1-(2-fluorenyl)-2,2,2-trifluoroethane (TFA10)</p>	 <p style="text-align: right;">41</p>
<p>1,1-bis(3-methyl-4-aminophenyl)-1-(2-fluorenyl)-2,2,2-trifluoroethane (TFA11)</p>	 <p style="text-align: right;">42</p>
<p>1,1-bis(3,5-dimethyl-4-aminophenyl)-1-(2-fluorenyl)-2,2,2-trifluoroethane (TFA12)</p>	 <p style="text-align: right;">43</p>

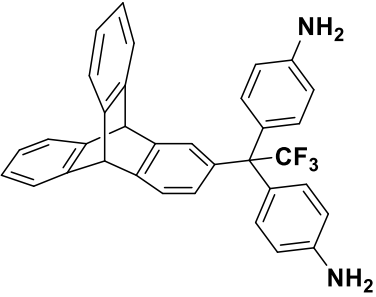
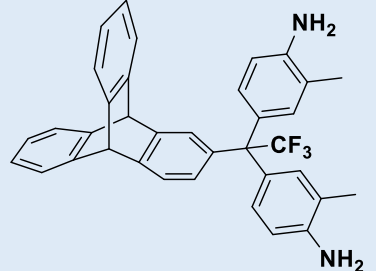
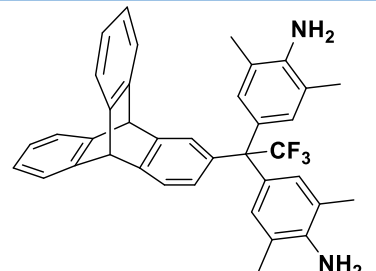
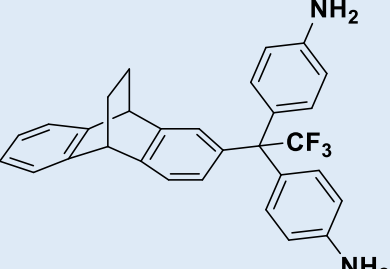
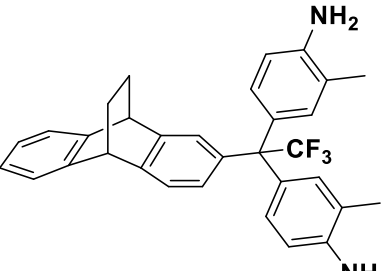
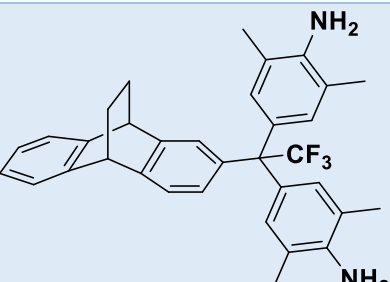
<p>1,1-bis(4-aminophenyl)-1-(2-triptyceny)-2,2,2-trifluoroethane (TFA13)</p>	 <p style="text-align: right;">44</p>
<p>1,1-bis(3-methyl-4-aminophenyl)-1-(2-triptyceny)-2,2,2-trifluoroethane (TFA14)</p>	 <p style="text-align: right;">45</p>
<p>1,1-bis(3,5-dimethyl-4-aminophenyl)-1-(2-triptyceny)-2,2,2-trifluoroethane (TFA15)</p>	 <p style="text-align: right;">46</p>
<p>1,1-bis[(4-aminophenyl)-1-(2-(9,10-dihydro-9,10-ethanoanthracenyl))]-2,2,2-trifluoroethane (TFA16)</p>	 <p style="text-align: right;">47</p>
<p>1,1-bis[(3-methyl-4-aminophenyl)-1-(2-(9,10-dihydro-9,10-thanoanthracenyl))]-2,2,2-trifluoroethane (TFA17)</p>	 <p style="text-align: right;">48</p>
<p>1,1-bis[(3,5-dimethyl-4-aminophenyl)-1-(2-(9,10-dihydro-9,10-ethanoanthracenyl))]-2,2,2-trifluoroethane (TFA18)</p>	 <p style="text-align: right;">49</p>

Table of Contents

Declaration	i
Acknowledgements	ii
Abstract	iii
Abbreviations	iv
Table of Molecules	v
Chapter One: Introduction	1
Part One	1
1.1: Porous Materials	1
1.2: Microporous Materials	2
1.3: Zeolites	2
1.4: Metal-Organic Frameworks	3
1.5: Covalent Organic Frameworks	4
1.6: Activated Carbons	5
1.7: Porous Aromatic Frameworks	5
1.8: Hyper Cross-Linked Polymers	6
1.9: Polymers of Intrinsic Microporosity	7
1.10: Linear Polymers	8
1.10.1: Polyacetylenes	8
1.10.2: PIM Polyimides	9
1.11: Ladder Polymers	11
1.11.1: Polybenzodioxane	11
1.11.2: Tröger-base Polymers	14
1.12: Network Polymers	15
Part Two:	17
1.13: Determination of Surface Area	17
1.14: Introduction of Membrane for gas separation	19
1.14.1: Mechanisms for gas separation	19
1.14.2: Dual-Mode Sorption Model	20
1.14.3: Transport Parameters	21
1.14.4: Robeson Plots	23
Chapter Two: Project Aims	25
Chapter 3: Monomer Synthesis	26
3.1: Introduction	26
3.2: Synthesis of 1,4-bis(di-aryl-hydroxymethyl)benzene compounds	26
3.3: Synthesis of aryl-2,2,2-trifluoromethyl ketones	26
3.3.1: 4-(trifluoromethyl)-α,α,α-trifluoroacetophenone	27
3.3.2: Aryl-2,2,2-trifluoromethyl ketones synthesis by Friedel-Crafts acylation	27
3.4: Bis-catechol monomers	28
3.4.1: Synthesis of p-bis (3,4-dihydroxyphenyldiphenylmethyl) benzene (BAB4)	28
3.4.2: Synthesis of 1,3-bis(3,4-dihydroxyphenyl)adamantane (BDA)	29
3.4.3: Synthesis of 1,1-bis(catechol)-2,2,2-trifluoro-1-arylethane	29

3.5: Diamino monomers.....	31
3.5.1: Synthesis of diamino-1,4-ditrylbenzene monomers 24, 25 and 26	31
3.5.2: Adamantane-based monomers	31
3.5.2.1: Synthesis of (AD2) and (AD3)	31
3.5.2.2: Synthesis of monomers AD4, AD5 and AD6.....	32
3.5.2.3: Synthesis of trifluorodiaminoaryl-based monomers.....	33
Chapter 4: Polybenzodioxane	36
4.1: Introduction to polybenzodioxane polymers	36
4.2: Synthesis of polymers containing of p-bis(3,4-dihydroxyphenyldiphenylmethyl) benzene (PIM-BAB4)	37
4.3: Synthesis of polymers derived from 1,3-bis(3,4-dihydroxyphenyl)adamantane (PIM-BDA)	37
4.4: Synthesis of Polymers Containing CF ₃ (PIM-TF 1-9).....	38
4.5: Synthesis of co-polymers containing CF ₃ with PIM-1 (PIM-1-co-TF(1-9)).....	40
Chapter 5: Träger Base polymers	46
5.1: Introduction to Träger Base polymers	46
5.2: Synthesis of PIM-BAB1-TB and PIM-BAB3-TB.....	46
5.3: Synthesis of PIM-AD2-TB	47
5.4: Synthesis of TB Polymers Containing CF ₃ (PIM-TFA-TB).....	48
Chapter 6: Polyimides	52
6.1: Introduction to polyimides.....	52
6.2: The Synthesis of BAB1-PI and BAB2-PI.....	54
6.3: Synthesis of Adamantane based Polyimides (PIM-AD1-6-PI)	54
6.4: Synthesis of (PIM-TFA-PI) polymers	60
Chapter 7: Future work	67
Conclusions.....	70
Chapter 8: Experimental.....	71
8.1: General Methods and Equipment	71
8.2: Monomers Synthesis.....	73
8.3: Polymer Synthesis	103
Bibliography	142
Appendix.....	154

Chapter 1: Introduction

Part One:

1.1: Porous Materials

A porous material is defined as a solid material which has cavities, channels or interstices¹ all of which can be defined as a pore. The structure of a pore is different according to the material and can also be dependent on the history and manipulation of the material. According to IUPAC, porosity is classified, depending on size, shape and accessibility to an external fluid as macroporous (> 50 nm), mesoporous (2-50 nm) and microporous (< 2 nm).¹ Fig 1.1¹ shows pores availability to an external fluid including closed pores (a) which are totally isolated from their neighbours, thus inaccessible to external fulfilment such as fluids and gas molecules. This region is not available for adsorption of gases, but does influence macroscopic properties such as bulk density, mechanical strength and thermal conductivity. The open pores like (b), (c), (d), (e) and (f) have a continuous channel of communication with the external surface. Pores with only one end (like b) and (f) can be described as blind pores. The rest are open at two ends, like (e) and they are mainly responsible for the adsorption of gases and liquids. Noted, (g) are rough surfaces and don't consider as a porous because must be deeper than they are wide to be defined as pores.

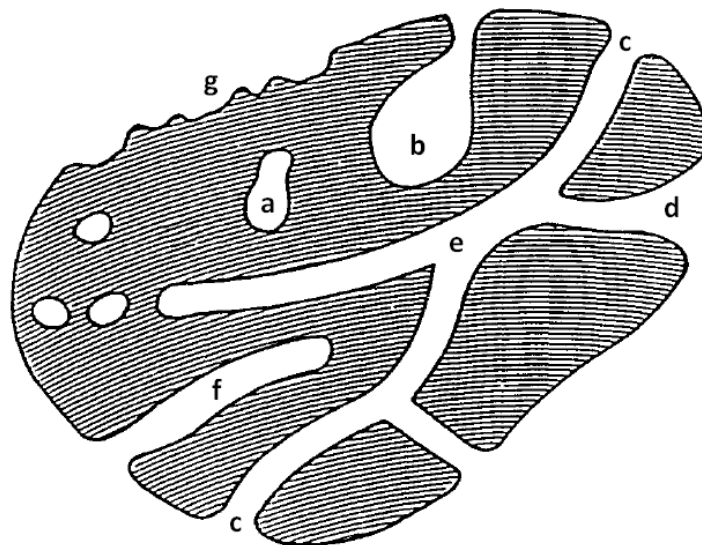


Fig 1.1: Schematic Cross-Section of a Porous Solid.

1.2: Microporous Materials

In the last decades, microporous materials have become increasingly important for both academic and industrial research, due to the great variety of applications and potential applications including adsorption,^{3,4} sensors,⁵ catalysis,⁶⁻⁹ liquid purification,¹⁰ ion exchange,^{11, 12} gas purification,¹³⁻¹⁷ hydrogen storage¹⁸⁻²² and carbon dioxide capture.²³

There are two main categories of conventional microporous materials: *ordered crystalline frameworks*, such as zeolites, metal-organic frameworks (MOFs) and covalent organic frameworks (COFs), and *amorphous networked structures* such as activated carbons, hyper cross-linked polymers (HCPs) and the many novel forms of porous polymers.^{24, 25}

1.3: Zeolites

Zeolites are a family of inorganic microporous crystalline materials with open three-dimensional microporous structures. Usually, the structures are comprised of interconnected aluminosilicate building blocks, i.e., $[\text{AlO}_4]^{5-}$ and $[\text{SiO}_4]^{4-}$ with molecular sized interconnected pores. They were first discovered by the Swedish mineralogist Axel Fredrick Cronstedt in 1756. He noted that the mineral stilbite absorbed water and released it as steam upon heating. This observation led to the name zeolite, which is derived from the Greek words *zeo* meaning “boiling” and *lithos* meaning “rock”.²⁶⁻²⁸

Since their discovery chemists have prepared a number of synthetic zeolites, to date there are over 230 unique zeolite architectures known.^{29, 30}

The cage-like framework structures (Fig 1.3³²), have tetrahedral vertices which form open channels of molecular dimensions (1-20 Å)^{31, 32} with BET surface areas ranging from 400 – 900 m² g⁻¹.^{7, 33, 34} The main applications of zeolites are as molecular sieves,³⁵ gas sensors,³⁶ purifications of gases and liquids by adsorption of impurities,^{37, 38} gas separation membranes,³⁹ hydrogen storage⁴⁰ and catalysis in petrochemical industries.⁴¹

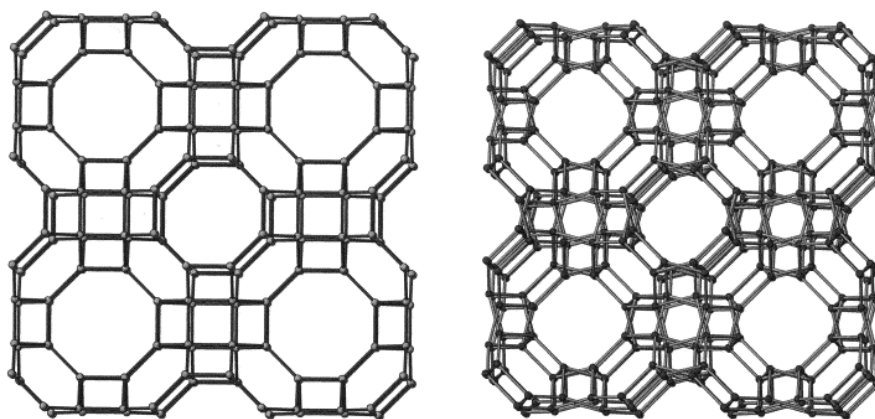


Fig 1.3: Framework structure of hydrated (left side) and dehydrated (right side) zeolite rho. The tetrahedral atoms (Si or Al) are directly connected and all oxygen atoms are omitted

1.4: Metal-Organic Frameworks (MOFs)

Metal-organic frameworks (MOFs) are a family of porous crystalline materials composed of metal ions or clusters, coordinated to organic molecules to form one-, two-, or three-dimensional structures.⁴² In 2004 Yaghi and co-workers reported the first MOF with a surface area higher than activated carbons, MOF-177 [$\text{Zn}_4\text{O}(1,3,5\text{-benzenetribenzoate})_2$] (Fig 1.4) with BET surface area of over $4500 \text{ m}^2 \text{ g}^{-1}$.⁴³ In 2012 Farha *et al.* reported a new MOF with ultrahigh surface area of $7140 \text{ m}^2 \text{ g}^{-1}$ (NU-110, Fig 1.4).⁴⁴ MOFs have a wide range of potential applications including catalysis,^{45, 46} sensors,⁴⁷ gas separation and purification,⁴⁸ hydrogen storage,⁴⁹ carbon dioxide capture⁵⁰ and drug delivery.^{51, 52}

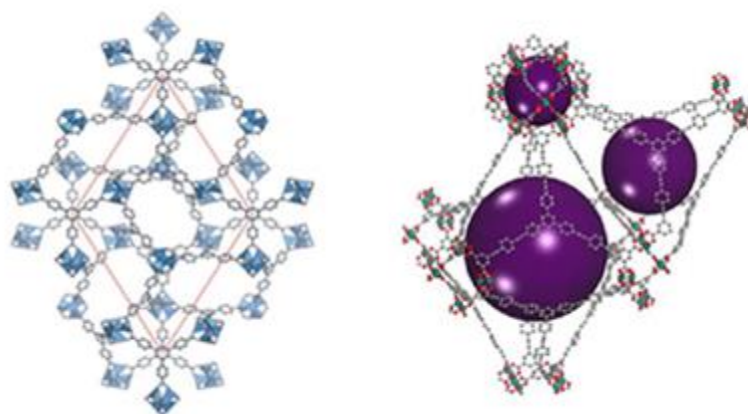


Fig 1.4: The structure of MOF-177 (left) and the structure of MOF NU-110 showing pore volumes (purple), largest of which was measured to be 35 \AA (right)

1.5: Covalent Organic Frameworks (COFs)

Covalent organic frameworks (COFs) are a family of porous crystalline macromolecules made entirely from light elements (H, B, C, N, and O) linked together through strong covalent bonds.^{53, 54} COFs possess low densities, high thermal stability (up to 600 °C), rigid structures, long-range order, and permanent porosity with extremely high surface areas, up to 6450 m² g⁻¹.¹ One of their disadvantages, shared with most MOFs, is their instability towards hydrolysis.⁵⁵ They are also very microporous, with surface areas ranging from 1590-6450 m² g⁻¹.⁵⁴⁻⁵⁷ Noteworthy, there are several potential applications of COFs including catalysis,⁵⁸ optoelectronics,⁵⁹ filtrations,⁶⁰ hydrogen storage⁶¹ and carbon dioxide capture.⁶²

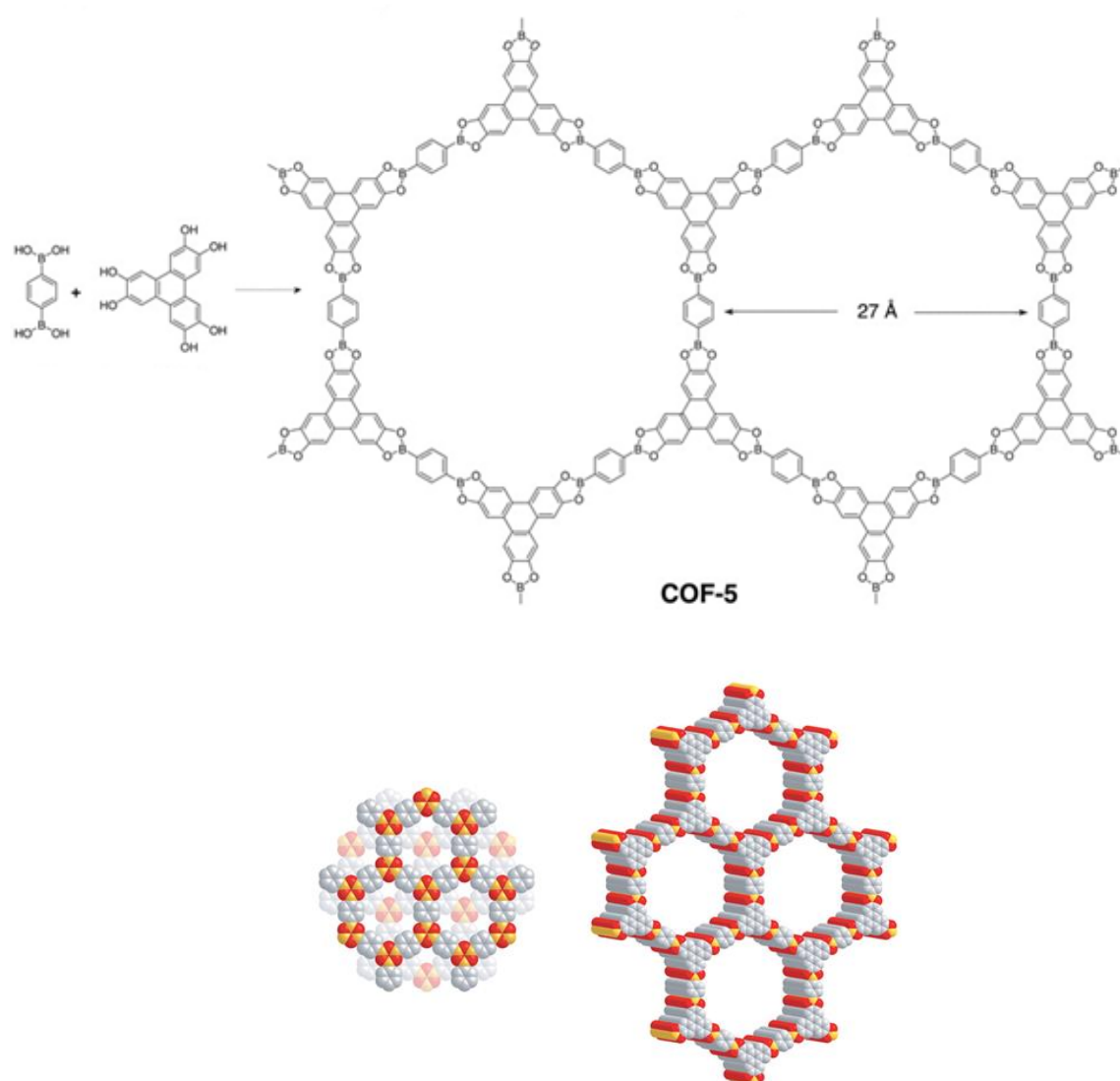


Fig 1.5⁵⁴: the condensation reaction of COF-5 (up) and building blocks and structure model of COF-5, C grey; H white, B orange and O red (down)

1.6: Activated Carbons

Activated carbons are amorphous materials which contain very small graphite domains.⁶³ They have typical pores of size around 1 nm with surface area up to $3000 \text{ m}^2 \text{ g}^{-1}$.⁶⁴ Applications vary widely from hydrogen storage,⁶⁶ carbon dioxide capture,⁶⁷ catalyst⁶⁸ and water purification.⁶⁹ Until this moment, the structure of activated carbons is not well-defined but one theory suggests that the small carbon sheets and other structural types of carbons are linked together by aliphatic units⁷⁰ (Fig 1.6⁷¹).

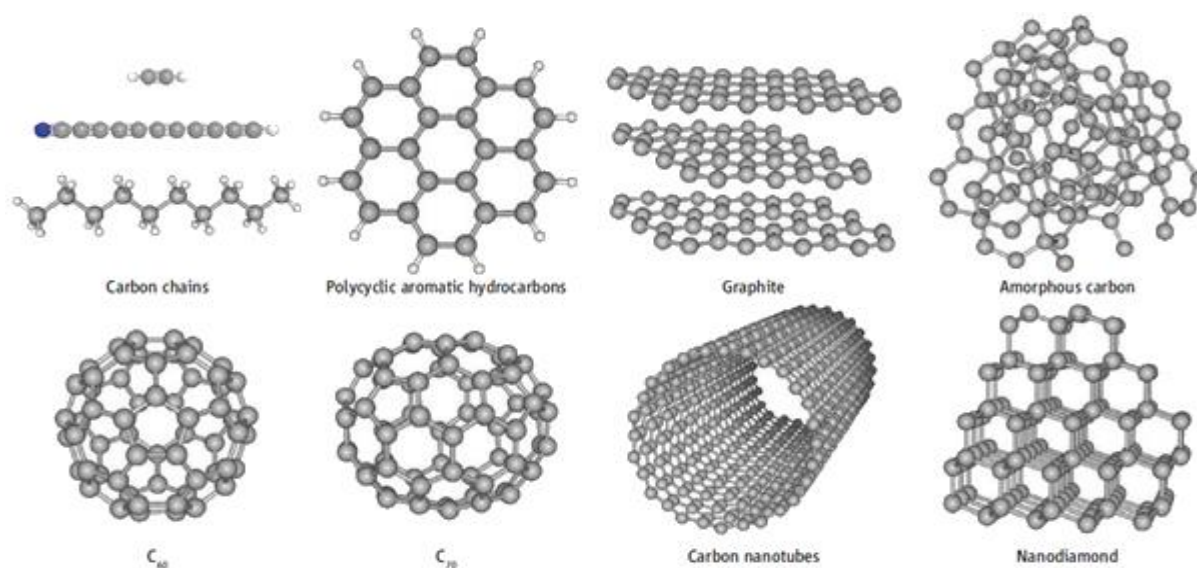
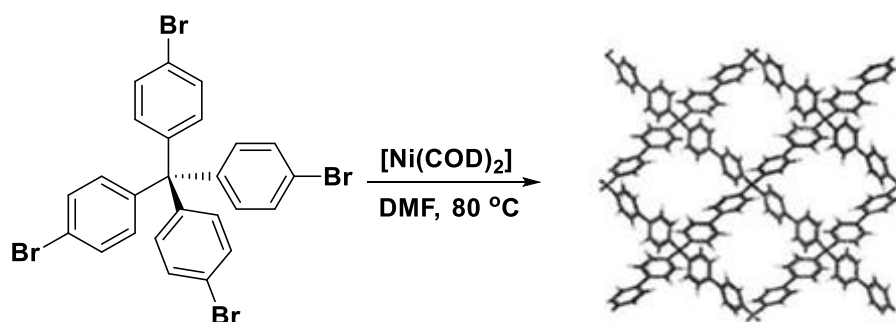


Fig 1.6: various known allotropes of carbon

1.7: Porous Aromatic Frameworks (PAFs)

Porous aromatic frameworks (PAFs) are synthetic microporous materials with amorphous structures based on diamond-like linkages of tetraphenylmethane.^{72, 73} Despite the lack of crystalline structure, these material shows high stability and massive surface areas ($> 5000 \text{ m}^2 \text{ g}^{-1}$). The amorphous structure of PAFs is proven by transmission electron microscopy (TEM) and powder X-ray diffraction (PXRD). This means that crystallinity is not a requirement for preparing “ultrahigh” surface area materials.⁷⁴ PAF-1 was first polymer of this family and it was prepared from, nickel(0)-catalysed, Yamamoto-type Ullmann cross-coupling reaction of tetrakis(4-bromophenyl)methane (Scheme 1.7.a⁷²) and recorded a BET surface area of $5640 \text{ m}^2 \text{ g}^{-1}$.



Scheme 1.7.a: Synthesis of PAF-1 with a simulated structure model

PAF-1 also showed high uptake of carbon dioxide (1300 mg/g at 40 bar, 298 K) which makes this polymer a potential material for CO_2 capture.^{72, 75} There have been reported several modifications of PAFs to increase gas adsorption capacity, for instance changing a carbon atom of the monomer with silicon or germanium or bulky groups like adamantane⁷⁶⁻⁷⁸ (Fig 1.7.b⁷⁸).

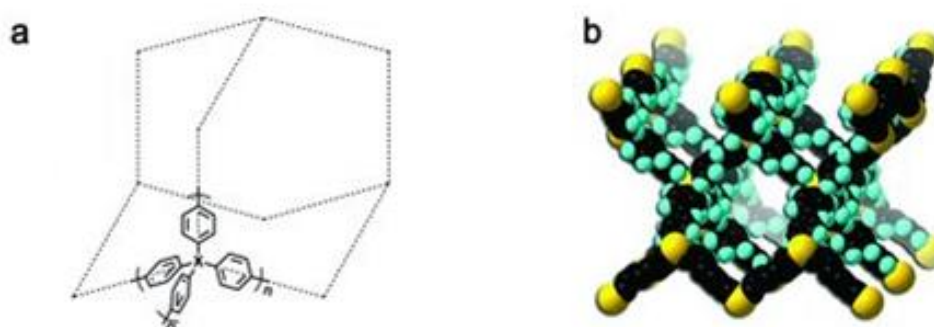


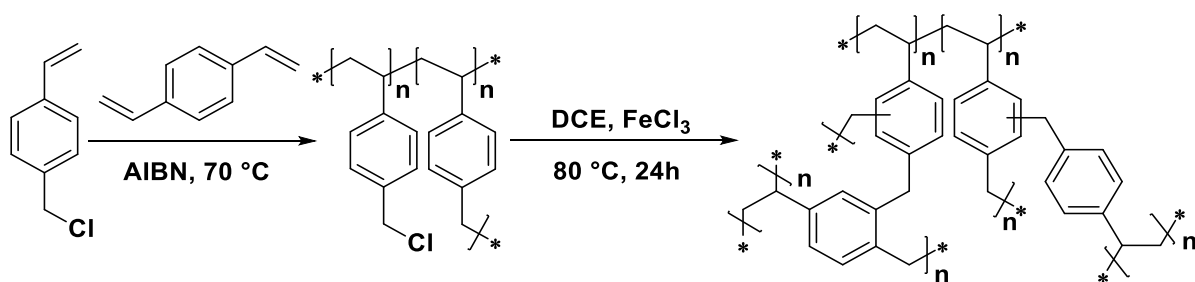
Fig 1.7.b: a) Structures of PPN-3 (X = adamantane), PPN-4 (X = Si), PPN-5 (X = Ge)

b) diamondoid network of PPN-4 (black, C; blue, H; yellow, Si)

1.8: Hyper-Cross-Linked Polymers (HCPs)

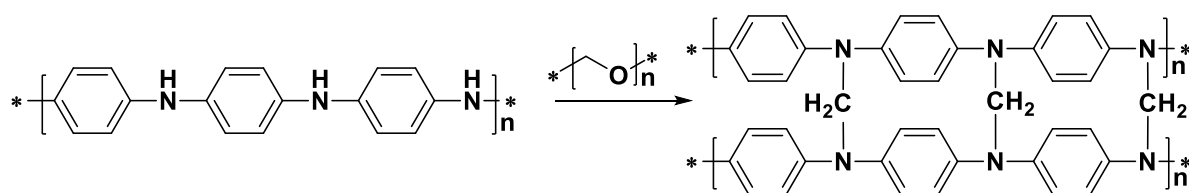
Hyper-cross-linked polymers (HCPs) are amorphous organic materials in which polymer chains are joined together to make cross-linked polymers. They possess a highly rigid structure, small pore sizes and moderately high BET surface area.⁷⁹

Davankov *et al.* synthesised the first HCPs, known today as ‘Davankov resins’⁸⁰ in two-steps, initially polymerising vinylbenzyl chloride, in the presence of a small amount of divinylbenzene which acts as a cross-linker, then preparing the ‘hyper-cross-linked’ copolymer via a Friedel-Crafts alkylation, to form the resins (Scheme 1.8.a).⁸¹



Scheme 1.8.a: Davankov resin synthesis

Ahn *et al.* found out that the properties of HCPs are heavily influenced according to the hyper-cross-linking procedure, especially when they are allowed to swell in either polar or non-polar solvents.⁸²⁻⁸⁴ Recently, several reactions have used to modify the structure of HCP by using the residual chloromethyl groups,⁸⁵ as well as the application of Davankov methodology to provide rigid porous polyacrylate and polysulfone networks.⁸⁰ Paraformaldehyde and several diiodoalkanes have been successfully used as cross-linkers, starting from commercial polyaniline (Scheme 1.8.b).⁸⁶ In addition, Friedel-Crafts alkylations were carry out on furan, pyrrole or thiophene with dimethoxymethane as methylene supplier to create a new series of HCPs. These polymers have surface areas between 437–726 m² g⁻¹ and are of interest due to their carbon dioxide adsorption capacities.⁸⁷ There are numerous potential applications of HCPs including hydrogen storage⁸⁴ and a number of real-world applications including ion exchange resins⁸⁸ and chromatography.⁸⁹



Scheme 1.8.b: Hyper cross-linking of polyaniline with paraformaldehyde

1.9: Polymers of Intrinsic Microporosity (PIMs)

Intrinsic microporosity within a polymer is defined as “a continuous network of interconnected intermolecular voids that forms as a direct consequence of the shape and rigidity of the component macromolecules”.⁹⁰ These polymeric materials, made from light elements (C, H, N, O), can be considered as the organic equivalent of amorphous activated

carbons.⁹¹ Usually, organic polymers are not porous because the backbone has adequate flexibility to twist and bend to reach a dense structure in order to maximise inter-chain cohesive forces and minimise free volume.⁶³ However, polymers of intrinsic microporosity (PIMs) have high rigidity and contorted structures, which greatly restricts flexibility of polymer chains. The inefficient packing of polymer chains leads to high fractional free volume (FFV), which makes them suitable for gas separation.^{91, 92}

The molecular chain configurations of PIMs show the possibility of formation of three different classes of polymers: linear, ladder and network.

Generally, the linear polymers are soluble and have only a single bond between monomers, so in order to make a high FFV polymers of this kind, the shape of the monomeric unit must ensure that the rotation around the single bonds is hindered and therefore the chain remains rigid. Examples of this kind of polymers include polynorbornenes,⁹³ perfluoropolymers,^{94, 95} polyacetylenes^{13, 96} and polyimides.⁹⁷

Ladder polymers instead, have two bonds between the monomeric units in order to prevent rotation so, in general, they generate more porosity than the corresponding linear polymers. Typical examples of monomeric building units are triptycenes⁹⁸ or spirobisindanes.⁹⁹ An example of polymerisation which produces ladder PIMs is the poly-dibenzodioxin formation to form the archetypal PIM-1.⁹⁹

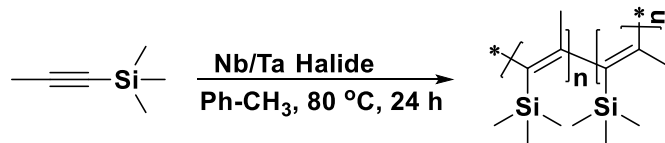
Network PIMs are prepared from monomers similar to the ones used to make ladder polymers, but in this case at least one of them must have a functionality average (f_{av}) higher than two, so that the polymer branches in three dimensions and results an intricate network structure. Examples of these PIMs are phthalocyanine-PIMs¹⁰⁰ and triptycene-PIMs¹⁰¹. The main difference between ladder and network polymers is that the latter, due to the branched structure, are insoluble in any solvent but they typically possess higher BET surface areas.

1.10: Linear Polymers

1.10.1: Polyacetylenes

In 1983 Masuda *et al.* reported the synthesised poly-[(1-trimethylsilyl)-1-propyne] (PTMSP), which formed films with very high gas permeability (e.g. O₂ permeability up to 9000 Barrer).¹³ This glassy material was prepared by polymerization of 1-(trimethylsilyl)-1-propyne using a range of different transition metal catalysts such as niobium (V) and tantalum (V) halides to yield contorted and rigid polymeric structures (Scheme 1.10.1). The backbone of this

polymer has single and double bonds, which offer an alternated *cis/trans* repeated unit. Izumikawa *et al.* studied the effect that the catalyst has over the polymerisation and they found that by using NbCl₅ over a TaCl₅ as a catalyst they obtain a *cis*-enriched structure, which also has slightly different gas permeability properties.^{102, 103}



Scheme 1.10.1: Synthesis of poly[(1-trimethylsilyl)-1-propyne] (PTMSP).

1.10.2: PIM-Polyimides

In 1955 the US company DuPont developed a new class of polymer termed aromatic polyimides.¹⁰⁴ They were synthesised via a two-stage polycondensation of dianhydride and aromatic diamine monomers, which gave a high molecular weight material.¹⁰⁵ Kapton® was the first commercial polymer of this kind prepared from pyromellitic dianhydride and 4,4'-oxydianiline.¹⁰⁶ The physical properties of this polymer showed good chemical resistance and thermal stability prompting its use in many different applications.¹⁰⁷ Many other aromatic polyimides have been assessed as membranes for gas separation.¹⁰⁸ For example, Matrimid® (Fig 1.10.2.a) is one of the few polymers currently used for gas separation membranes in industry.^{109, 110}

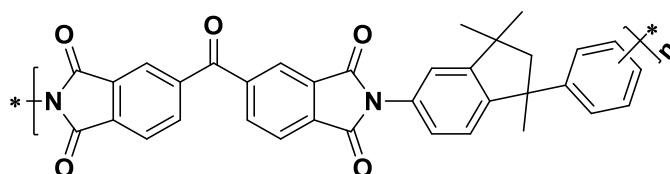


Fig 1.10.2.a: structure of the Matrimid®

Many other polyimides have been prepared during the last decades to improve the performance of Matrimid®.¹¹¹⁻¹¹⁵ In 2007, Zhang and *et al.* reported several polyimides based on spirobisindane-dianhydride, they showed good solubility in organic solvent, high T_g and they have been successfully used for gas separation applications.¹¹⁶ Ghanem *et al.* in 2008 reported three polyimides designed using the concept of intrinsic microporosity (Fig 1.10.2.b: structure of PIM-PI-8), also based on spirobisindane-dianhydride, which showed enhanced permeability and selectivity for several gas pairs.⁹⁷

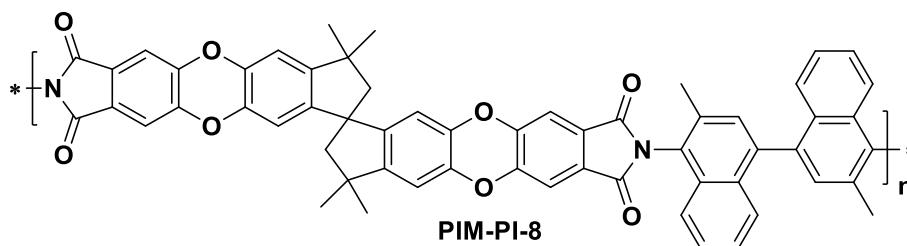


Fig 1.10.2.b: structure of PIM-PI-8

Studies on molecular modelling, proved that the dibenzodioxin units are more flexible than initially expected.¹¹⁷ Therefore, to improve the gas separation performance, several PIM-PIs were prepared without the benzodioxin unit to provide a more rigid structure. These PIM-PIs showed enhanced performance.¹¹⁸ For example, Ma *et al.* synthesised a spirobifluorene-dianhydride and reacted it with 3,3'-dimethylnaphthidine (DMN) to form SBFDA-DMN (Fig 1.10.2.c). The obtained polymer showed high BET surface area ($686 \text{ m}^2 \text{ g}^{-1}$) and high permeability, paired with moderate selectivity for O_2/N_2 and H_2/N_2 .¹¹⁹

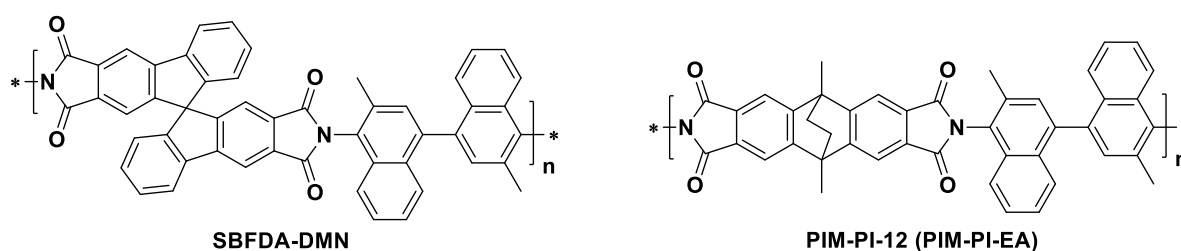


Fig 1.10.2.c: structure of SBFDA-DMN and of PIM-PI-EA

In 2014 Rogan *et al.* reported a novel polyimide derived from an ethanoanthracene-dianhydride (PIM-PI-12, Fig 1.10.2.c). It proved even more permeable than the related spiro-containing polyimides. This is probably attributable to the increased rigidity conferred by the bridged bicyclic ethanoanthracene monomer, allowing the polymer to outperform the previously synthesised PIs for important gas pairs, such as O_2/N_2 , H_2/N_2 , CO_2/CH_4 and CO_2/N_2 .¹¹⁰

A further improvement was reported by a research group at King Abdullah University of Science and Technology (KAUST), Saudi Arabia. They prepared a series of triptycene-based polyimides with several bis-amino monomers. These materials showed ultramicroporosity due to enhanced rigidity of the triptycene unit, in addition to the presence of bulky isopropyl placed at the bridgehead. Their best result showed a BET surface area of

750 m² g⁻¹, which is lower than other PIM-PIs but displays higher selectivity for several gas pairs making it the best performing PIM-PI to date (Fig 1.10.2.d: KAUST-1).¹²⁰⁻¹²³

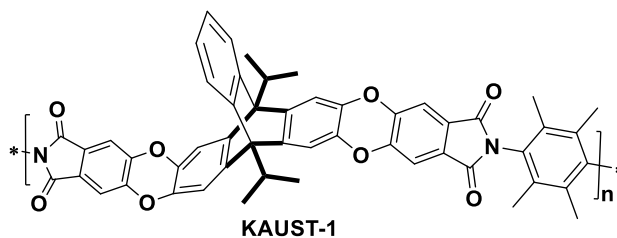
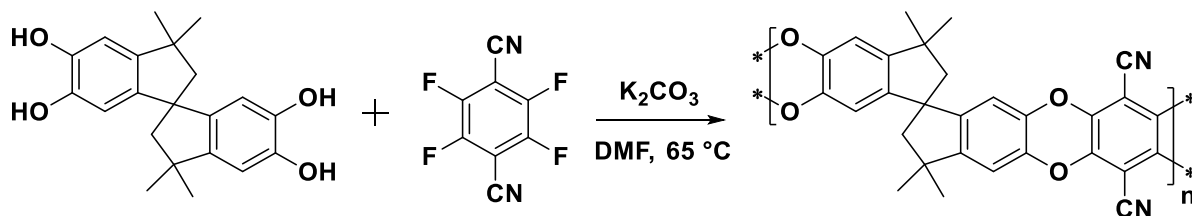


Fig 1.10.2.d: structure of KAUST-1

1.11: Ladder Polymers

1.11.1: Polybenzodioxins

As already mentioned, a ladder polymer possesses two bonds between the two monomeric components. For example, ‘PIM-1’, is obtained by step-growth polymerisation, involving a double nucleophilic aromatic substitution reaction between the commercial monomers 5,5',6,6'-tetrahydroxy-3,3,3',3'-tetramethyl-1,1'-spirobisindane and 2,3,5,6-tetrafluoroterephthalonitrile (scheme 1.11.1.a).⁹⁹



Scheme 1.11.1.a: synthesis of PIM-1

PIM-1 proved to be an amorphous, highly yellow fluorescent powder, of high molecular mass ($M_w = > 100000$ g mol⁻¹) and high BET surface area (up to 870 m² g⁻¹). This is attributed to the contribution of the high rigidity of spirobisindane units, in combination with the planarity of the benzodioxin unit, which confers on to the material a highly contorted structure that packs inefficiently in the solid state, leaving pores of nano-dimension^{92, 124} (Fig 1.11.1.b¹²⁴). There are numerous studies of PIM-1 which prove its high free volume.^{111, 112, 117, 145, 126}

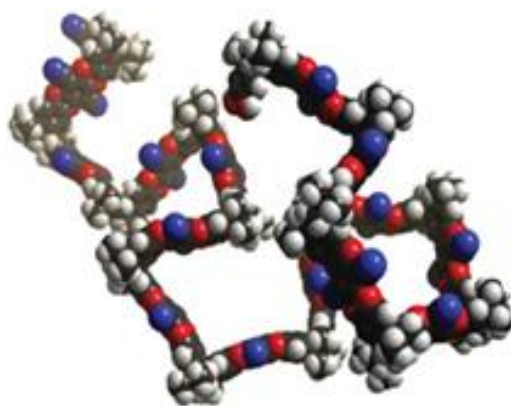


Fig 1.11.1.b: the model of a fragment of PIM-1 to illustrate contorted structure

Given the success of PIM-1, there have been several studies aimed to modify and improve its structure, for instance reaction of nitrile groups (-CN), such as hydrolysis to transform them into carboxylic groups. The carboxylated polymer, c-PIM-1, was first prepared by basic hydrolysis of the powder form with sodium hydroxide, to give three different degree of hydrolysis, this modification showed lower permeability for several gases but a much increased selectivity (Fig 1.11.1.c).¹²⁷⁻¹²⁸

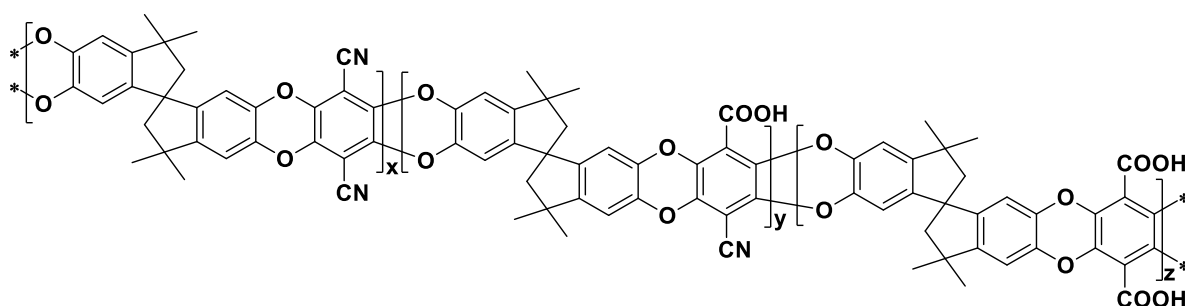


Fig 1.11.1.c: Structure of PIM-1 carboxylate

Another post-polymerisation modification of PIM-1 is represented by the reaction of the nitriles group with sodium azide and zinc chloride to form tetrazole rings (TZ-PIM) which showed high gas selectivity, particularly for CO₂, but, again at the expense of permeability.¹²⁹ Other modifications of PIM-1 consist of blending it with various polymers in attempts to improve the physical properties such as gas permeability. For instance, the blending of PIM-1 with Matrimid, in different ratios, resulted in increased permeability of O₂/N₂ with increasing PIM-1 contribution but this is accompanied by slight decrease of O₂/N₂ selectivity.¹³⁰

Several copolymerisations of PIM-1 synthesised to improve the PIM-1 physical properties such as the report in 2008 from Du *et al.* where they used heptafluoro-*p*-

tolylphenylsulfone (HFTPS) with 5,5',6,6'-tetrahydroxy-3,3,3',3'-tetramethylspirobisindane with different ratios of tetrafluoroterephthalonitrile (TFTPN). These copolymers show increasing selectivity with decreasing of permeability for the O₂/N₂ gas, pair as compared to PIM-1, with increasing HFTPS ratio (Fig 1.11.1.d).¹³¹

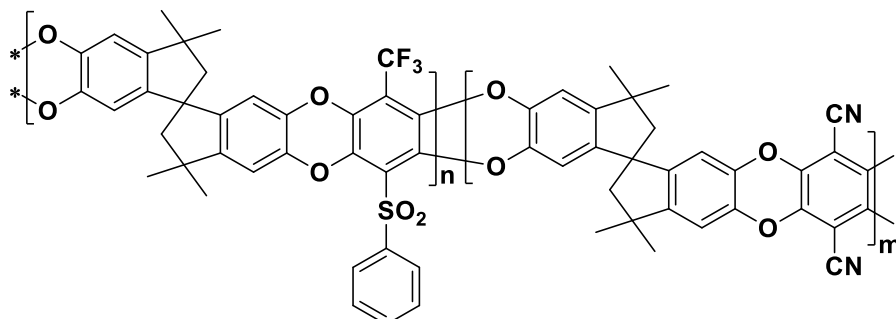


Fig 1.11.1.d: structure of co-PIM-1

Other polybenzodioxin-based PIMs:

Since PIM-1 was reported several bis-catechol have been used to make novel polybenzodioxin polymers for gas separation applications, for example PIM-7 (Fig 1.11.1.e).⁹¹

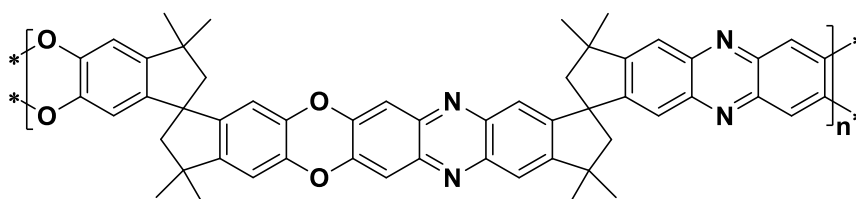


Fig 1.11.1.e: structure of PIM-7

This polymer is soluble in chloroform and has a rigid and contorted backbone where both monomeric units contain a spiro-centred site of contortion providing microporosity as demonstrated with a BET surface area of 680 m² g⁻¹.¹³² Gas permeability measurements showed that PIM-7 has a higher selectivity than PIM-1.^{133, 134} In 2008, Ghanem and *et al.* reported several kinds of PIMs based on bis(phenazyl) similar to PIM-7, for example, cardo-PIM-1 which showed lower permeability and selectivity than PIM-7.¹³² In 2012, Bezzu *et al.* synthesised a new PIM based on spirobifluorene which showed a similar BET surface area and permeability but higher selectivity for most gas pairs as compared to PIM-1 (Fig. 1.11.1.f (left)).¹³⁵ Recently, the synthesis of PIMs based on hexaphenylbenzene was achieved however these polymers demonstrated lower BET surface area and permeability as compared to PIM-1 (Fig. 1.11.1.f (right)).¹³⁶

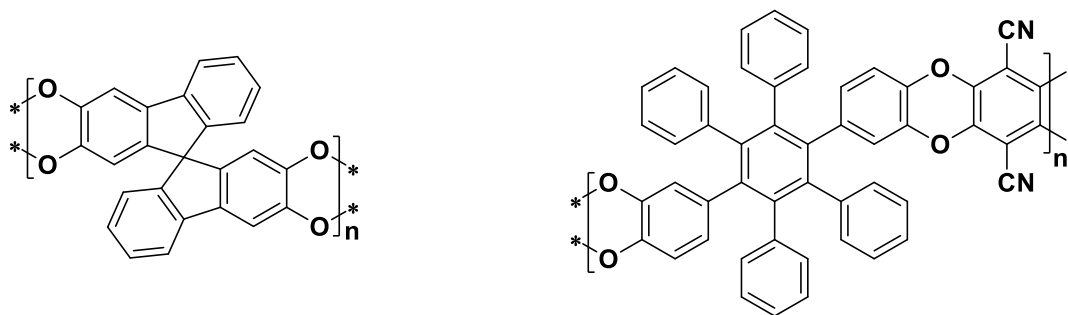
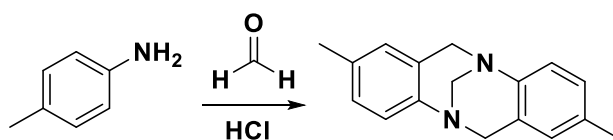


Fig1.11.1.f: structure of SBF-PIM (left) and PIM based hexaphenylbenzene (right)

1.11.2: Träger-base (TB) Polymers

In 1887 Julius Tröger synthesised and isolated (2,8-dimethyl-6*H*,12*H*-5,11-methanodibenzo[*b,f*][1,5]diazocine) now termed Tröger base **1** from the condensation of formaldehyde with 4-aminotoluene (*p*-toluidine) in acid-catalysed media (Scheme 1.11.2.a).¹³⁷



Scheme 1.11.2.a: synthesis of Tröger base **1**

In 1935, M. A. Spielman proved the structure of Tröger base through acylation, nitrosation and reduction to conclude that it was 2,8-dimethyl-6*H*,12*H*-5,11-methanodibenzo[*b,f*][1,5]diazocine.¹³⁸ In 1986, Larson and Wilcox confirmed this structure by single crystal X-ray diffraction.¹³⁹ Tröger base (TB) contains two stereogenic nitrogen atoms in its rigid twisted V-shaped structure (Fig1.11.2.b).¹⁴⁰ Enantiomers of chiral amines (N-centred) often cannot be determined because of rapid inversion at room temperature but the rigid bicyclic unit prevents inversion of the bridgehead N atoms, so TB exists as two enantiomers.^{141, 142}

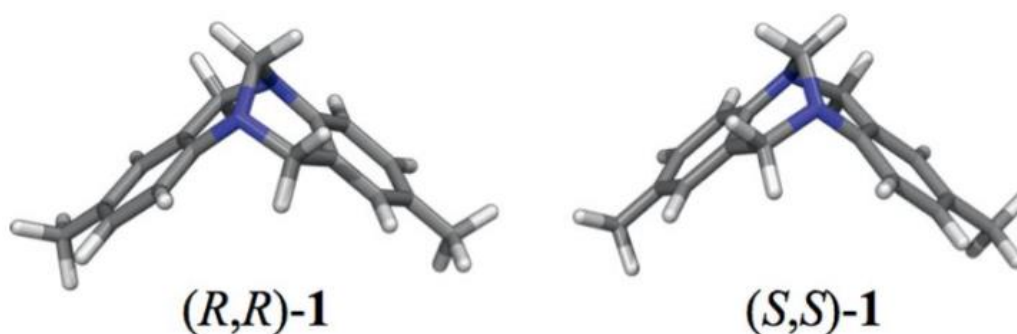
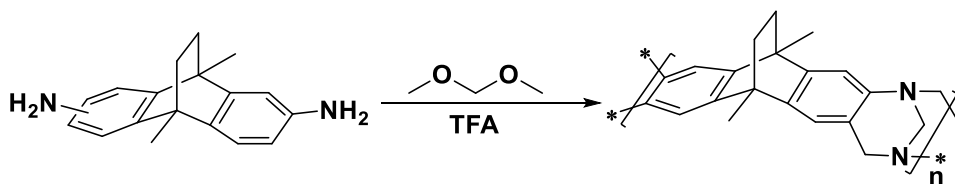


Fig 1.11.2.b: Molecular model of the TB enantiomers

TB was thought to be only weakly basic¹⁴³ however, it has higher hydrogen bonding acceptor strength compared to other aromatic amines.¹⁴⁴ This basicity is attributed to the rigid V-shaped structure which prevents conjugation between the aromatic rings and the lone pairs of the bridgehead nitrogens. There are several methods reported to synthesise TB, in addition to the original procedure¹⁴⁵ with a range of different "methylene supplier" such as formaldehyde,¹³⁷ paraformaldehyde,¹⁴⁶ hexamethylenetetramine¹⁴⁷ and dimethoxymethane¹⁴⁸ all of which involve an aromatic amine derivative reacting under acidic conditions. It is also possible to use different acids as solvent and catalyst such as hydrochloric acid,¹³⁷ methanesulfonic acid¹⁴⁹ and trifluoroacetic acid.¹⁴⁷ In 2010, a patent application by Carta *et al.* described the formation of polymers of intrinsic microporosity based on TB formation using bifunctional aniline monomers and dimethoxymethane as a methylene supplier in a solution of trifluoroacetic acid (TFA).¹⁵⁰

In 2013, Carta *et al.* reported the polymerisation of PIM-EA-TB using bridged bicyclic 2,6(7)-diamino-9,10-dimethylethanoanthracene monomer (Scheme 1.11.2.c). This polymer showed a very high BET surface area (1028 m² g⁻¹) and also demonstrated high performance for gas separations of some gas pairs H₂/CO₂, H₂/N₂, H₂/CH₄ and O₂/N₂.¹⁵¹



Scheme 1.11.2.c: synthesis of PIM-EA-TB

Noteworthy, TB polymers have been used for various applications such as heterogeneous catalysis¹⁵²⁻¹⁵⁴ and also show the potential to increase affinity for CO₂ in capture materials.^{155, 156}

1.12: Network Polymer of Intrinsic Microporosity

Network PIMs have structures similar to activated carbon where they show high BET surface areas up to 2000 m² g⁻¹ with a wide distribution of pore sizes.¹⁵⁷ Examples of network polymers are those based on triptycene made by the reaction of hexahydroxy triptycene monomers, containing various lengths of alkyl chains attached to the bridgehead position (R), with tetrafluorophthalonitrile. The BET surface areas of these polymers are high due to internal molecular free volume of triptycene molecules¹⁵⁸ but it was also found that the surface area

depends on the number of carbon atom on the alkyl chains so that Trip-Me-PIM is a highest surface area of $1760 \text{ m}^2 \text{ g}^{-1}$ while H and Et have a similar value of $1400 \text{ m}^2 \text{ g}^{-1}$. Increasing the number of carbon atoms in the bridgehead chain decreases surface area. This result is attributed to occupation of the free volume by the flexible side chains (Fig 1.12 (left)).^{98, 101}

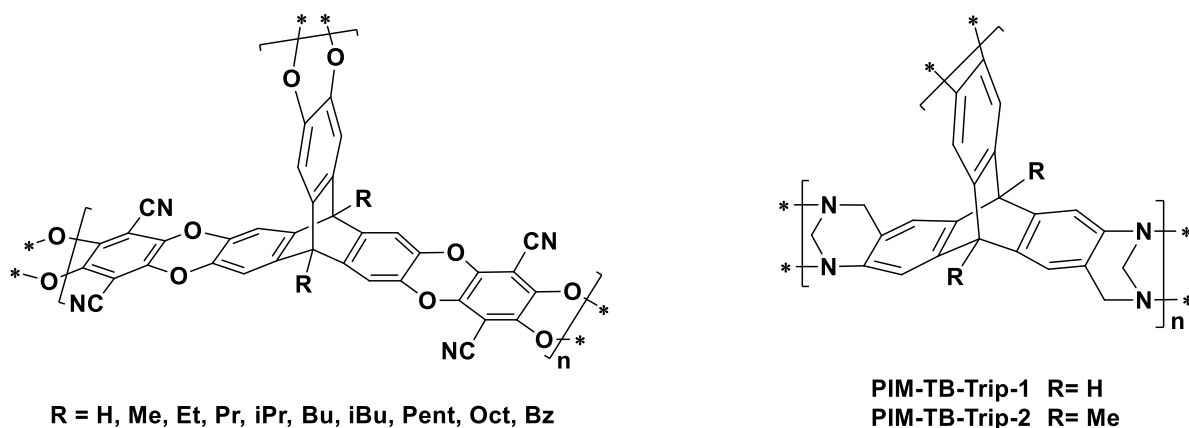


Fig 1.12: structure of triptycene polybenzodioxane network (left) and triptycene TB polymer network (right)

Recently, Carta *et al.* reported a network PIM based on Tröger base in which they used triamino-triptycene monomers to form PIM-TB-Trip-1 and PIM-TB-Trip-2 which showed high BET surface areas of 1035 and $752 \text{ m}^2 \text{ g}^{-1}$, respectively (Fig. 1.12 (right)).¹⁵⁹

Part Two:

1.13: Determination of Surface Area

The determination of surface area for a porous material is a measurement of the total irregular internal surface that the object occupies, which is predominantly on a microscopic scale. There are several methods for quantifying the surface area of materials including optical methods,¹⁶⁰ computational methods^{161, 162} and porosimetry methods using a non-wetting liquid such as mercury.¹⁶³ Usually, gas adsorption (both adsorption and desorption) is widely used to determine the surface area and relative pore size distributions of a porous material. The adsorption is facilitated by interactions between the solid and adsorbate molecules. There are two kinds of interaction between the gas molecule with the surface: either chemical adsorption (chemisorption) or physical adsorption (physisorption). Chemical adsorption (chemisorption) is the phenomenon that takes place between a surface and a gas molecule due to the formation of a chemical bond. Physical adsorption (physisorption) is the phenomenon that takes place between a surface and a gas molecule due to Van der Waals or weak interactions and is reversible. This process can thus be exploited to determine the surface area of the material. Surface area can be estimated by the amount of gas adsorbed by the surface of the sample, either by a change in the volume of the probe gas (volumetric analysis) or by change in sample weight (gravimetric analysis). The volumetric technique often uses Brunauer-Emmett-Teller (BET) theory,¹⁶⁴ which was developed from Langmuir theory for monolayer molecular adsorption. Irving Langmuir developed a mathematical model to depict physisorption in a gas-solid system. In this system equilibrium is established between the free gas molecules and the gas molecules adsorbed onto the surface. This equilibrium depends on the relative stabilities of the species, the pressure of the gas above the surface and the temperature of the system. Low temperature and high pressure are necessary to keep the surface saturated with gas molecules.¹⁶⁵

The Langmuir adsorption isotherm is based on a number of assumptions:

- 1- Adsorption cannot proceed beyond monolayer coverage.
- 2- There are no adsorbate-adsorbate interactions.
- 3- All surface sites are equivalent and can accommodate, at most, one adsorbed molecule.
- 4- In the gas phase, the adsorbate behaves ideally.
- 5- An adsorbed molecule is immobile.

Langmuir theory was built to account for monolayer adsorption, while BET theory builds on these ideas,¹⁶⁴ but to account for multilayer adsorption with the following assumptions:

- 1- Langmuir theory can be applied to each separate layer.
- 2- There are no interactions between each adsorption layer.
- 3- Gas molecules can physically adsorb to a surface in an infinite number of layers.

The specific BET surface area (S_{BET} (m²g⁻¹)) of the sample is then calculated from V_m using the following equation:

$$S_{BET} = \frac{V_m N_A \sigma}{WMv}$$

Where: V_m = the volume of gas required to form a monolayer, N_A = Avogadro's constant (6.022×10^{23} mol⁻¹), W = weight of sample (g), Mv = Molar volume occupied by a gas at 273.15 K and 1 atm (22414 ml), σ = Effective cross-sectional area of one nitrogen molecule (16.2 Å²).¹⁶⁶

Nitrogen is the most commonly used gas probe for BET measurements and can be applied to materials with surface areas ranging from 0.01 to 6000 m²/g. As well as the surface area, the pore size distribution can be calculated from the isotherm using an assessment model, based on shape and size, of pores ranging in size from a few Angstroms to half a micron.¹

A plot of the volume of gas adsorbed V against P/P_0 results in an adsorption isotherm. IUPAC definitions can be categorized into six main types (Fig 1.13¹⁶⁷: microporous (< 2 nm), mesoporous (2-50 nm) and macroporous (>50 nm) and each has a different adsorption isotherm profile.^{1,167}

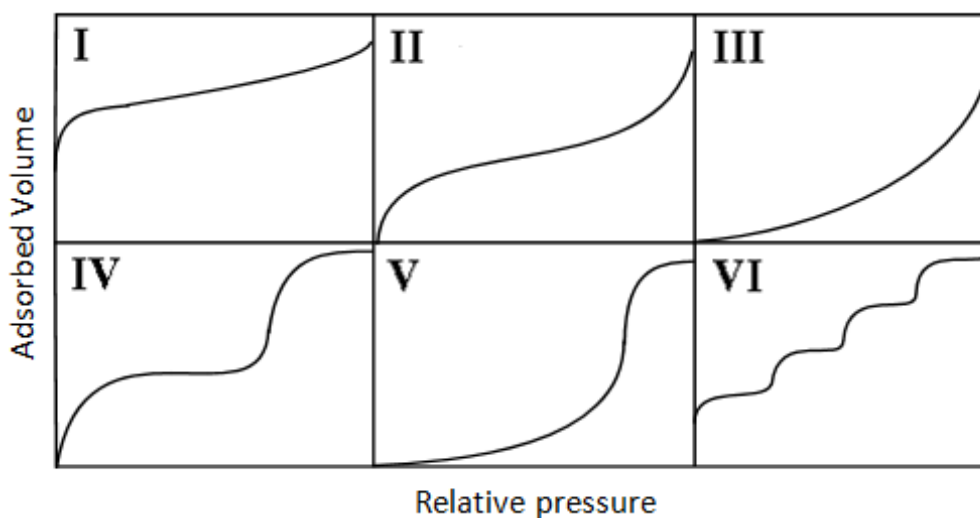


Fig 1.13: The IUPAC classification of adsorption isotherms

Type I isotherms of microporous materials show high surface areas through a large gas uptake at low partial pressures. The isotherm climbs the y-axis until the surface becomes largely covered with adsorbate molecules. Then, the plot passes through an almost linear region from $0.05 \leq P/P_0 \leq 0.35$ where the first monolayer is full. More layers are built on top of the first layer and the pores completely fill with adsorbate until a saturation point is reached at $P/P_0=1$. Macroporous materials show type II, III and VI isotherms while the mesoporous materials show type IV and V isotherms.

1.14: Introduction to membranes for gas separation

One definition of a membrane is “a phase or a group of phases that lies between two different phases, which is physically and/or chemically distinctive from both of them and which, due to its properties and the force field applied, is able to control the mass transport between these phases”.¹⁶⁸ This is a broad definition which includes a range of membranes in different fields (e.g. biological membranes). It can be applied to a range of membrane applications like those used for applications in gas separation, pervaporation, electrodialysis and reverse osmosis.¹⁶⁹ Transport of permeate through a membrane is as a result of a driving force generated either by concentration, differences in pressure, temperature or electrical potential. Differences in chemical and/or physical properties between the membrane and permeate achieves the separation of one component from the other.¹⁷⁰

1.14.1: Mechanisms for gas separation

There are different mechanisms for the transport of gas molecules through a membrane, which have been suggested based on pore size (Fig 1.14.1.a¹⁷¹).

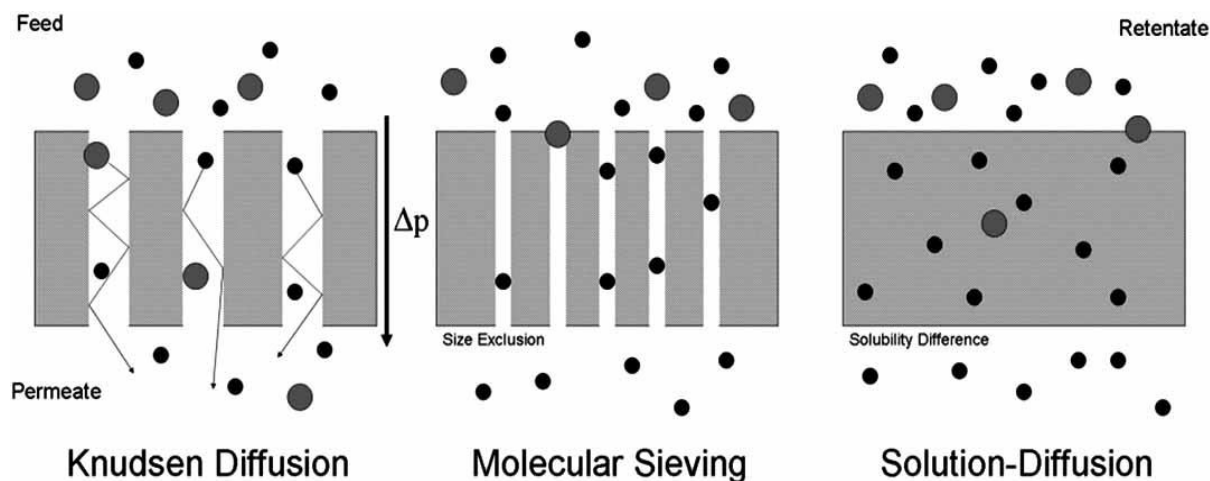


Fig 1.14.1.a: membrane separation mechanisms for gases

Knudsen diffusion occurs when membranes have pore sizes (0.002-0.1 μm). The pores are large and of adequate size to accommodate both components of the gas mixture however, there is a variance in the mean free path for both components in the mixture based on the size of the molecule because the collision between larger gas molecules and pore walls with a greater frequency than smaller molecules. So, the separation is achieved due to differences in velocities of the gaseous species.¹⁷²

Molecular sieving occurs when membranes have pore size in the range 0.0005-0.002 μm . These pore are very small and provide size exclusion whereby mixtures are separated depending on the kinetic diameter of the gas molecules. As a result, the pore size allows the permeation of smaller gas molecules through the membrane.¹⁷³

In 1866 Graham suggested the solution-diffusion model as a way to describe the transport of gases through a nonporous membrane.¹⁷⁴ Separation is achieved by the differential solubility of compounds into the membrane surface from the gas phase on the feed side (fig 1.14.1.b).¹⁷⁵ Due to the difference in solubility there will be a difference in the ability of components to evaporate from the membrane surface into the gas phase on the permeate side.¹⁷⁶ This kind of sorption follows Henry's law of solubility¹⁶⁸ where the solubility of a gas in the membrane is directly proportional to the partial pressure of the gas. However, the structure of glassy polymers, like PIMs, are not homogeneous and have a distribution of unrelaxed free volume. This causes a big deviation from Henry's law which is best explained by the Dual-Mode sorption model.¹⁷⁷

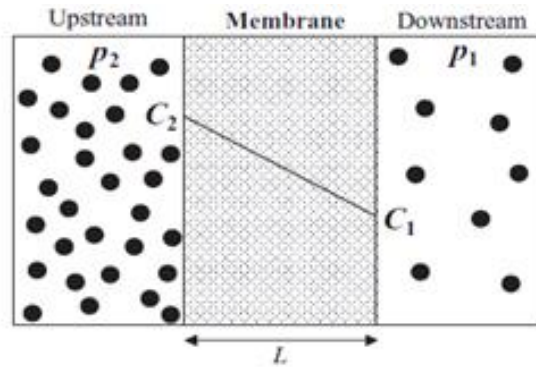


Fig 1.14.1.b: A gas separation membrane with concentration gradient across the membrane

1.14.2: Dual-Mode Sorption Model

As noted, Henry's law is the best description of the gas sorption in rubbery polymer membranes where the solubility is independent of the concentration thus the concentration inside the membrane is proportional to the applied pressure.^{168, 177} In glassy polymers Henry's law will be non-ideal to describe the gas sorption because the transport parameters dependent on variables like pressure and permeate concentration. In 1976, the dual-mode sorption model was suggested to explain the gas sorption in glassy polymers and was based on both Langmuir sorption models and Henry's law to explain the differences between glassy and rubbery polymers. The model concludes that the permeate gas dissolved in the membrane can be divided into two phases, each with different diffusive properties in equilibrium.¹⁷⁸

In glassy polymers, the permeate dissolves in the bulk polymer (Henry's law type sorption) where diffusion may occur and there is also adsorption of the permeate inside a number of transient microvoids distributed throughout the polymer (Langmuir type sorption). Diffusion occurs via a "hopping" mechanism¹⁷⁵ where permeate molecules are restricted inside the free volume until they find enough energy to "hop" to next the free volume element. The energy barrier to achieve this depends on a several factors like temperature, concentration, size of penetrant molecule, polymer rigidity and the degree of the interconnectivity of free volume elements. The physical ageing of thin membranes occurs due to the relaxation of polymer chains into a denser solid where the free volume is reduced resulting in a reduction in permeability.^{179, 180}

1.14.3: Transport Parameters

The permeability coefficient P is defined as ratio between the flow J (volume of the permeate crossing out of a unit area of the membrane per unit time) and its concentration tendency Δ_C over the membrane of thickness l and is conveniently reported in "Barrer" (1 Barrer = 10^{-10} (cm³(STP)/cm s cmHg).

$$P = \frac{J}{\Delta_C / l}$$

The solution-diffusion model suggests that the permeability coefficient P of a gas through a membrane is the product of the diffusion coefficient and the solubility coefficient.

$$P = SD$$

Where S the solubility coefficient with unit (cm³ cm⁻³ bar⁻¹). D the diffusion or diffusivity coefficient with unit (m² s⁻¹). The selectivity or "permselectivity" (α) is a measure of the gas separating ability of the membrane. The selectivity of a gas pair is acquired as the ratio of the permeability coefficient for each of the two gases.

$$\alpha_{XY} = \frac{P_x}{P_y}$$

The selectivity of a membrane has components from both diffusion and solubility coefficients with thus the selectivity for a gas pair can be decoupled into diffusivity-selectivity and solubility-selectivity:

$$\alpha_{XY} = \frac{S_x}{S_y} \cdot \frac{D_x}{D_y}$$

It is usual to report the selectivity values for each gas relatively to the permeability of nitrogen ($\alpha (P_x/P_{N_2})$), ($\alpha (S_x/S_{N_2})$) and ($\alpha (D_x/D_{N_2})$) as it is usually the least permeable of the gases.

$$\alpha_{XY} = \frac{S_x}{S_{N_2}} \cdot \frac{D_x}{D_{N_2}}$$

Molecular sieving materials are less permeable to gas molecules with larger kinetic diameters ($d_k(\text{\AA})$) than to smaller diameters and so the order of gas permeabilities are typically: He (2.6) > H₂ (2.89) > CO₂ (3.3) > O₂ (3.46) > N₂ (3.64) > CO (3.76) > CH₄ (3.8).¹⁸¹ This kind of membrane is known as "*forward selective*". For membranes acting by the solution-diffusion mechanism, the orders of gas permeabilities are typically: CO₂>H₂>O₂>He>CH₄>CO>N₂. This kind of membrane is known as "*reverse selective*". The cause for this order is the relative differences in solubility and diffusion coefficients of the gases. For example, below is a plot

(Fig 1.14.3.a)¹⁸² of the solubility and diffusion coefficients vs the Lennard-Jones diameter of a number of gases for a natural rubber membrane.

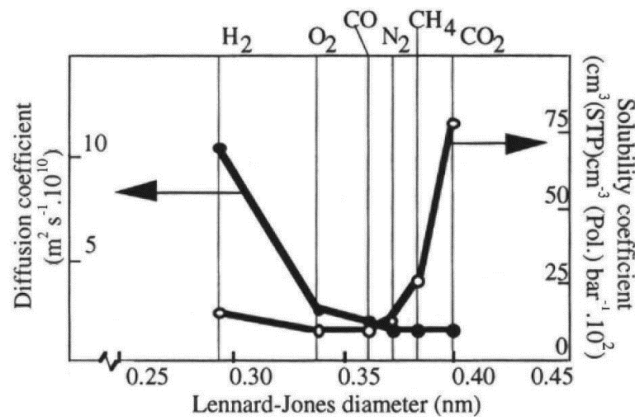


Fig1.14.3.a: Lennard-Jones Diameter of Gases Vs Solubility & Diffusion Coefficients for a Natural Rubber Membrane

According to the solution diffusion model (i.e. $P = SD$) these data can be combined to prove the total effect the diameter of the penetrant gas has on the permeability coefficient. A plot below of the permeability coefficients vs the Lennard-Jones diameter for the same natural rubber membrane (Fig 1.14.3.b)¹⁸² shows the relative permeability of the gases in the order $CO_2 > H_2 > O_2 > CH_4 > CO > N_2$.

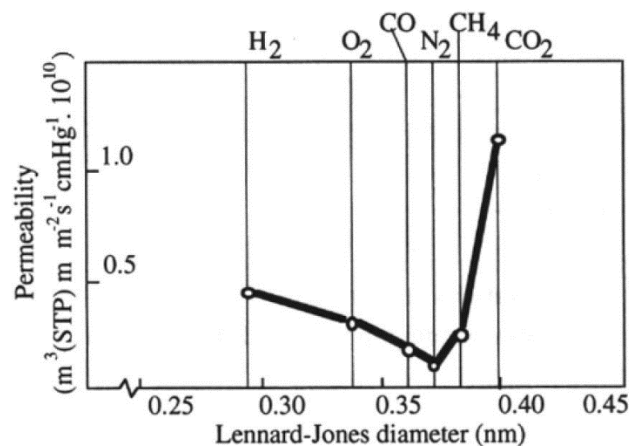


Fig 1.14.3.b: Lennard-Jones Diameter of Gases Vs Permeability Coefficients for a Natural Rubber Membrane

1.14.4: Robeson Plots

Both high permeability and high selectivity are desirable for a polymer membrane but there is an inverse relationship between permeability (P_x) and selectivity ($\alpha_{xy} = P_x/P_y$).¹⁸³ In 1991, Lloyd Robeson proposed an ‘upper bound’ to show a limit for this trade-off between high selectivity and high permeability.¹⁸⁴ The data from many references for polymer

permeability was collected and plotted for a number of dual gas mixtures as $\log \alpha_{xy}$ versus $\log P_x$ (Fig 1.14.4).¹⁸⁵. Over time, polymer materials were synthesised which surpassed the 1991 upper bound¹⁴⁵. In 2008, Robeson updated the plot taking into account newly published data including that of PIM-1 and PIM-7 with a new upper limits known as the "*Robeson (2008) upper bounds*".¹⁸⁵

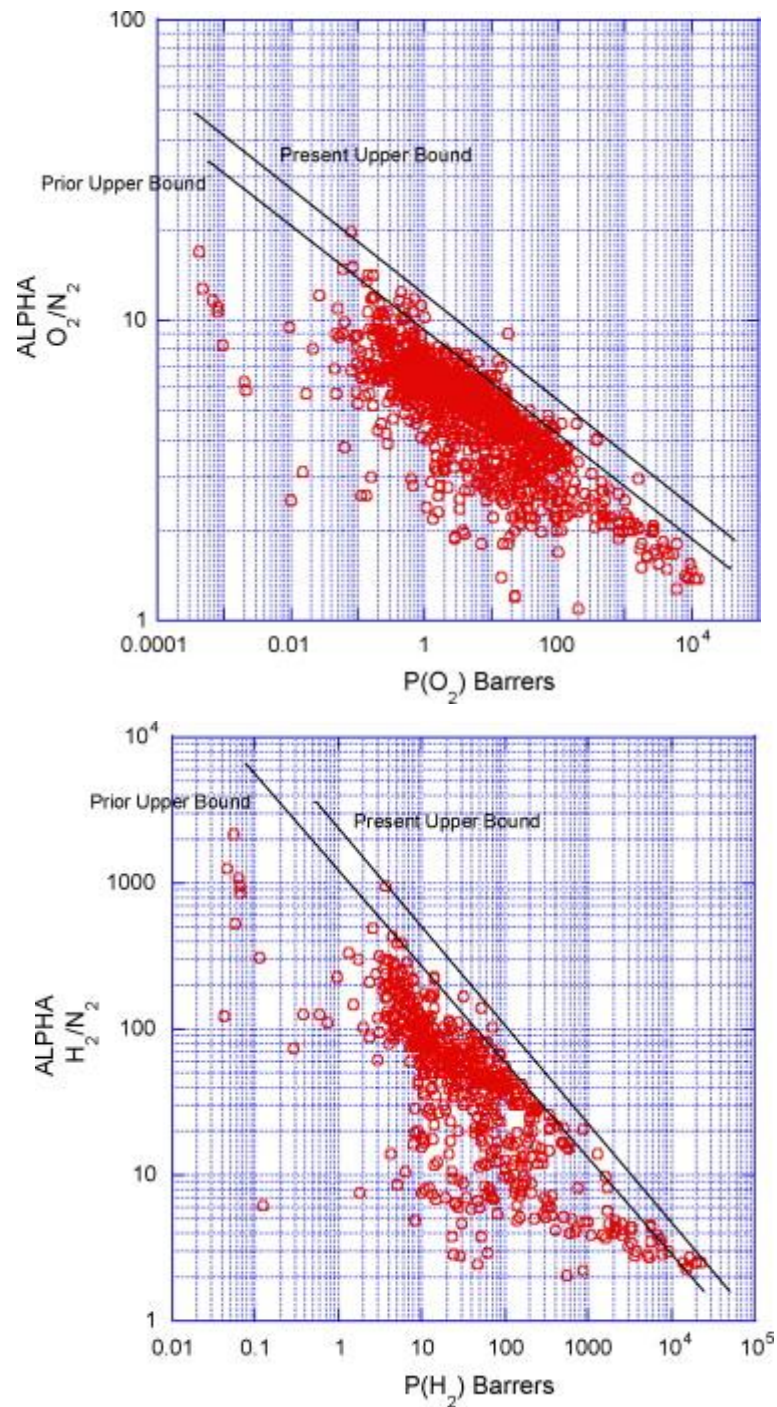


Fig 1.14.4: Robeson plot for O_2/N_2 and H_2/N_2 showing present and prior upper bound

Chapter Two: Project Aims

As noted, PIMs show remarkable potential as gas separation materials.^{124,186} Therefore, we were interested to synthesise novel PIMs for this application using three established polymerisation methods but using novel monomers specifically designed for this programme of research (Chapter 3).

The types of polymers of interest are (fig 2.1):

1. Polybenzodioxin (Chapter 4)
2. Tröger's base polymers (Chapter 5) and
3. Polyimides (Chapter 6)

Soluble, film-forming polymers obtained from these studies will have their gas transport parameters evaluated at The Institute of Membrane Technology (ITM) CNR (Calabria, Italy).

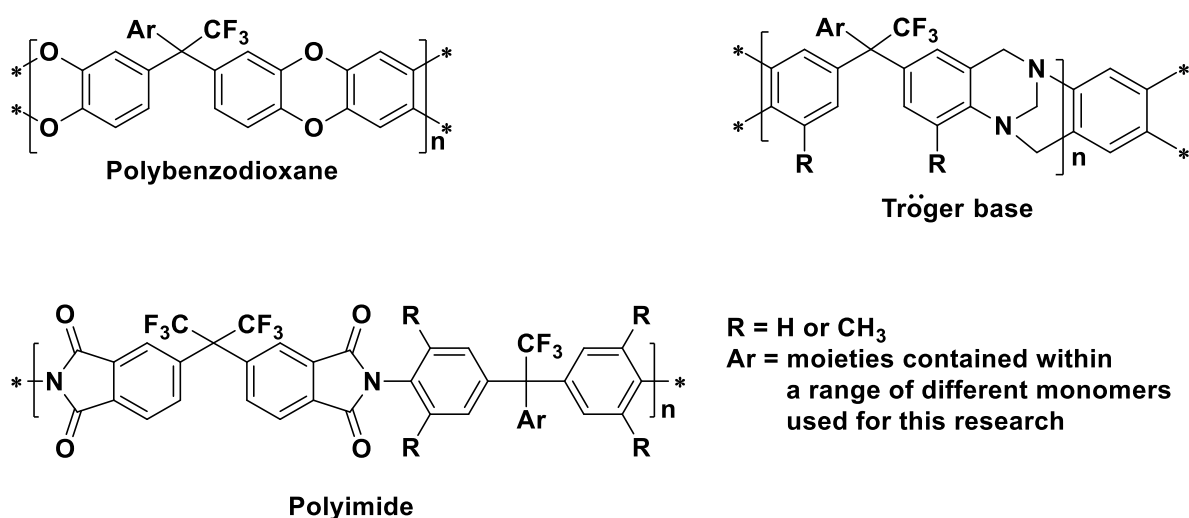


Fig 2.1: General structures of the three classes of polymer reported in this thesis

Chapter Three: Monomer Synthesis

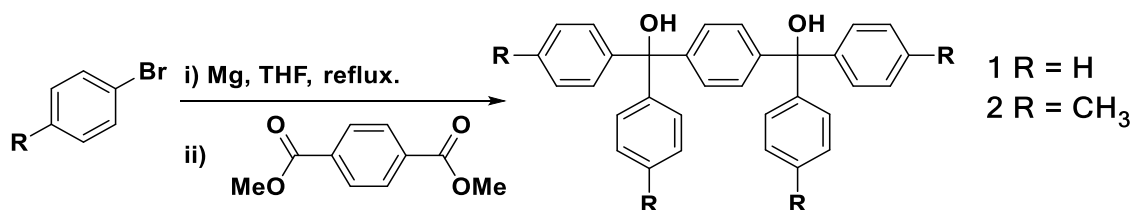
3.1: Introduction

Some of the monomers reported in this thesis were already described in the literature, but the majority were prepared specifically for the project. The monomers used for this work are based on “1,4-ditriptylbenzene”, bis(aryl)adamantane and 2,2,2-trifluoro-1-arylethane derivatives. All were prepared by electrophilic aromatic substitution of purposely synthesised substrates on catechol or aniline molecules. Thus, they can be separated into two groups by functionality: biscatechols and bisanilines. Whereas the first can be used only for the synthesis of novel benzodioxin-based polymers (i.e. similar to PIM-1), some of the bisanilines could be used for the synthesis of both polyimides and Tröger’s Base polymers (TB-PIMs).

All reactions were tested to be complete using thin layer chromatography and all compounds were fully characterised to confirm structure and purity using melting point, ^1H , ^{13}C and, when necessary, also ^{19}F nuclear magnetic resonance (NMR), FT-IR and mass spectrometry.

3.2: Synthesis of 1,4-bis(di-aryl-hydroxymethyl)benzene compounds

Precursors 1,4-bis(diphenylhydroxymethyl)benzene (**1**) and 1,4-bis(di-*p*-toluenylhydroxymethyl)benzene (**2**) were synthesised according to a reported procedure,¹⁸⁷ by reacting dimethyl terephthalate with the appropriate Grignard reagent (scheme 3.1).



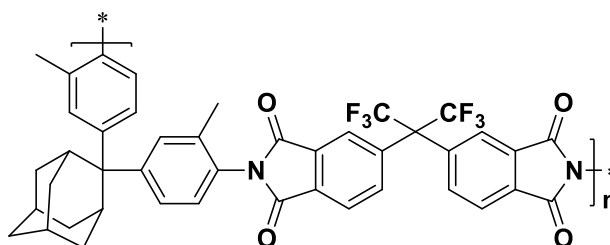
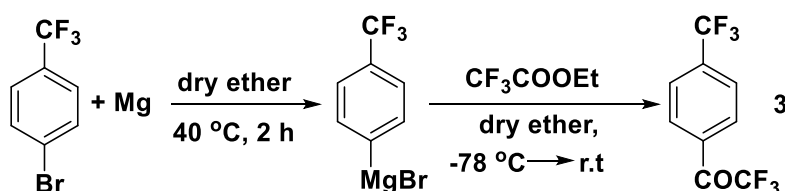
Scheme 3.2: Synthesis of 1,4-bis(diphenylhydroxymethyl)benzene and 1,4-bis(ditoluylhydroxymethyl)benzene

3.3: Synthesis of aryl-2,2,2-trifluoromethyl ketones

Most of the ketones used for this work were synthesised by Friedel-Crafts acylation. However, 4-(trifluoromethyl)- α,α,α -trifluoroacetophenone was prepared by a Grignard reaction and trifluoroacetophenone was commercially available.

3.3.1: 4-(trifluoromethyl)- α,α,α -trifluoroacetophenone

The Grignard reagent *p*-(trifluoromethyl)benzene magnesium bromide was freshly prepared as reported in the literature,¹⁸⁸ then transferred to a dropping funnel and added dropwise to a solution of ethyl trifluoroacetate in diethyl ether at $-78\text{ }^{\circ}\text{C}$, then the mixture was allowed to reach room temperature and stirred at this temperature overnight. The product was isolated in a good yield after quenching the reaction with diluted HCl and extraction with diethyl ether. Various methods for the preparation of this ketone are reported¹⁸⁹ but the above procedure was chosen because it was simple, allowed the use of cheap starting materials and afforded the product in high yield. Grignard reagents are extremely reactive and in reactions with esters to form alcohols the intermediate ketones cannot be isolated, but in this case the electron-withdrawing trifluoromethyl group stabilizes the tetrahedral intermediate allowing the ketone to be isolated in a good yield. (Scheme 3.3.1).

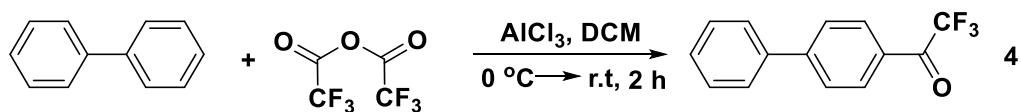


Scheme 3.3.1: Synthesis of 4-(trifluoromethyl)- α,α,α -trifluoroacetophenone (**3**)

3.3.2: Aryl-2,2,2-trifluoromethyl ketones synthesis by Friedel-Crafts acylation

Several aryl trifluoromethyl ketones, some of which are novel, were synthesised by Friedel-Crafts acylation, according to reported procedures.¹⁹⁰ The acylation reaction was performed by adding the aromatic compound (i.e. biphenyl in Scheme 3.3.2.a) to trifluoroacetic anhydride (TFAA) and anhydrous AlCl_3 in DCM. All the ketones could be easily purified by recrystallization with petroleum ether or Et_2O . This method was preferred to others, such as Grignard¹⁹¹ or Suzuki cross-coupling reactions (as previously used for **4** and **5**),¹⁹² because it allowed the use of cheap starting materials and catalyst, affording high purity products in very

good yields and in short reaction times. The results for these reactions are reported in (Table 3.3.2.b).



Scheme 3.3.2.a: synthesis of 4-biphenyl trifluoromethyl ketone

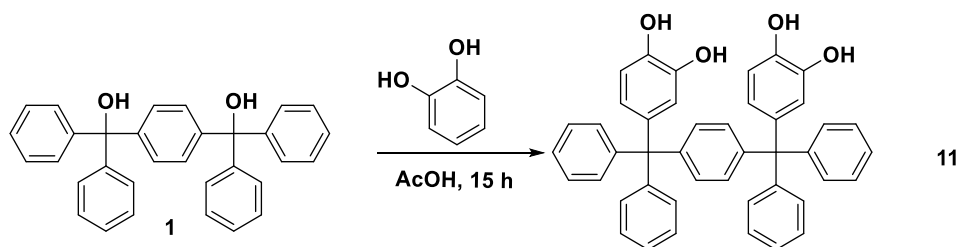
Table (3.3.2.b): Trifluoromethyl ketones, yields and reaction times

No.	Aromatic Compounds	Aryl-2,2,2-trifluoromethyl ketones	% Yield	Reaction time, h
1			80	6
2			81	2
3			70	2
4			90	10
5			70	16
6			63	16

3.4: Bis-catechol monomers

3.4.1: Synthesis of *p*-bis (3,4-dihydroxyphenyldiphenylmethyl) benzene (BAB4):

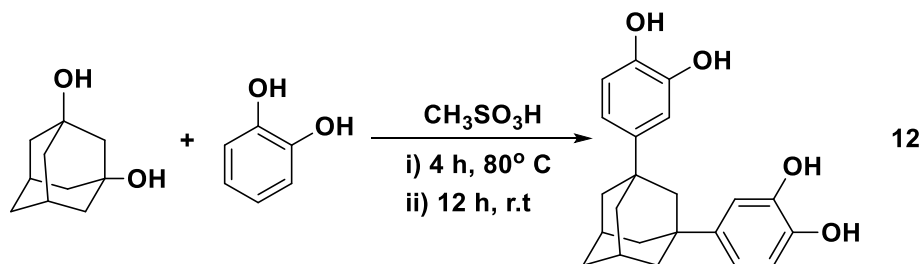
The diol (**1**) was reacted with catechol in presence of acetic acid as a solvent to form a novel biscatechol monomer (BAB4) (**11**) in good yield (69%) (Scheme 3.4.1).



Scheme 3.4.1: synthesis of BAB4 monomer

3.4.2: Synthesis of 1,3-bis(3,4-dihydroxyphenyl)adamantane (BDA)

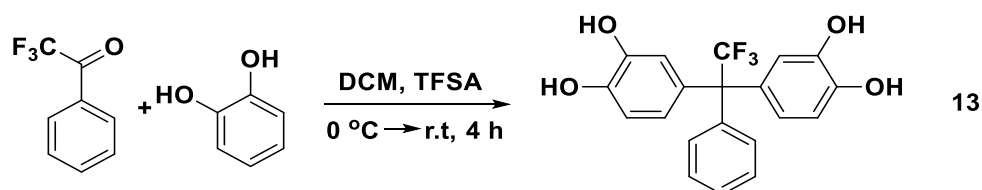
This bis-catechol monomer (BDA) (**12**) (scheme 3.4.2) was synthesised according to a procedure reported in the literature,¹⁹³ by reacting 1,3-adamantane diol with catechol in methanesulfonic acid. The reaction afforded the product in a low yield (24%), probably because of the scarce reactivity of the adamantane diol, some of which was recovered unreacted.



Scheme 3.4.2: Synthesis of PIM-BDA

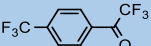
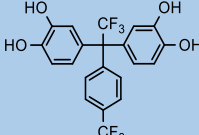
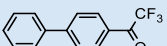
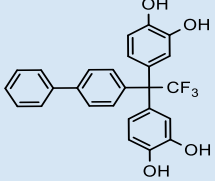
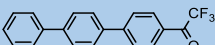
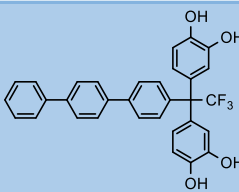
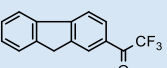
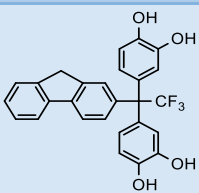
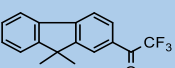
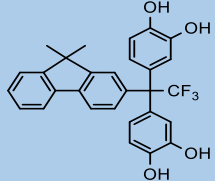
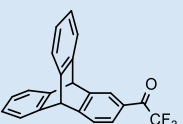
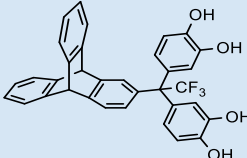
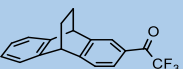
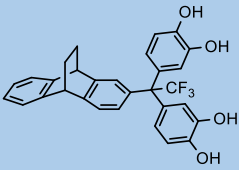
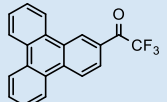
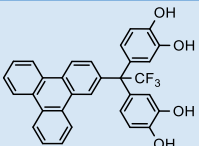
3.4.3: Synthesis of 1,1-bis(catechol)-2,2,2-trifluoro-1-arylethane

Recently, the synthesis of 1,1-bis(3,4-dihydroxy-phenyl)-2,2,2-trifluoro-1-phenylethane, by a condensation reaction of trifluoroacetophenone with catechol (Scheme 3.4.3.a), was reported.¹⁹⁴ This simple and high yielding method was employed for the synthesis of all 1,1-bis(catechol)-2,2,2-trifluoro-1-arylethane monomers. Trifluoromethanesulfonic acid (TFSA) was used as a catalyst for the reactions, which were conducted at room temperature and afforded the desired monomers in moderate to high yields. The time of reaction demonstrated a strong dependence on concentration and reactivity of ketones. The overall results for the monomers prepared in this way are reported in (Table 3.4.3.b).



Scheme 3.4.3.a: Synthesis of 1,1-bis(3,4-dihydroxy-phenyl)-2,2,2-trifluoro-1-phenylethane (TF1) (**13**)

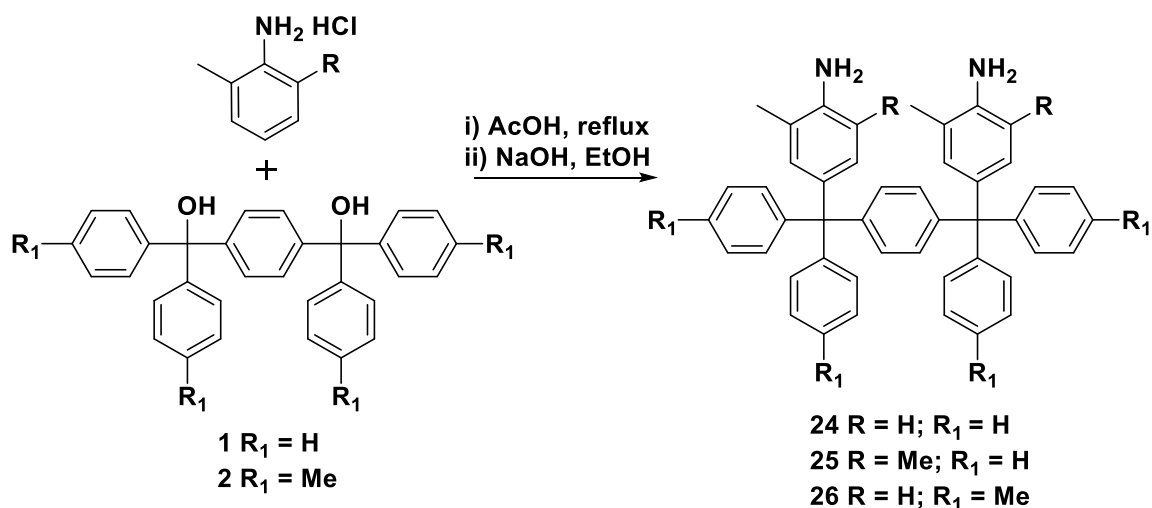
Table (3.4.3.b): 1,1-Bis(catechol)-2,2,2-trifluoro-1-arylethane monomers, yields and reaction time.

No	Ketones	Bis-catechol	Yield %	Reaction time, h
1	 3	 14	71	16
2	 4	 15	70	5
3	 5	 16	82	5
4	 6	 17	57	24
5	 7	 18	77	16
6	 8	 19	41	24
7	 9	 20	71	10
8	 10	 21	70	5

3.5: Diamino monomers

3.5.1: Synthesis of diamino-1,4-ditritylbenzene monomers **24**, **25** and **26**

In a similar way as previously reported for the biscatechol monomers, bisanilines were prepared as they can be used for the synthesis of both novel polyimides and in some cases Tröger's base PIMs. In this way we can compare how similar monomers behave using three different types of polymerisation. The diol (**1**) was reacted with *o*-toluidine hydrochloride and 2,6-dimethylaniline hydrochloride in a double electrophilic aromatic substitution reaction to form *p*-bis-(4-amino-3-methylphenyldiphenylmethyl)benzene (**24**) and *p*-bis-(4-amino-3,5-dimethylphenyldiphenylmethyl)benzene (**25**), respectively, (Scheme 3.5.1.a). The same procedure was also used to prepare the diamino monomer (**26**) from the diol (**2**). The resulting bisaniline monomer was purified by removing the hydrochloride salt by basic work-up.



Scheme 3.5.1.a: Synthesis of BAB1, BAB2 and BAB3

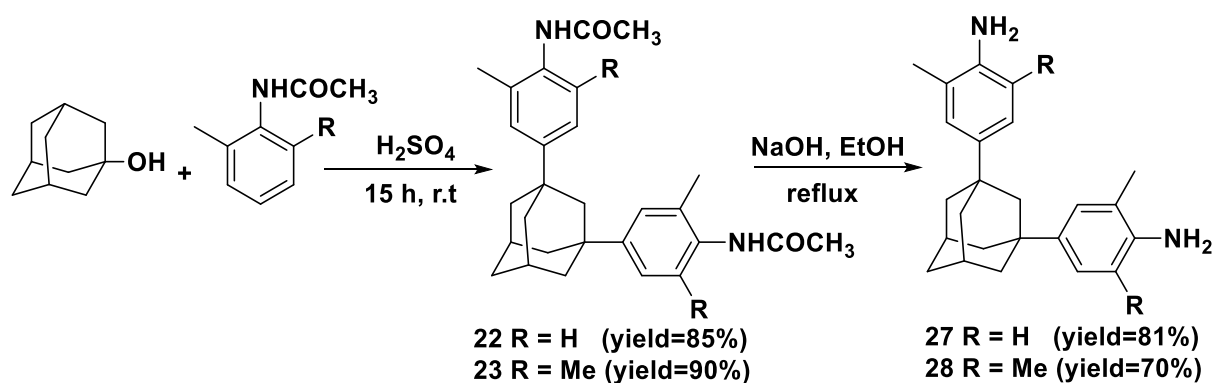
All monomers were formed with good yields, due to the high stability of the intermediate triphenylmethyl carbocations. The products were poorly soluble in common solvents such as CHCl₃ but were fully soluble in pyridine and NMP.

3.5.2: Adamantane-based monomers

3.5.2.1: Synthesis of (AD2) and (AD3)

Following the objective of comparing similar structural building units for different polymerisations, we decided to prepare a series of adamantane-based bisanilines. In the first attempted reaction, adamantane bis-alkylacetanilide protected monomers were prepared by the reaction of 1-adamantanol with the corresponding alkylacetanilide (scheme 3.5.2.1) in

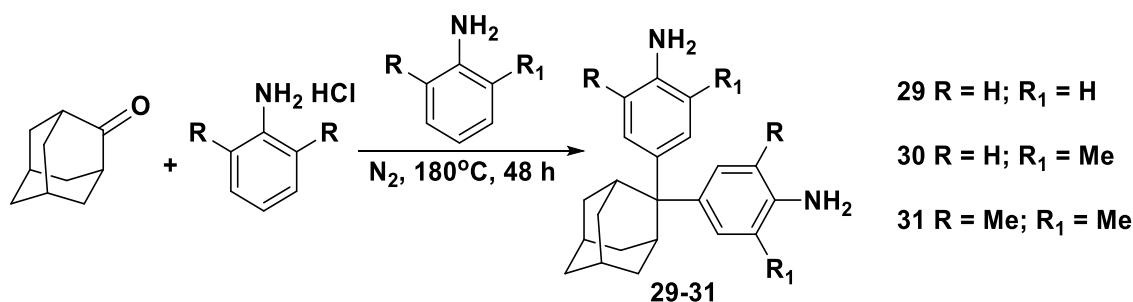
strong acidic medium, achieving the desired monomers in very good yields. The acetanilide derivatives were used because of their higher stability under these reaction conditions, compared to aniline salts such as aniline hydrochloride. The deprotection reaction, via basic hydrolysis, was performed with NaOH in refluxing ethanol for 24-48 hours (scheme 3.5.2.1).



Scheme 3.5.2.1: Synthesis of adamantane derivatives (**22** & **23**) and AD2 (**27**) & AD3 (**28**)

3.5.2.2: Synthesis of monomers AD4, AD5 and AD6

We anticipated that placing the substitution reaction on the same carbon would create a more rigid monomer, compared with the previously used monomers in which the aryl groups were on different carbons of the adamantane core, inducing higher porosity in the subsequently prepared polymer. With that in mind we synthesised three monomers (Scheme 3.5.2.2) from 2-adamantanone, using its condensation with, respectively: aniline hydrochloride in aniline, *o*-toluidine hydrochloride in *o*-toluidine and 2,6-dimethylaniline hydrochloride in 2,6-dimethylaniline. The monomers were treated with ammonium hydroxide to release the desired product. The monomers were obtained in low yields, (between 31% and 36%) probably because of the steric hindrance and rigidity of 2-adamantanone, which has to undergo a double substitution at the same position.

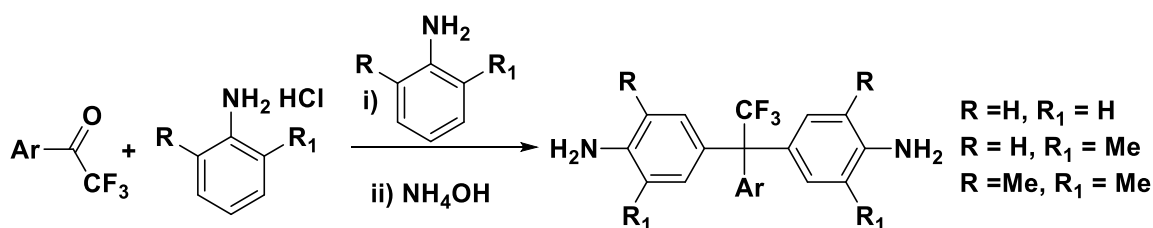


Scheme 3.5.2.2: synthesis of **29** (AD4), **30** (AD5) and **31** (AD6)

3.5.2.3: Synthesis of trifluorodiaminoaryl-based monomers

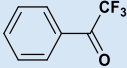
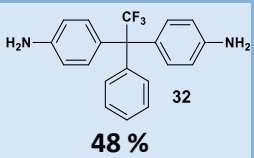
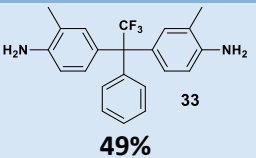
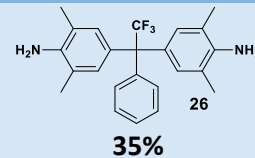
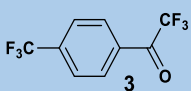
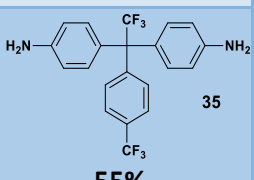
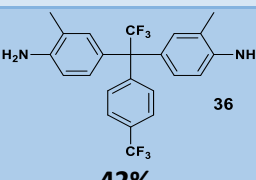
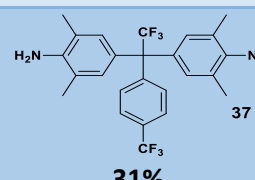
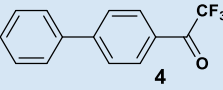
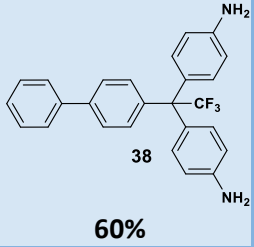
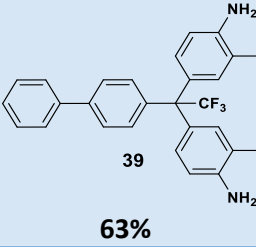
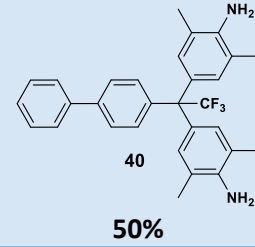
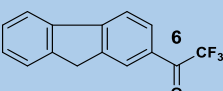
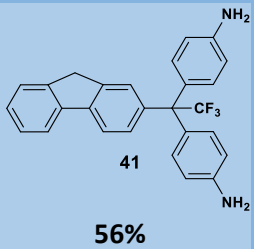
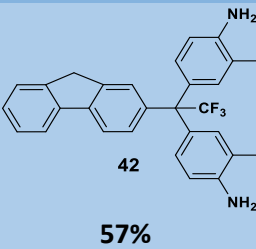
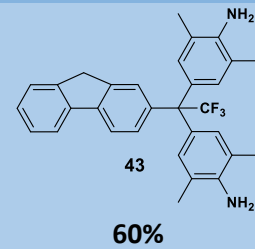
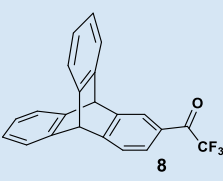
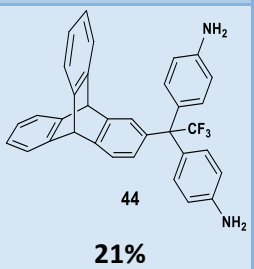
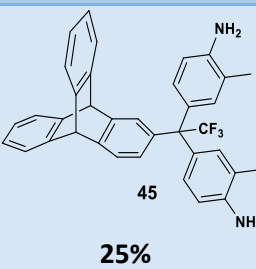
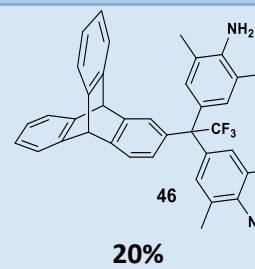
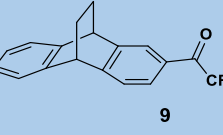
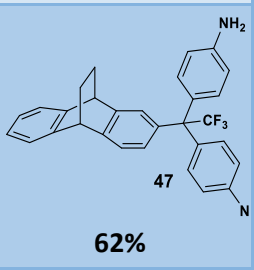
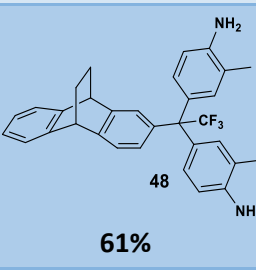
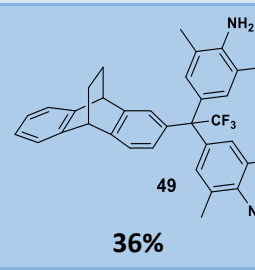
As the CF_3 group typically helps in tuning the gas permeability properties of certain polymers, we attempted its insertion in some diamino monomers, by using similar Friedel-Craft acylation chemistry. Two possible methods could be used to prepare this kind of monomer and in both of them an acid is used as catalyst for the reaction. In the first, the ketone is reacted with aniline or alkylated aniline in presence of trifluoromethanesulfonic acid (TFSA) as catalyst,¹⁹⁵ while in the second method HCl is employed for the condensation reaction between a ketone and either aniline,¹⁹⁶ 2-methylaniline¹⁹⁷ or 2,6-dimethylaniline¹⁹⁸ which are cheap and readily available starting materials.

A series of novel diamine monomers were prepared, using the second method, by reacting aryl-2,2,2-trifluoromethyl ketone with aniline hydrochloride salt or alkylated aniline hydrochloride salt. This one-step procedure proved to be quite simple and afforded highly pure monomers although in moderate yields (Table 3.5.3.b). The condensation reaction between an aniline salt with aryl-2,2,2-trifluoromethyl ketones is carried out at high temperature, enough to dissolve all the starting materials into the corresponding free aniline solvent. The reactions were carried out under nitrogen atmosphere to avoid any degradation of the product. The reaction is mediated by the protonation of the carbonyl group, which can more readily be attacked by the aniline salt, via a double aromatic substitution. The bisubstituted monomer salt is then hydrolysed with aqueous ammonia to give the desired diamino product (Scheme 3.4.3.a).



Scheme 3.4.3.a: synthesis of trifluorodiaminoaryl

Table (3.5.3.b): Ketone and bis-aniline monomers.

Ketones		Monomers		
		Structure & yield	Structure & yield	Structure & yield
1		 32 48 %	 33 49%	 26 35%
2		 35 55%	 36 42%	 37 31%
3		 38 60%	 39 63%	 40 50%
4		 41 56%	 42 57%	 43 60%
5		 44 21%	 45 25%	 46 20%
6		 47 62%	 48 61%	 49 36%

By reacting the aromatic ketone with-aniline, 2-methylaniline and 2,6-dimethylaniline, three different diamine monomers were obtained from each (Table 3.5.3.b). We observed increased yields on products when large-scale reaction was performed. Some of these

monomers have a bulky pendant group, which is anticipated to create steric hindrance between the chains of the target polymers, inducing microporosity. The use of these monomers for the synthesis of high molecular weight polyimides and Tröger's base polymers will be discussed in Chapter 5.

Chapter Four: Polybenzodioxin

4.1: Introduction to polybenzodioxin polymers

Following the synthesis of the bis-catechol monomers, the goal was to make several polybenzodioxin polymers using the reaction between novel bis-catechol monomers (Chapter Three) and tetrafluoroterephthalonitrile.

The general procedure used for polymerisation was similar to that developed for PIM-1⁹⁹ with some modifications. The step-growth polymerisation was conducted in a suitable solvent (dry DMF or DMAc) under an inert nitrogen atmosphere in the presence of potassium carbonate. After accurate measurement of the mass of monomers, DMF or DMAc was added with stirring until all monomers had dissolved. Potassium carbonate was added to the mixture and the reaction was gently heated for an appropriate time and temperature depending upon the reactivity of the monomer, resulting in a yellow precipitate being formed after a short time. The mixture was quenched with water and the polymer was purified according to its solubility in organic solvents. From all the synthesised polymers we succeeded in forming robust solvent-cast films from only two, with others proving brittle and not suitable for gas permeation measurements.

The structure of all polymers were confirmed by ¹H-NMR and ¹³C-NMR. Solid state FTIR was also used to show characteristic absorption bands at ~2100 cm⁻¹ (CN), ~1015 cm⁻¹ (Ar-O-Ar), and also ~1111, ~1015 cm⁻¹ (asymmetric and symmetric respectively) for polymers containing CF₃. The absence of OH stretching or bending, typical of monomers, provides good evidence that the reaction of bis-catechol with tetrafluoroterephthalonitrile was complete (Fig 4.1).

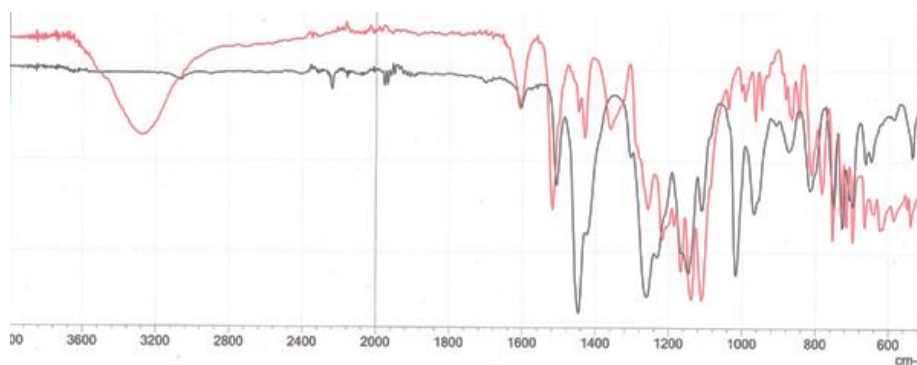
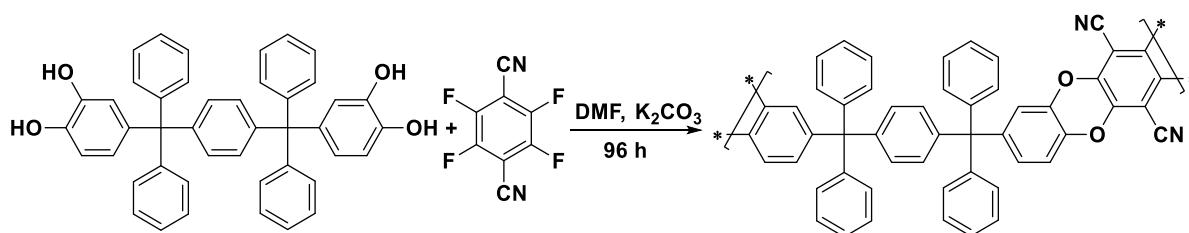


Fig 4.1: FTIR spectrum of TF1 monomer (red) and PIM-TF1 polymer (black)

4.2: Synthesis of polymers containing of *p*-bis(3,4-dihydroxyphenyldiphenylmethyl) benzene (PIM-BAB4)

The polymerisation yielded a yellow powder (79%) but unfortunately, the polymer (Scheme 4.2.1) did not form a film due to its low molecular weight ($M_w = 7050$ g/mol). The measured BET surface area (144 m²/g) was much lower than that of PIM-1 (760 m²/g).⁹⁹ This lower surface area is perhaps due to rotation of the single bonds linking the phenyl groups.



Scheme 4.2.1: Synthesis of PIM-BAB4

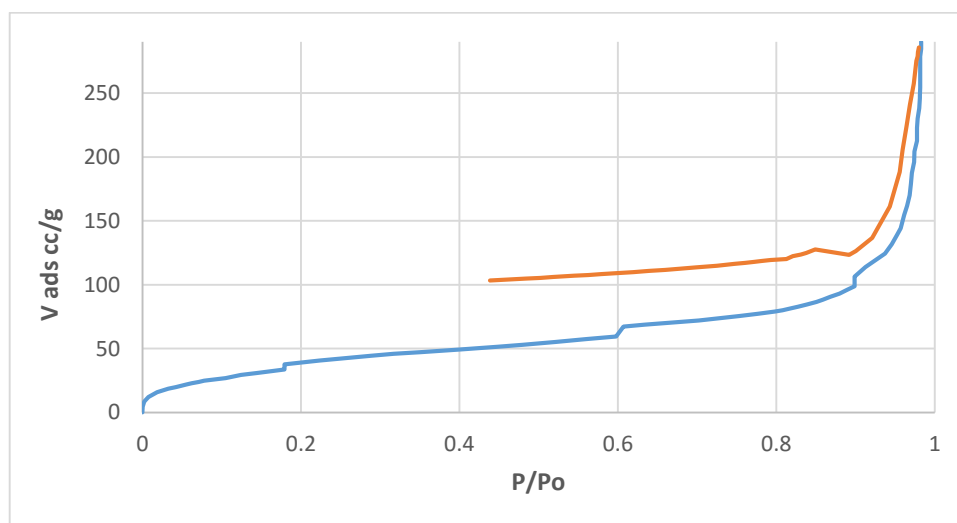
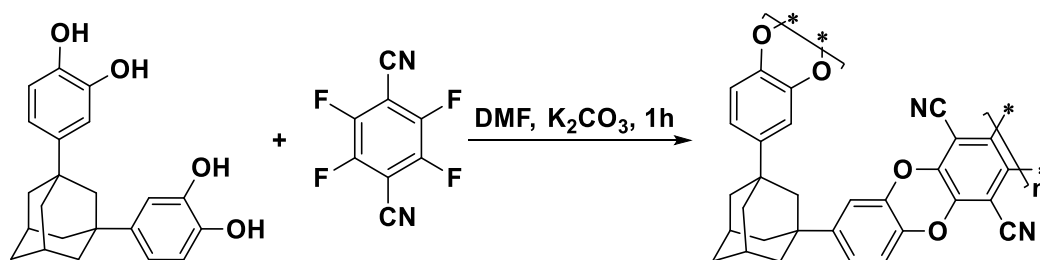


Fig 4.2.2: Nitrogen adsorption isotherms at 77 K for PIM-BAB4

4.3: Synthesis of polymers derived from 1,3-bis(3,4-dihydroxyphenyl)adamantane (PIM-BDA)

The polymerisation yielded a yellow powder (82%) but unfortunately, the polymer was insoluble in any common solvent (scheme 4.3.1). A low BET surface area (180 m²/g) was demonstrated which can be attributed to the rotation of the single bonds connecting the phenyl groups to the adamantyl cage.



Scheme 4.3.1: Synthesis of PIM-BDA

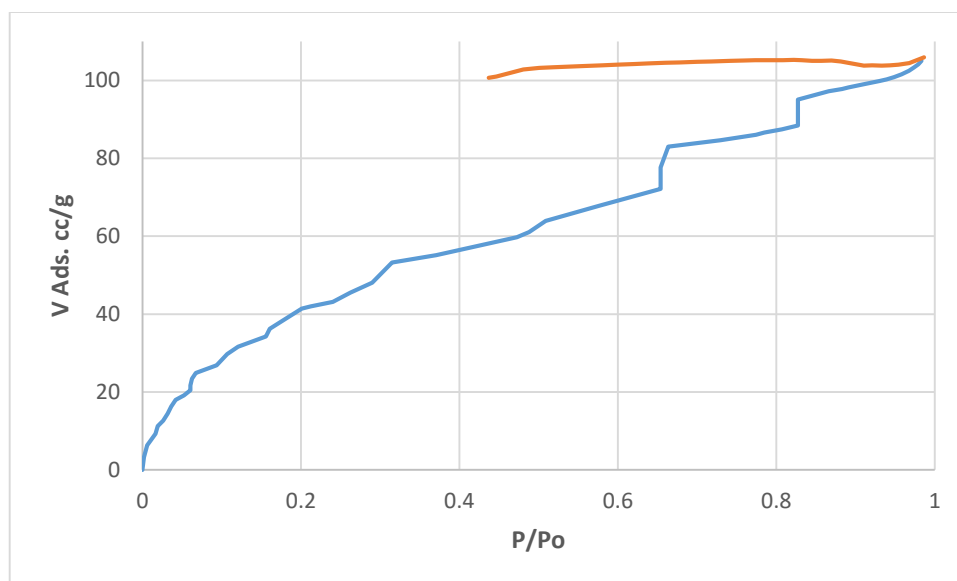
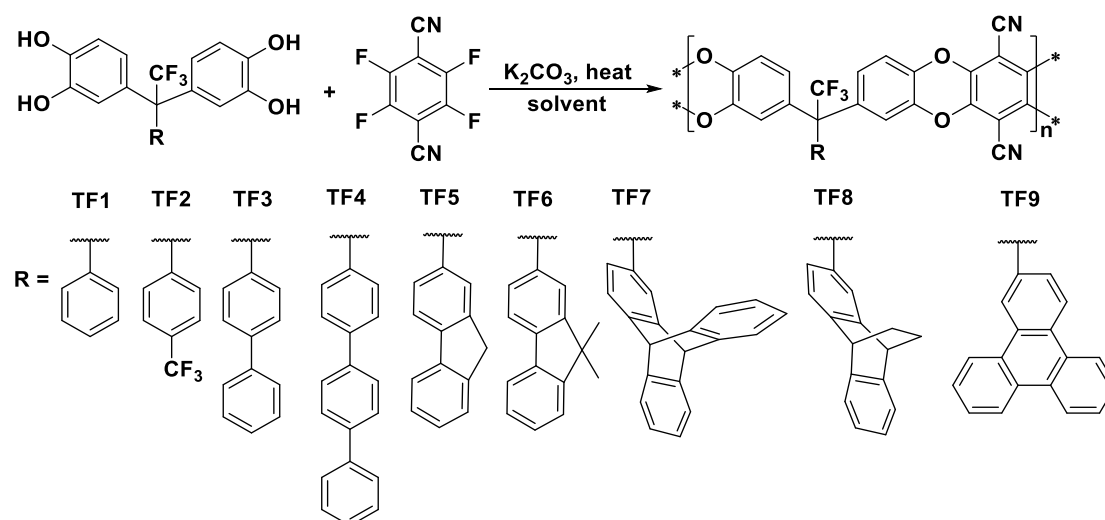


Fig 4.3.2: Nitrogen adsorption isotherms at 77 K for PIM-BDA

4.4: Synthesis of Polymers Containing CF₃ (PIM-TF 1-9)

The trifluoromethyl group (CF₃) is electron-withdrawing and is used to lower the basicity of organic compounds or to give distinctive solvation properties.¹⁹⁹ Fluorinated polymers showed distinctive characteristics such as low intramolecular and intermolecular interactions, hence leading to low cohesive energy and to lower density. They also show a higher thermal stability and are not chemically reactive.²⁰⁰ The first polybenzodioxin polymer containing CF₃ was synthesised by Du *et al.* and showed good physical properties such as high molecular weight and good solubility but with lower gas permeability and higher selectivity than PIM-1.¹³¹ Therefore, we decided to make a range of CF₃ containing polymers with different pendant groups from the monomers described in Chapter Three (Scheme 4.4.1, Table 4.4.2).



Scheme 4.4.1: Synthesis of PIM-TF

Table 4.4.2: shown the BET surface area, GPC, TGA and film formation of PIM-TF (1-9)

PIM-TF	BET Analysis		GPC			TGA	Film Formation
	BET Surface area (m ² g ⁻¹)	Pore Volume (cm ³ g ⁻¹) at (P/Po 0.98)	Mw	Mn	Mw/Mn (PDI)	T _{DEC} (°C)	
PIM-TF1	456	0.37	13000	6200	2.1	461	Brittle
PIM-TF2	20	0.08	2500	1200	2.1	416	No
PIM-TF3	20	0.08	3500	1200	3.0	365	No
PIM-TF4	20	0.03	2900	1500	2.0	335	No
PIM-TF5	565	0.56	-	-	-	370	Insoluble
PIM-TF6	120	0.17	1660	1000	1.7	309	No
PIM-TF7	30	0.16	1100	600	1.8	350	No
PIM-TF8	400	0.34	17000	8900	1.9	278	Brittle
PIM-TF9	405	0.35	-	-	-	438	Insoluble

As reported in Table 4a and from the N₂ adsorption isotherms (Fig 4.4.3), polymers PIM-TF1, PIM-TF5, PIM-TF8 and PIM-TF9 show BET surfaces areas which were equal to or higher than 400 m²/g with typical Type I isotherm²⁰¹ but these values are lower than that of PIM-1. The other polymers displayed low porosity in which the BET surfaces area were between 20 - 120 m²/g. This can be attributed to rotation of pendant groups, in addition to the single bonds linking the phenyl groups to the carbon containing the CF₃ group. It could also be due to the

CF₃ group filling the pore volume, reducing the fractional free volume (FFV).¹³¹ The GPC result of these polymers showed very different values, except for where PIM-TF5 and PIM-TF9 which were completely insoluble in any common solvent possibly due to cross-linking or strong cohesive forces between the pendant groups (fluorenyl and terphenyl), while PIM-TF2, PIM-TF3, PIM-TF4, PIM-TF6 and PIM-TF7 showed molecular weight lower than 4000 g/mol. Both PIM-TF1 and PIM-TF8 showed a higher molecular weight compared to the rest of the polymers. Unfortunately, PIM-TF1 and PIM-TF8 formed only a brittle film, which did not resist the gas permeation measurement. The TGA result of these polymers showed thermal stability above 300 °C except PIM-TF8 where the initial weight loss due to thermal degradation commences at ~ 278 °C with a 4% decrease in mass consistent with the loss of an ethylene fragment from the ethanoanthracene unit via a retro Diels-Alder reaction.²⁰²

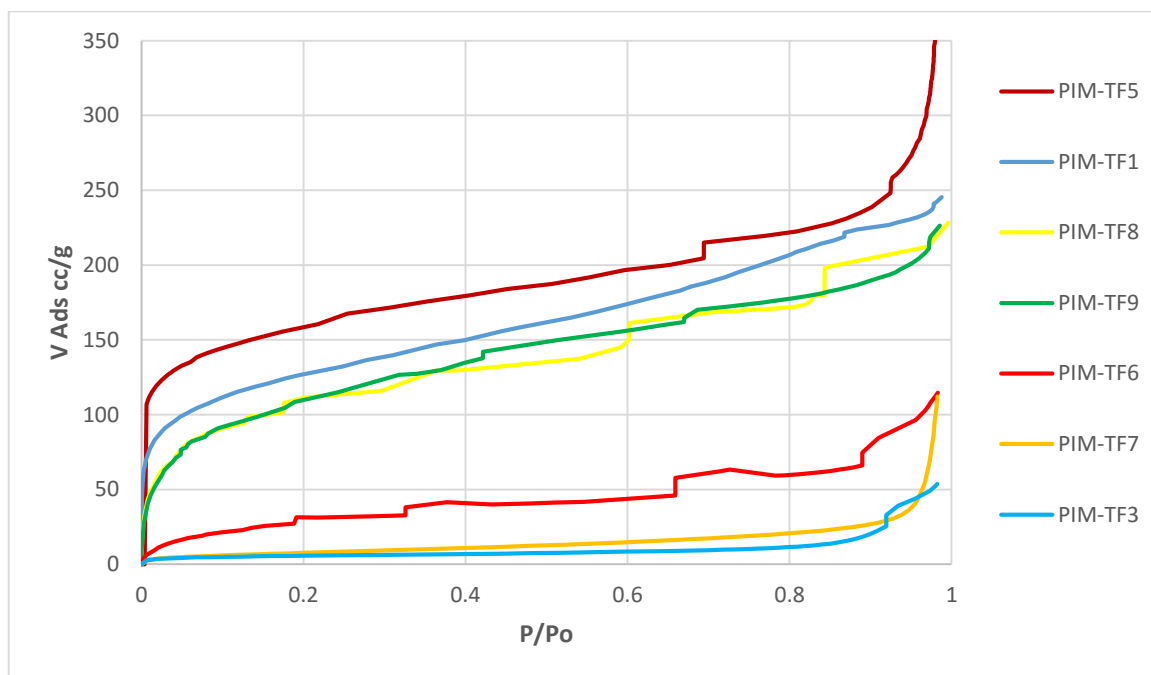
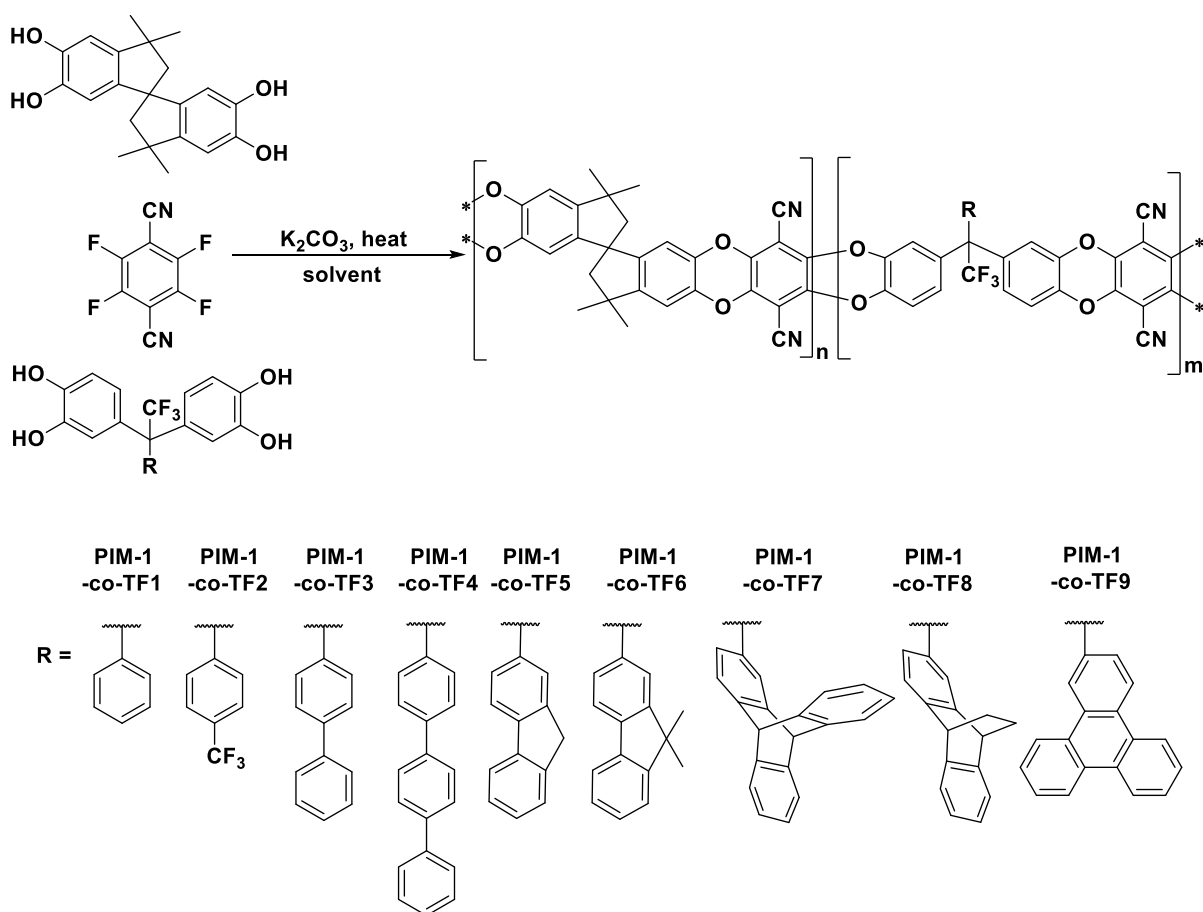


Fig 4.4.3: Nitrogen adsorption isotherms at 77 K for some PIM-TF

4.5: Synthesis of co-polymers containing CF₃ with PIM-1 (PIM-1-co-TF(1-9))

A series of PIM copolymer was synthesised in 2008 by Du *et al.* which used different ratios of monomers from 5,5',6,6'-tetrahydroxy-3,3,3'3'-tetramethyl-1,1'-spirobisindane, heptafluoro-*p*-tolylphenylsulfone (HFTPS) and tetrafluoroterephthalonitrile. The result of the copolymerisations were higher molecular weight polymers which demonstrated high

selectivity of gases compared to PIM-1.¹³¹ Since that time several PIM copolymers were reported.⁹⁹ Since it was not possible to form films from the polymers described in the previous section, we decided to synthesise copolymers in an attempt to make materials with higher molecular weight. The ratio of these copolymers were (50-50) of 5,5',6,6'-tetrahydroxy-3,3,3'-tetramethyl-1,1'-spirobisindane to monomers TF (1-9) with double the ratio of tetrafluoroterephthalonitrile (scheme 4.5.1).



Scheme 4.5.1: Synthesis of PIM-1-co-TF (1-9)

Table 4.5.2: shown the BET surface area, GPC, TGA and film formation of PIM-1-co-TF(1-9)

PIM-1-co-TF (1-9)	BET Analysis		GPC			TGA	Film Formation
Polymer	BET Surface area (m² g⁻¹)	Pore Volume (cm³ g⁻¹)	Mw	Mn	Mw/ Mn (PDI)	T_{DEC} (°C)	
PIM-1-co-TF1	600	0.45	66000	35000	1.9	452	Yes
PIM-1-co-TF2	505	0.35	4270	3340	1.3	452	Brittle
PIM-1-co-TF3	660	0.51	61000	30000	2.0	427	Yes
PIM-1-co-TF4	460	0.35	4800	2800	1.7	443	No
PIM-1-co-TF5	700	0.55	-	-	-	450	Insoluble
PIM-1-co-TF6	500	0.37	4000	2000	2.0	433	No
PIM-1-co-TF7	572	0.42	5000	2100	2.4	370	No
PIM-1-co-TF8	583	0.43	20000	12000	1.6	275	Brittle
PIM-1-co-TF9	452	0.35	-	-	-	433	Insoluble

The polymerisation yielded yellow powders in a range of 55-95%. All copolymers show microporosity with the BET surface area in the range of 452-700 m²/g (Fig 4.5.3) with a typical type I isotherm²⁰¹ but with values lower than that of PIM-1. The spirobisindane unit in PIM-1 induced high free volume which increased the BET surface area.²⁰³ Unfortunately, it appears that the free rotation in the novel monomeric units and the CF₃ group in these co-polymers combine to reduce free volume. Similar to the homopolymers PIM-TF5 and PIM-9, the copolymers PIM-1-co-TF5 and PIM-1-co-TF9 were completely insoluble in any common organic solvent. The GPC results of the soluble polymers showed different values with PIM-1-co-TF2, PIM-1-co-TF4, PIM-1-co-TF6 and PIM-1-co-TF7 giving low molecular weight (<5100 g/mol) that might be attributed to lower reactivity of the CF₃ monomers. PIM-1-co-TF1 and PIM-1-co-TF3 successfully formed films and were tested for permeability. Unfortunately, PIM-1-co-TF8 formed a film but it proved brittle after it was completely dried after solvent casting. The TGA result of these polymers similar thermal stability to that of PIM-1⁹⁹ (>350 °C) except for PIM-1-co-TF8 which showed initial weight loss to ethylene fragment to ethanoanthracene unit at ~ 275 °C.

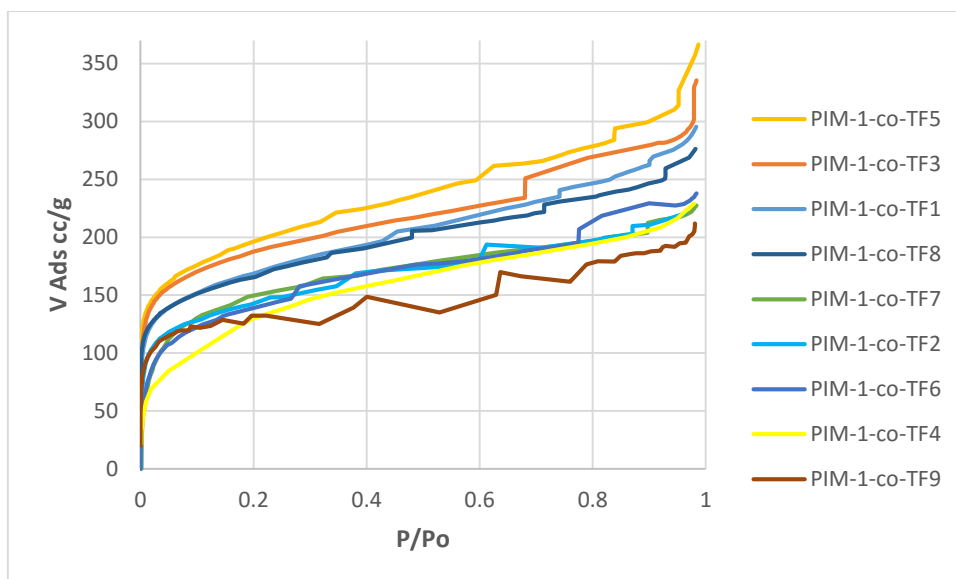


Fig 4.5.3: Nitrogen adsorption isotherms at 77 K for PIM-1-co-TF(1-9)

Although PIM-1-co-TF1 and PIM-1-co-TF3 formed films, PIM-1-co-TF3 did not resist methanol treatment and so methanol treated values could not be measured.

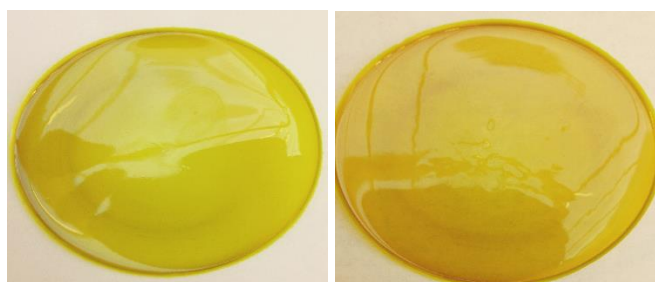
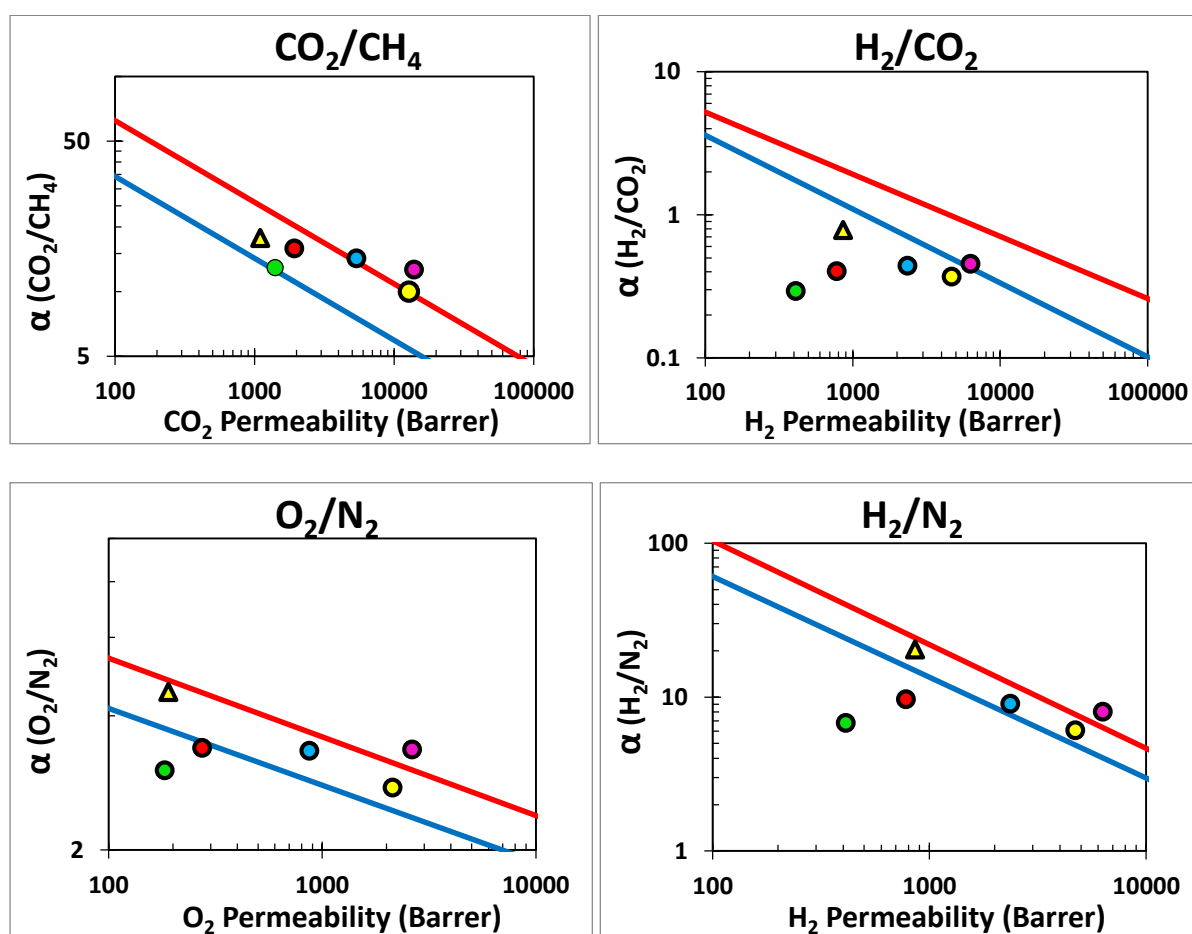


Fig 4.5.4: Films of PIM-1-co-TF1(left) and PIM-1-co-TF3 (right)

Table 4.5.5: polybenzodioxane membrane permeability measurements

Transport parameter	Membranes	Thickness	N ₂	O ₂	CO ₂	CH ₄	H ₂	He
P_x [Barrer]	PIM-1-co-TF1	66 μ m As Cast	80.8	274	1879	122	781	412
	PIM-1-co-TF3	167 μ m As cast	60.6	179	1350	108	412	224
	PIM-1-co-TF1	70 μ m MeOH	261	871	5381	378	2363	1061
$\alpha(P_x/PN_2)$	PIM-1-co-TF1	66 μ m As Cast	-	3.4	23.26	1.5	9.67	5.1
	PIM-1-co-TF3	167 μ m As cast	-	2.95	22.28	1.79	6.80	3.70
	PIM-1-co-TF1	70 μ m MeOH	-	3.34	20.62	1.45	9.05	4.07

The order of gas permeabilities for all samples was ($\text{CO}_2 > \text{H}_2 > \text{He} > \text{O}_2 > \text{N}_2 > \text{CH}_4$) which is consistent with PIM-7¹³² but different of that of PIM-1 and PIM-SBF where $\text{O}_2 > \text{He}$ which can be attributed to the presence of the CF_3 group which increased the selectivity of the polymer. Interestingly, fluorinated polymers are noted for their high He permeability and selectivity.¹⁸⁵ The results for PIM-1-co-TF1 and PIM-1-co-TF3 show high selectivity and almost reached the Robeson 2008 upper bound for several gases (CO_2/CH_4 , O_2/N_2 , H_2/N_2 , H_2/CH_4) also the rest of the results were between the 1991 and 2008 upper bounds and are comparable with most spirobisindane/benzodioxin-based PIMs but inferior to the more rigid spirobifluorene-based PIMs (e.g. PIM-SBF).¹³⁵



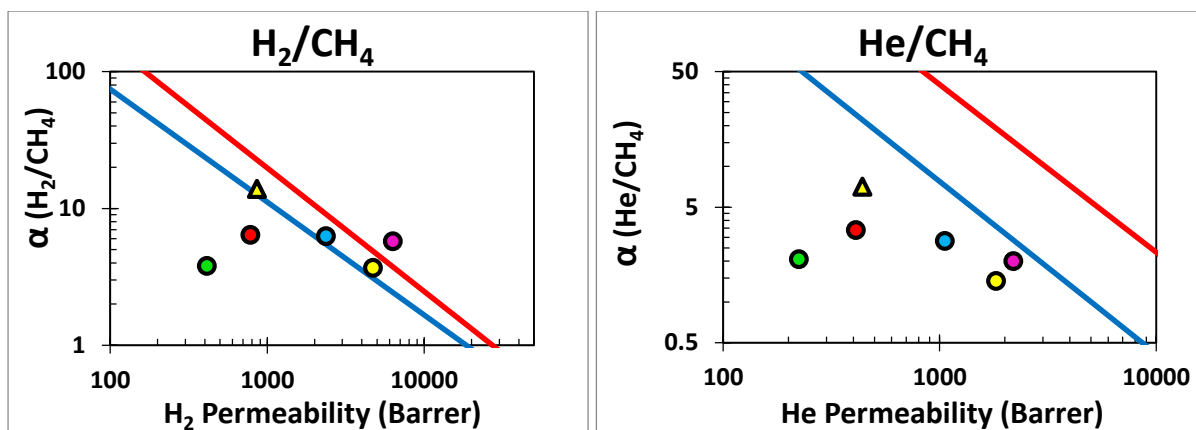
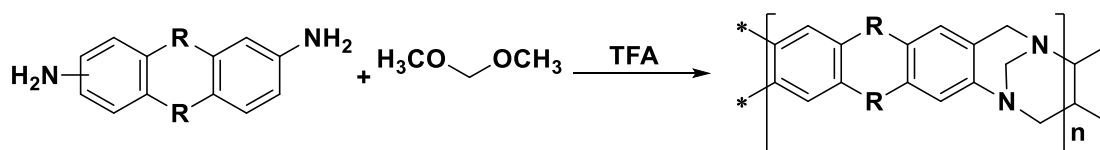


Fig 4.5.6: Robeson plots of selected gas pairs for PIM-1-co-TF1 as cast, PIM-1-co-TF1 MeOH and PIM-1-co-TF3 with 1991 (—) and 2008 (—) upper bounds: PIM-1-co-TF1 MeOH (●), PIM-1-co-TF1 as cast (●) and PIM-1-co-TF3 as cast (●) compared to PIM-1 (●), PIM-7 (▲) and PIM-SBF (●).

Chapter Five: Tröger Base Polymers

5.1: Introduction to Tröger Base polymers

In 2010 a patent from M. Carta *et. al*¹⁵⁰ described the synthesis of a new kind of PIM based on Tröger base formation from dianiline monomers (Scheme 5.1: synthesis of PIM-TB polymer).

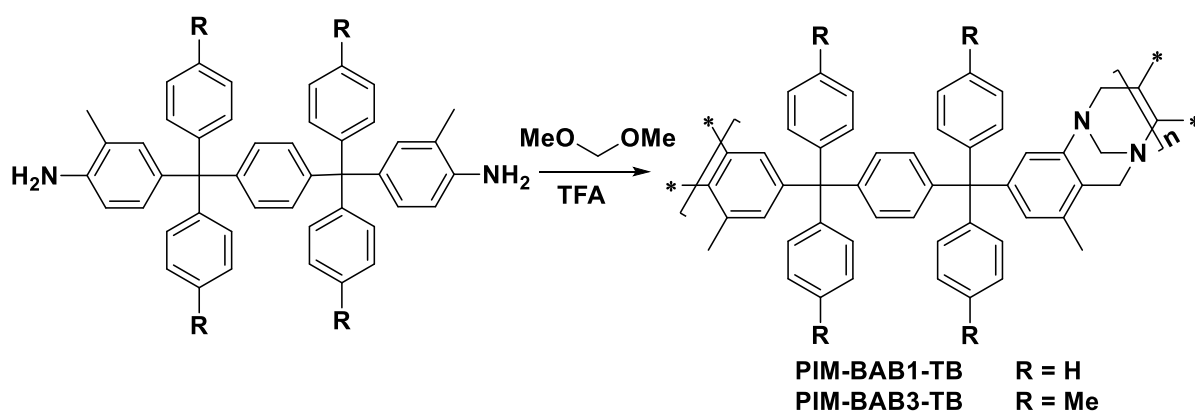


Scheme 5.1: synthesis of PIM-TB polymer

The goal of research described in this chapter is the exploitation of this efficient polymerisation reaction to prepare PIM-TB polymers, for which only a single type of synthetic monomer (containing two or more amino groups) is required, with the linking group formed from a "methylene" source, usually dimethoxymethane (DMM) in a strongly acidic solvent such as trifluoroacetic acid (TFA). In this chapter fifteen novel polymers are reported from using this methodology.

5.2: Synthesis of PIM-BAB1-TB and PIM-BAB3-TB

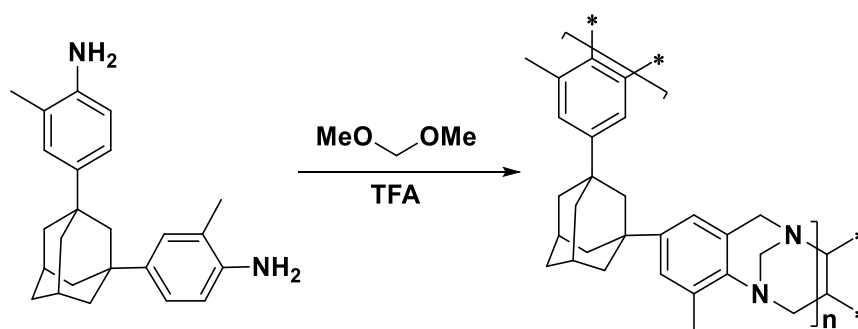
The monomers BAB1 (24) and BAB3(25) were only partially soluble in the DMM and TFA polymerisation mixture so DCM was used as a solvent. The polymerisation of BAB1 and BAB3 yielded off-white powders in yields of 76 and 83%, respectively. Unfortunately, the polymers (Scheme 5.2) did not form films due to their low molecular weight as confirmed by GPC measurements (Table 5.3.2). The values for BET surface area of PIM-BAB1-TB and PIM-BAB3-TB obtained by nitrogen adsorption at 77 K were low (Table 5.3), perhaps due to rotation of the single bonds linking the phenyl groups within the monomeric units. TGA results shows the stability of polymers up to 300 °C.



Scheme 5.2: synthesis of PIM-BAB1-TB and PIM-BAB3-TB

5.3: Synthesis of PIM-AD2-TB

In 2014, M. Carta *et. al*²⁰⁴ reported TB cardo-polymers based on 2,2-substituted adamantane. Therefore, an interesting target was to prepare a polymer based 1,3-disubstituted adamantane for comparison. PIM-AD2-TB was synthesised in 70% yield from the TB polymerisation of 1,3-bis(3-methyl-4-aminophenyl)adamantane (AD2) at a concentration of 25 ml of TFA per gram of monomer over 72 h (Scheme 5.3.2) using DCM as a solvent to afford a pale yellow powder. The excess of TFA helped to increase the monomer solubility within the polymerisation mixture. Unfortunately, GPC results showed only low molecular weight polymer had been prepared. BET surface area results show a low value that can be attributed to the free rotation of phenyl groups about the adamantyl group. TGA results show stability of polymer up to 325 °C (table 5.3).



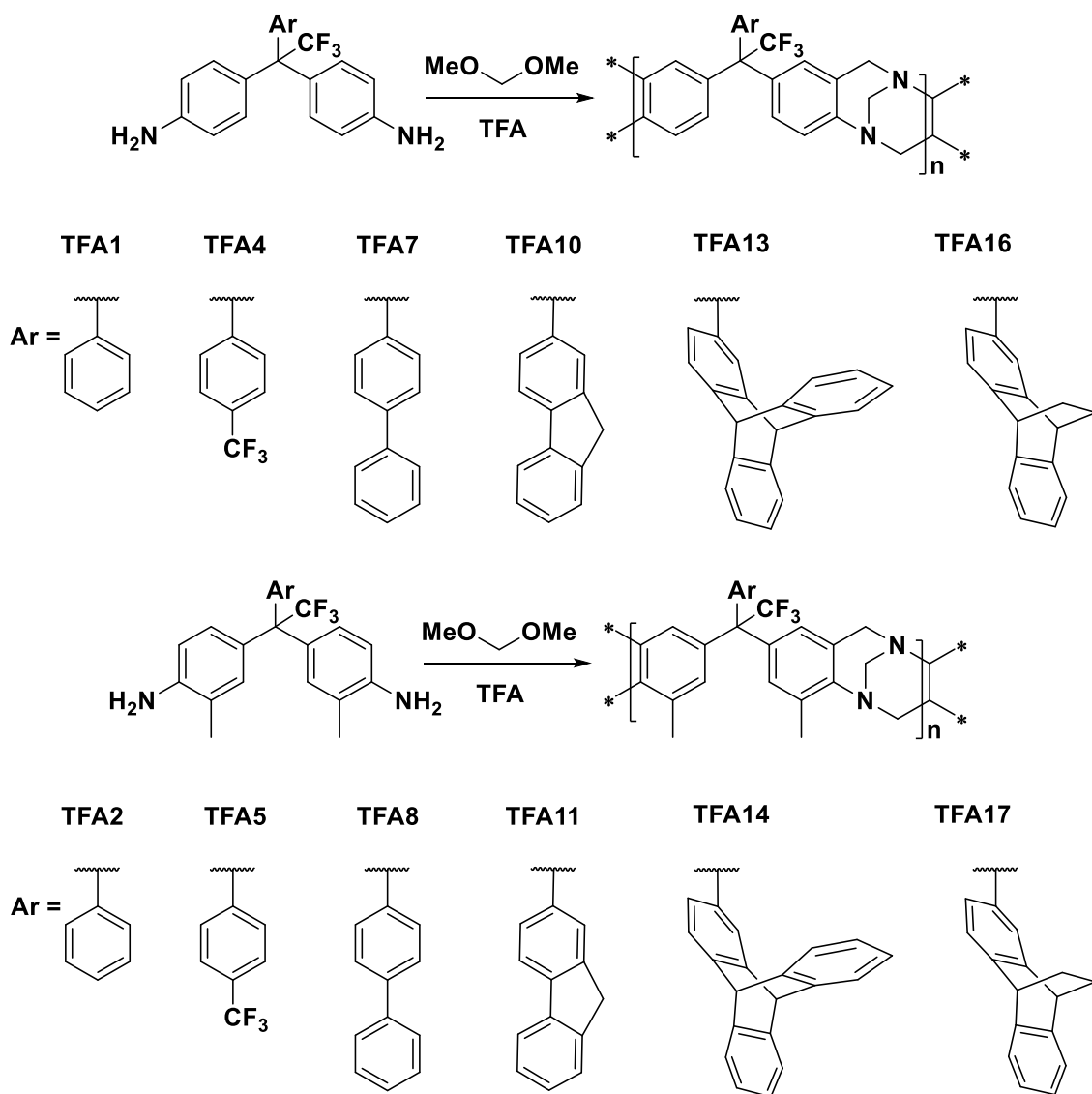
Scheme 5.3.1: synthesis of PIM-AD2-TB

Table 5.3.2: shown the BET surface area of TB polymer with thermal stability and film formation

Polymer	BET Analysis		GPC			TGA	Film Formation
	BET Surface area (m ² g ⁻¹)	Pore Volume (cm ³ g ⁻¹)	Mw	Mn	Mw/Mn (PDI)	T _{DEC} (°C)	
PIM-BAB1-TB	40	0.09	19400	11400	1.7	390	No
PIM-BAB3-TB	22	0.04	5500	3500	1.6	325	No
PIM-AD2-TB	30	0.09	2500	1350	1.9	360	No

5.4: Synthesis of TB Polymers Containing CF₃ (PIM-TFA-TB)

Twelve TB polymers all possessing the -CF₃ substituent were synthesised from specially prepared diamines (Chapter 3) by reaction with DMM in TFA. It was decided to prepare polymers from monomers in which the aniline had either H or CH₃ next to the amino group in order to assess the effect of the CH₃ on the physical properties of the polymer, especially microporosity and the film forming properties. The polymers were prepared as light brown to off-white powders with yields between 55-91% (Scheme 5.4.1, Table 5.4.2). The N₂ adsorption isotherms (Fig 5.4.3) of these polymers allow BET surfaces areas to be calculated which were in the range 24-510 m²/g. The polymers that have a methyl group next to the TB unit have much higher BET surface areas compared to those without. This can be attributed to methyl groups pushing chains apart thus creating higher free volume. Other structural factors appeared less important, for example, the extra CF₃ group on PIM-TFA4-TB and PIM-TFA5-TB appears to provide a small increase in the BET surface area. The extra phenyl group on PIM-TFA7-TB and PIM-TFA8-TB appears to decrease the apparent surface area as compared to PIM-TFA2-TB possibly due to the increased free rotation of the phenyl group along with its pore-filling effect. However, the steric bulk of the fluorene, triptycene and ethanoanthracene units on PIM-TFA11-TB, PIM-TFA14-TB and PIM-TFA17-TB appear to generate higher intrinsic microporosity. Unfortunately, none of these polymers made a film suitable for gas permeation measurements. The TGA result of these polymers showed thermal stability above 300 °C except PIM-TFA16-TB and PIM-TFA17-TB where the initial weight loss due to thermal degradation commences at ~ 280 and 290 °C with a 6 and 5% respectively, decrease in mass consistent with the loss of an ethylene fragment from the ethanoanthracene unit via a retro Diels-Alder reaction.²⁰²



Scheme 5.4.1: synthesis of PIM-TFA-TB

Table 5.4.2: shown the BET surface area of TB polymer with thermal stability and film formation.

PIM-TFA-TB	BET Analysis		GPC			TGA	Film Formation
	BET Surface area (m ² g ⁻¹)	Pore Volume (cm ³ g ⁻¹)	Mw	Mn	Mw/Mn (PDI)	T _{DEC} (°C)	
PIM-TFA1-TB	38	0.13	---	---	---	325	part soluble
PIM-TFA2-TB	220	0.30	30000	16500	1.8	353	Yes but brittle
PIM-TFA4-TB	255	0.31	5000	2100	2.4	362	No
PIM-TFA5-TB	377	0.24	6300	3000	2.1	375	No
PIM-TFA7-TB	30	0.08	7000	4050	1.7	325	No
PIM-TFA8-TB	70	0.31	29000	12600	2.3	387	Yes but brittle
PIM-TFA10-TB	24	0.06	----	----	-----	308	part soluble
PIM-TFA11-TB	381	0.40	48000	20000	2.4	369	Yes but brittle
PIM-TFA13-TB	70	0.23	----	----	----	348	part soluble
PIM-TFA14-TB	510	0.23	5000	2900	1.7	364	No
PIM-TFA16-TB	90	0.23	8500	5000	1.7	280	No
PIM-TFA17-TB	445	0.59	10000	6500	1.5	290	No

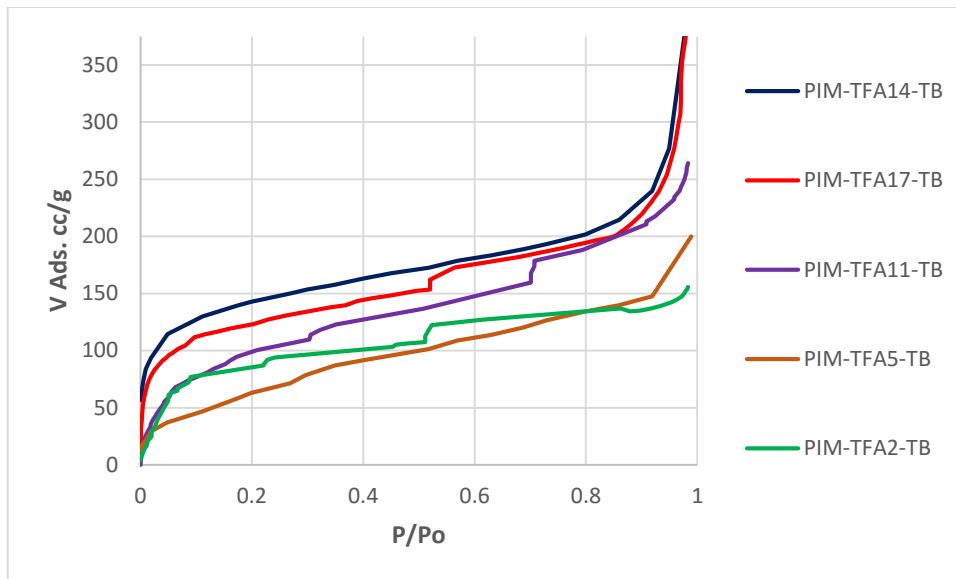
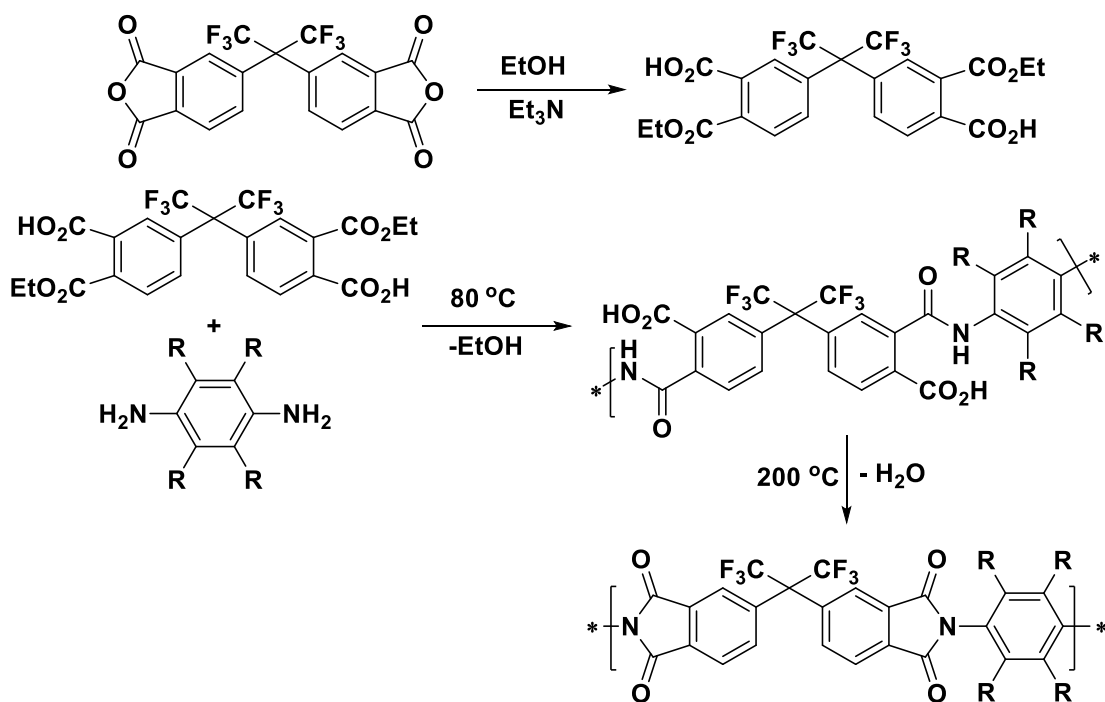


Fig 5.3.3: Nitrogen adsorption isotherms at 77 K of some PIM-TFA-TB

Chapter Six: Polyimides

6.1: Introduction to polyimides

Several polyimides were prepared from aromatic amines with the commercially available 4,4'-(hexafluoroisopropylidene)diphthalic anhydride (6FDA). The principal reason why 6FDA has been frequently used for making polyimides is because the $-\text{C}(\text{CF}_3)_2-$ group increases chain stiffness, which in turn increases free volume, thus providing polyimides with a good balance between permeability and selectivity.^{205, 206} Polyimides are classically synthesised by a cycloimidisation polycondensation reaction between a dianhydride and diamine monomer. The synthesis of the polyimides described in this thesis were performed via an ester acid intermediate compound, the production of which is described in literature.²⁰⁷ It typically affords high molecular weight and soluble polyimides with a high degree of imidisation. This procedure (Scheme 6.1.1) first involves conversion of the dianhydride monomer to a diester-diacid by refluxing it in ethanol in the presence of trimethylamine as a base. After one hour the residual ethanol and triethylamine are then removed under heat by evaporation, to leave a highly viscous liquid. At this point, the diamine monomer is added as a solution in 1-methyl-2-pyrrolidone (NMP) as solvent. The mixture of the diamine, diester-diacid and NMP are reacted under a nitrogen atmosphere at a low temperature (80 °C) for one hour to form a polyamic acid as an intermediate polymer. The mixture is then heated gently to 200 °C and the water produced during the imidisation reaction is left to evaporate helped by a gentle nitrogen gas flow. The mixture is left for 24-72 hours and then purified by reprecipitation from a good solvent into a poor solvent.



Scheme 6.1.1: Synthesis of polyimides using the ester acid route

All polyimide structures were confirmed by ¹H and ¹³C NMR. In addition, solid state FTIR showed the typical peaks assigned to polyimides, such as 1786 (C=O asymm), 1724 (C=O symm), ~1368 (C-N stretch) cm⁻¹. Importantly, the absence of the polyamic acid, is indicated by the lack of typical peaks, such as ~2700 (OH stretch), as reported.^{208, 209} In figure 6.1.2 is reported the overlay of the two structures, the monomer (e.g. TFA-12, red) and the resulting polyimide (black).

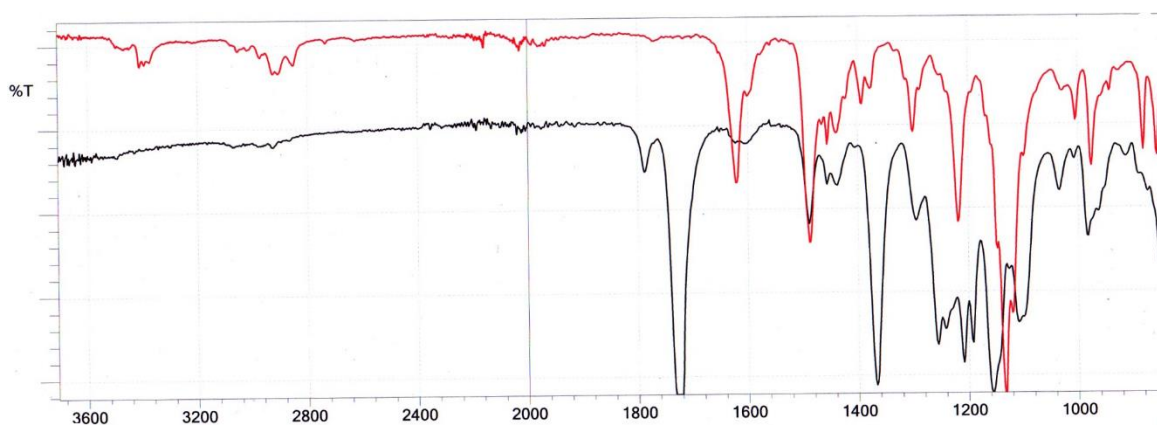
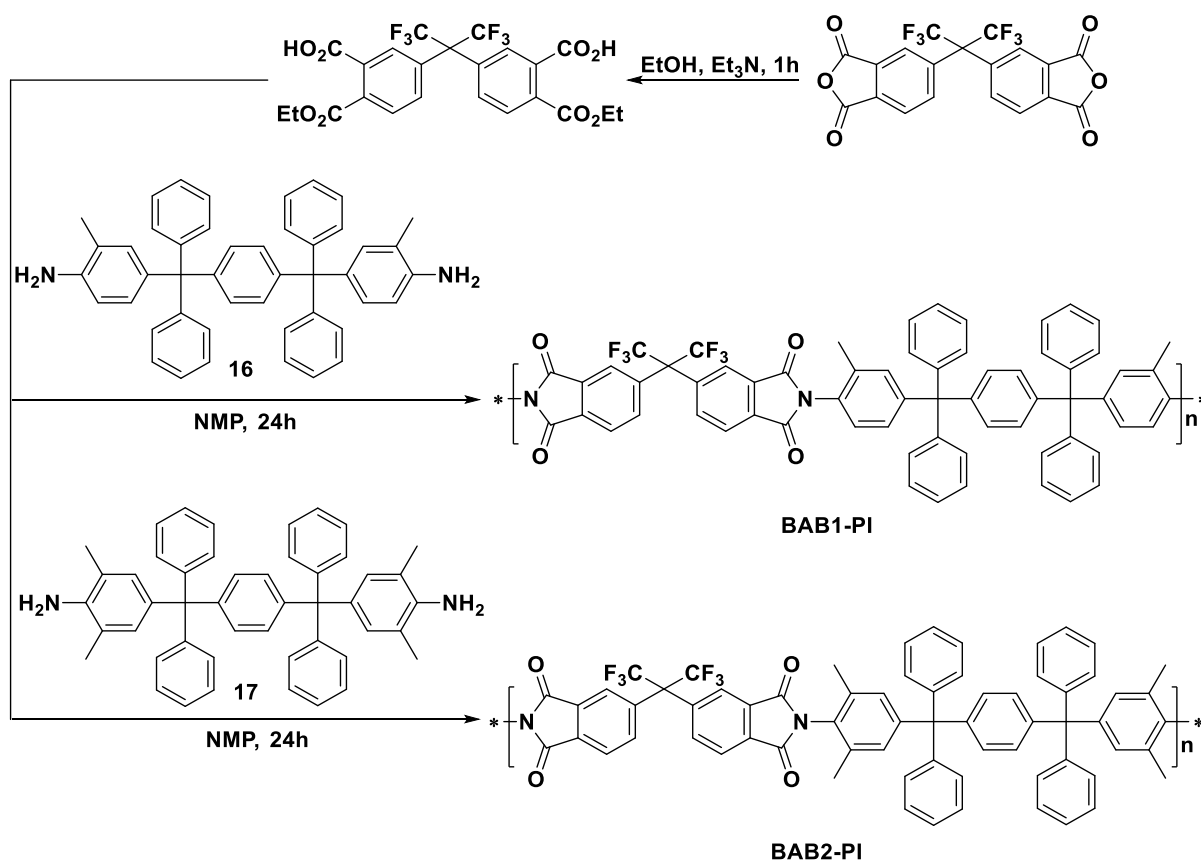


Fig 6.1.2: FTIR of monomer TFA12 (red) and polyimide PIM-TFA12-PI (black)

6.2: The Synthesis of BAB1-PI and BAB2-PI

Two polyimides BAB1-PI and BAB2-PI were synthesised, again using 6FDA as a co-monomer, with yields of 37 and 38% respectively, as light brown powders. The GPC results showed low molecular mass with a range from $M_w = 17000$ to $M_w = 20200$ g/mol respectively. This disappointing result is possibly due to relatively low concentration of reactive amine functionality due to the large size of the monomer, which prohibits efficient polymerisation. Thermal gravimetric analysis (TGA) shows stability up to 420 °C and a mass loss of ~ 20% below 440 °C. Apparent BET surface area, measured by isothermal nitrogen adsorption, for BAB1-PI and BAB2-PI show values between 8 and 63 m²/g, respectively. This result is not totally unexpected, as the high free rotation around the phenyl groups, along with the free rotation around the imide ring, allows the polymer to pack efficiently in the solid state, not inducing the microporosity which is typical of PIMs.



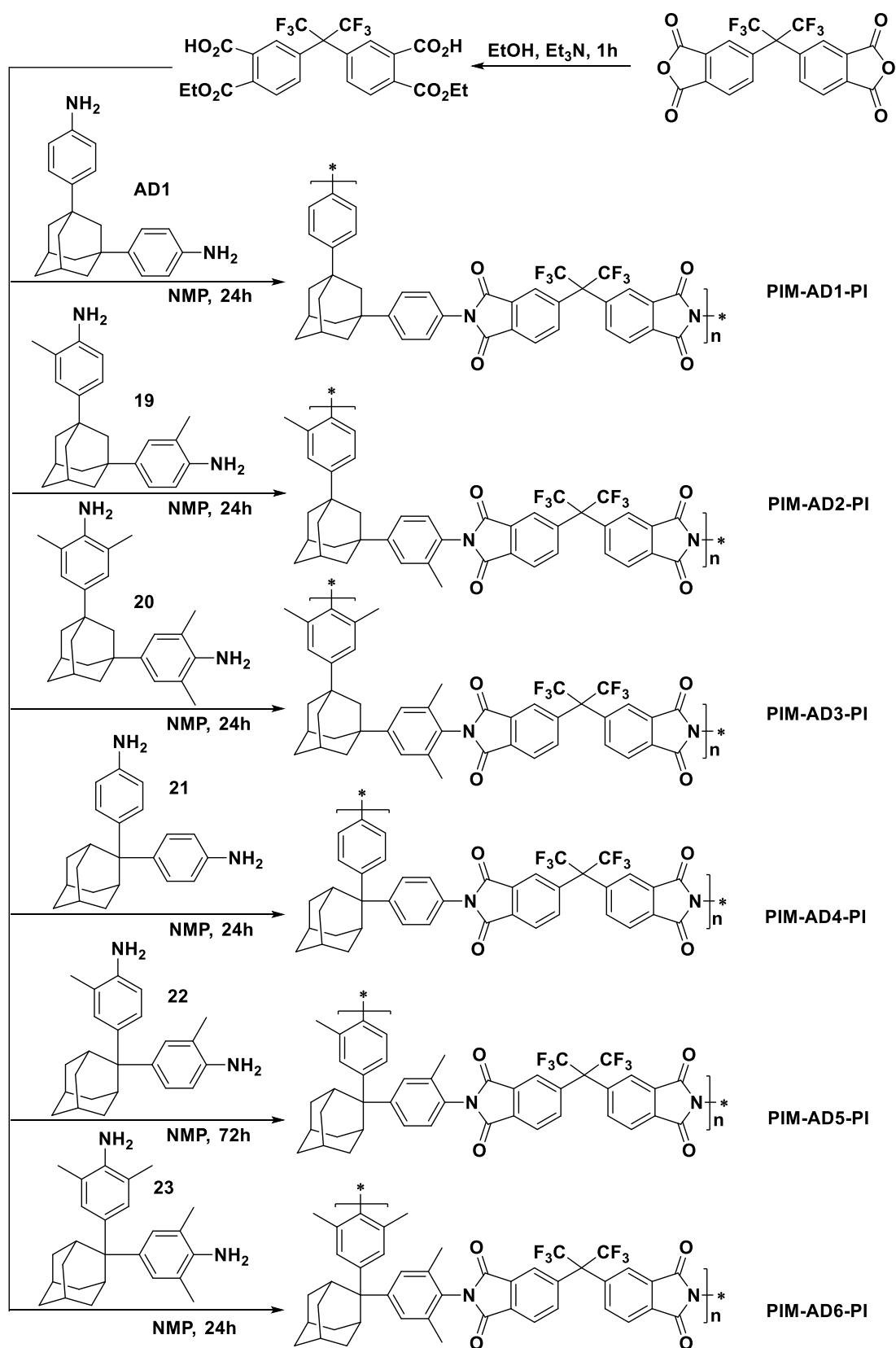
Scheme 6.2.1: Synthesis of BAB1-PI and BAB2-PI

6.3: Synthesis of Adamantane based Polyimides (PIM-AD1-6-PI)

Six polyimides containing the adamantane group were synthesised via the reaction of the corresponding monomers with 6FDA. The AD1 is a commercial monomer and PIM-AD1-PI

was synthesised following the literature procedure.²¹⁰ Although not novel, it was decided to prepare this polymer to test the reaction and for comparison with the rest of the polymers synthesised in this work. As described in Chapter 3, we prepared two different kinds of monomers: one with the 4-aminophenyl groups attached to two different carbons on the adamantyl, the second one where the 4-aminophenyl groups are connected to the same carbon adamantyl unit. The first kind of polymers resulted in a light brown powders with yields of 33, 32 and 32% (PIM-AD1-PI, PIM-AD2-PI and PIM-AD3-PI), respectively. The second monomers yielded 48, 76 and 71% (PIM-AD4-PI, PIM-AD5-PI and PIM-AD6-PI), respectively (Scheme 6.3.1).

Unfortunately, the low molecular mass of PIM-AD1-PI, PIM-AD2-PI and PIM-AD3-PI prevented the formation of robust films. They also showed low BET surface areas as compared with PIM-AD4-PI, PIM-AD5-PI and PIM-AD6-PI. Again, this is attributable to the greater freedom of rotation around the C-C bond between the adamantyl unit and the phenyl groups. In contrast, the rotation within PIM-AD6-PI is more restricted, due to the methyl groups next to the amine moiety, leading to enhanced porosity.



Scheme 6.3.1: Synthesis of PIM-AD1-PI, PIM-AD2-PI & PIM-AD3-PI

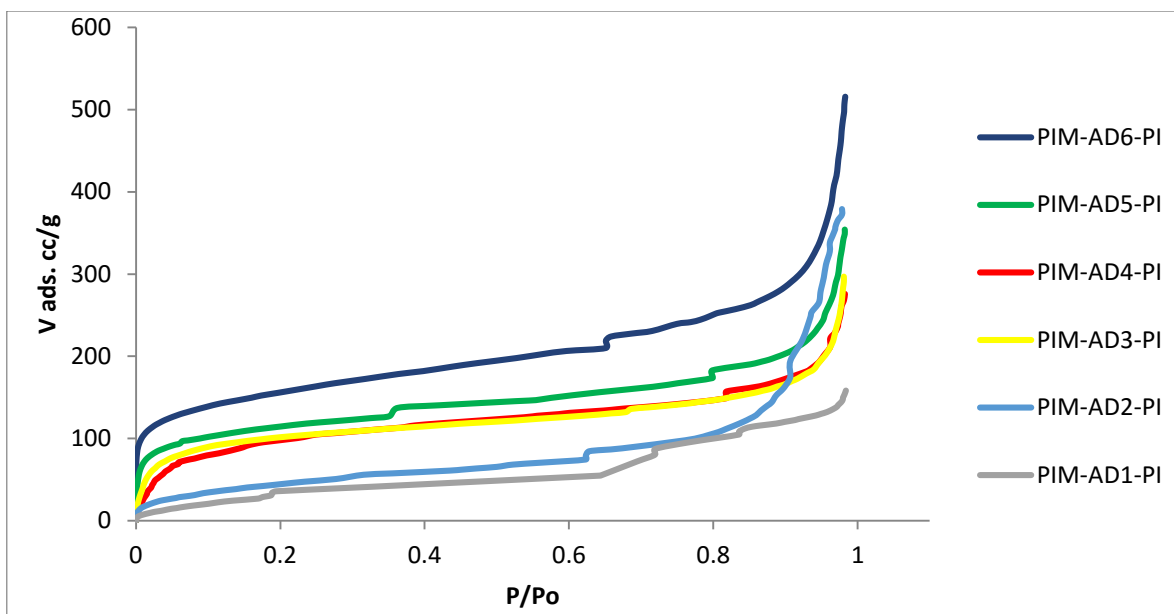


Fig 6.3.2: Nitrogen adsorption isotherms at 77 K for PIM-AD1-6-PI

Table 6.3.3: Adamantane polyimides, BET surface area, GPC, TGA and film formation.

Adamantane Polyimides	BET Analysis		GPC			TGA	Film Formation
	BET Surface area (m ² g ⁻¹)	Pore Volume (cm ³ g ⁻¹) at (P/Po 0.98)	Mw	Mn	Mw/Mn (PDI)	T _{DEC} (°C)	
PIM-AD1-PI	175	0.58	10000	4000	2.5	447	✗
PIM-AD2-PI	250	0.24	18000	5600	3.2	466	✗
PIM-AD3-PI	370	1.76	19300	6000	3.2	390	✗
PIM-AD4-PI	370	0.42	16000	9300	1.7	450	✗
PIM-AD5-PI	430	0.54	47300	23600	2.0	450	✓
PIM-AD6-PI	560	0.78	131200	62500	2.1	465	✓

From all the above PIM-AD(1-6)-PI polymers, unfortunately, only PIM-AD5-PI and PIM-AD6-PI are demonstrated a molecular mass high enough to allow the formation of a self-standing film, PIM-AD6-PI (Fig 6.3.4).

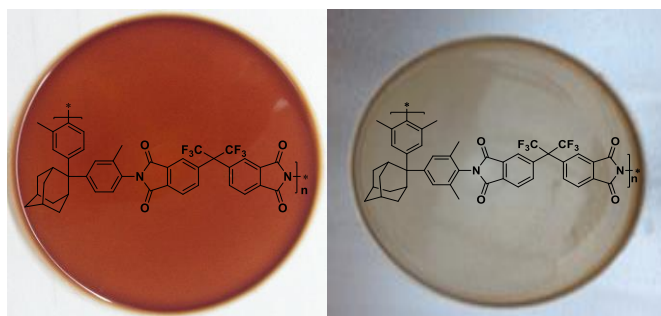


Fig 6.3.4: Film of PIM-AD5-PI (left) and PIM-AD6-PI(right)

Table 6.3.5: results of gas permeation tests after methanol treatment of PIM-AD5-PI and PIM-AD6-PI films.

Transport parameter	Membrane	N ₂	O ₂	CO ₂	CH ₄	H ₂	He
P_x [Barrer]	PIM-AD5-PI	34.5	142.7	573.0	19.3	682.0	385.2
	PIM-AD6-PI	143	451	2167	152	1582	776
$\alpha(P_x/PN_2)$	PIM-AD5-PI	-	4.14	16.61	0.56	19.77	11.17
	PIM-AD6-PI	-	3.16	15.18	1.06	11.08	5.44

In agreement with the BET surface area, the permeability for PIM-AD6-PI was higher than PIM-AD5-PI, this is consistent with effect of the two aromatic methyl groups adjacent to the imide linking bonds which restricts the free rotation as compared with PIM-AD5-PI, which has only one methyl next to the imide bond. As mentioned previously, the methanol treatment helps the complete removal of the casting solvent, increasing the permeability for all tested gases.

The order of gas permeability for PIM-AD5-PI was ($H_2 > CO_2 > He > O_2 > N_2 > CH_4$) which is similar to that of KAUST-1 reported by Pinnau *et al.*¹²¹ but it is different from the result obtained with PIM-1¹³³ and PIM-PI-EA.¹¹⁰ Indeed, for most PIMs CO₂ permeates faster than H₂, which is due to their much higher solubility coefficients that boosts the CO₂ permeability over H₂. PIM-AD5-PI, instead, shows greater molecular sieving behaviour. This is an indication that the diffusivity selectivity is more important for this polymer, facilitating the gas transport. The order of gas permeability for CO₂ and H₂ of PIM-AD6-PI was reversed indicating that polymer is more typical of that of a PIM. The high permeability of He, H₂ and O₂ PIM-AD6-PI is attributable to high diffusivity (being small gases) while the permeability of CO₂ appears to be related to its higher solubility in PIM-AD6-PI, with a compromise between molecular sieving and solution-diffusion models. In general terms, the two polymers show good results for the important H₂/CH₄ and CO₂/CH₄ gas pairs, in addition, they have been

synthesised using commercially available starting monomers (6FDA) or those readily prepared from cheap precursors. According to the Robeson¹⁸⁵ plot, the two novel polymers show the typical trade-off relationship between permeability and selectivity, with PIM-AD6-PI being more permeable but less selective, compared with PIM-AD5-PI.

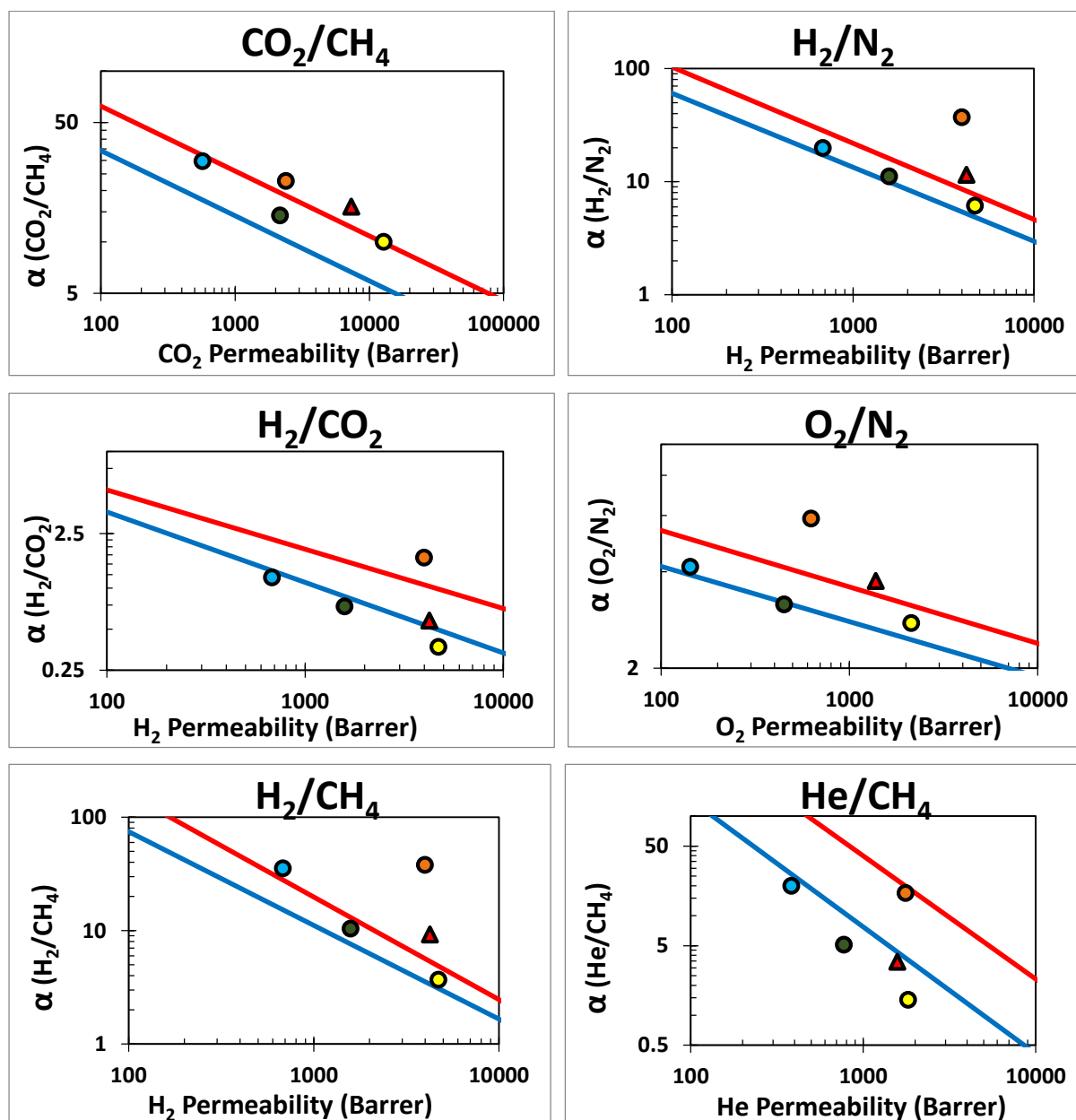
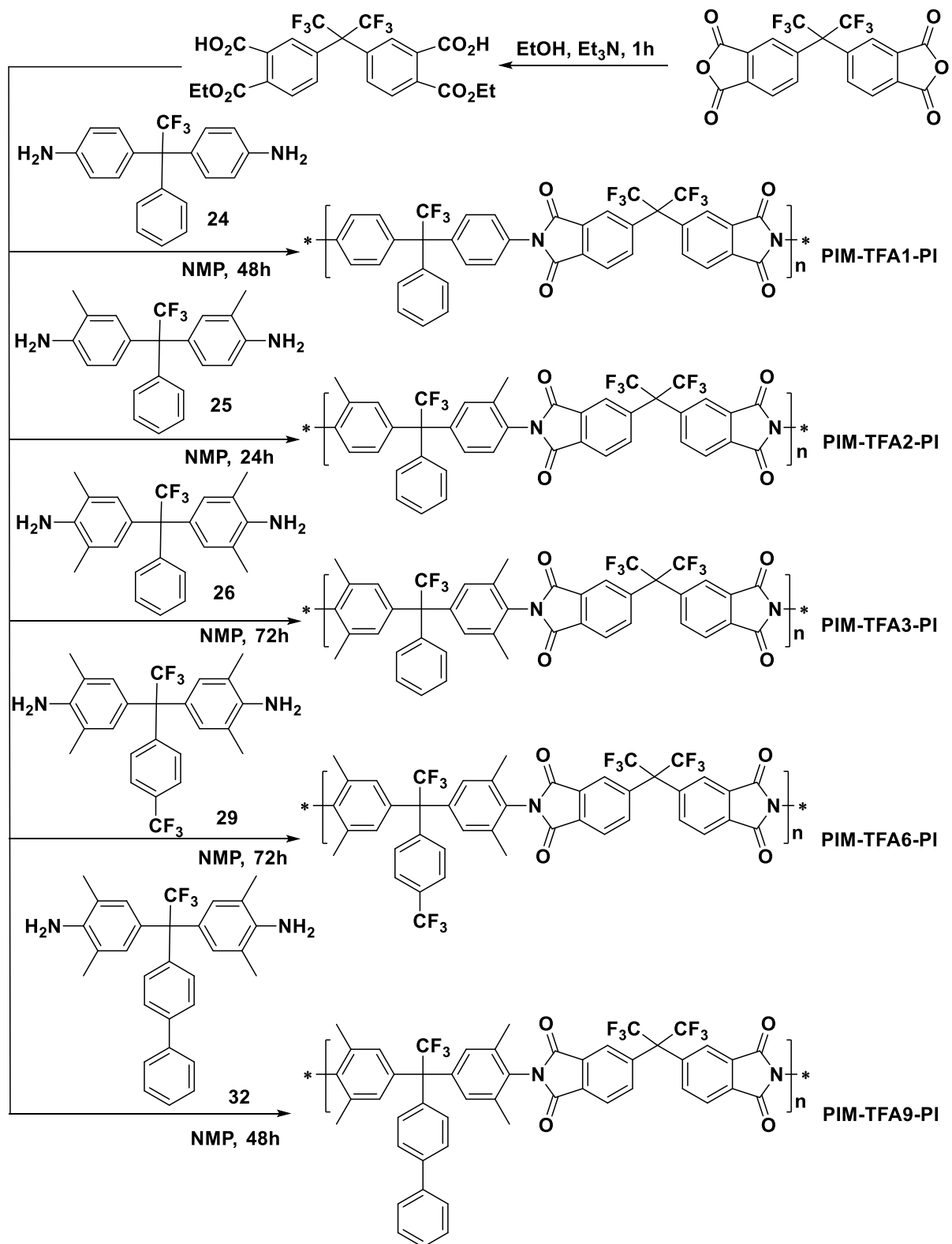


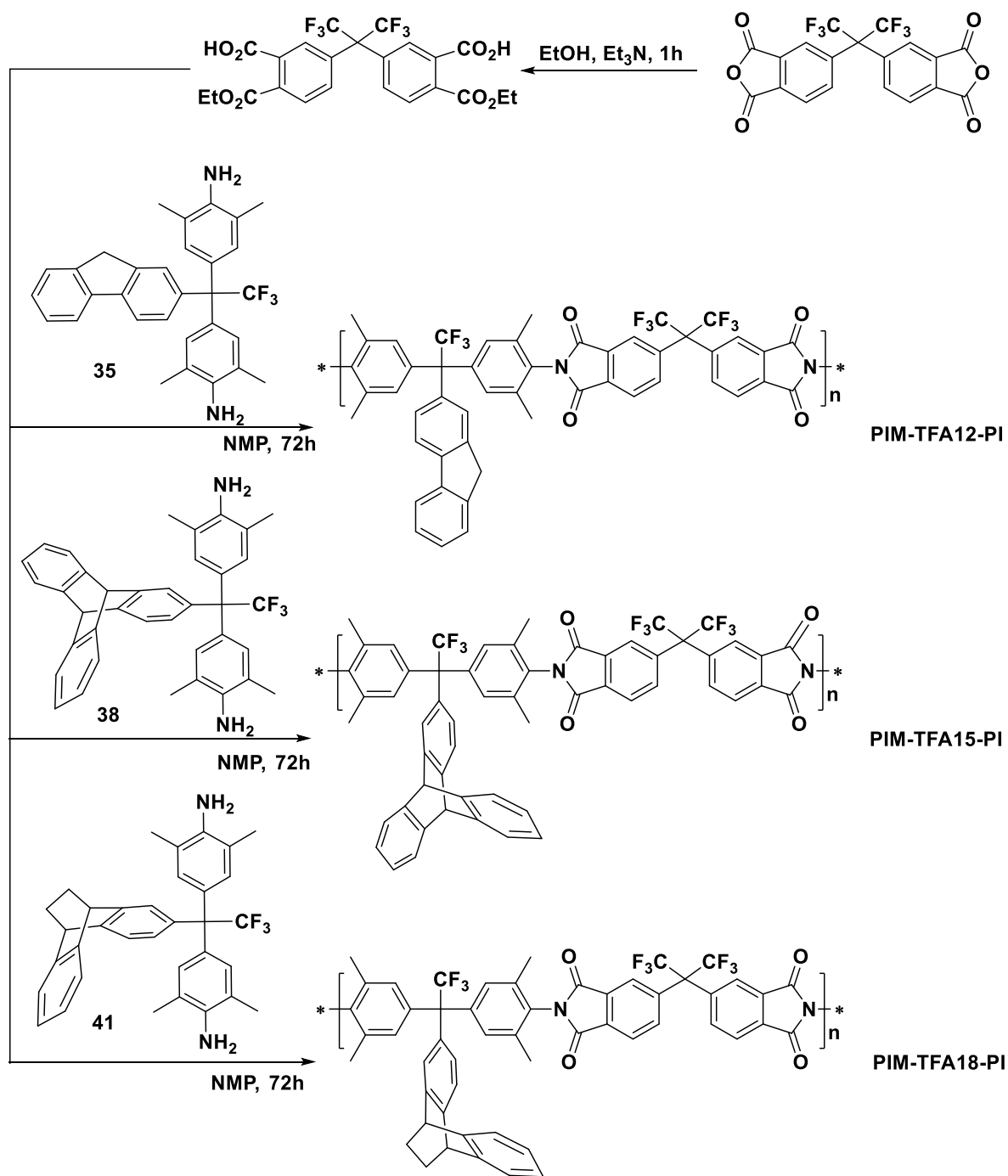
Fig 6.3.6: Robeson plots of selected gas pairs for PIM-AD-5 and PIM-AD6-PI with 1991 (—) and 2008 (—) upper bounds: PIM-AD5-PI MeOH (●) and PIM-AD6-PI MeOH (●) compared to PIM-1 (●), PIM-PI-EA (▲) and KAUST-PI-1 (●)

6.4: Synthesis of (PIM-TFA-PI) polymers

Eight PI polymers all possessing the $-CF_3$ substituents were synthesised from specially prepared diamine monomers (Chapter 3) by reaction with 6FDA dianhydride. Firstly, we decided to prepare the ones in which the aniline had different substituents next to the amino group (H, CH_3 and $2 \times CH_3$) to test how the substituents affect the physical properties of the polymer, especially microporosity and the film forming properties. The polymers were prepared as light brown powders with yields of 53, 36, 67, 83, 92, 95, 94 and 82% for PIM-TFA1-PI, PIM-TFA2-PI, PIM-TFA3-PI, PIM-TFA6-PI, PIM-TFA9-PI, PIM-TFA12-PI, PIM-TFA15-PI and PIM-TFA18-PI, respectively (Scheme 6.4.1). Thermal gravimetric analysis shows that polyimides are stable up to ~ 400 °C with all polymers showing an initial decrease in mass loss $\sim 40\%$ commencing at ~ 450 °C except for PIM-TFA18-PI which uniquely showed a loss of 5% at 275 °C due to the loss of the ethylene fragment from the ethanoanthracene unit due to a retro Diels-Alder reaction (Table 6.4.3).

BET surface areas calculated from nitrogen isotherms were dependent on the degree of substitution adjacent to the amine units on the monomer (i.e. $H < CH_3 < 2 \times CH_3$). Again, the trend observed from the BET surface areas showed that the introduction of a methyl next to the amine group increased the microporosity. Other structural factors appeared less important, for example, the extra CF_3 group on PIM-TFA6-PI, which displayed a value similar to PIM-TFA3-PI. The introduction of the extra phenyl group on PIM-TFA9-PI led to a decrease in apparent surface area as compared to PIM-TFA3-PI possibly due to the increased free rotation of the phenyl group along with its pore-filling effect. However the steric bulk of the triptycene and ethanoanthracene units on PIM-TFA15-PI and PIM-TFA18-PI do appear to generate higher intrinsic microporosity.





Scheme 6.4.1: Synthesis of PIM-TFA-PIs

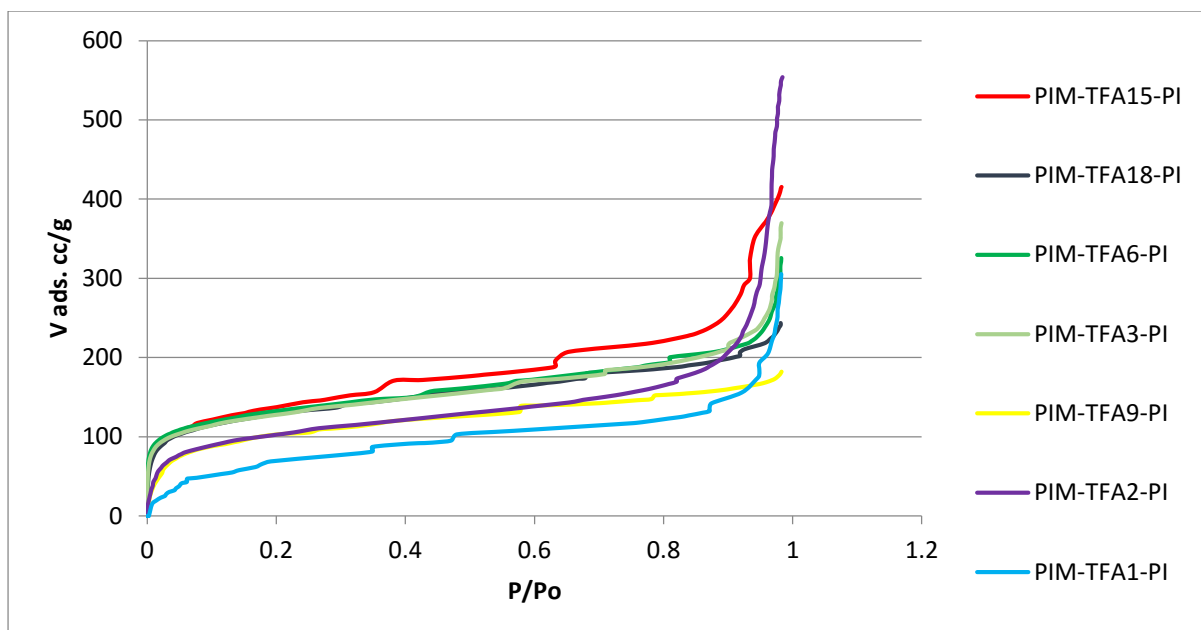


Fig 6.4.2: Nitrogen adsorption isotherm at 77 K of PIM-TFA-PI

Table 6.4.3: PIM-TFA-PI polymers, BET surface area, GPC, TGA and film formation.

PIM-TFA-PI	BET Analysis		GPC			TGA	Film Formation
	BET Surface area (m ² g ⁻¹)	Pore Volume (cm ³ g ⁻¹) at (P/Po 0.98)	Mw	Mn	Mw/Mn (PDI)	T _{DEC} (°C)	
PIM-TFA1-PI	270	0.45	68300	42300	1.6	459	✓
PIM-TFA2-PI	375	0.84	48400	28100	1.7	457	✓
PIM-TFA3-PI	460	0.56	103300	81400	1.2	462	✓
PIM-TFA6-PI	470	0.49	42500	30000	1.4	471	✓
PIM-TFA9-PI	375	0.28	77750	46000	1.7	450	✓
PIM-TFA12-PI	450	0.46	321000	203400	1.6	465	✓
PIM-TFA15-PI	500	0.37	91500	45050	2.0	474	✓
PIM-TFA18-PI	490	0.63	4300	3250	1.3	275	✗

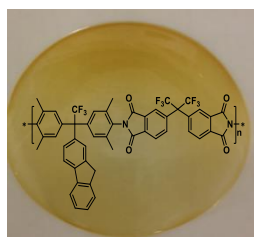


Fig 6.4.4: film of PIM-TFA12-PI

All polymers (PIM-TFA1-15-PI) formed a self-standing film except PIM-TFA18-PI which showed a very low molecular mass as measured by GPC. Despite the successful formation of the film, for PIM-TFA1-PI and PIM-TFA6-PI they did not resist methanol treatment, which typically boosts the permeability, so the results in table 6.4.5 represent only the ‘as cast’ measurement. All the synthesised PIs however, showed a good compromise between a good permeability with moderate selectivity, which is typical of PIMs.

Table 6.4.5: films permeability measurements with selectivity coefficient of PIM-TFA-PI.

Transport parameter	Membrane	N ₂	O ₂	CO ₂	CH ₄	H ₂	He
P_x [Barrer]	PIM-TFA1-PI As Cast	2.8	9.5	59.7	1.8	57.3	57.3
	PIM-TFA2-PI MeOH	13	66	327	9	355	313
	PIM-TFA3-PI MeOH	33.2	147.5	814.0	32.5	645.1	427.8
	PIM-TFA6-PI As Cast	23.2	89.1	507.3	22.3	354.6	269.0
	PIM-TFA9-PI MeOH	32	104	608	8	427	789
	PIM-TFA12-PI MeOH	42.5	170.3	948.4	39.2	759.4	467.0
	PIM-TFA15-PI MeOH	60.1	277	1215	55	946	537
$\alpha(P_x/PN_2)$	PIM-TFA1-PI As Cast	-	3.36	21.23	0.64	20.39	20.38
	PIM-TFA2-PI MeOH	-	3.21	24.66	0.66	26.69	23.60
	PIM-TFA3-PI MeOH	-	4.44	24.52	0.98	19.43	12.89
	PIM-TFA6-PI As Cast	-	3.84	21.88	0.96	15.29	11.61
	PIM-TFA9-PI MeOH	-	3.24	19.07	0.25	13.39	24.72
	PIM-TFA12-PI MeOH	-	4.01	22.32	0.92	17.87	10.99
	PIM-TFA15-PI MeOH	-	4.61	20.23	0.91	15.75	8.94

As anticipated from its apparent BET surface area, PIM-TF1-PI did not demonstrate good performance both in terms of permeability and selectivity, although its particularly low permeability is likely to be due to the measurements being made without methanol treatment, which it did not resist. In general, for polyimides, the permeability and apparent surface area, increase with number of methyl group adjacent to imides ring, for example, the permeability and selectivity of previously prepared PIM-PI-2 proved higher than PIM-PI-3.²¹¹ Similarly for the present series of polymers, the permeability and selectivity of PIM-TFA2-PI was higher than PIM-TFA1-PI but lower than PIM-TFA3-PI. The order of gas permeability of PIM-TFA1-PI ($\text{CO}_2 > \text{H}_2 > \text{He} > \text{O}_2 > \text{N}_2 > \text{CH}_4$) are similar to PIM-TF3-PI, while PIM-TF2-PI gave $\text{H}_2 > \text{CO}_2 > \text{He} > \text{O}_2 > \text{N}_2 > \text{CH}_4$. PIM-TF2-PI compensated for its lower permeability with higher selectivity, with data close to the 2008 Robeson upper bounds for the CO_2/CH_4 and H_2/CH_4 gas pairs showing that this polymer behaves as a good molecular sieving material where the permeability of H_2 is higher than CO_2 . PIM-TFA3-PI shows lower selectivity than PIM-TFA2-PI but with a higher permeability, in accordance with the Robeson trade-off, in addition the order of gas was $\text{CO}_2 > \text{H}_2 > \text{He} > \text{O}_2 > \text{N}_2 > \text{CH}_4$ showing reverse-selectivity which is typical of PIMs. Unfortunately, PIM-TFA6-PI did not resist the methanol treatment due to its lower molecular weight not allowing a full comparison with other polymers. PIM-TFA12-PI shows reverse selectivity (i.e. $\text{CO}_2 > \text{H}_2$), with results similar to PIM-TFA3-PI, but with a slightly higher permeability showing that the fluorenyl group, which is a more rigid substituent than biphenyl, enhances the permeability by increasing the free volume of the polymer. Overall the most impressive performance was demonstrated by PIM-TFA15-PI, which shows the same order of gas permeability ($\text{CO}_2 > \text{H}_2 > \text{He} > \text{O}_2 > \text{N}_2 > \text{CH}_4$) but greater values than PIM-TFA3-PI and PIM-TFA12-PI due to the structure of triptycene unit. Triptycene is highly rigid and shape persistent, with concave spaces between the aromatic rings resulting in inefficient packing and enhanced intrinsic microporosity.¹⁵⁸ This is evident also looking at Table 6.4.3 where the polymer displays the highest pore volume of the whole set. The data for PIM-TFA15-PI falls close to the 2008 Robeson upper bounds for CO_2/CH_4 , O_2/N_2 and H_2/CH_4 .

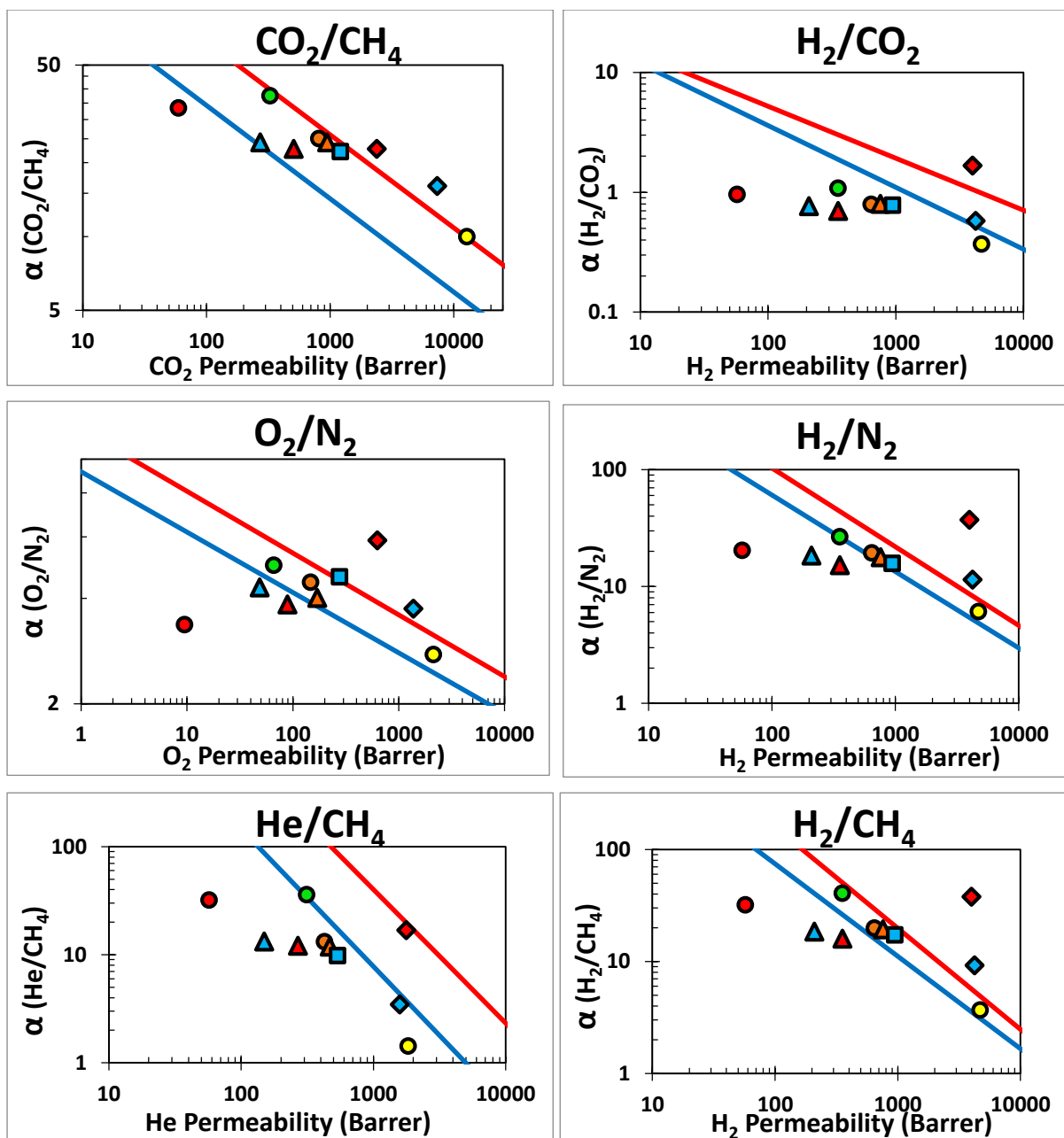


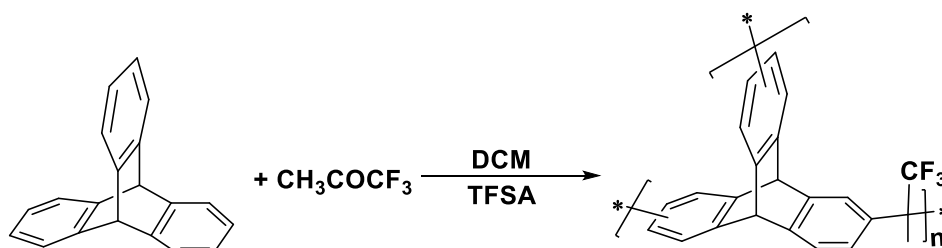
Fig 6.4.6: Robeson plots of selected gas pairs for PIM-TFA1-15-PI with 1991 (—) and 2008 (—) upper bounds: PIM-TFA1-PI as cast (●), PIM-TFA2-PI MeOH (●), PIM-TFA3-PI MeOH (●), PIM-TFA6-PI as cast (▲), PIM-TFA9-PI as cast (▲), PIM-TFA12-PI MeOH (▲) and PIM-TFA15-PI MeOH (■) compared PIM-1 (●), PIM-PI-EA (◆), KAUST-PI-1 (◆)

Chapter 7: Future work

At the end of the PhD programme the synthesis of some novel PIMs were attempted but were not completed due to lack of time and some relevant examples are reported in this chapter. In particular, we followed literature procedures^{212, 213} to make aromatic fluorinated polymers based upon polymerisation reaction in strong acid involving the addition of two aromatic rings to aryl-2,2,2-trifluoromethyl ketones.

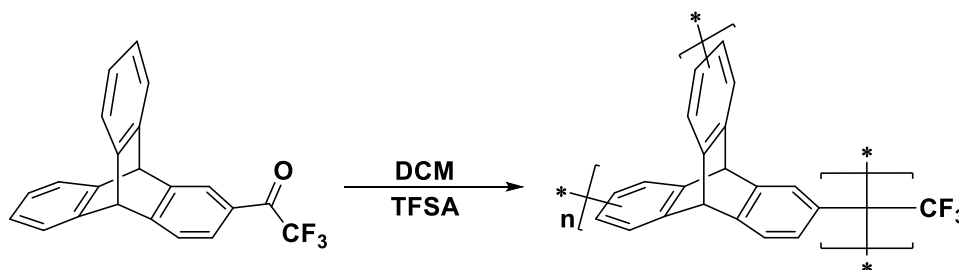
Polymer Synthesis

The commercially available 1,1,1-trifluoroacetone and triptycene were reacted to form a networked polymer denoted PIM-CF₃-A1 which proved insoluble in any common solvent but demonstrated an apparent BET surface area of 520 m²/g. The relatively high surface area is attributed to higher internal free volume given by the triptycene.^{214, 215} TGA analysis showed high thermal stability with a decomposition temperature over 450 °C (scheme 7.1)



Scheme 7.1: synthesis of PIM-CF₃-A1

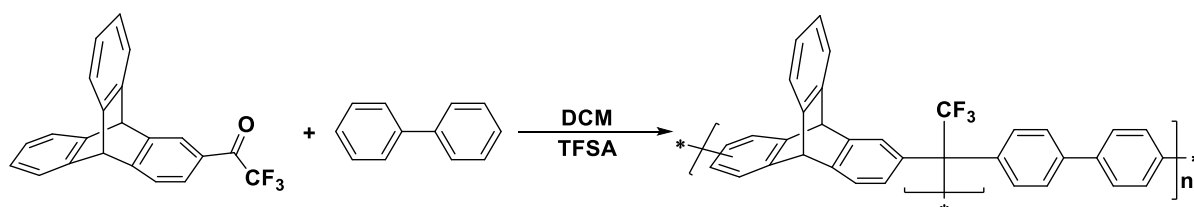
In a similar way, the self-polymerisation of the novel ketone 2-triptycenylnitrifluoromethyl ketone gave insoluble polymer PIM-CF₃-A2 (scheme 7.2) with an apparent BET surface area of 790 m²/g.



Scheme 7.2: synthesis of PIM-CF₃-A2

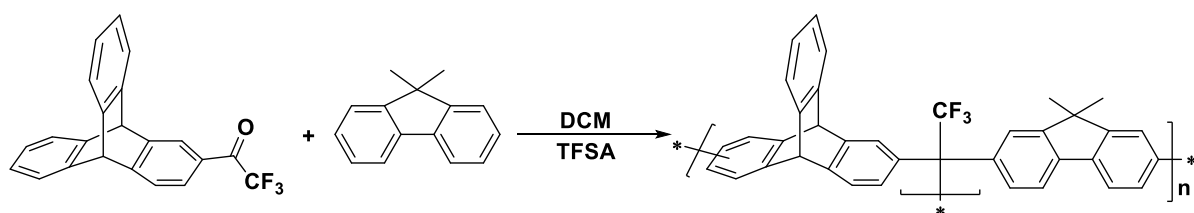
In an effort to prepare a soluble polymer using the same chemistry, we attempted the polymerisation of the 2-triptycenylnitrifluoromethyl ketone with biphenyl (Scheme 7.3).

Unfortunately, GPC analysis of the product mixture showed only low molecular weight and the BET analysis gave an apparent surface area of 500 m²/g, similar to PIM-CF₃-A1 but lower than PIM-CF₃-A2, this is probably due to the free rotation around the biphenyl unit which allows the polymer to pack more efficiently.



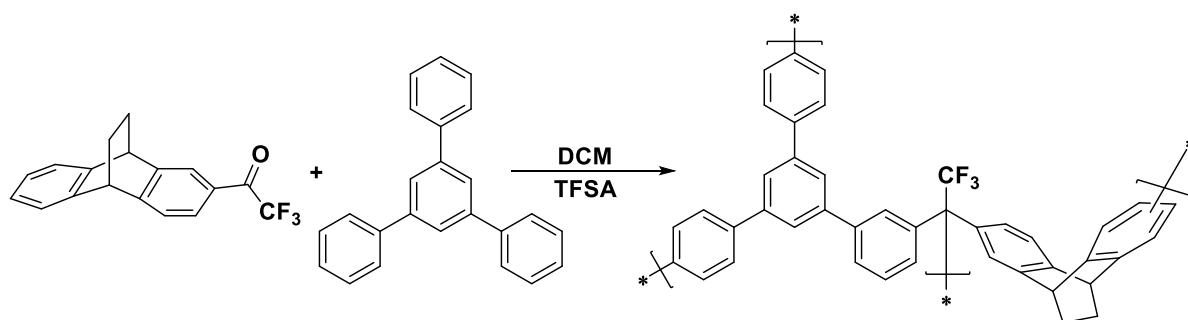
Scheme 7.3: synthesis of PIM-CF₃-A3

In another effort to synthesise a more soluble polymer, 2-tripticenyl trifluoromethyl ketone was polymerised with 9,9-dimethylfluorene (Scheme 7.4). The GPC analysis of this polymer again shows only a low molecular weight and the polymer displayed a BET surface area of 400 m²/g.



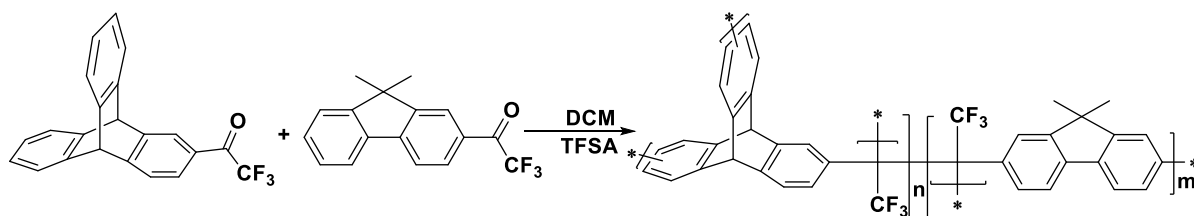
Scheme 7.4: synthesis of PIM-CF₃-A4

In addition, 2-(9,10-dihydro-9,10-ethanoanthracenyl)trifluoromethyl ketone was polymerised with 1,3,5-triphenylbenzene to afford the networked polymer PIM-CF₃-A5. The thermal stability was ~ 256 °C due to the loss of an ethylene fragment from the ethanoanthracene unit via a retro Diels-Alder reaction.²⁰² The BET surface area was 955 m²/g, the highest value for these polymers.



Scheme 7.5: synthesis of PIM-CF₃-A5

Finally, 2-triptycenyyl trifluoromethyl ketone and (9,9-dimethyl)fluorenyl trifluoromethyl ketone were co-polymerised to afford an insoluble polymer. The thermal stability was over ~ 382 °C and BET surface area was 735 m²/g.



Scheme 7.6: synthesis of PIM-CF3-A6

Hopefully in the future, other ketones **3**, **4**, **5** and **6** can be reacted with similar or different aromatic compounds to produce high performing PIMs. We anticipate that this polymerisation reaction could yet provide soluble polymers with a high degree of microporosity by further screening of monomers and reaction conditions.

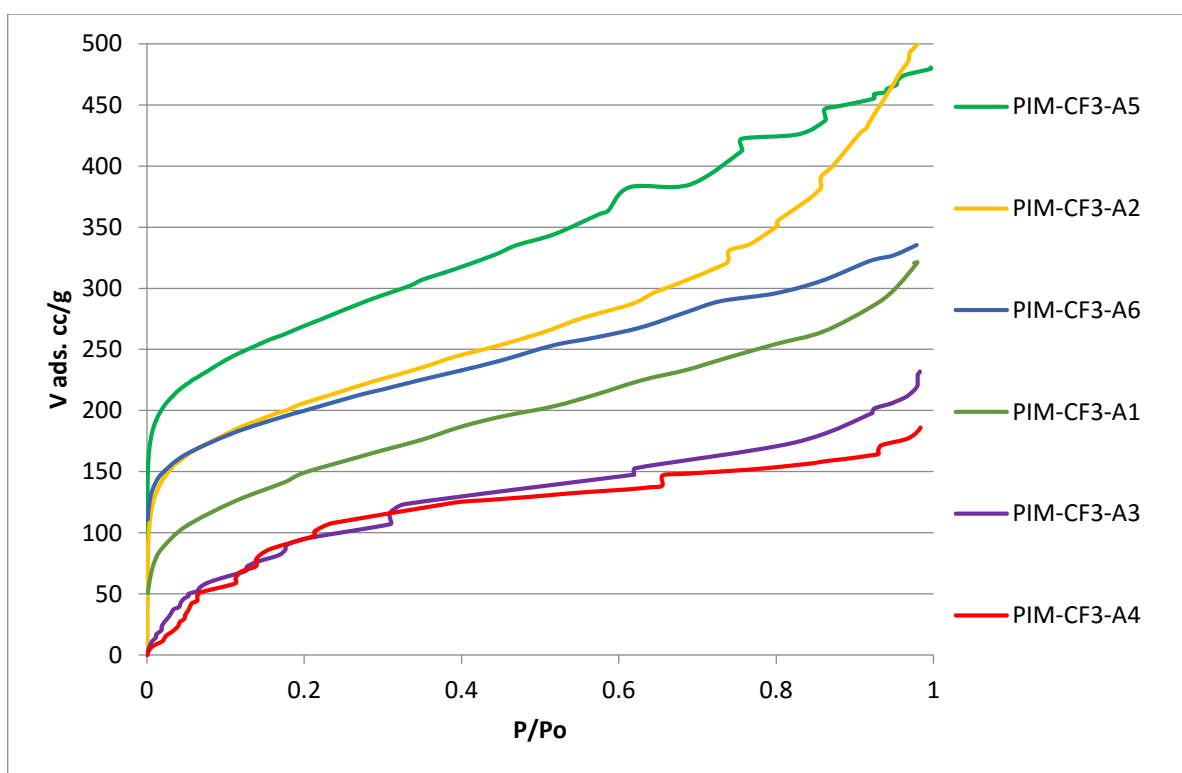


Fig 7.7: Nitrogen adsorption isotherms at 77 K for PIM-CF3-A1-6

Conclusions:

This thesis describes the successful synthesis of novel polymers, some of which conform to the PIM design concept, belonging to three classes of polymer from a range of new aromatic tetrahydroxy and diamine monomers. Although none of the polymers show gas permeability data that competes with the current best performing PIMs such as KAUST-PI-1, PIM-Trip-TB or TPIM-1, the simple synthesis of the monomers used in the present study provides an advantage over these highly sophisticated polymers made using a multi-step synthesis. In addition, it should be noted that for the PIM-TFA-PI series, described in Section 6.4, some very respectable gas permeation data were obtained. These polymers were derived from novel aromatic diamine monomers and the dianhydride 6FDA, which is relatively flexible but was used due to its commercial availability. Use of more rigid commercial dianhydrides such as pyromellitic anhydride might provide PIMs with excellent performance but with greater potential for scale-up and, hence, commercial exploitation.

Chapter Eight: Experimental

8.1: General Methods and Equipment

All reactions using air/moisture sensitive reagents were performed in oven-dried apparatus, under a nitrogen atmosphere. TLC analysis refers to analytical thin layer chromatography, using aluminium sheets (TLC) 60 GF₂₅₄ from Analytical Chromatography. Product spots were viewed by UV fluorescence. Column chromatography was performed over a silica gel (pore size 60 Å, particle size 40-63 µm) stationary phase.

Melting Points (Mp)

Melting points were recorded using a Sturat Melting Point SMP10 apparatus.

Fourier Transform Infrared Spectra (FTIR)

Fourier transform infrared adsorption spectra were recorded in the range 4000-400 cm⁻¹ using FTIR spectrophotometer as a solid (powder) and liquid by Shimadzu IRAffinity-1S.

Nuclear Magnetic Resonance (NMR)

¹H, ¹³C and ¹⁹F NMR spectra were recorded in a suitable deuterated solvent using Bruker Ascend™ 500 at the School of Chemistry, University of Edinburgh. Solid-State ¹³C NMR spectra were recorded by the EPSRC funded solid state NMR service at Durham University. Multiplicity is reported as singlet (s), doublet (d), doubled-doublet (dd), doubled-triplet (dt), triplet (t), quartet (q), pentet (p) or multiplet (m). Broad peaks are further labelled br. Coupling constants (*J*) are quoted in Hz.

Mass Spectrometry

Small molecule (MW < 1000 g mol⁻¹) low-resolution mass spectrometric (LRMS) and high-resolution mass spectrometric (HRMS) were obtained using a Thermo MAT 900 XP, double focusing sector at The University of Edinburgh also Fisons VG Platform II quadrupole instrument at Cardiff University.

BET Surface Areas

Low-temperature (77 K) nitrogen adsorption/desorption isotherms were obtained using a Coulter SA3100 surface area analyser or Quardrasorb Quantachrome Instruments. Weighed powdered samples of roughly 0.10 g were degassed for 15 h at 120 °C under high vacuum prior to analysis unless otherwise stated.

Thermo-Gravimetric Analysis (TGA)

Thermo-gravimetric analyses were performed on a Thermal Analysis SDT Q600 system, heating samples (~ 10 mg) at a rate of 10 °C/min from 50 °C to 1000 °C under a nitrogen atmosphere.

Gel Permeation Chromatography (GPC).

Gel permeation chromatography (GPC) analyses were performed on chloroform solutions (2 mg ml⁻¹) using a GPC MAX variable loop equipped with two KF-805L SHODEX columns and a RI(VE3580) detector, operating at a flow rate of 1 ml min⁻¹. Calibration was achieved using Viscotek polystyrene standards (M_w 1000 – 1,000,000 g mol⁻¹).

Film Fabrication for Membrane Gas Permeation Studies

Film formation was achieved by preparing a solution of polymer (e.g. 0.70 g for a 180 µm film and 0.35 g for a 90 µm film) in chloroform (15 ml), which was filtered through glass wool and poured into a 10 cm circular Teflon mould. The film was allowed to form by slow solvent evaporation for 96 h in a desiccator. Membranes were treated with MeOH to cancel casting history and to remove traces of residual solvent. This treatment consists in soaking overnight in MeOH and drying for 24h under ambient conditions.

Measurement of Membrane Gas Permeabilities

Low temperature measurements were carried out by the Institute on Membrane Technology (ITM-CNR), Calabria-Italy. Gas permeation tests of single gases were carried out at 25 °C and at a feed pressure of 1 bar, using a fixed-volume pressure increase instrument, described in the background theory section. Before analysis, the membrane samples were carefully evacuated to remove previously dissolved species. The gases were tested in the following order: He, N₂, O₂, CH₄ and CO₂. A total membrane area of 2.14 cm² was used and five thickness measurements were made for each membrane sample with a digital micrometer (Mitutoyo). The pressure increase in the permeate volume was monitored by a pressure transducer, starting from the instant of exposure of the membrane to the feed gas. All values were calculated from the slope of the pressure-time curves by methods described in background theory section.

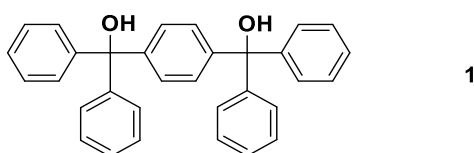
8.2: Monomers Synthesis

8.2.1: Diols

X1: General Procedure for 1,4-bis-(di-aryl-hydroxymethyl)benzene

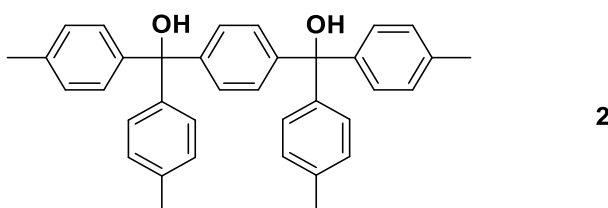
Under a nitrogen atmosphere, magnesium and an iodine crystal (~5 mg) was suspended in dry THF. With vigorous stirring, a corresponding aryl halide was injected drop-wise and the mixture was refluxed until the magnesium was consumed. A solution of dimethyl terephthalate in THF was injected drop-wise and the mixture was allowed to reflux for another 6 h. The mixture was then cooled down to room temperature, poured into water and extracted with diethyl ether. The organic layer was dried over MgSO₄ and the solvent was removed under vacuum. The crude product was recrystallised from toluene.

1.1: 1,4-Bis(diphenylhydroxymethyl)benzene¹⁸⁷



General procedure (X1) was followed using magnesium (5.00 g, 205.72 mmol), THF (150 ml), bromobenzene (31.40 g, 200.00 mmol) and dimethyl terephthalate (5.00 g, 25.75 mmol) in dry THF (100 ml). The pure product 1,4-bis(diphenylhydroxymethyl)benzene (**1**) (9.40 g, 82%) was isolated as a white powder. Mp = 168–170 °C (lit 169 °C); FTIR (solid, cm⁻¹) ν = 3451, 3059, 3024, 1605, 1491, 1445, 1013, 1001, 891, 826, 756, 700; ¹H NMR (500 MHz, CDCl₃) δ _H = 7.33 (m, 24H, ArH), 3.95 (s, br, 2H, OH); ¹³C NMR (126 MHz, CDCl₃) δ _C = 146.9, 145.9, 128.1, 128.0, 127.7, 127.4, 82.0; LRMS (EI, m/z): calculated for C₃₂H₂₆O₂ 442.6, found 422.2 (M⁺).

1.2: 1,4-Bisdi-*p*-tolylhydroxymethyl)benzene²¹⁶

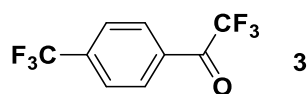


General procedure (X1) was followed using magnesium (5.00 g, 205.72 mmol), THF (150 ml), *p*-bromotoluene (34.21 g, 200.00 mmol) and dimethyl terephthalate (4.05 g, 20.85 mmol), in dry THF (100 ml). The pure product 4-bis(di-*p*-tolylhydroxymethyl)benzene (**2**)

(8.65 g, 83%) was isolated as a white powder as a white powder. Mp = 153–157 °C; FTIR (solid, cm⁻¹) ν = 3345, 1628, 1508, 1437, 1406, 1281, 1105, 1018; ¹H NMR (500 MHz, CDCl₃) δ_{H} = 8.21 (d, J_{HH} = 8.5 Hz, 8H, ArH), 8.08 (d, J_{HH} = 8.5 Hz, 8H, ArH), 7.99 (d, J_{HH} = 8.5 Hz, 2H, ArH), 7.44 (d, J_{HH} = 8.5 Hz, 2H, ArH), 3.99 (br. s, 2H, OH), 2.36 (s, 12H); ¹³C NMR (126 MHz, CDCl₃) δ_{C} = 146.1, 144.3, 137.0, 128.9, 128.7, 127.9, 127.6, 81.8, 21.2; HRMS (EI, m/z): calculated for C₃₆H₃₄O₂ 498.2553, found 498.2536 (M⁺).

8.2.2: Aryl-2,2,2-trifluoromethyl ketones

2.1: 4-(Trifluoromethyl)- α,α,α -trifluoroacetophenone ¹⁸⁸



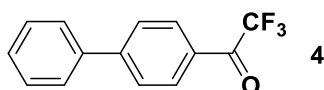
Under a nitrogen atmosphere, magnesium (4.00 g, 164.54 mmol) and an iodine crystal (5 mg) was suspended in dry diethyl ether (150 ml) and *p*-(trifluoromethyl)bromobenzene (25.00 g, 111.11 mmol) was injected as drop-wise and refluxed until the magnesium was consumed. The reagent was transferred to a dropping funnel and added drop-wise to a solution of ethyl trifluoroacetate (15.78 g, 111.11 mmol) in diethyl ether at -78 °C. The mixture was allowed to warm to room temperature for 16 h. The mixture was treated with dilute HCl then extracted with ether and the solvent was removed under vacuum. The crude product was distilled under vacuum to afford 4-(trifluoromethyl)- α,α,α -trifluoroacetophenone (**3**) (16.50 g, 71%, lit. 72%) as a colourless liquid; FTIR (liquid, cm⁻¹) ν = 1730, 1610, 1414, 1325, 1165, 1128, 1082, 1067, 1020, 943, 839, 743; ¹H NMR (500 MHz, CDCl₃) δ_{H} = 8.19 (d, J_{HH} = 8.9 Hz, 2H, ArH), 7.82 (d, J_{HH} = 8.9 Hz, 2H, ArH); ¹³C NMR (126 MHz, CDCl₃) δ_{C} = 180.0 (q, $J_{\text{C-F}}$ = 36.0 Hz), 136.8 (q, $J_{\text{C-F}}$ = 33.1 Hz), 132.8, 130.62 (q, $J_{\text{C-F}}$ = 2.1 Hz), 126.32 (q, $J_{\text{C-F}}$ = 3.8 Hz), 117.8, 115.4; ¹⁹F NMR (471 MHz, CDCl₃) δ_{F} = -64.0, -72.1; LRMS (EI, m/z): calculated for C₉H₄F₆O 242.1, found 242.0 (M⁺).

X2: General Procedure of Synthesis of Aryl Trifluoromethyl Ketones

Under a nitrogen atmosphere, anhydrous aluminium chloride was suspended in DCM with vigorous stirring and it was cooled in an ice bath. A mixture of TFAA and DCM was added drop-wise to the suspension. The mixture was stirred for 15 min at -5 °C. A solution of the corresponding aromatic reagent in DCM was injected as drop-wise over 60 min. The mixture was allowed to warm to room temperature for an appropriate time. The reaction mixture was poured into a mixture of concentrated HCl (250 ml), water (750 ml) and ice (750

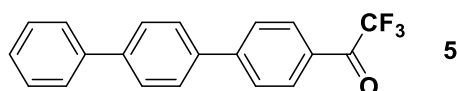
g) with vigorous stirring. The mixture was extracted with DCM and the solvent was removed under vacuum. The crude product was recrystallised from petroleum ether to give the pure product.

2.2: 4-Biphenyl trifluoromethyl ketone¹⁹¹



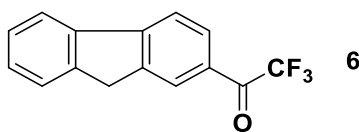
General procedure (X2) was followed using anhydrous aluminium chloride (13.30 g, 100.00 mmol) in DCM (250 ml), TFAA (21.00 g, 100.00 mmol) in DCM (75 ml) and biphenyl (7.70 g, 49.93 mmol) in DCM (50 ml). The mixture was stirred for 2 h to afford 4-biphenyl trifluoromethyl ketone (**4**) (5.81 g, 75%, lit. 70%) as colourless crystals. Mp = 102–104 °C (lit. 102–103 °C); FTIR (solid, cm⁻¹) ν = 3061, 3034, 1714, 1601, 1479, 1429, 1344, 1180, 1171, 1136, 1076, 1005, 941, 745, 725, 650, 689; ¹H NMR (500 MHz, CDCl₃) δ_{H} = 8.16 (dd, J_{HH} = 8.8, 1.1 Hz, 2H, ArH), 7.78 (m, 2H, ArH), 7.65 (m, 2H, ArH), 7.51 (m, 2H, ArH), 7.45 (m, 1H, ArH); ¹³C NMR (500 MHz, CDCl₃) δ_{C} = 180.42 (q, $J_{\text{C-F}}$ = 35.0 Hz), 148.65, 139.57, 131.16 (q, $J_{\text{C-F}}$ = 2.2 Hz), 129.54, 129.31, 129.15, 129.03, 128.06, 127.77, 117.18 (q, $J_{\text{C-F}}$ = 291.6 Hz); ¹⁹F NMR (471 MHz, CDCl₃) δ_{F} = -71.3; LRMS (EI, m/z): calculated for C₁₄H₉F₃O 250.2, found 250.1 (M⁺).

2.3: 4-Terphenyl trifluoromethyl ketone



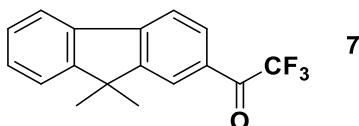
General procedure (X2) was followed using anhydrous aluminium chloride (13.30 g, 100.00 mmol) in DCM (250 ml), TFAA (21.00 g, 100.00 mmol) in DCM (75 ml) and *p*-terphenyl (11.49 g, 49.90 mmol) in DCM (100 ml). The mixture was stirred for 6 h to afford 4-terphenyl trifluoromethyl ketone (**5**) (13.00 g, 80%) as an off-white powder. Mp = 170–173 °C. FTIR (solid, cm⁻¹) ν = 3061, 3034, 1714, 1598, 1479, 1454, 1402, 1207, 1179, 1138, 1003, 941, 837, 745, 687, 638; ¹H NMR (500 MHz, CDCl₃) δ_{H} = 8.18 (d, J_{HH} = 7.7 Hz, 2H, ArH), 7.83 (m, 1H, ArH), 7.65 (m, 4H, ArH), 7.47 (m, 4H, ArH), 7.40 (m, 2H, ArH); ¹³C NMR (126 MHz, CDCl₃) δ_{C} = 180.1, 140.9, 140.3, 136.1, 131.0, 130.9 (q, $J_{\text{C-F}}$ = 2.2 Hz), 129.1, 129.0, 128.0, 127.9, 127.7, 127.5, 127.3, 127.2; ¹⁹F NMR (471 MHz, CDCl₃) δ_{F} = -71.3; HRMS (EI, m/z): calculated for C₂₀H₁₃F₃O 326.0913, found 326.0914 (M⁺).

2.4: 2-Fluorenyl trifluoromethyl ketone¹⁹¹



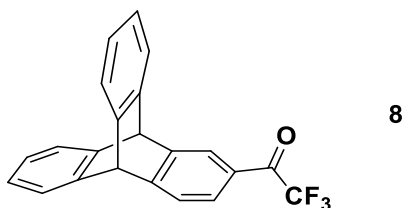
General procedure (X2) was followed using anhydrous aluminium chloride (13.30 g, 100.00 mmol) in DCM (250 ml), TFAA (21.00 g, 100.00 mmol) in DCM (75 ml) and fluorene (8.31g, 50.00 mmol) in DCM (50 ml). The mixture was stirred for 2 h to afford 2-fluorenyl trifluoromethyl ketone (**6**) (6.75 g, 81%, lit. 75%⁵) as light yellow crystals. Mp = 83-85 °C (lit. 83 °C); FTIR (solid, cm⁻¹) ν = 3057, 2930, 2902, 1703, 1603, 1566, 1396, 1350, 1240, 1190, 1096, 1028, 958, 748, 729; ¹H NMR (500 MHz, CDCl₃) δ_{H} = 8.25 (m, 1H, ArH), 8.14 (m, 1H, ArH), 7.92 (m, 2H, ArH), 7.63 (m, 1H, ArH), 7.45 (m, 2H, ArH), 4.01 (s, 2H, CH₂); ¹³C NMR (126 MHz, CDCl₃) δ_{C} = 180.4 (q, $J_{\text{C-F}}$ = 34.7 Hz), 149.1, 145.1, 143.7, 140.0, 129.9 (q, $J_{\text{C-F}}$ = 2.1 Hz), 129.1, 128.3, 127.5, 126.9 (q, $J_{\text{C-F}}$ = 2.1 Hz), 125.6, 121.6, 120.3, 117.1 (q, $J_{\text{C-F}}$ = 291.6 Hz), 37.1; ¹⁹F NMR (471 MHz, CDCl₃) δ_{F} = -70.9; LRMS (EI, m/z): calculated for C₁₅H₉F₃O 262.1, found 262.0 (M⁺).

2.5: 2-(9,9-Dimethyl)fluorenyl trifluoromethyl ketone



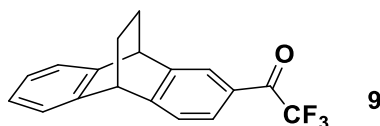
General procedure (X2) was followed using anhydrous aluminium chloride (13.74 g, 103.1 mmol) in DCM (250 ml), TFAA (21.70 g, 103.1 mmol) in DCM (75 ml) and 9,9-dimethylfluorene (10.00 g, 51.50 mmol) in DCM (50 ml). The mixture was stirred for 2 h to afford 2-(9,9-dimethyl)fluorenyl trifluoromethyl ketone (**7**) (10.50 g, 70%) as light yellow crystals. Mp = 63 - 65 °C; FTIR (solid, cm⁻¹) ν = 3065, 2963, 2928, 2970, 1705, 1604, 1470, 1447, 1425, 1350, 1200, 1169, 1153, 1136, 1078, 1007, 977, 930, 814, 760, 738, 729; ¹H NMR (500 MHz, CDCl₃) δ_{H} = 8.14 (s, 1H, ArH), 8.09 (d, J_{HH} = 8.1 Hz, 1H, ArH), 7.85 (d, J_{HH} = 8.1, 1H, ArH), 7.82 (dd, J_{HH} = 7.3, 1.5, Hz, 1H, ArH), 7.50 (dd, J_{HH} = 7.3, 1.5, Hz, 1H, ArH), 7.46 (d, J_{HH} = 1.3 Hz, 1H, ArH), 7.45 (d, J_{HH} = 1.3 Hz, 1H, ArH), 1.54 (s, 6H, CH₃); ¹³C NMR (126 MHz, CDCl₃) δ_{C} = 180.3 (q, $J_{\text{C-F}}$ = 34.5 Hz), 154.4, 146.9, 137.4, 130.3, 130.2 (q, $J_{\text{C-F}}$ = 2.6 Hz), 129.7, 128.7, 127.7, 124.5, 123.1, 121.7, 120.4 (q, $J_{\text{C-F}}$ = 1.8 Hz), 116.0, 47.4, 27.0; ¹⁹F NMR (471 MHz, CDCl₃) δ_{F} = -70.8; HRMS (EI, m/z): calculated for C₁₇H₁₃F₃O 290.0913, found 290.0917 (M⁺).

2.6: 2-Triptycenyyl trifluoromethyl ketone



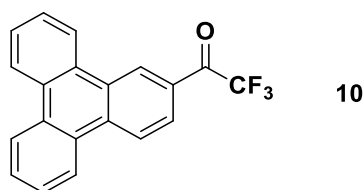
General procedure (X2) was followed using anhydrous aluminium chloride (6.65 g, 50.00 mmol) in DCM (125 ml), TFAA (10.50 g, 50.00 mmol) in DCM (37.5 ml) and triptycene (6.36 g, 25.00 mmol) in DCM (25 ml). The mixture was stirred for 10 h to afford 2-triptycenyyl trifluoromethyl ketone (**8**) (7.50 g, 90%) as a light pink powder. Mp = 150-153 °C. FTIR (solid, cm^{-1}) ν = 3069, 3040, 3021, 2968, 1703, 1614, 1601, 1454, 1431, 1190, 1145, 1115, 986, 797, 739, 694, 625, 613; ^1H NMR (500 MHz, CDCl_3) δ_{H} = 8.06 (s, 1H, ArH), 7.78 (d, $J_{\text{HH}} = 7.8$ Hz, 1H, ArH), 7.54 (d, $J_{\text{HH}} = 7.8$ Hz, 1H, ArH), 7.42 (m, 4H, ArH), 7.45 (m, 4H, ArH), 5.54 (s, 1H, CH), 5.53 (s, 1H, CH); ^{13}C NMR (126 MHz, CDCl_3) δ_{C} = 180.1 (q, $J_{\text{C-F}} = 34.9$ Hz), 145.4, 144.4, 143.7, 126.3 (q, $J_{\text{C-F}} = 202.0$), 126.0, 125.9, 125.3, 124.2, 124.1, 123.7, 54.4, 54.3; ^{19}F NMR (471 MHz, CDCl_3) δ_{F} = -71.2; HRMS (EI, m/z): calculated for $\text{C}_{22}\text{H}_{13}\text{F}_3\text{O}$ 350.0913, found 350.0914 (M^+).

2.7: 2-(9,10-Dihydro-9,10-ethanoanthracenyl) trifluoromethyl ketone



General procedure (X2) was followed using anhydrous aluminium chloride (12.93 g, 96.95 mmol) in DCM (250 ml), TFAA (17.65 g, 96.95 mmol) in DCM (75 ml) and 9,10-dihydro-9,10-ethanoanthracene (10.00 g, 48.47 mmol) in DCM (25 ml). The mixture was stirred for 16 h to afford 2-(9,10-dihydro-9,10-ethanoanthracenyl) trifluoromethyl ketone (**9**) (10.25 g, 70%) as yellow crystals. Mp = 96-98 °C; FTIR (solid, cm^{-1}) ν = 3073, 3048, 2953, 1707, 1610, 1570, 1474, 1460, 1190, 1145, 1215, 1190, 1182, 1146, 1121, 986, 970, 941, 756, 750, 556; ^1H NMR (500 MHz, CDCl_3) δ_{H} = 8.00 (s, 1H, ArH), 7.95 (dd, $J_{\text{HH}} = 7.9, 1.5$ Hz, 1H, ArH), 7.90 (dd, $J_{\text{HH}} = 7.9, 1.5$ Hz, 1H, ArH), 7.50 (d, $J_{\text{HH}} = 7.8$ Hz, 2H, ArH), 7.46 (d, $J_{\text{HH}} = 7.8$ Hz, 2H, ArH), 4.47 (m, 2H, CH), 1.80 (m, 4H, CH_2); ^{13}C NMR (126 MHz, CDCl_3) δ_{C} = 180.3, 152.5, 145.0, 142.8, 142.0, 128.7, 127.6, 126.2, 126.2, 124.6, 124.0, 123.7, 123.6, 117.0 (q, $J_{\text{C-F}} = 291.6$ Hz), 44.4, 44.0, 26.3, 26.1; ^{19}F NMR (471 MHz, CDCl_3) δ_{F} = -71.0; HRMS (EI, m/z): calculated for $\text{C}_{18}\text{H}_{13}\text{F}_3\text{O}$ 302.0913, found 302.0901 (M^+).

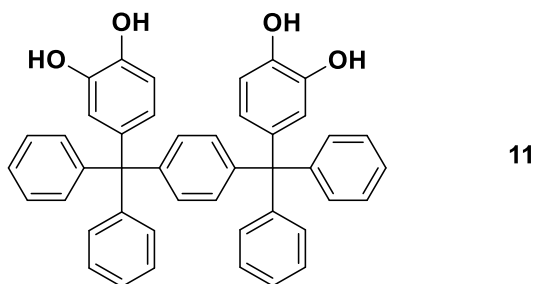
2.8: 2-Triphenylyl trifluoromethyl ketone



General procedure (X2) was followed using anhydrous aluminium chloride (4.62 g, 34.68 mmol) in DCM (250 ml), TFAA (9.17 g, 43.68 mmol) in DCM (25 ml) and triphenylene (5.00 g, 17.34 mmol) in DCM (125 ml). The mixture was stirred for 16 h to afford 2-triphenylyl trifluoromethyl ketone (**10**) (4.50 g, 63%) as light yellow crystals. Mp = 140-143 °C; FTIR (solid, cm^{-1}) ν = 3078, 3038, 1707, 1609, 1495, 1433, 1242, 1186, 1167, 950, 733, 715, 702; ^1H NMR (500 MHz, CDCl_3) δ_{H} = 9.35 (s, 1H, ArH), 8.70 (d, $J_{\text{HH}} = 8.7$ Hz, 1H, ArH), 8.69 (m, 3H, ArH), 8.23 (m, 2H, ArH), 7.69 (m, 4H, ArH); ^{13}C NMR (126 MHz, CDCl_3) δ_{C} = 180.5 (d, $J_{\text{C-F}} = 34.9$ Hz), 135.3, 131.4, 129.9, 129.3, 128.4, 128.0, 127.8, 127.4, 127.1 (q, $J_{\text{C-F}} = 2.4$ Hz), 126.6, 124.5, 123.4, 118.3; ^{19}F NMR (471 MHz, CDCl_3) δ_{F} = -70.8; HRMS (EI, m/z): calculated for $\text{C}_{20}\text{H}_{11}\text{F}_3\text{O}$ 324.0757, found 324.0762 (M^+).

8.2.3: Bis-catechol Monomers

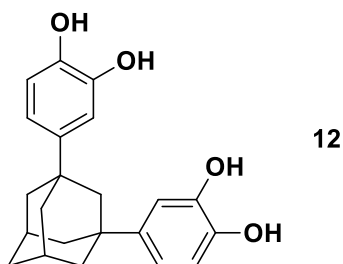
3.1: Synthetic of *p*-bis(3,4-dihydroxyphenyldiphenylmethyl)benzene (BAB4)



A mixture of 1,4-bis(diphenylhydroxymethyl)benzene (**1**) (5.00 g, 11.30 mmol), catechol (10.00 g, 90.82 mmol) and acetic acid (50 ml) was mixed at room temperature. The mixture was refluxed for 16 h then cooled to room temperature, filtered and washed with hot water. The crude product was dissolved into ethyl acetate and re-precipitated with petroleum ether, dried under nitrogen to afford *p*-bis(3,4-dihydroxyphenyldiphenylmethyl)benzene (BAB4) (**11**) (4.9 g, 69%) as a white powder. Mp = 245-248 °C; FTIR (solid, cm^{-1}) ν = 3505, 3350, 3062, 3032, 1606, 1491, 1441, 1287, 1184, 702; ^1H NMR (500 MHz, CD_3OD) δ_{H} = 7.53 (m, 22H, ArH), 7.08 (s, 2H, ArH), 6.65 (d, $J_{\text{HH}} = 2.0$ Hz, 2H, ArH), 6.46 (m, 4H, ArH), 3.33 (br. s, 4H, OH); ^{13}C NMR (126 MHz, CD_3OD) δ_{C} = 148.6, 146.1, 134.6, 132.3, 132.3, 131.2,

131.0, 131.0, 129.3, 128.3, 126.9, 123.7, 30.7; HRMS (EI, m/z) calculated for C₄₄H₃₄O₄ 626.2452, found 626.2460 (M⁺).

3.2: Synthesis of 1,3-Bis(3,4-dihydroxyphenyl)adamantane (BDA)

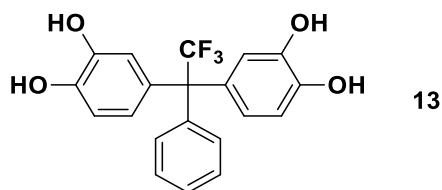


According to a patent procedure,¹⁹³ methanesulfonic acid (80 ml) was added drop-wise to a mixture of catechol (10.00 g, 90.82 mmol) and 1,3-adamantandiol (5.00 g, 29.72 mmol) at room temperature, the mixture was heated to 80 °C for 4 h then removed from heating to cool to room temperature and left stirring for 12 h. Water was added to the mixture and extracted with 10% methanol in CHCl₃ for three times, the solvent was removed under vacuum to afford an off-white solid. The crude product was subjected to column chromatography (eluent: 20% MeOH in chloroform) to afford 1,3-bis(3,4-dihydroxyphenyl)adamantane (**12**) (2.50 g, 24%, lit. 20%); as a white powder. Mp = 209-210 °C; FTIR (solid, cm⁻¹) ν = 3440, 3254, 2913, 2882, 2845, 1603, 1520, 1466, 1445, 1371, 1341, 1327, 1270, 1213, 1190, 1175, 1167, 1100, 797; ¹H NMR (500 MHz, CD₃OD) δ_{H} = 6.84 (s, 2H, ArH), 6.75 (d, J_{HH} = 2.0 Hz, 2H, ArH), 6.65 (d, J_{HH} = 2.0 Hz, 4H, ArH), 2.15 (s, 2H, CH₂), 1.87 (m, 8H, CH₂), 1.76 (br. s, 2H, CH₂); ¹³C NMR (126 MHz, CD₃OD) δ_{C} = 145.7, 144.4, 143.8, 117.1, 116.0, 113.4, 50.9, 43.8, 37.7, 37.05, 31.2; LRMS (EI, m/z): calculated for C₂₂H₂₄O₄ 352.4, found 352.1 (M⁺).

X3: General Procedure of Synthesis of Trifluorotetrahydroxyaryl

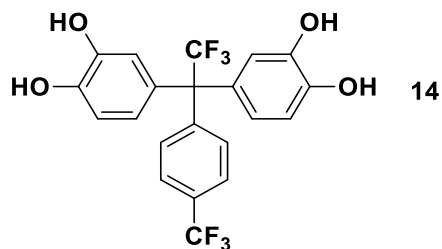
Under a nitrogen atmosphere, a mixture of the aryl-2,2,2-trifluoromethyl ketones, catechol and DCM were mixed, then TFSA was added drop-wise and stirred for an appropriate time at room temperature. The precipitate was filtered and washed with hot water, then DCM and dried under nitrogen.

3.3: Synthesis of 1,1-Bis(3,4-dihydroxyphenyl)-2,2,2-trifluoro-1-phenylethane (TF1) ¹⁹⁴



General procedure (X3) was followed using trifluoroacetophenone (5.00 g, 28.72 mmol), catechol (6.32 g, 57.44 mmol), DCM (60 ml) and TFSA (2.1539 g, 14.36 mmol). The mixture was stirred for 5 h to afford 1,1-bis(3,4-dihydroxyphenyl)-2,2,2-trifluoro-1-phenylethane (TF1) (**13**) (8.63 g, 80%, lit. 80%) as an off-white powder. Mp = 199–201 °C; FTIR (solid, cm⁻¹) ν = 3277, 1609, 1518, 1429, 1360, 1258, 1219, 1186, 1167, 1138, 1109, 964, 812, 754, 716, 665; ¹H NMR (500 MHz, CDCl₃) δ_{H} = 7.31 (m, 2H, ArH), 7.15 (m, 2H, ArH), 6.87 (m, 1H, ArH), 6.80 (m, 2H, ArH), 6.66 (d, J_{HH} = 5.4 Hz, 1H, ArH), 6.58 (d, J_{HH} = 5.4 Hz, 1H, ArH), 5.26 (br. s, 1H, OH), 5.07 (br. s, 1H, OH); ¹³C NMR (126 MHz, CDCl₃) δ_{C} = 143.3, 142.9, 140.5, 133.2, 130.0 (q, $J_{\text{C-F}}$ = 289 Hz), 129.3, 128.2, 127.8, 123.2, 117.6, 114.9, 64.3 (q, $J_{\text{C-F}}$ = 22.9 Hz); ¹⁹F NMR (471 MHz, CDCl₃) δ_{F} = -58.8; LRMS (EI, m/z): calculated for C₂₀H₁₅F₃O₄ 376.3, found 376.1 (M⁺).

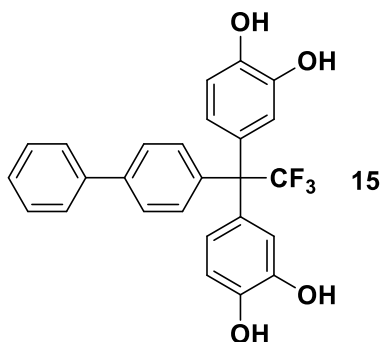
3.4: Synthesis of 1,1-Bis(3,4-dihydroxyphenyl)-2,2,2-trifluoro-1-(4-trifluorotoluy)ethane (TF2)



General procedure (X3) was followed using 2,2,2-trifluoro-4'-(trifluoromethyl)acetophenone (**3**) (5.00 g, 20.65 mmol), catechol (4.54 g, 41.30 mmol), DCM (50 ml) and TFSA (1.55 g, 10.33 mmol). The mixture was stirred for 16 h to afford 1,1-bis(3,4-dihydroxyphenyl)-2,2,2-trifluoro-1-(4-trifluorotoluy)ethane (TF2) (**14**) (6.50 g, 71%) as a white powder. Mp = 153-155 °C; FTIR (solid, cm⁻¹) ν = 3402, 1610, 1526, 1433, 1327, 1294, 1254, 1233, 1173, 1152, 1107, 1070, 1020, 849, 829, 814, 789, 730, 621; ¹H NMR (500 MHz, DMSO-d₆) δ_{H} = 8.92 (br. s, 4H, OH), 7.77 (d, J_{HH} = 8.4 Hz, 2H, ArH), 7.29 (d, J_{HH} = 8.4 Hz, 2H, ArH), 6.49 (d, J_{HH} = 2.4 Hz, 2H, ArH), 6.26 (d, J_{HH} = 2.4 Hz, 2H, ArH), 5.75 (s, 2H, ArH); ¹³C NMR (126 MHz, DMSO-d₆) δ_{C} = 145.0, 144.8, 144.2, 129.8, 128.13 (q, $J_{\text{C-F}}$ = 32.0 Hz),

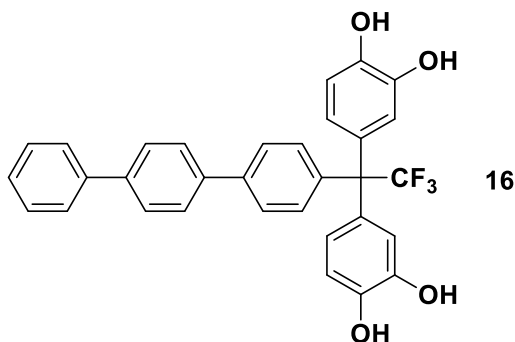
125.0 (q, $J_{C-F} = 3.7$ Hz), 123.0, 120.5, 119.2, 117.1, 115.7, 115.1, 63.43 (q, $J = 23.4$ Hz); ^{19}F NMR (471 MHz, CDCl_3) $\delta_{\text{F}} = -58.8, -62.7$; HRMS (EI, m/z): calculated for $\text{C}_{21}\text{H}_{14}\text{F}_6\text{O}_4$ 444.0791, found 444.0784 (M^+).

3.5: Synthesis of 1,1-Bis(3,4-dihydroxyphenyl)-2,2,2-trifluoro-1-(4-biphenyl)ethane (TF3)



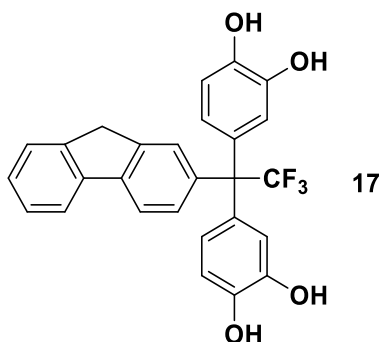
General procedure (X3) was followed using 4-biphenyl trifluoromethyl ketone (**4**) (4.00 g, 15.99 mmol), catechol (3.52 g, 31.99 mmol), DCM (40 ml) and TFSA (1.20 g, 7.99 mmol). The mixture was stirred for 5 h to afford 1,1-bis(3,4-dihydroxyphenyl)-2,2,2-trifluoro-1-(4-biphenyl)ethane (TF3) (**15**) (7.28 g, 70%) as a white powder. Mp = 180-183 °C; FTIR (solid, cm^{-1}) $\nu = 3333, 1612, 1522, 1435, 1288, 1256, 1223, 1138, 1105, 816, 764, 716, 625$; ^1H NMR (500 MHz, DMSO-d_6) $\delta_{\text{H}} = 9.01$ (br. s, 4H, OH), 7.69 (td, $J_{\text{HH}} = 7.0, 1.8$ Hz, 2H, ArH), 7.47 (t, $J_{\text{HH}} = 7.7$ Hz, 1H, ArH), 7.37 (m, 1H, ArH), 7.14 (d, $J_{\text{HH}} = 8.4$ Hz, 1H, ArH), 6.70 (d, $J_{\text{HH}} = 8.4$ Hz, 1H, ArH), 6.55 (d, $J_{\text{HH}} = 2.4$ Hz, 1H, ArH), 6.46 (s, 2H, ArH), 6.32 (d, $J_{\text{HH}} = 2.4$ Hz, 2H, ArH), 6.30 (d, $J_{\text{HH}} = 2.4$ Hz, 2H, ArH); ^{13}C NMR (126 MHz, DMSO-d_6) $\delta_{\text{C}} = 144.8, 144.6, 139.7, 139.2, 139.1, 130.5, 129.9, 129.0, 128.2$ (q, $J_{C-F} = 143.3$ Hz), 127.7, 126.6, 126.2, 120.6, 117.2, 115.0, 63.2 (q, $J_{C-F} = 23.2$ Hz); ^{19}F NMR (471 MHz, CDCl_3) $\delta_{\text{F}} = -58.8$; HRMS (EI, m/z): calculated for $\text{C}_{26}\text{H}_{19}\text{F}_3\text{O}_4$ 452.1230, found 452.1245 (M^+).

3.6: Synthesis of 1,1-Bis(3,4-dihydroxyphenyl)-2,2,2-trifluoro-1-(4-terphenyl)ethane (TF4)



General procedure (X3) was followed using 4-terphenyl trifluoromethyl ketone (**5**) (3.50 g, 10.73 mmol), catechol (2.37 g, 21.46 mmol), DCM (50 ml) and TFSA (1.15 g, 7.66 mmol). The mixture was stirred for 5 h to afford 1,1-bis(3,4-dihydroxyphenyl)-2,2,2-trifluoro-1-(4-terphenyl)ethane (TF4) (**16**) (4.64 g, 82%) as an off-white powder. Mp = 218-220 °C; FTIR (solid, cm⁻¹) ν = 3383, 1614, 1520, 1481, 1435, 1286, 1260, 1225, 1204, 1182, 1103, 941, 814, 765, 731, 626; ¹H NMR (500 MHz, CDCl₃) δ_{H} = 7.82 (d, J_{HH} = 8.5 Hz, 2H, ArH), 7.66 (m, 5H, ArH), 7.59 (d, J_{HH} = 8.5 Hz, 2H, ArH), 7.47 (m, 2H, ArH), 7.26 (s, 2H, ArH), 7.24 (m, 2H, ArH), 6.83 (s, 2H, ArH), 6.81 (s, 2H, ArH), 6.64 (d, J_{HH} = 2.3 Hz, 2H, ArH), 6.62 (d, J_{HH} = 2.3 Hz, 2H, ArH), 5.33 (br. s, 4H, OH); ¹³C NMR (126 MHz, CDCl₃) δ_{C} = 143.4, 143.0, 140.8, 140.3, 140.0, 139.6, 139.2, 133.0, 130.5, 129.1, 129.0, 127.7, 127.6, 127.5, 127.2, 126.6, 123.2, 117.6, 114.9, 64.0; ¹⁹F NMR (471 MHz, CDCl₃) δ_{F} = -58.8; HRMS (EI, m/z): calculated for C₃₂H₂₃F₃O₄ 528.1543, found 528.1530 (M⁺).

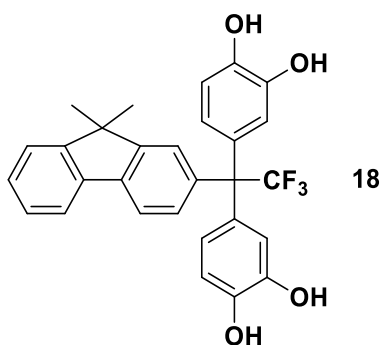
3.7: Synthesis of 1,1-Bis(3,4-dihydroxyphenyl)-2,2,2-trifluoro-1-(2-fluorenyl)ethane (TF5)



General procedure (X3) was followed using 2-fluorenyltrifluoromethyl ketone (**6**) (5.00g, 19.07 mmol), catechol (4.20 g, 38.14 mmol), DCM (50 ml) and TFSA (1.43 g, 9.54

mmol). The mixture was stirred for 24 h to afford 1,1-bis(3,4-dihydroxyphenyl)-2,2,2-trifluoro-1-(2-fluorenyl)ethane (TF5) (**17**) (5.02 g, 57%) as an off-white powder. Mp = 120-123 °C; FTIR (solid, cm⁻¹) ν = 3287, 1607, 1518, 1456, 1257, 1224, 1161, 1146, 1029, 822, 766, 733; ¹H NMR (500 MHz, DMSO-d₆) δ_{H} = 8.99 (s, 4H, OH), 7.78 (d, J_{HH} = 7.5 Hz, 2H, ArH), 7.57 (d, J_{HH} = 7.5 Hz, 2H, ArH), 7.39 (td, J_{HH} = 7.4, 1.2 Hz, 1H, ArH), 7.32 (td, J_{HH} = 7.4, 1.2 Hz, 1H, ArH), 7.26 (d, J_{HH} = 1.8 Hz, 1H, ArH), 7.11 (d, J_{HH} = 1.8 Hz, 1H, ArH), 6.71 (s, 1H, ArH), 6.70 (s, 1H, ArH), 6.55 (d, J_{HH} = 2.4 Hz, 1H, ArH), 6.33 (d, J_{HH} = 2.4 Hz, 1H, ArH), 6.31 (d, J = 2.5 Hz, 1H, ArH), 3.90 (s, 2H, CH₂); ¹³C NMR (126 MHz, DMSO-d₆) δ_{C} = 144.7, 144.6, 143.4, 142.7, 140.4, 140.3, 139.3, 130.8, 128.2, 128.3 (q, $J_{\text{C-F}}$ = 143.5 Hz), 127.0, 126.8, 125.9, 125.1, 120.7, 120.2, 119.4, 117.3, 115.0, 63.6 (q, $J_{\text{C-F}}$ = 23.0 Hz), 56.03; ¹⁹F NMR (471 MHz, CDCl₃) δ_{F} = -58.5; HRMS (EI, m/z): calculated for C₂₇H₁₉F₃O₄ 464.1230, found 464.1214 (M⁺).

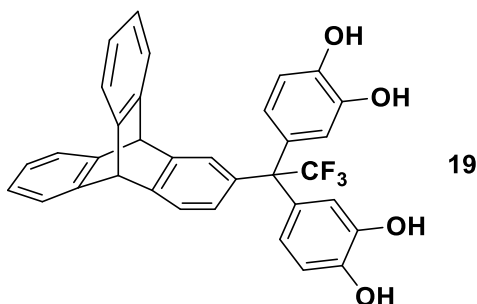
3.8: Synthesis of 1,1-Bis(3,4-dihydroxyphenyl)-2,2,2-trifluoro-1-(9,9-dimethyl-2-fluorenyl)ethane (TF6)



General procedure (X3) was followed using 2-(9,9-dimethyl)fluorenyltrifluoromethyl ketone (**7**) (10.00 g, 34.47 mmol), catechol (7.58 g, 68.89 mmol), DCM (50 ml) and TFSA (2.58 g, 17.2 mmol). The mixture was stirred for 16 h to afford 1,1-bis(3,4-dihydroxyphenyl)-2,2,2-trifluoro-1-(9,9-dimethyl-2-fluorenyl)ethane (TF6) (**18**) (13.01 g, 77%) as an off-white powder. Mp = 140-143 °C; FTIR (solid, cm⁻¹) ν = 3300, 2950, 1614, 1531, 1441, 1260, 1213, 1170, 1148, 1140, 1117, 804, 783, 738; ¹H NMR (500 MHz, DMSO-d₆) δ_{H} = 8.97 (br. s, 4H, OH), 7.36 (dd, J_{HH} = 7.4, 1.5 Hz, 1H, ArH), 7.32 (dd, J_{HH} = 7.4, 1.5 Hz, 1H, ArH), 6.99 (d, J_{HH} = 1.8 Hz, 1H, ArH), 6.97 (d, J_{HH} = 1.8 Hz, 1H, ArH), 6.71 (s, 1H, ArH), 6.70 (s, 2H, ArH), 6.67 (d, J_{HH} = 2.5 Hz, 1H, ArH), 6.56 (d, J_{HH} = 2.5 Hz, 1H, ArH), 6.33 (d, J_{HH} = 2.5 Hz, 2H, ArH), 6.31 (d, J_{HH} = 2.5 Hz, 2H, ArH), 1.35 (s, 6H, CH₃); ¹³C NMR (126 MHz, CDCl₃) δ_{C} = 143.3, 142.9, 139.6, 138.6, 133.5, 129.2, 127.7, 127.2, 124.2, 123.3, 122.8, 120.3, 119.4, 117.6,

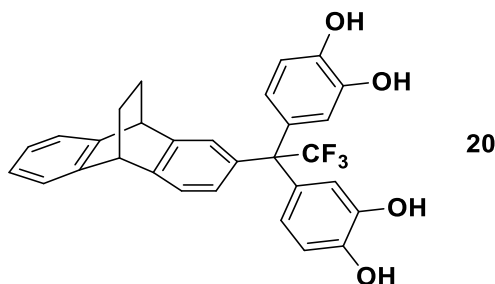
114.9, 64.4, 47.1, 27.1; ^{19}F NMR (471 MHz, CDCl_3) $\delta_{\text{F}} = -58.6$; HRMS (EI, m/z): calculated for $\text{C}_{29}\text{H}_{23}\text{F}_3\text{O}_4$ 492.1541, found 492.1543 (M^+).

3.9: Synthesis of 1,1-bis(3,4-dihydroxyphenyl)-2,2,2-trifluoro-1-(2-triptyceny)ethane (TF7)



General procedure (X3) was followed using 2-triptycenytrifluoromethyl ketone (**8**) (4.00 g, 11.42 mmol), catechol (2.51 g, 22.83 mmol), DCM (50 ml) and TFSA (0.86 g, 5.71 mmol). The mixture was stirred for 24 h to afford 1,1-bis(3,4-dihydroxyphenyl)-2,2,2-trifluoro-1-(2-triptyceny)ethane (TF7) (**19**) (2.60 g, 41%) as an off-white powder. Mp = 217-220 °C; FTIR (solid, cm^{-1}) $\nu = 3503, 3069, 2970, 1606, 1520, 1456, 1285, 1261, 1226, 1163, 1146, 1134, 1109, 850, 790, 739, 625$; ^1H NMR (500 MHz, CDCl_3) $\delta_{\text{H}} = 7.55$ (d, $J_{\text{HH}} = 8.4$ Hz, 4H, ArH), 7.32 (d, $J_{\text{HH}} = 8.4$ Hz, 4H, ArH), 7.26 (s, 1H, ArH), 6.83 (d, $J_{\text{HH}} = 2.4$ Hz, 1H, ArH), 6.71 (d, $J_{\text{HH}} = 2.4$ Hz, 1H, ArH), 6.70 (d, $J_{\text{HH}} = 2.3$ Hz, 2H, ArH), 6.60 (d, $J_{\text{HH}} = 2.3$ Hz, 2H, ArH), 6.59 (s, 2H, ArH), 3.69 (br. s, 4H, OH), 2.11 (s, 2H, CH); ^{13}C NMR (126 MHz, CDCl_3) $\delta_{\text{C}} = 145.6, 144.1, 131.9, 130.5, 129.8, 129.7, 129.5, 129.4, 129.3$ (q, $J_{\text{C-F}} = 211.4$ Hz), 128.8, 125.3, 124.9, 123.2, 121.9, 114.4, 64.1 (q, $J_{\text{C-F}} = 23.6$ Hz), 31.1; ^{19}F NMR (471 MHz, CDCl_3) $\delta_{\text{F}} = -58.8$; HRMS (EI, m/z): calculated for $\text{C}_{34}\text{H}_{23}\text{F}_3\text{O}_4$ 552.1543, found 552.1538 (M^+).

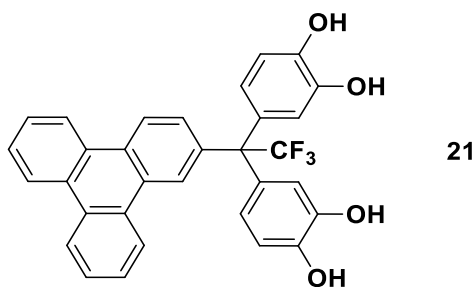
3.10: Synthesis of 1,1-Bis[(3,4-dihydroxyphenyl)-2,2,2-trifluoro-1-(2-(9,10-dihydro-9,10-ethanoanthracenyl))]ethane (TF8)



General procedure (X3) was followed using 2-(9,10-dihydro-9,10-ethanoanthracenyl)trifluoromethyl ketone (**9**) (6.61 g, 21.88 mmol), catechol (4.82 g, 43.76 mmol), DCM (50 ml)

and TFSA (1.64 g, 10.94 mmol). The mixture was stirred for 10 h to afford 1,1-bis[(3,4-dihydroxyphenyl)-2,2,2-trifluoro-1-(2-(9,10-dihydro-9,10-ethanoanthracenyl))]ethane (TF8) (**20**) (5.63 g, 51%) as an off-white powder. Mp = 130-133 °C; FTIR (solid, cm⁻¹) ν = 3343, 2955, 2940, 1608, 1520, 1435, 1258, 1223, 1161, 1151, 1134, 1111, 806, 785, 731; ¹H NMR (500 MHz, CDCl₃) δ_{H} = 7.40 (m, 2H, ArH), 7.36 (s, 1H, ArH), 7.34 (m, 2H, ArH), 7.22 (s, 2H, ArH), 6.97 (d, J_{HH} = 2.0 Hz, 1H, ArH), 6.95 (d, J_{HH} = 2.0 Hz, 1H, ArH), 6.87 (d, J_{HH} = 2.3 Hz, 2H, ArH), 6.85 (d, J_{HH} = 2.3 Hz, 2H, ArH), 6.53 (d, J_{HH} = 2.4 Hz, 1H, ArH), 6.51 (d, J_{HH} = 2.4 Hz, 1H, ArH), 4.67 (br. s, 2H, OH), 4.64 (br. s, 2H, OH), 4.12 (q, J_{HH} = 7.1 Hz, 2H, CH₂), 3.48 (q, J_{HH} = 7.0 Hz, 2H, CH₂), 2.05 (t, J_{HH} = 7.0 Hz, 1H, CH), 1.21 (t, J_{HH} = 7.0 Hz, 1H, CH); ¹³C NMR (126 MHz, CHCl₃) δ_{C} = 144.2, 144.1, 144.0, 143.9, 143.8, 143.7, 143.6, 137.9, 132.5, 127.2, 124.5, 123.4, 122.8, 122.0, 117.4, 114.8, 114.7, 64.0 (q, J = 23.3 Hz), 43.9, 43.3; ¹⁹F NMR (471 MHz, CDCl₃) δ_{F} = -58.5; HRMS (EI, m/z): calculated for C₃₀H₂₃F₃O₄ 504.1543, found 504.1543 (M⁺).

3.11: Synthesis of 1,1-Bis(3,4-dihydroxyphenyl)-2,2,2-trifluoro-1-(2-triphenyl)ethane (TF9) (21)



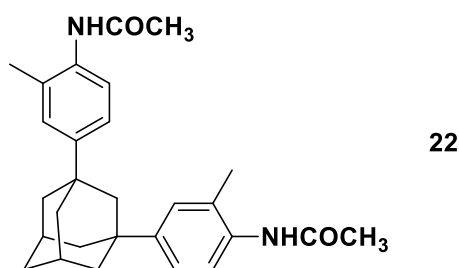
General procedure (X3) was followed using 2-triphenyltrifluoromethyl ketone (**10**) (4.00 g, 12.33 mmol), catechol (2.72 g, 24.67 mmol), DCM (50 ml) and TFSA (0.93 g, 6.17 mmol). The mixture was stirred for 16 h to afford 1,1-bis(3,4-dihydroxyphenyl)-2,2,2-trifluoro-1-(2-triphenyl)ethane (TF9) (**21**) (3.20 g, 49%) as an off-white powder. Mp = 180–183 °C; FTIR (solid, cm⁻¹) ν = 3392, 1608, 1514, 1433, 1260, 1234, 1171, 1138, 951, 864, 813, 779, 734; ¹H NMR (500 MHz, CDCl₃) δ_{H} = 8.62 (m, 4H, ArH), 8.42 (s, 1H, ArH), 8.25 (m, 1H, ArH), 7.59 (m, 6H, ArH), 6.86 (d, J_{HH} = 8.5 Hz, 1H, ArH), 6.72 (m, 4H, ArH), 5.26 (s, 2H, OH), 5.02 (s, 2H, OH); ¹³C NMR (126 MHz, CDCl₃) δ_{C} = 146.2, 143.0, 142.9, 136.9, 133.2, 129.4, 127.7, 127.6, 127.4, 126.4, 125.6, 125.3, 122.4, 121.5, 118.3, 72.2; ¹⁹F NMR (471 MHz, CDCl₃) δ_{F} = -58.5; HRMS (EI, m/z): calculated for C₃₂H₂₁F₃O₄ 526.1387, found 526.1367 (M⁺).

8.2.4: Adamantane Derivatives

X4: General Procedure for Adamantane Derivatives

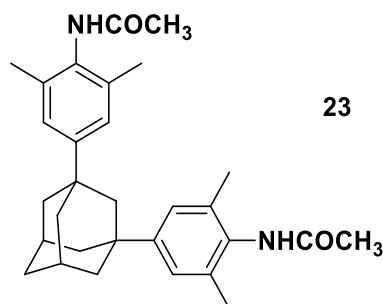
A mixture of 1-adamantanol (10.00 g, 65.68 mmol) and the corresponding alkylatedacetanilide was cooled in an ice bath. H₂SO₄ (500 ml) was added drop-wise under vigorous stirring. After the addition, the mixture was allowed to warm to room temperature and stirred for 15 h. The mixture was then poured into ice and stirred for 30 min, filtered and dried under vacuum to obtain the product as a white powder.

4.1: Synthesis of 1,3-bis(3-methyl-4-acetynilide)adamantane



General procedure (X4) was followed using 2-methylacetanilide (19.60 g, 131.37 mmol), to afford 1,3-bis(3-methyl-4-acetynilide)adamantane (**22**) (48.10 g, 85%). Mp = 113–115 °C; FTIR (solid, cm⁻¹) ν = 3263, 3040, 2900, 2847, 1650, 1600, 1560, 1508, 1444, 1411, 1369, 1340, 1294, 1126, 1037, 1016, 974, 877, 810, 719; ¹H NMR (500 MHz, CDCl₃) δ _H = 7.73 (d, J_{HH} = 11.7 Hz, 2H, ArH), 7.63 (d, J_{HH} = 11.7 Hz, 2H, ArH), 7.19 (s, 2H, ArH), 7.13 (br. s, 2H, NH), 2.26 (s, 2H, CH₂), 2.22 (s, 6H, CH₃), 2.19 (s, 6H, CH₃), 1.92 (m, 10H, CH₂ & CH), 1.76 (m, 2H, CH₂); ¹³C NMR (126 MHz, CDCl₃) δ _C = 168.5, 149.6, 135.5, 130.4, 123.6, 123.5, 122.4, 49.1, 43.3, 42.4, 37.9, 29.7, 28.5; HRMS (EI, m/z): calculated for C₂₈H₃₄N₂O₂ 430.2615, found 430.2630 (M⁺).

4.2: Synthesis of 1,3-bis(3,5-dimethyl-4-acetynilide)adamantane



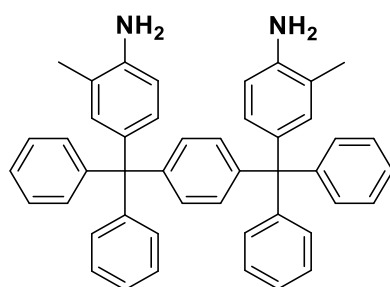
General procedure (X4) was followed using 2,6-dimethylacetanilide (21.44 g, 131.36 mmol), to afford 1,3-bis(3,5-dimethyl-4-acetimidyl)adamantane (**23**) (54.10 g, 90%). Mp = 148–150 °C; FTIR (solid, cm⁻¹) ν = 3251, 3040, 2900, 2847, 1655, 1603, 1520, 1489, 1484, 1369, 1352, 1342, 1277, 1174, 1103, 1037, 999, 970, 866, 831, 812, 798, 719; ¹H NMR (500 MHz, CDCl₃) δ_{H} = 7.75 (s, 2H, ArH), 7.09 (br. s, 4H, NH), 2.27 (s, 2H, CH₂), 2.24 (s, 6H, CH₃), 2.21 (s, 12H, CH₃), 1.88 (d, J_{HH} = 3.1 Hz, 8H, CH₂), 1.79 (d, J_{HH} = 3.1 Hz, 2H, CH₂), 1.76 (m, 2H, CH); ¹³C NMR (126 MHz, CDCl₃) δ_{C} = 168.8, 149.9, 135.1, 135.0, 125.1, 49.1, 43.3, 42.4, 37.9, 28.5, 23.4, 18.9; HRMS (EI, m/z): calculated for C₂₈H₃₄N₂O₂ 458.2928, found 458.2950 (M⁺).

8.2.5: Diamino Monomers

X5: General Procedure for BAB1, BAB2 and BAB3

A mixture of diol, alkylated aniline hydrochloric salt and acetic acid (50 ml) was mixed at room temperature. The mixture was refluxed for 8 h then the mixture was cooled to room temperature, filtered and washed with acetic acid and diethyl ether to afford the diamine salt. That salt was poured in a large volume of ethanol and neutralized with sodium hydroxide solution to afford a monomer crude. The monomer was purified with dissolve into pyridine and re-precipitated with water to afford as a white powder.

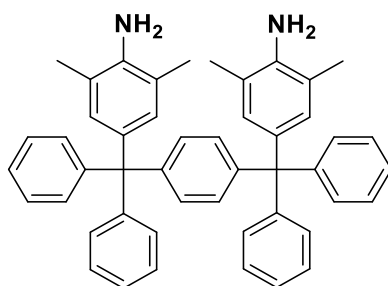
5.1: *p*-Bis(4-amino-3-methylphenyldiphenylmethyl)benzene (BAB1)



24

General procedure (X5) was followed using 1,4-bis(diphenylhydroxymethyl)benzene (**1**) (4.60 g, 10.39 mmol) and 2-toluidine hydrochloride (2.99 g, 20.78 mmol), to afford *p*-bis(4-amino-3-methylphenyldiphenylmethyl)benzene (BAB1) (**24**) (4.00 g, 62%). Mp > 300 °C; FTIR (solid, cm⁻¹) ν = 3387, 1620, 1500, 1489, 1439, 1292, 817, 698; ¹H NMR (500 MHz, CDCl₃) δ_{H} = 7.19 (m, 28H, ArH), 7.03 (s, 2H, ArH), 3.54 (br. s, 4H, NH₂), 2.06 (s, 6H, CH₃); ¹³C NMR (126 MHz, CDCl₃) δ_{C} = 147.5, 144.7, 142.4, 137.2, 133.5, 131.4, 130.3, 130.0, 127.3, 125.8, 121.2, 114.0, 110.1, 64.1, 17.8; HRMS (EI, m/z): calculated for C₄₆H₄₀N₂ 620.3186, found 620.3183 (M⁺).

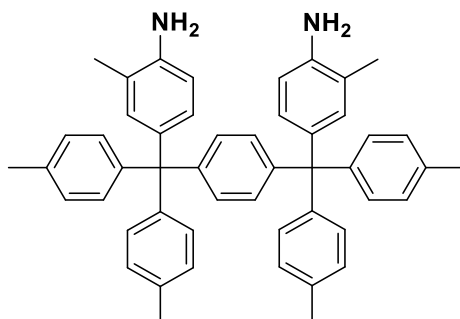
5.2: *p*-Bis(4-amino-3,5-dimethylphenyldiphenylmethyl)benzene (BAB2)



25

General procedure (X5) was followed using 1,4-bis(diphenylhydroxymethyl)benzene (**1**) (4.60 g, 10.39 mmol) and 2,6-dimethylaniline hydrochloride (3.28 g, 20.78 mmol) to afford *p*-bis(4-amino-3,5-dimethylphenyldiphenylmethyl)benzene (BAB2) (**25**) (4.10 g, 61%). Mp = 288–291 °C; FTIR (solid, cm⁻¹) ν = 3476, 3391, 2957, 2860, 1622, 1599, 1487, 1441, 1140, 1034, 756, 700; ¹H NMR (500 MHz, CDCl₃) δ_{H} = 7.20 (m, 24H, ArH), 6.69 (s, 4H, ArH), 3.50 (br. s, 4H, NH₂), 2.08 (s, 12H, CH₃); ¹³C NMR (126 MHz, CDCl₃) δ_{C} = 147.6, 144.8, 140.6, 136.4, 131.5, 131.4, 130.3, 128.0, 127.3, 125.8, 120.5, 64.1, 18.1; HRMS (EI, m/z): calculated for C₄₈H₄₄N₂ 648.3499, found 648.3522 (M⁺).

5.3: *p*-Bis(4-amino-3-methylphenyldi(*p*-tolyl)methyl)benzene (BAB3)



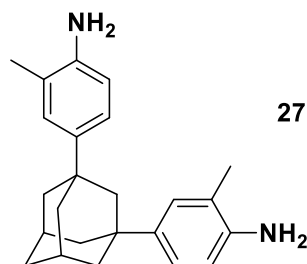
26

General procedure (X5) was followed using 1,4-bis(*p*-tolylhydroxymethyl)benzene (**2**) (2.00 g, 4.01 mmol) and 2-toluidine hydrochloride (1.15 g, 8.02 mmol) to afford *p*-bis(4-amino-3-methylphenyldi(*p*-tolyl)methyl)benzene (BAB3) (**26**) (2.20 g, 81%). Mp > 300 °C; FTIR (solid, cm⁻¹) ν = 3395, 3300, 1622, 1555, 1504, 1408, 1020, 804; ¹H NMR (500 MHz, CDCl₃) δ_{H} = 7.03 (m, 20H, ArH), 6.80 (s, 2H, ArH), 6.78 (d, J_{HH} = 8.1 Hz, 2H, ArH), 6.53 (d, J_{HH} = 8.1 Hz, 2H, ArH), 3.52 (br. s, 4H, NH₂), 2.31 (s, 12H, CH₃), 2.06 (s, 6H, CH₃); ¹³C NMR (126 MHz, CDCl₃) δ_{C} = 144.9, 144.7, 142.3, 137.6, 135.2, 133.5, 131.3, 130.2, 130.0, 128.0, 128.0, 121.1, 114.0, 63.3, 21.0, 17.8; HRMS (EI, m/z): calculated for C₅₀H₄₈N₂ 676.3812, found 676.3803 (M⁺).

X6: General Procedure for 1,3-Adamantane Monomers (AD2) & (AD3)

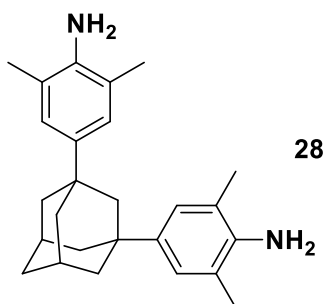
An aqueous solution of sodium hydroxide (5 M) (100 ml) was added to a mixture of the 1,3-adamantane salt in ethanol (300 ml) and the mixture was refluxed for an appropriate time. The mixture was cooled to room temperature and poured into water with vigorous stirring to afford an off-white powder.

5.4: Synthesis 1,3-Bis(3-methyl-4-aminophenyl)adamantane (AD2)



General procedure (X6) was followed using 1,3-bis(3-methyl-4-acetimidide)adamantane (**22**) (10.00 g, 23.22 mmol) with a reflux time of 24 h to afford 1,3-bis(3-methyl-4-aminophenyl)adamantane (AD2) (**27**) (8.10 g, 81%) as a white powder. Mp = 130–133 °C; FTIR (solid, cm^{-1}) ν = 3448, 3360, 3008, 2897, 2845, 1620, 1572, 1510, 1448, 1418, 1354, 1315, 1273, 1155, 1101, 864, 802; ^1H NMR (500 MHz, CDCl_3) δ_{H} = 7.70 (d, J_{HH} = 17.2 Hz, 2H, ArH), 7.20 (d, J_{HH} = 17.2 Hz, 2H, ArH), 7.12 (s, 2H, ArH), 4.74 (br. s, 4H, NH_2), 3.56 (s, 2H, CH_2), 2.22 (m, 14H, CH_3 & CH_2), 1.97 (m, 2H, CH), 1.75 (s, 2H, CH_2); ^{13}C NMR (126 MHz, CDCl_3) δ_{C} = 168.6, 130.4, 123.4, 122.4, 120.93, 115.1, 49.1, 42.4, 37.9, 29.7, 28.5, 24.3; HRMS (EI, m/z): calculated for $\text{C}_{24}\text{H}_{30}\text{N}_2$ 346.2403, found 346.2403 (M^+).

5.5: Synthesis of 1,3-Bis(3,5-dimethyl-4-aminophenyl)adamantane (AD3)



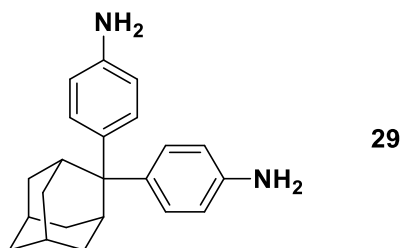
General procedure (X6) was followed using 1,3-bis(3,5-dimethyl-4-acetimidide)adamantane (**23**) (10.00 g, 21.80 mmol) with a reflux time of 48 h to afford 1,3-bis(3,5-dimethyl-4-aminophenyl)adamantane (AD3) (**28**) (7.00 g, 70%) as a white powder. Mp = 102–105 °C; FTIR (solid, cm^{-1}) ν = 3458, 3361, 3045, 2899, 2845, 1662, 1622, 1600, 1490,

1444, 1418, 1367, 1319, 1255, 1157, 1103, 1026, 866, 734; ^1H NMR (500 MHz, CDCl_3) δ_{H} = 6.99 (s, 4H, ArH), 4.65 (br. s, 4H, NH_2), 2.32 (s, 2H, CH_2), 2.24 (m, 20H, CH_3 & CH_2), 1.92 (m, 2H, CH), 1.76 (s, 2H, CH_2); ^{13}C NMR (126 MHz, CDCl_3) δ_{C} = 135.1, 132.6, 125.1, 125.0, 42.8, 37.9, 37.1, 29.2, 28.5, 18.3; HRMS (EI, m/z): calculated for $\text{C}_{26}\text{H}_{34}\text{N}_2$ 374.2716, found 374.2700 (M^+).

X7: General Procedure for Diamino Monomers from Ketones

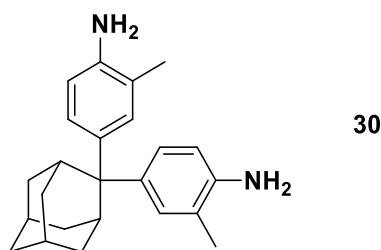
Under a nitrogen atmosphere, a mixture of the ketone, aniline and aniline hydrochloride were mixed together at room temperature. The mixture was heated to 180-185 °C for an appropriate time. The reaction was quenched with water (100 ml) at 140 °C and refluxed for 1h then cooled to room temperature. The mixture was poured into ammonia solution (35%) and stirred for 30 min. The mixture was extracted with chloroform (3 x 300 ml) and washed with water. The organic layer was dried over MgSO_4 and the solvent was removed under vacuum to give a brown oil product. The crude product was subjected to column chromatography (eluent: 6:4 petrolumether: ethyl acetate). The product was washed with methanol to afford the pure product.

5.6: Synthesis of 2,2-Bis(4-aminophenyl)adamantane (AD4)^{204, 217}



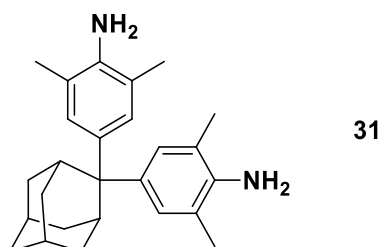
General procedure (X7) was followed using 2-adamantanone (10.00 g, 66.57 mmol), aniline hydrochloride (18.98 g, 146.45 mmol) and aniline (18.59 g, 199.71 mmol). The mixture was refluxed for 48 h to afford 2,2-bis(4-aminophenyl)adamantane (AD4) (**29**) (6.58 g, 31%) as a grey powder. Mp = 242–245 °C, (lit. 242 °C); FTIR (solid, cm^{-1}) ν = 3452, 3348, 3367, 3022, 2886, 2852, 1612, 1505, 1466, 1449, 1358, 1282, 1205, 1205, 1184, 1124, 1099, 1076, 1039, 980, 862, 808, 735; ^1H NMR (500 MHz, CDCl_3) δ_{H} = 7.14 (d, J_{HH} = 8.6 Hz, 4H, ArH), 6.56 (d, J_{HH} = 8.6 Hz, 4H, ArH), 3.21 (br. s, 4H, NH_2), 3.11 (s, 2H, CH_2), 2.05 (m, 8H, CH_2) 1.79 (m, 2H, CH_2); ^{13}C NMR (126 MHz, CDCl_3) δ_{C} = 142.9, 139.6, 126.4, 115.4, 49.1, 39.3, 38.2, 33.4, 32.0, 27.7; LRMS (EI, m/z): calculated for $\text{C}_{22}\text{H}_{26}\text{N}_2$ 318.5, found 318.2 (M^+).

5.7: Synthesis of 2,2-Bis(3-methyl-4-aminophenyl)adamantane (AD5) ^{204, 217}



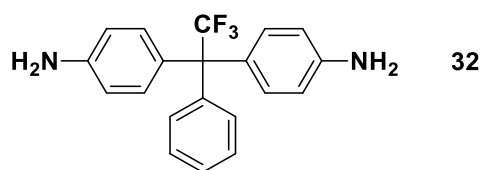
General procedure (X7) was followed using 2-adamantanone (10.00 g, 66.57 mmol), 2-methylaniline hydrochloride (21.03 g, 146.45 mmol) and 2-methylaniline (21.40 g, 199.71 mmol). The mixture was refluxed for 48 h to afford 2,2-bis(3-methyl-4-aminophenyl)adamantane (AD5) (**30**) (7.85 g, 34%) as an off-white powder. Mp = 260–263 °C (lit. 261-263 °C); FTIR (solid, cm^{-1}) ν = 3414, 3362, 3339, 3019, 2905, 2851, 1697, 1622, 1578, 1500, 1468, 1449, 1356, 1300, 1273, 1200, 1147, 1101, 883, 806, 735; ^1H NMR (500 MHz, CDCl_3) δ_{H} = 7.05 (m, 4H, ArH), 6.55 (d, J_{HH} = 8.0 Hz, 2H, ArH), 3.12 (m, 6H, NH_2 & CH_2), 2.10 (m, 10H, CH_2), 1.79 (m, 2H, CH_2), 1.71 (s, 6H, CH_3); ^{13}C NMR (126 MHz, CDCl_3) δ_{C} = 141.0, 139.7, 127.7, 124.1, 122.3, 115.3, 49.0, 38.3, 33.5, 32.0, 27.8, 17.9; LRMS (EI, m/z): calculated for $\text{C}_{24}\text{H}_{30}\text{N}_2$ 346.5, found 346.2 (M^+).

5.8: Synthesis of 2,2-bis(3,5-di methyl-4-aminophenyl)adamantane (AD6)



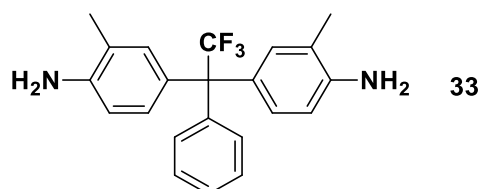
General procedure (X7) was followed using 2-adamantanone (10.00 g, 66.57 mmol), 2,6-dimethylaniline hydrochloride (23.08 g, 146.45 mmol) and 2,6-dimethylaniline (24.20 ml, 199.71 mmol). The mixture was refluxed for 48 h to afford 2,2-bis(3,5-dimethyl-4-aminophenyl)adamantane (AD6) (**31**) (8.98 g, 36%) as a white powder. Mp = 284–285 °C; FTIR (solid, cm^{-1}) ν = 3458, 3379, 3035, 2960, 2905, 2851, 1734, 1616, 1599, 1475, 1469, 1448, 1439, 1373, 1361, 1355, 1292, 1198, 1150, 1120, 1084, 1028, 982, 880, 864, 827, 743; ^1H NMR (500 MHz, CDCl_3) δ_{H} = 6.93 (s, 4H, ArH), 3.13 (br. s, 4H, NH_2), 2.11 (s, 12H, CH_3), 2.06 (m, 10H, CH & CH_2), 1.78 (m, 4H, CH & CH_2); ^{13}C NMR (126 MHz, CDCl_3) δ_{C} = 139.3, 139.0, 125.7, 121.8, 48.9, 38.5, 33.7, 32.0, 27.9, 18.3; HRMS (EI, m/z): calculated for $\text{C}_{26}\text{H}_{34}\text{N}_2$ 374.2717, found 374.2717 (M^+).

5.9: Synthesis of 1,1-Bis(4-aminophenyl)-1-phenyl-2,2,2-trifluoroethane (TFA1)



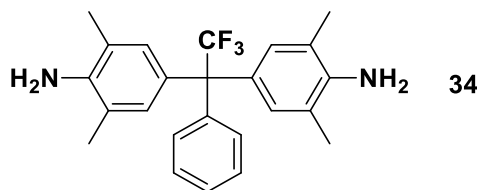
General procedure (X7) was followed using trifluoroacetophenone (20.00 g, 114.86 mmol), aniline hydrochloride (44.65 g, 344.58 mmol) and aniline (53.48 g, 574.32 mmol). The mixture was refluxed for 48 h to afford 1,1-bis(4-aminophenyl)-1-phenyl-2,2,2-trifluoroethane (TFA1) (**32**) (20.91 g, 48%) as a white powder. Mp = 202-205 °C (201-204 °C²¹⁸); FTIR (solid, cm⁻¹) ν = 3483, 3383, 3036, 1620, 1514, 1499, 1445, 1290, 1225, 1196, 1159, 1125, 1115, 1086, 916, 819, 758, 773, 714, 700; ¹H NMR (500 MHz, CDCl₃) δ_{H} = 7.29 (m, 5H, ArH), 6.91 (d, J_{HH} = 8.3 Hz, 4H, ArH), 6.60 (d, J_{HH} = 8.3 Hz, 4H, ArH), 3.69 (br. s, 4H, NH₂); ¹³C NMR (126 MHz, CDCl₃) δ_{C} = 145.7, 142.6, 131.1, 130.6, 130.1, 128.0, 127.5, 116.0 (q, $J_{\text{C-F}}$ = 177.7 Hz), 114.6, 29.9; ¹⁹F NMR (471 MHz, CDCl₃) δ_{F} = -59.0; LRMS (EI, m/z): calculated for C₂₀H₁₇F₃N₂ 342.4, found 342.1 (M⁺).

5.10: Synthesis of 1,1-Bis(3-methyl-4-aminophenyl)-1-phenyl-2,2,2-trifluoroethane (TFA2)



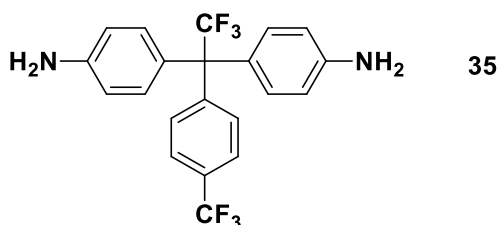
General procedure (X7) was followed using trifluoroacetophenone (20.00 g, 114.86 mmol), 2-methylaniline hydrochloride (49.50 g, 344.68 mmol) and 2-methylaniline (67.70 g, 632.00 mmol). The mixture was refluxed for 48 h to afford 1,1-bis(3-methyl-4-aminophenyl)-1-phenyl-2,2,2-trifluoroethane (TFA2) (**33**) (20.91 g, 49%) as an off-white powder. Mp = 192-195 °C; FTIR (solid, cm⁻¹) ν = 3455, 3389, 1622, 1504, 1447, 1302, 1285, 1234, 1234, 1219, 1175, 1126, 887, 826, 818, 754, 739, 716, 700, 662; ¹H NMR (500 MHz, CDCl₃) δ_{H} = 7.29 (m, 1H, ArH), 7.16 (m, 4H, ArH), 6.87 (d, J_{HH} = 2.3 Hz, 2H, ArH), 6.74 (d, J_{HH} = 2.3 Hz, 2H, ArH), 6.66 (s, 1H, ArH), 3.69 (br. s, 4H, NH₂), 2.13 (s, 6H, CH₃); ¹³C NMR (126 MHz, CDCl₃) δ_{C} = 142.7, 141.3, 132.1, 131.5, 130.1, 129.0, 128.0, 127.4, 127.3 (q, $J_{\text{C-F}}$ = 188.8 Hz), 122.5, 115.0, 64.1, 17.9; ¹⁹F NMR (471 MHz, CDCl₃) δ_{F} = -58.6; HRMS (EI, m/z): calculated for C₂₂H₂₁F₃N₂ 370.1651, found 370.1669 (M⁺).

5.11: Synthesis of 1,1-Bis(3,5-dimethyl-4-aminophenyl)-1-phenyl-2,2,2-trifluoro-ethane (TFA3)



General procedure (X7) was followed using trifluoroacetophenone (15.00 g, 86.15 mmol), 2,6-dimethylaniline hydrochloride (29.87 g, 189.53 mmol) and 2,6-dimethylaniline (57.42 g, 473.82 mmol). The mixture was refluxed for 48 h to afford 1,1-bis(3,5-dimethyl-4-aminophenyl)-1-phenyl-2,2,2-trifluoroethane (TFA3) (**34**) (12.00 g, 35%) as a pale yellow powder. Mp = 170-175 °C; FTIR (solid, cm^{-1}) ν = 3458, 3370, 2967, 2928, 1622, 1491, 1441, 1377, 1227, 1145, 1130, 870, 849, 741, 706; ^1H NMR (500 MHz, CDCl_3) δ_{H} = 7.29 (m, 3H, ArH), 7.17 (m, 2H, ArH), 6.70 (s, 4H, ArH), 3.70 (br. s, 4H, NH_2), 2.12 (s, 12H, CH_3); ^{13}C NMR (126 MHz, CDCl_3) δ_{C} = 141.8, 141.6, 130.2, 130.1, 130.0, 129.1 (q, $J_{\text{C-F}}$ = 169.4 Hz), 127.9, 127.3, 121.2, 64.1, 18.1; ^{19}F NMR (471 MHz, CDCl_3) δ_{F} = -58.2; HRMS (EI, m/z): calculated for $\text{C}_{24}\text{H}_{25}\text{F}_3\text{N}_2$ 398.1964, found 398.1972 (M^+).

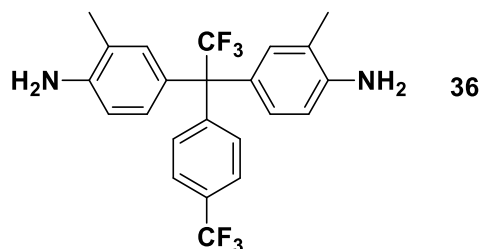
5.12: Synthesis of 1,1-Bis(4-aminophenyl)-1-(4-trifluorotoluy)l)-2,2,2-trifluoroethane (TFA4)



General procedure (X7) was followed using 4-trifluoromethyl-2,2,2-trifluoroacetophenone (**3**) (23.00 g, 94.99 mmol), aniline hydrochloride (27.08 g, 208.99 mmol) and aniline (48.65 g, 522.44 mmol). The mixture was refluxed for 72 h to afford 1,1-bis(4-aminophenyl)-1-(4-trifluorotoluy)l)-2,2,2-trifluoroethane (TFA4) (**35**) (21.30 g, 55%) as an off-white powder. Mp = 160–163 °C; FTIR (solid, cm^{-1}) ν = 3483, 3399, 1622, 1514, 1331, 1227, 1198, 1175, 1130, 1117, 1070, 1016, 824, 714; ^1H NMR (500 MHz, CDCl_3) δ_{H} = 7.55 (d, J = 8.2 Hz, 2H, ArH), 7.34 (d, J_{HH} = 8.3 Hz, 2H, ArH), 6.89 (d, J_{HH} = 8.6 Hz, 4H, ArH), 6.61 (d, J_{HH} = 8.7 Hz, 4H, ArH), 3.72 (br. s, 4H, NH_2); ^{13}C NMR (126 MHz, CDCl_3) δ_{C} = 146.0, 145.4, 131.0, 131.0, 130.5, 130.5, 129.7, 124.9 (q, $J_{\text{C-F}}$ = 3.7 Hz), 119.42 (q, $J_{\text{C-F}}$ =

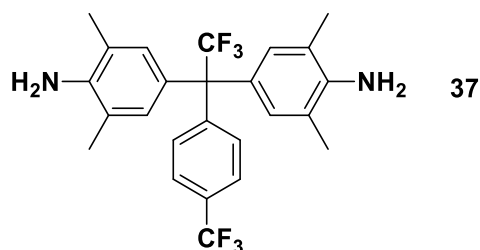
136.08 Hz), 114.7, 64.0 (q, $J_{C-F} = 23.9$ Hz); ^{19}F NMR (471 MHz, CDCl_3) $\delta_{\text{F}} = -59.1, -62.5$; HRMS (EI, m/z): calculated for $\text{C}_{21}\text{H}_{16}\text{F}_6\text{N}_2$ 410.1212, found 410.1202 (M^+).

5.13: Synthesis of 1,1-bis(3-methyl-4-aminophenyl)-1-(4-trifluorotoluy)-2,2,2-trifluoroethane (TFA5)



General procedure (X7) was followed using 4-trifluoromethyl-2,2,2-trifluoroacetophenone (**3**) (22.50 g, 92.92 mmol), 2-methylaniline hydrochloride (29.36 g, 204.42 mmol) and 2-methylaniline (59.70 g, 557.57 mmol). The mixture was refluxed for 72 h to afford 1,1-bis(3-methyl-4-aminophenyl)-1-(4-trifluorotoluy)-2,2,2-trifluoroethane (TFA5) (**36**) (17.10 g, 42%) as a white powder. Mp = 167–170 °C; FTIR (solid, cm^{-1}) $\nu = 3364, 3377, 2950, 1622, 1504, 1330, 1233, 1219, 1188, 1163, 1132, 1114, 1072, 1018, 887, 820, 737$; ^1H NMR (500 MHz, CDCl_3) $\delta_{\text{H}} = 7.63$ (d, $J_{\text{HH}} = 8.5$ Hz, 2H, ArH), 7.54 (d, $J_{\text{HH}} = 8.5$ Hz, 2H, ArH), 7.45 (m, 4H, ArH), 6.92 (s, 2H, ArH), 3.64 (br. s, 4H, NH_2), 2.13 (s, 6H, CH_3); ^{13}C NMR (126 MHz, CDCl_3) $\delta_{\text{C}} = 143.9, 140.6, 140.5, 131.3$ (q, $J_{\text{C-F}} = 91.61$ Hz), 130.0, 128.9, 128.9, 127.5, 127.2, 126.5, 121.8, 63.9 (q, $J_{\text{C-F}} = 23.4$ Hz), 17.82; ^{19}F NMR (471 MHz, CDCl_3) $\delta_{\text{F}} = -58.7, -62.6$; HRMS (EI, m/z): calculated for $\text{C}_{23}\text{H}_{20}\text{F}_6\text{N}_2$ 438.1525, found 438.1515 (M^+).

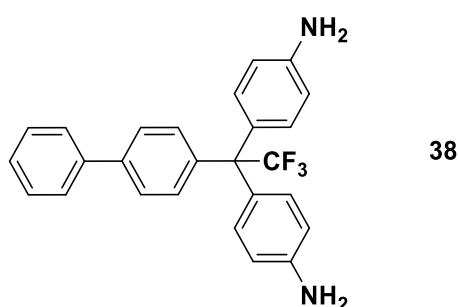
5.14: Synthesis of 1,1-Bis(3,5-dimethyl-4-aminophenyl)-1-(4-trifluorotoluy)-2,2,2-trifluoroethane (TFA6)



General procedure (X7) was followed using 4-trifluoromethyl-2,2,2-trifluoroacetophenone (**3**) (14.00 g, 57.80 mmol), 2,6-dimethylaniline hydrochloride (27.34 g, 173.46 mmol) and 2,6-dimethylaniline (42.00 g, 346.80 mmol). The mixture was refluxed for 48 h to afford 1,1-bis(3,5-dimethyl-4-aminophenyl)-1-(4-trifluorotoluy)-2,2,2-trifluoro-

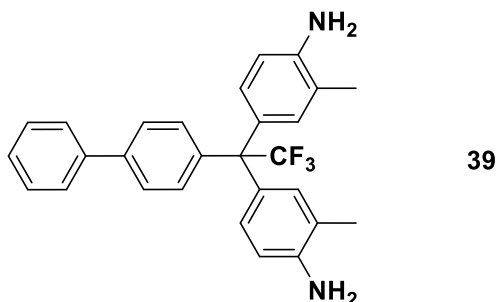
ethane (TFA6) (**37**) (8.41 g, 31%) as a white powder. Mp = 195–197 °C; FTIR (solid, cm^{-1}) ν = 3422, 3404, 2920, 2857, 1618, 1490, 1323, 1227, 1190, 1165, 1152, 1138, 1119, 1070, 1018, 872, 843, 820, 741; ^1H NMR (500 MHz, CDCl_3) δ_{H} = 7.55 (d, J_{HH} = 8.4 Hz, 2H, ArH), 7.32 (d, J_{HH} = 8.3 Hz, 2H, ArH), 6.68 (s, 4H, ArH), 3.64 (br. s, 4H, NH_2), 2.12 (s, 12H, CH_3); ^{13}C NMR (126 MHz, CDCl_3) δ_{C} = 145.7, 142.3, 130.6, 129.9, 129.2, 127.5 (q, $J_{\text{C-F}}$ = 94.8 Hz), 126.8, 124.0 (q, $J_{\text{C-F}}$ = 189.6 Hz), 121.2, 64.1 (q, $J_{\text{C-F}}$ = 23.5 Hz), 18.1; ^{19}F NMR (471 MHz, CDCl_3) δ_{F} = -58.4, -62.6; HRMS (EI, m/z): calculated for $\text{C}_{25}\text{H}_{24}\text{F}_6\text{N}_2$ 466.1838, found 466.1858 (M^+).

5.15: Synthesis of 1,1-bis(4-aminophenyl)-1-(4-biphenyl)-2,2,2-trifluoroethane (TFA7)



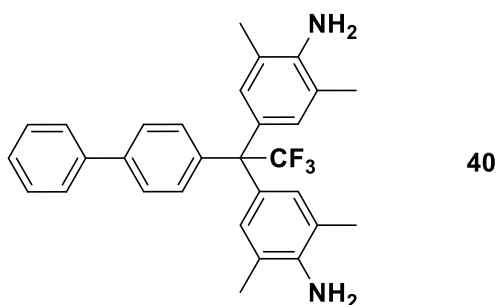
General procedure (X7) was followed using 4-biphenyl trifluoromethyl ketone (**4**) (20.00 g, 79.93 mmol), aniline hydrochloride (22.79 g, 175.85 mmol) and aniline (44.66 g, 479.57 mmol). The mixture was refluxed for 72 h to afford 1,1-bis(4-aminophenyl)-1-(4-biphenyl)-2,2,2-trifluoroethane (TFA7) (**38**) (20.00 g, 60%) as a white powder. Mp = 150–153 °C; FTIR (solid, cm^{-1}) ν = 3472, 3379, 1622, 1514, 1499, 1489, 1225, 1194, 1126, 1078, 916, 824, 735, 694; ^1H NMR (500 MHz, CDCl_3) δ_{H} = 7.61 (d, J_{HH} = 8.5 Hz, 2H, ArH), 7.53 (d, J_{HH} = 8.5 Hz, 2H, ArH), 7.31 (m, 3H, ArH), 6.96 (d, $J_{\text{C-F}}$ = 8.7 Hz, 2H, ArH), 6.68 (m, 4H, ArH), 6.62 (d, J_{HH} = 8.7 Hz, 4H, ArH), 3.70 (br. s, 4H, NH_2); ^{13}C NMR (126 MHz, CDCl_3) δ_{C} = 140.5, 140.4, 131.1, 130.5, 130.5, 129.5, 129.4, 128.9, 127.5, 127.2, 126.6, 118.3 (q, $J_{\text{C-F}}$ = 45.99 Hz), 114.6; ^{19}F NMR (471 MHz, CDCl_3) δ_{F} = -59.1; HRMS (EI, m/z): calculated for $\text{C}_{26}\text{H}_{21}\text{F}_3\text{N}_2$ 418.1651, found 418.1663 (M^+).

5.16: Synthesis of 1,1-bis(3-methyl-4-aminophenyl)-1-(4-biphenyl)-2,2,2-trifluoroethane (TFA8)



General procedure (X7) was followed using 4-biphenyl trifluoromethyl ketone (**4**) (20.00 g, 79.93 mmol), 2-methylaniline hydrochloride (25.25 g, 175.85 mmol) and 2-methylaniline (51.39 g, 479.58 mmol). The mixture was refluxed for 72 h to afford 1,1-bis(3-methyl-4-aminophenyl)-1-(4-biphenyl)-2,2,2-trifluoroethane (TFA8) (**39**) (22.50 g, 63%) as a white powder. Mp = 192–195 °C; FTIR (solid, cm^{-1}) ν = 3478, 3389, 1622, 1504, 1489, 1300, 1233, 1219, 1128, 817, 761, 739; ^1H NMR (500 MHz, CDCl_3) δ 7.64 (d, $J_{\text{HH}} = 8.5$ Hz, 2H, ArH), 7.55 (d, $J_{\text{HH}} = 8.5$ Hz, 2H, ArH), 7.45 (t, $J_{\text{HH}} = 7.5$ Hz, 2H, ArH), 7.36 (t, $J_{\text{HH}} = 7.5$ Hz, 2H, ArH), 7.27 (m, 1H, ArH), 6.92 (s, 2H, ArH), 6.81 (d, $J_{\text{HH}} = 8.4$ Hz, 2H, ArH), 6.62 (d, $J_{\text{HH}} = 8.4$ Hz, 2H, ArH), 3.65 (br. s, 4H, NH_2), 2.13 (s, 6H, CH_3); ^{13}C NMR (126 MHz, CDCl_3) δ_{C} 143.9, 140.5, 140.0, 132.0, 132.0, 130.6, 130.6, 130.5, 128.9, 127.5, 127.2, 126.5, 121.8, 114.4, 64.6, 17.8; ^{19}F NMR (471 MHz, CDCl_3) $\delta_{\text{F}} = -58.7$; HRMS (EI, m/z): calculated for $\text{C}_{28}\text{H}_{25}\text{F}_3\text{N}_2$ 446.1964, found 446.1952 (M^+).

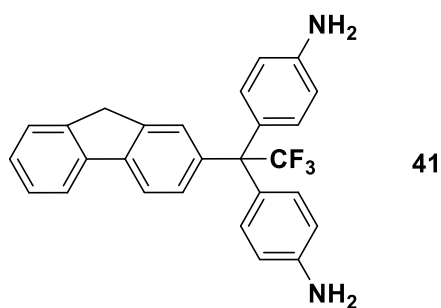
5.17: Synthesis of 1,1-Bis(3,5-dimethyl-4-aminophenyl)-1-(4-biphenyl)-2,2,2-trifluoroethane (TFA9)



General procedure (X7) was followed using 4-biphenyl trifluoromethyl ketone (**4**) (15.00 g, 59.94 mmol), 2,6-dimethylaniline hydrochloride (28.34 g, 179.82 mmol) and 2,6-dimethylaniline (43.58 g, 359.64 mmol). The mixture was refluxed for 48 h to afford 1,1-bis(3,5-dimethyl-4-aminophenyl)-1-(4-biphenyl)-2,2,2-trifluoroethane (TFA9) (**40**) (14.21

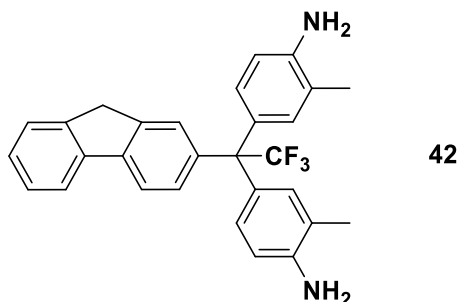
g, 50%) as an off-white powder. Mp = 230–233 °C; FTIR (solid, cm^{-1}) ν = 3412, 3394, 2970, 2922, 1622, 1487, 1441, 1300, 1220, 1136, 1126, 1007, 871, 843, 820, 735, 698; ^1H NMR (500 MHz, CDCl_3) δ 7.63 (m, 1H, ArH), 7.53 (d, J_{HH} = 8.4 Hz, 2H, ArH), 7.39 (m, 4H, ArH), 7.23 (d, J_{HH} = 8.4 Hz, 2H, ArH), 6.75 (s, 4H, ArH), 4.32 (br. s, 4H, NH_2), 2.16 (s, 12H, CH_3); ^{13}C NMR (126 MHz, CDCl_3) δ_{C} = 140.6, 140.5, 139.9, 130.7, 130.5, 130.0 (q, $J_{\text{C-F}}$ = 102.0 Hz), 130.1, 128.9, 128.8, 127.5, 127.2, 126.5, 121.9, 60.6, 18.2; ^{19}F NMR (471 MHz, CDCl_3) δ_{F} = -58.3; HRMS (EI, m/z): calculated for $\text{C}_{28}\text{H}_{25}\text{F}_3\text{N}_2$ 474.2277, found 474.2270 (M^+).

5.18: Synthesis of 1,1-bis(4-aminophenyl)-1-(2-fluorenyl)-2,2,2-trifluoroethane (TFA10)



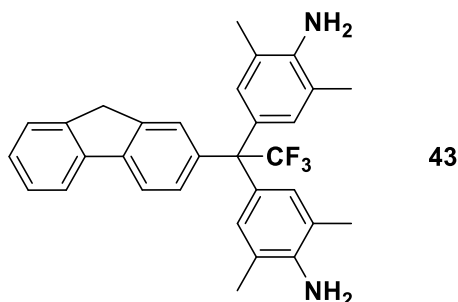
General procedure (X7) was followed using 2-fluorenyl trifluoromethyl ketone (**6**) (25.00 g, 95.34 mmol), aniline hydrochloride (27.18 g, 209.75 mmol) and aniline (53.27 g, 570.02 mmol). The mixture was refluxed for 72 h to afford 1,1-bis(4-aminophenyl)-1-(2-fluorenyl)-2,2,2-trifluoroethane (TFA10) (**41**) (23.01 g, 56%) as a white powder. Mp = 142–146 °C; FTIR (solid, cm^{-1}) ν = 3451, 3364, 1620, 1514, 1495, 1225, 1194, 1130, 1119, 1097, 824, 772, 750, 739; ^1H NMR (500 MHz, CDCl_3) δ_{H} = 7.78 (d, J_{HH} = 7.8 Hz, 1H, ArH), 7.70 (d, J_{HH} = 7.8 Hz, 1H, ArH), 7.38 (m, 5H, ArH), 6.97 (d, J_{HH} = 8.7 Hz, 4H, ArH), 6.62 (d, J_{HH} = 8.7 Hz, 4H, ArH), 3.85 (br. s, 4H, NH_2), 3.70 (s, 2H, CH_2); ^{13}C NMR (126 MHz, CDCl_3) δ_{C} = 145.7, 143.8, 143.1, 141.3, 141.0, 139.9, 131.1, 131.1, 130.8, 128.9, 127.0, 126.9, 125.2, 120.2, 119.2, 118.9 (q, $J_{\text{C-F}}$ = 43.47 Hz), 114.6, 64.2 (q, $J_{\text{C-F}}$ = 23.6 Hz), 37.2; ^{19}F NMR (471 MHz, CDCl_3) δ_{F} = -58.7; HRMS (EI, m/z): calculated for $\text{C}_{27}\text{H}_{21}\text{F}_3\text{N}_2$ 430.1651, found 430.1669 (M^+).

5.19: Synthesis of 1,1-bis(3-methyl-4-aminophenyl)-1-(2-fluorenyl)-2,2,2-trifluoroethane (TFA11)



General procedure (X7) was followed using 2-fluorenyl trifluoromethyl ketone (**6**) (24.00 g, 91.52 mmol), 2-methylaniline hydrochloride (28.92 g, 201.34 mmol) and 2-methylaniline (58.85 g, 549.12 mmol). The mixture was refluxed for 72 h to afford 1,1-bis(3-methyl-4-aminophenyl)-1-(2-fluorenyl)-2,2,2-trifluoro ethane (TFA11) (**42**) (24.00 g, 57%) as an off-white powder. Mp = 197–200 °C; FTIR (solid, cm⁻¹) ν = 3441, 3362, 1624, 1508, 1456, 1302, 1233, 1219, 1177, 1155, 1150, 819, 738; ¹H NMR (500 MHz, CDCl₃) δ_{H} = 7.78 (d, J = 7.9 Hz, 1H, ArH), 7.69 (d, J_{HH} = 7.9 Hz, 1H, ArH), 7.53 (d, J_{HH} = 7.4 Hz, 1H, ArH), 7.37 (m, 2H, ArH), 7.30 (d, J_{HH} = 7.4, 1H, ArH), 7.21 (d, J_{HH} = 8.3, 2H, ArH), 6.90 (s, 2H, ArH), 6.80 (d, J_{HH} = 8.3 Hz, 2H, ArH), 6.61 (s, 1H, ArH), 3.85 (s, 2H, CH₂), 3.64 (br. s, 4H, NH₂), 2.11 (s, 6H, CH₃); ¹³C NMR (126 MHz, CDCl₃) δ_{C} = 143.8, 143.0, 141.4, 140.9, 140.1, 132.1, 132.0, 131.0, 129.0, 126.9, 126.9, 126.7, 126.7, 125.2, 121.8, 120.1, 119.2, 114.4, 64.3 (d, $J_{\text{C-F}}$ = 23.4 Hz), 37.3, 17.8; ¹⁹F NMR (471 MHz, CDCl₃) δ_{F} = -58.5; HRMS (EI, m/z): calculated for C₂₉H₂₅F₃N₂ 458.1964, found 458.1974 (M⁺).

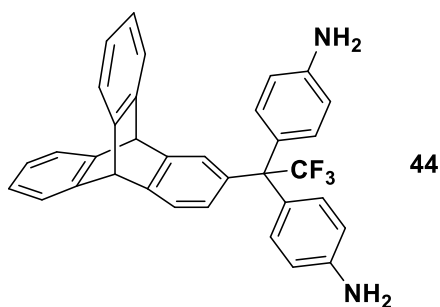
5.20: Synthesis of 1,1-bis(3,5-dimethyl-4-aminophenyl)-1-(2-fluorenyl)-2,2,2-trifluoroethane (TFA12)



General procedure (X7) was followed using 2-fluorenyl trifluoromethyl ketone (**6**) (20.00 g, 76.27 mmol), 2,6-dimethylaniline hydrochloride (36.06 g, 228.80 mmol) and 2,6-dimethylaniline (55.45 g, 457.62 mmol). The mixture was refluxed for 48 h to afford 1,1-

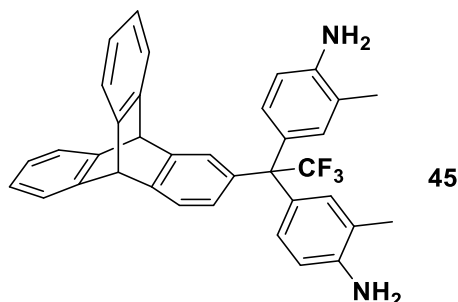
bis(3,5-dimethyl-4-aminophenyl)-1-(2-fluorenyl)-2,2,2-trifluoroethane (TFA12) (**43**) (22.30 g, 60%) as an off-white powder. Mp = 227–230 °C; FTIR (solid, cm⁻¹) ν = 3410, 3374, 2972, 2907, 2851, 1620, 1487, 1456, 1439, 1393, 1300, 1219, 1134, 1121, 1004, 976, 881, 856, 835, 822, 735; ¹H NMR (500 MHz, CDCl₃) δ_{H} = 7.78 (d, J_{HH} = 7.5 Hz, 1H, ArH), 7.68 (d, J_{HH} = 8.3 Hz, 1H, ArH), 7.53 (d, J_{HH} = 7.5 Hz, 1H, ArH), 7.34 (m, 3H, ArH), 7.18 (d, J_{HH} = 8.3 Hz, 1H, ArH), 6.73 (s, 4H, ArH), 3.85 (s, 2H, CH₂), 3.61 (br. s, 4H, NH₂), 2.11 (s, 12H, CH₃); ¹³C NMR (126 MHz, CDCl₃) δ_{C} = 130.5, 130.4, 130.3, 130.2, 130.2, 130.1, 130.0, 126.9, 125.2, 124.6 (q, $J_{\text{C-F}}$ = 276.2 Hz), 124.2, 122.9, 121.2, 120.2, 120.1, 119.1, 115.2, 113.1, 103.0, 55.42, 37.29, 18.09; ¹⁹F NMR (471 MHz, CDCl₃) δ_{F} = -58.5; HRMS (EI, m/z): calculated for C₃₁H₂₉F₃N₂ 486.2277, found 486.2298 (M⁺).

5.21: Synthesis of 1,1-bis(4-aminophenyl)-1-(2-triptyceny)-2,2,2-trifluoroethane (TFA13)



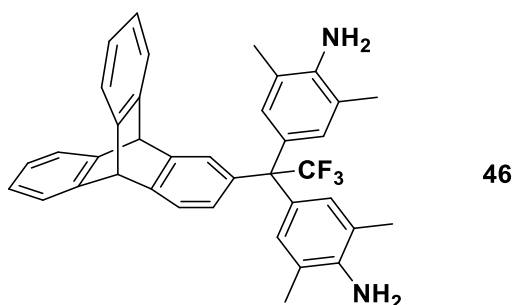
General procedure (X7) was followed using 2-triptyceny trifluoromethyl ketone (**8**) (16.50 g, 47.09 mmol), aniline hydrochloride (18.31 g, 141.29 mmol) and aniline (26.31 g, 282.54 mmol). The mixture was refluxed for 72 h to afford 1,1-bis(4-aminophenyl)-1-(2-triptyceny)-2,2,2-trifluoroethane (TFA13) (**44**) (5.10 g, 21%) as an off-white powder. Mp = 278–281 °C; FTIR (solid, cm⁻¹) ν = 3456, 3371, 3017, 1620, 1512, 1458, 1285, 1146, 822, 745; ¹H NMR (500 MHz, CDCl₃) δ_{H} = 7.16 (d, J_{HH} = 8.4 Hz, 4H, ArH), 7.09 (d, J_{HH} = 8.4 Hz, 4H, ArH), 7.07 (s, 1H, ArH), 6.91 (d, J_{HH} = 8.4 Hz, 1H, ArH), 6.86 (d, J_{HH} = 8.4 Hz, 1H, ArH), 6.76 (d, J_{HH} = 7.8 Hz, 4H, ArH), 6.60 (d, J_{HH} = 7.8 Hz, 4H, ArH), 5.39 (s, 1H, CH), 5.37 (s, 1H, CH), 3.58 (br. s, 4H, NH₂); ¹³C NMR (126 MHz, CDCl₃) δ_{C} = 145.3, 131.1, 130.2, 129.4, 127.9, 127.4, 125.5, 125.3, 123.9, 123.8, 118.7, 117.3, 115.0, 62.8, 54.2, 53.9; ¹⁹F NMR (471 MHz, CDCl₃) δ_{F} = -58.8; HRMS (EI, m/z): calculated for C₃₄H₂₅F₃N₂ 518.1964, found 518.1986 (M⁺).

5.22: Synthesis of 1,1-bis(3-methyl-4-aminophenyl)-1-(2-triptyceny)-2,2,2-trifluoroethane (TFA14)



General procedure (X7) was followed using 2-triptyceny trifluoromethyl ketone (**8**) (18.50 g, 52.80 mmol), 2-methylaniline hydrochloride (22.75 g, 158.41 mmol) and 2-methylaniline (33.95 g, 316.80 mmol). The mixture was refluxed for 48 h to afford 1,1-bis(3-methyl-4-aminophenyl)-1-(2-triptyceny)-2,2,2-trifluoroethane (TFA14) (**45**) (6.40 g, 25%) as a white powder. Mp > 300 °C; FT-IR (solid, cm⁻¹) ν = 3476, 3383, 2936, 2866, 1622, 1506, 1458, 1219, 1128, 822, 625; ¹H NMR (500 MHz, CDCl₃) δ _H = 7.35 (m, 4H, ArH), 7.21 (d, J_{HH} = 1.9 Hz, 2H, ArH), 6.90 (m, 3H, ArH), 6.73 (d, J_{HH} = 1.9 Hz, 1H, ArH), 6.72 (d, J_{HH} = 2.0 Hz, 1H, ArH), 6.66 (d, J_{HH} = 2.3 Hz, 2H, ArH), 6.64 (d, J_{HH} = 2.3 Hz, 2H, ArH), 6.62 (s, 2H, ArH), 5.41 (s, 1H, CH), 5.32 (s, 1H, CH), 4.59 (br. s, 4H, NH₂), 2.10 (s, 6H, CH₃); ¹³C NMR (126 MHz, CDCl₃) δ _C = 145.6, 145.4, 145.0, 144.4, 138.0, 132.0, 131.8, 129.1, 127.3, 125.2, 125.2, 123.9, 123.7, 122.9, 122.7, 54.3, 53.8, 17.8; ¹⁹F NMR (471 MHz, CDCl₃) δ _F = -58.5; HRMS (EI, m/z): calculated for C₃₆H₂₉F₃N₂ 546.2277, found 546.2291 (M⁺).

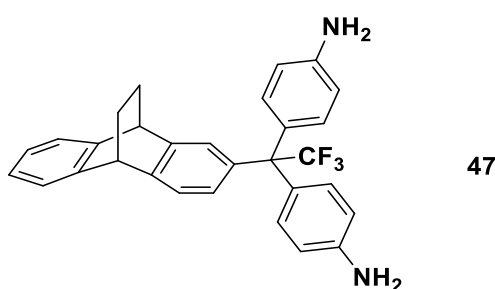
5.23: Synthesis of 1,1-bis(3,5-dimethyl-4-aminophenyl)-1-(2-triptyceny)-2,2,2-trifluoroethane (TFA15)



General procedure (X7) was followed using 2-triptyceny trifluoromethyl ketone (**8**) (7.00 g, 19.98 mmol), 2,6-dimethylaniline hydrochloride (9.45 g, 59.94 mmol) and 2,6-dimethylaniline (14.53 g, 119.88 mmol). The mixture was refluxed for 48 h to afford 1,1-bis(3,5-dimethyl-4-aminophenyl)-1-(2-triptyceny)-2,2,2-trifluoroethane (TFA15) (**46**) (2.30

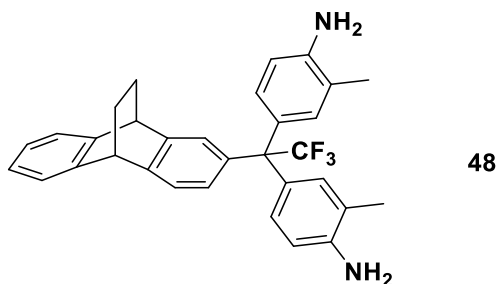
g, 20%) as a pale yellow powder. Mp > 300 °C; FT-IR (solid, cm⁻¹) ν = 3477, 3384, 2937, 2867, 1622, 1506, 1458, 1219, 1128, 822, 625; ¹H NMR (500 MHz, CDCl₃) δ_{H} = 7.38 (m, 4H, ArH), 7.35 (m, 4H, ArH), 7.27 (s, 1H, ArH), 7.26 (s, 4H, ArH), 7.0 (m, 2H, ArH), 5.38 (s, 1H, CH), 5.34 (s, 1H, CH), 4.56 (br. s, 4H, NH₂), 2.11 (s, 12H, CH₃); ¹³C NMR (126 MHz, CDCl₃) δ_{C} = 145.3, 143.8, 143.1, 142.2, 138.7, 135.3, 135.0, 134.9, 134.5, 132.1, 131.9, 125.6 (q, $J_{\text{C-F}}$ = 124.11Hz), 125.4, 123.3, 122.5, 54.3, 43.8, 19.2; ¹⁹F NMR (471 MHz, CDCl₃) δ_{F} = -58.1; HRMS (EI, m/z): calculated for C₃₈H₃₃F₃N₂ 574.2880, found 574.2895 (M⁺).

5.24: Synthesis of 1,1-bis[(4-aminophenyl)-1-(2-(9,10-dihydro-9,10-ethanoanthracenyl))]-2,2,2-trifluoroethane (TFA16)



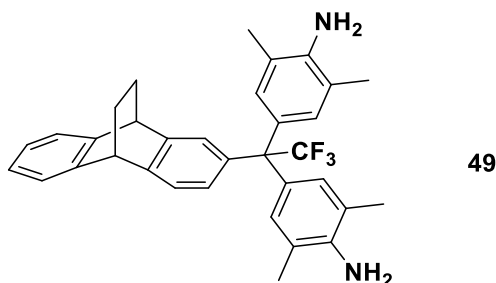
General procedure (X7) was followed using 2-(9,10-dihydro-9,10-ethanoanthracenyl) trifluoromethyl ketone (**9**) (25.00 g, 82.70 mmol), aniline hydrochloride (23.57 g, 181.94 mmol) and aniline (46.21 g, 496.20 mmol). The mixture was refluxed for 72 h to afford 1,1-bis[(4-aminophenyl)-1-(2-(9,10-dihydro-9,10-ethanoanthracenyl))]-2,2,2-trifluoroethane (TFA16) (**47**) (24.20 g, 62%) as a white powder. Mp = dec. 170 °C; FTIR (solid, cm⁻¹) ν = 3460, 3368, 3034, 2938, 2868, 1622, 1510, 1500, 1460, 1447, 1278, 1229, 1194, 1143, 1125, 760, 752; ¹H NMR (500 MHz, CDCl₃) δ_{H} = 7.23 (m, 3H, ArH), 7.13 (m, 2H, ArH), 6.95 (m, 2H, ArH), 6.88 (d, J_{HH} = 2.8 Hz, 4H, ArH), 6.87 (d, J_{HH} = 2.8 Hz, 4H, ArH), 4.31 (d, J_{HH} = 3.7 Hz, 1H, CH), 4.21 (d, J_{HH} = 3.7, 1H, CH), 3.67 (br. s, 4H, NH₂), 1.68 (m, 4H, CH₂); ¹³C NMR (126 MHz, CDCl₃) δ_{C} = 145.5, 142.4, 141.3, 138.0, 135.5, 131.2, 129.5, 127.8, 127.0, 126.0, 125.8, 125.7, 123.6, 123.0, 118.7, 60.2, 44.9, 44.4, 32.9, 23.8; ¹⁹F NMR (471 MHz, CDCl₃) δ_{F} = -58.8; HRMS (EI, m/z): calculated for C₃₀H₂₅F₃N₂ 470.1964, found 470.1959 (M⁺).

5.25: Synthesis of 1,1-bis[(3-methyl-4-aminophenyl)-1-(2-(9,10-dihydro-9,10-ethanoanthracenyl))]-2,2,2-trifluoroethane (TFA17)



General procedure (X7) was followed using 2-ethanoanthracenyl trifluoromethyl ketone (**9**) (10.00 g, 33.08 mmol), 2-methylaniline hydrochloride (10.45 g, 72.77 mmol) and 2-methylaniline (21.27 g, 198.48 mmol). The mixture was refluxed for 72 h to afford 1,1-bis[(3-methyl-4-aminophenyl)-1-(2-(9,10-dihydro-9,10-ethanoanthracenyl))]-2,2,2-trifluoroethane (TFA17) (**48**) (10.01 g, 61%) as a white powder. Mp = 147–150 °C; FTIR (solid, cm^{-1}) ν = 3468, 3383, 2943, 2870, 1624, 1504, 1474, 1290, 1221, 1161, 1129, 820, 748; ^1H NMR (500 MHz, CDCl_3) δ_{H} = 7.27 (m, 5H, ArH), 7.16 (d, $J_{\text{HH}} = 7.9$ Hz, 1H, ArH), 7.13 (m, 2H, ArH), 6.88 (m, 3H, ArH), 6.72 (d, $J_{\text{HH}} = 2.4$ Hz, 1H, ArH), 6.69 (d, $J_{\text{HH}} = 2.4$ Hz, 1H, ArH), 4.29 (m, 2H, CH), 3.61 (br. s, 4H, NH_2), 2.10 (m, 4H, CH_2), 1.89 (s, 6H, CH_3); ^{13}C NMR (126 MHz, CDCl_3) δ_{C} = 144.0, 143.7, 143.3, 138.6, 132.0, 131.0 (d, $J_{\text{C-F}} = 2.6$ Hz), 129.0, 127.5, 125.6, 124.9, 123.5, 123.3, 122.6, 121.6 (d, $J_{\text{C-F}} = 2.6$ Hz), 114.3, 64.0 (q, $J_{\text{C-F}} = 23.2$ Hz), 44.3, 43.8, 26.9, 26.9, 17.8; ^{19}F NMR (471 MHz, CDCl_3) δ_{F} = -58.4; HRMS (EI, m/z): calculated for $\text{C}_{32}\text{H}_{29}\text{F}_3\text{N}_2$ 498.2277, found 498.2261 (M^+).

5.26: Synthesis of 1,1-bis[(3,5-dimethyl-4-aminophenyl)-1-(2-(9,10-dihydro-9,10-ethanoanthracenyl))]-2,2,2-trifluoroethane (TFA18)



General procedure (X7) was followed using 2-ethanoanthracenyl trifluoromethyl ketone (**9**) (14.00 g, 46.31 mmol), 2,6-dimethylaniline hydrochloride (16.06 g, 101.88 mmol) and 2,6-dimethylaniline (30.08 g, 254.70 mmol). The mixture was refluxed for 72 h to afford 1,1-

bis[(3,5-dimethyl-4-aminophenyl)-1-(2-(9,10-dihydro-9,10-ethanoanthracenyl))]-2,2,2-trifluoroethane (TFA18) (**49**) (8.80 g, 36%) as a pale yellow powder. Mp = dec. 225 °C; FTIR (solid, cm⁻¹) ν = 3489, 3391, 2940, 2866, 1622, 1491, 1443, 1227, 1134, 754, 557; ¹H NMR (500 MHz, CDCl₃) δ_{H} = 7.23 (m, 2H, ArH), 7.12 (m, 2H, ArH), 6.80 (d, J_{HH} = 2.0 Hz, 1H, ArH), 6.79 (d, J_{HH} = 2.0 Hz, 1H, ArH), 6.68 (s, 1H, ArH), 6.66 (s, 4H, ArH), 4.27 (m, 4H, CH₂), 3.87 (br. s, 4H, NH₂), 2.15 (m, 2H, CH₂), 1.67 (s, 12H, CH₃); ¹³C NMR (126 MHz, CDCl₃) δ_{C} = 144.0, 143.9, 143.3, 142.7, 138.6, 130.1, 127.6, 126.6 (q, $J_{\text{C-F}}$ = 124.11Hz), 125.6, 125.6, 124.9, 123.5, 123.3, 122.5, 44.3, 43.8, 26.9, 18.16; ¹⁹F NMR (471 MHz, CDCl₃) δ_{F} = -58.1; HRMS (EI, m/z): calculated for C₃₄H₃₃F₃N₂ 526.2590, found 526.2581 (M⁺).

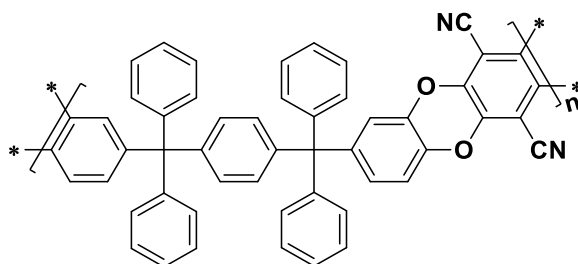
8.3: Polymer Synthesis

8.3.1: Synthesis of Poly-benzodioxanes

X8: General Procedure for synthesis of Poly-benzodioxanes

Under a nitrogen atmosphere, a mixture of biscatechol, tetrafluoroterephthalonitrile and anhydrous DMF or DMAc was mixed at room temperature and then anhydrous potassium carbonate was added. The mixture was stirred for the stated time at the stated temperature. The mixture was added to water (500 ml) with stirring for 30 min. and the *pH* of the aqueous mixture was adjusted to 6 with aqueous HCl and the solid collected by filtration. The crude polymer was dissolved into CHCl₃ and re-precipitated with a suitable solvent (e.g. methanol). The polymer was dried under vacuum oven to afford a yellow powder.

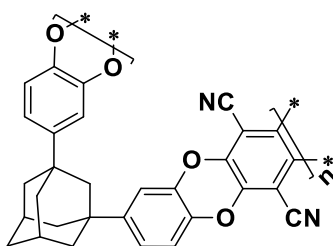
1.1: Synthesis of PIM-BAB4



General procedure (X8) was followed using *p*-bis(3,4-dihydroxyphenyl)diphenylmethyl)benzene (BAB4) (**11**) (1.00 g, 1.59 mmol), tetrafluoroterephthalonitrile (0.32 g, 1.59 mmol), anhydrous DMF (50 ml) and anhydrous potassium carbonate (1.75 g, 12.72 mmol). The mixture was heated to 80 °C for 96 h to afford PIM-BAB4 (0.90 g, 79%); FTIR (solid, cm⁻¹) ν = 2100, 1599, 1503, 1450, 1418, 1267, 1016, 816, 746; ¹H NMR (500 MHz, CDCl₃) δ_{H} = 7.28 (br. d, J_{HH} = 7.8 Hz, 8H, ArH), 7.22 (br., 2H,

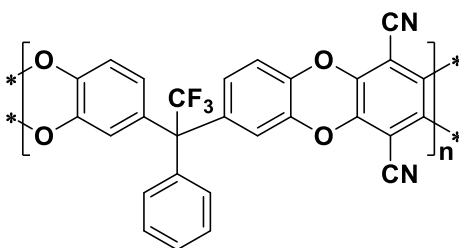
ArH), 7.15 (br. d, $J_{\text{HH}} = 7.8$ Hz, 8H, ArH), 7.07 (br. s, 2H, ArH), 6.86 (br. m, 10H, ArH); ^{13}C NMR (126 MHz, CDCl_3) $\delta_{\text{C}} = 145.8, 145.4, 144.1, 139.3, 138.8, 137.8, 131.0, 130.4, 129.6, 128.8, 128.5, 128.4, 128.4, 127.9, 126.5, 119.9, 115.8, 109.5, 94.4, 64.3$; BET surface area = $144 \text{ m}^2/\text{g}$, total pore volume = $0.38 \text{ cm}^3/\text{g}$; GPC: $M_{\text{n}} = 3020, M_{\text{w}} = 7050 \text{ g/mol}$; TGA analysis: Initial weight loss due to thermal degradation commences at $\sim 457 \text{ }^\circ\text{C}$ with a 30% loss of mass below $1000 \text{ }^\circ\text{C}$.

1.2: Synthesis of PIM-BDA



General procedure (X8) was followed using 1,3-bis(3,4-dihydroxyphenyl)adamantane (1.29 g, 2.83 mmol) (**12**), tetrafluoroterephthalonitrile (0.56 g, 2.83 mmol), anhydrous DMF (100 ml) and anhydrous potassium carbonate (3.12 g, 22.65 mmol). The mixture was heated to $60 \text{ }^\circ\text{C}$ for 1 h to afford PIM-BDA as an insoluble polymer in any common solvent (1.1 g, 82%); FTIR (solid, cm^{-1}) $\nu = 2900, 2849, 1508, 1450, 1414, 1265, 1009, 804, 750$; ^{13}C NMR (100.561 MHz, Solid) $\delta_{\text{C}} = 149.9, 139.3, 121.1, 114.5, 94.3, 44.0, 37.6$; BET surface area = $180 \text{ m}^2/\text{g}$, total pore volume = $0.16 \text{ cm}^3/\text{g}$ at (P/Po = 0.98); TGA analysis: Initial weight loss due to thermal degradation commences at $\sim 458 \text{ }^\circ\text{C}$ with a 39% loss of mass below $1000 \text{ }^\circ\text{C}$.

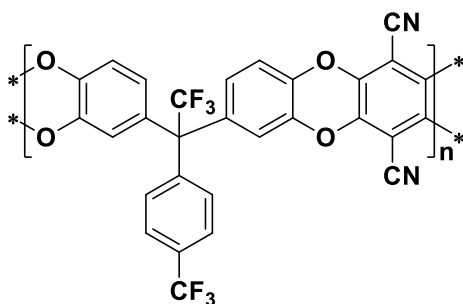
1.3: Synthesis of PIM-TF1



General procedure (X8) was followed using 1,1-bis(3,4-dihydroxyphenyl)-2,2,2-trifluoroacetophenone (TF1) (**13**) (1.00 g, 2.65 mmol), tetrafluoroterephthalonitrile (0.53 g, 2.65 mmol), anhydrous DMF (25 ml) and anhydrous potassium carbonate (2.93 g, 21.20 mmol). The mixture was heated to $90 \text{ }^\circ\text{C}$ for 72 h to afford PIM-TF1 (1.00 g, 70%); FTIR (solid, cm^{-1}) $\nu = 2241, 1604, 1506, 1446, 1260, 1111, 1016, 968, 816, 750, 727$; ^1H NMR (500

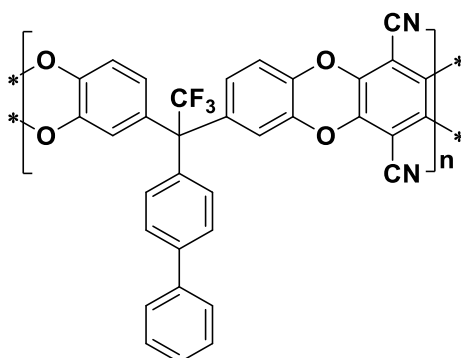
MHz, CDCl₃) δ_H = 7.36 (br. s, 1H, ArH), 7.11 (br. s, 1H, ArH), 7.85 (br. m, 1H, ArH), 6.74 (br. s, 1H, ArH); ¹³C NMR (126 MHz, CDCl₃) δ_C = 139.5, 139.3, 139.2, 138.1, 137.6, 129.6, 129.5, 128.9, 128.8, 127.4, 118.9, 116.9, 109.1, 94.7, 64.2; BET surface area 456 m²/g, total pore volume = 0.37 cm³/g at (P/Po = 0.98); GPC: M_n = 6200, M_w = 13000 g/mol; TGA analysis: Initial weight loss due to thermal degradation commences at ~ 461 °C with a 42% loss of mass below 1000 °C.

1.4: Synthesis of PIM-TF2



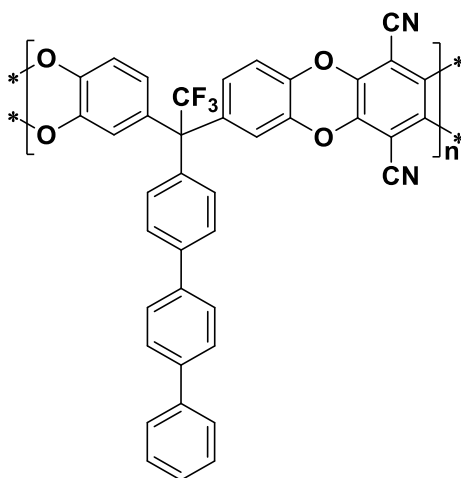
General procedure (X8) was followed using 1,1-bis(3,4-dihydroxyphenyl)-2,2,2-trifluoro-1-(4-trifluorotoluy)ethane (TF2) (**14**) (1.0 g, 2.25 mmol), tetrafluoroterephthalonitrile (0.45 g, 2.25 mol), anhydrous DMAc (30 ml) and anhydrous potassium carbonate (2.48 g, 18.00 mmol). The mixture was heated to 190 °C for 72 h to afford PIM-TF2 (0.5 g, 39%); FTIR (solid, cm⁻¹) ν = 2237, 1618, 1508, 1450, 1325, 1265, 1167, 1117, 1072, 1018, 951, 816, 746, 723; ¹H NMR (500 MHz, CDCl₃) δ_H = 8.19 (br. d, J_{HH} = 8.2 Hz, 2H, ArH), 7.73 (br. d, J_{HH} = 8.2 Hz, 2H, ArH), 7.54 (br. d, J_{HH} = 8.4 Hz, 2H, ArH), 7.05 (br. s, 2H, ArH), 6.70 (br. d, J_{HH} = 8.4 Hz, 2H, ArH); ¹³C NMR (126 MHz, CDCl₃) δ_C = 151.5, 148.6, 148.4, 142.7, 142.2, 139.8, 138.0, 137.3, 134.7, 127.1, 125.8, 120.6, 114.8, 110.0, 65.4; BET surface area = 20 m²/g, total pore volume = 0.08 cm³/g at (P/Po = 0.98); GPC: M_n = 1200, M_w = 2500 g/mol; TGA analysis: Initial weight loss due to thermal degradation commences at ~ 416 °C with a 36% loss of mass below 1000 °C.

1.5: Synthesis of PIM-TF3



General procedure (X8) was followed using 1,1-bis(3,4-dihydroxyphenyl)-2,2,2-trifluoro-1-(4-biphenyl)ethane (TF3) (**15**) (1.00 g, 2.21 mmol), tetrafluoroterephthalonitrile (0.44 g, 2.21 mmol), anhydrous DMF (25 ml) and anhydrous potassium carbonate (2.44 g, 17.68 mmol). The mixture was heated to 90 °C for 7 days to afford PIM-TF3 (0.50 g, 39%); FTIR (solid, cm^{-1}) $\nu = 2243, 1604, 1506, 1454, 1263, 1148, 1111, 1016, 968, 816, 752, 735$; ^1H NMR (500 MHz, CDCl_3) $\delta_{\text{H}} = 8.00$ (br. d, $J_{\text{HH}} = 7.0$ Hz, 2H, ArH), 7.60 (br. d, $J_{\text{HH}} = 7.0$ Hz, 2H, ArH), 7.41 (m, 3H, ArH), 7.19 (br. d, $J_{\text{HH}} = 7.2$ Hz, 2H, ArH), 7.03 (br. d, $J_{\text{HH}} = 7.2$ Hz, 2H, ArH), 6.86 (m, 4H, ArH); ^{13}C NMR (126 MHz, CDCl_3) $\delta_{\text{C}} = 139.6, 135.3, 134.7, 133.5, 132.8, 131.7, 129.6, 129.4, 129.0, 128.0, 127.9, 127.5, 127.4, 126.6, 123.7, 118.6, 116.3, 101.3, 64.9$; BET surface area = 20 m^2/g , total pore volume = 0.08 cm^3/g at ($P/P_0 = 0.98$); GPC: $M_n = 1200$, $M_w = 3500$ g/mol; TGA analysis: Initial weight loss due to thermal degradation commences at $\sim 365^\circ\text{C}$ with a 33% loss of mass below 1000 °C.

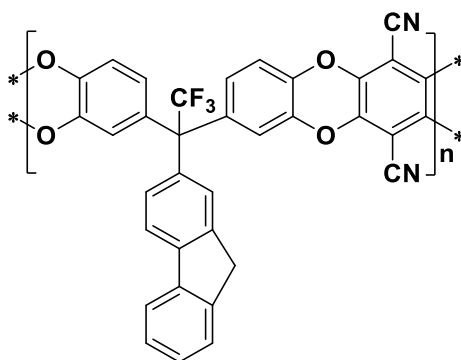
1.6: Synthesis of PIM-TF4



General procedure (X8) was followed using 1,1-bis(3,4-dihydroxyphenyl)-2,2,2-trifluoro-1-(4-terphenyl)ethane (TF4) (**16**) (1.0 g, 1.89 mmol), tetrafluoroterephthalonitrile

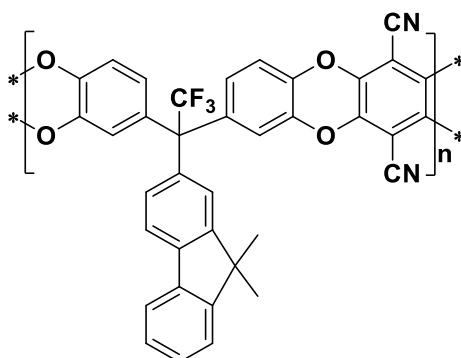
(0.37 g, 1.89 mmol), anhydrous DMAc (25 ml) and anhydrous potassium carbonate (2.09 g, 15.14 mmol). The mixture was heated to 125 °C for 96 h to afford PIM-TF4 (0.60 g, 49%); FTIR (solid, cm^{-1}) $\nu = 2241, 1601, 1506, 1483, 1425, 1306, 1264, 1150, 1111, 1005, 970, 816, 743, 733$; $^1\text{H NMR}$ (500 MHz, CDCl_3) $\delta_{\text{H}} = 7.67$ (br. m, 9H, ArH), 7.42 (br. m, 4H, ArH), 7.02 (br. m, 6H, ArH); $^{13}\text{C NMR}$ (126 MHz, CDCl_3) $\delta_{\text{C}} = 142.9, 141.7, 141.6, 141.0, 139.7, 139.1, 137.9, 136.6, 132.7, 131.9, 131.6, 129.0, 127.2, 126.5, 125.6, 124.3, 122.0, 120.0, 117.2, 116.5, 115.3, 114.9, 65.1$; BET surface area = 20 m^2/g , total pore volume = 0.03 cm^3/g at (P/Po = 0.98); GPC: $M_{\text{n}} = 1500$, $M_{\text{w}} = 2900$; TGA analysis: Initial weight loss due to thermal degradation commences at ~ 335 °C with a 34% loss of mass below 1000 °C.

1.7: Synthesis of PIM-TF5



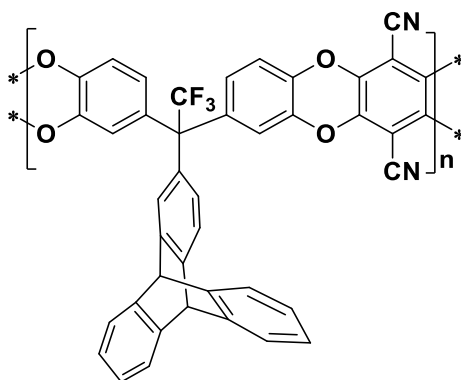
General procedure (X8) was followed using 1,1-bis(3,4-dihydroxyphenyl)-2,2,2-trifluoro-1-(2-fluorenyl)ethane (TF5) (**17**) (1.00 g, 2.15 mmol), tetrafluoroterephthalonitrile (0.43 g, 2.15 mmol), anhydrous DMF (35 ml) and anhydrous potassium carbonate (2.4 g, 17.23 mmol). The mixture was heated to 60 °C for 72 h to afford insoluble polymer in any common solvent PIM-TF5 (1.00 g, 75%); FTIR (solid, cm^{-1}) $\nu = 2239, 1605, 1506, 1450, 1263, 1161, 1113, 1018, 974, 818, 750, 735$; $^{13}\text{C NMR}$ (100.561 MHz, Solid) $\delta_{\text{C}} = 154.0, 145.4, 139.3, 124.1, 65.2, 55.3$; BET surface area = 565 m^2/g , total pore volume = 0.56 cm^3/g at (P/Po = 0.98); TGA analysis: Initial weight loss due to thermal degradation commences at ~ 370 °C with a 37% loss of mass below 1000 °C.

1.8: Synthesis of PIM-TF6



General procedure (X8) was followed using 1,1-bis(3,4-dihydroxyphenyl)-2,2,2-trifluoro-1-(9,9-dimethyl-2-fluorenyl)ethane (TF6) (**18**) (1.00 g, 2.03 mmol), tetrafluoroterephthalonitrile (0.40 g, 2.03 mmol), anhydrous DMAc (20 ml) and anhydrous potassium carbonate (2.24 g, 16.25 mmol). The mixture was heated to 125 °C for 72 h to afford PIM-TF6 (0.60 g, 50%); FTIR (solid, cm^{-1}) $\nu = 2950, 2241, 1607, 1508, 1452, 1263, 1150, 1113, 1078, 1016, 974, 818, 758, 739$; $^1\text{H NMR}$ (500 MHz, CDCl_3) $\delta_{\text{H}} = 7.70$ (br. m, 4H, ArH), 7.38 (br. s, 3H, ArH), 6.93 (br. s, 6H, ArH), 1.62 (br. s, 6H, CH_3); $^{13}\text{C NMR}$ (126 MHz, CDCl_3) $\delta_{\text{C}} = 150.3, 148.7, 146.7, 143.1, 142.8, 141.4, 140.9, 140.1, 135.9, 135.7, 130.1, 128.8, 127.9, 126.8, 124.9, 123.0, 120.6, 119.2, 118.3, 113.7, 107.5, 99.1, 64.0, 46.4, 32.3$; BET surface area = 120 m^2/g total pore volume = 0.17 cm^3/g at (P/Po = 0.98); GPC: $M_{\text{n}} = 1000$, $M_{\text{w}} = 1660$ g/mol; TGA analysis: Initial weight loss due to thermal degradation commences at ~ 309 °C with a 39% loss of mass below 1000 °C.

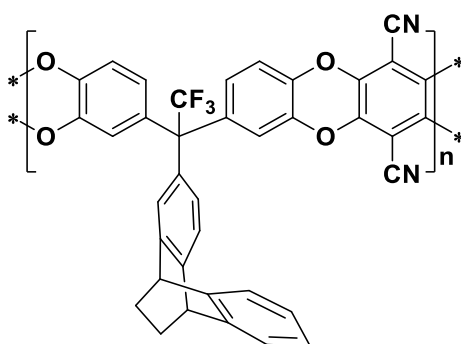
1.9: Synthesis of PIM-TF7



General procedure (X8) was followed using 1,1-bis(3,4-dihydroxyphenyl)-2,2,2-trifluoro-1-(2-tripticycnyl)ethane (TF7) (**19**) (0.8 g, 1.44 mmol), tetrafluoroterephthalonitrile (0.29 g, 1.44 mmol), anhydrous DMAc (20 ml) and anhydrous potassium carbonate (1.59 g,

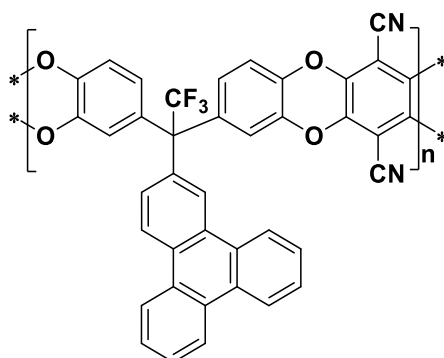
11.52 mmol). The mixture was heated to 190 °C for 72 h to afford PIM-TF7 (0.6 g, 65%); FTIR (solid, cm^{-1}) $\nu = 2237, 1605, 1508, 1452, 1263, 1233, 1161, 1115, 1015, 976, 874, 820, 745$; ^1H NMR (500 MHz, CDCl_3) $\delta_{\text{H}} = 7.46$ (br. m, 8H, ArH), 7.14 (br. s, 3H, ArH), 6.76 (br. m, 6H, ArH), 5.44 (br. s, 1H, CH), 5.35 (br. s, 1H, CH); ^{13}C NMR (126 MHz, CDCl_3) $\delta_{\text{C}} = 148.1, 146.1, 145.6, 145.3, 145.1, 145.0, 143.6, 142.8, 139.6, 129.0, 127.6, 125.6, 125.5, 125.4, 125.3, 124.1, 124.0, 123.9, 123.8, 53.7, 31.0$; BET surface area = 30 m^2/g , total pore volume = 0.16 cm^3/g at (P/Po = 0.98); GPC: $M_{\text{n}} = 600, M_{\text{w}} = 1100$ g/mol; TGA analysis: Initial weight loss due to thermal degradation commences at ~ 350 °C with a 29% loss of mass below 800 °C.

1.10: Synthesis of PIM-TF8



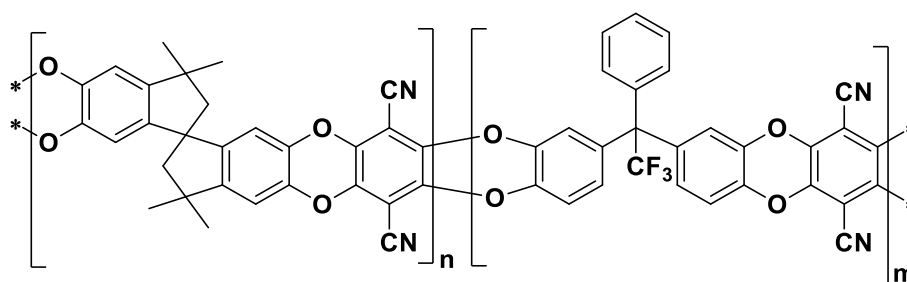
General procedure (X8) was followed using 1,1-bis[(3,4-dihydroxyphenyl)-2,2,2-trifluoro-1-(2-(9,10-dihydro-9,10-ethanoanthracenyl))]ethane (TF8) (**20**) (0.80 g, 1.58 mmol), tetrafluoroterephthalonitrile (0.31 g, 1.58 mmol), anhydrous DMF (40 ml) and anhydrous potassium carbonate (1.75 g, 12.68 mmol). The mixture was heated to 70 °C for 96 h to afford PIM-TF8 (0.80 g, 81%); FTIR (solid, cm^{-1}) $\nu = 2943, 2239, 1605, 1506, 1449, 1265, 1163, 1113, 1018, 974, 818, 752, 729$; ^1H NMR (500 MHz, CDCl_3) $\delta_{\text{H}} = 7.18$ (br. m, 4H, ArH), 6.97 (br.s, 1H, ArH), 6.79 (br. m, 8H, ArH), 4.31 (br., 4H, CH_2), 1.71 (br. s, 2H, CH); ^{13}C NMR (126 MHz, CDCl_3) $\delta_{\text{C}} = 144.5, 144.3, 143.4, 139.4, 139.3, 139.2, 137.9, 135.4, 127.6, 127.1, 125.9, 125.9, 124.2, 123.6, 123.5, 118.8, 116.8, 109.2, 94.7, 64.4, 44.4, 43.8$; BET surface area = 400 m^2/g , total pore volume = 0.34 cm^3/g at (P/Po = 0.98); GPC: $M_{\text{n}} = 8900, M_{\text{w}} = 17000$; TGA analysis: Initial weight loss due to thermal degradation commences at ~ 278 °C with a 4% consistent with the loss of an ethylene fragment from the ethanoanthracene unit via a retro Diels-Alder reaction²⁰² then at ~ 450 °C with a 30% loss of mass below 1000 °C.

1.11: Synthesis of PIM-TF9



General procedure (X8) was followed using 1,1-bis(3,4-dihydroxyphenyl)-2,2,2-trifluoro-1-(2-triphenyl)ethane (TF9) (**21**) (1.00 g, 1.90 mmol), tetrafluoroterephthalonitrile (0.38 g, 1.9 mmol), anhydrous DMF (60 ml) and anhydrous potassium carbonate (2.10 g, 15.19 mmol). The mixture was heated to 50 °C for 72 h to afford insoluble polymer in common solvent PIM-TF9 (1.1 g, 90%); FTIR (solid, cm⁻¹) ν = 2241, 1604, 1506, 1450, 1425, 1255, 1166, 1113, 1018, 970, 818, 752, 731; ¹³C NMR (100.561 MHz, Solid) δ_C = 139.3, 129.4, 123.6, 108.0, 94.3, 64.4, 24.7; BET surface area 405 m²/g, total pore volume = 0.35 ml/g at (P/Po = 0.98); TGA analysis: Initial weight loss due to thermal degradation commences at ~ 438 °C with a 34% loss of mass below 1000 °C.

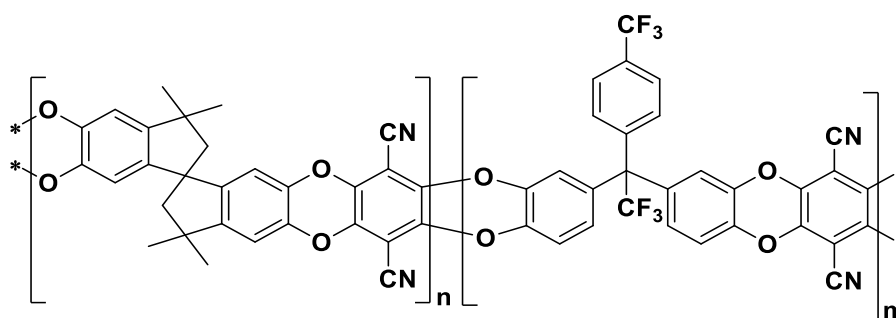
1.12: Synthesis of co-polymer PIM-1-co-TF1



General procedure (X8) was followed using 1,1-bis(3,4-dihydroxyphenyl)-2,2,2-trifluoroacetophenone (TF1) (**13**) (0.5 g, 1.32 mmol), 5,5',6,6'-tetra-hydroxy-3,3,3',3'-tetramethyl-1,1'-spirobisindane (0.45 g, 1.32 mmol), tetrafluoroterephthalonitrile (0.53 g, 2.65 mmol), anhydrous DMF (20 ml) and anhydrous potassium carbonate (2.93 g, 21.25 mmol). The mixture was heated to 65 °C for 72 h to afford PIM-1-TF1 (0.80 g, 63%); FTIR (solid, cm⁻¹) ν = 2955, 2862, 2241, 1605, 1508, 1447, 1263, 1211, 1169, 1152, 1109, 1013, 976, 959, 876, 813, 752; ¹H NMR (500 MHz, CDCl₃) δ_H = 7.38 (br. s, 2H, ArH), 7.12 (br. m, 2H, ArH), 6.96 (br. m, 2H, ArH), 6.76 (br. m, 5H, ArH), 6.42 (br. s, 4H, ArH), 1.57 (br. s, 4H, CH₂), 1.33 (br.

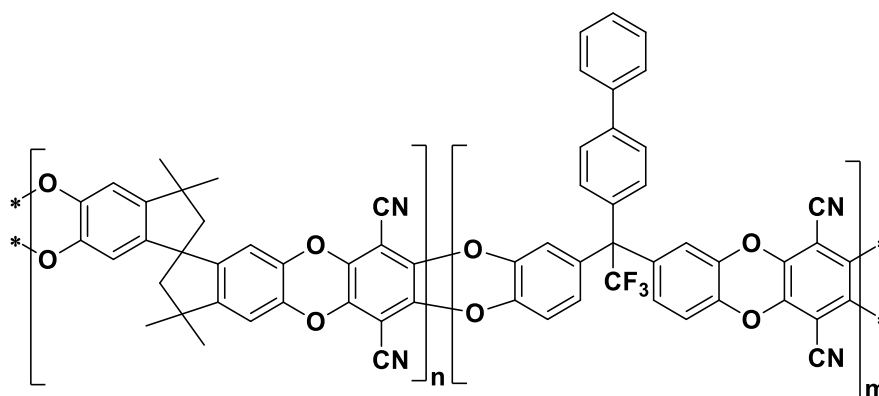
s, 12H, CH_3); ^{13}C NMR (126 MHz, $CDCl_3$) δ_C = 150.1, 147.2, 139.8, 139.6, 139.5, 139.4, 138.9, 129.6, 128.9, 127.4, 118.9, 116.9, 112.5, 110.71, 109.3, 94.6, 64.2, 59.0, 57.3, 51.0, 31.5, 30.1; BET surface area = 600 m^2/g , total pore volume = 0.45 cm^3/g at (P/P_0 = 0.98); GPC: M_n = 35000, M_w = 66000; TGA analysis: A 5% loss of weight occurred at between 50-235 $^\circ C$. Initial weight loss due to thermal degradation commences at ~ 452 $^\circ C$ with a 32% loss of mass below 1000 $^\circ C$.

1.13: Synthesis of co-polymer PIM-1-co-TF2



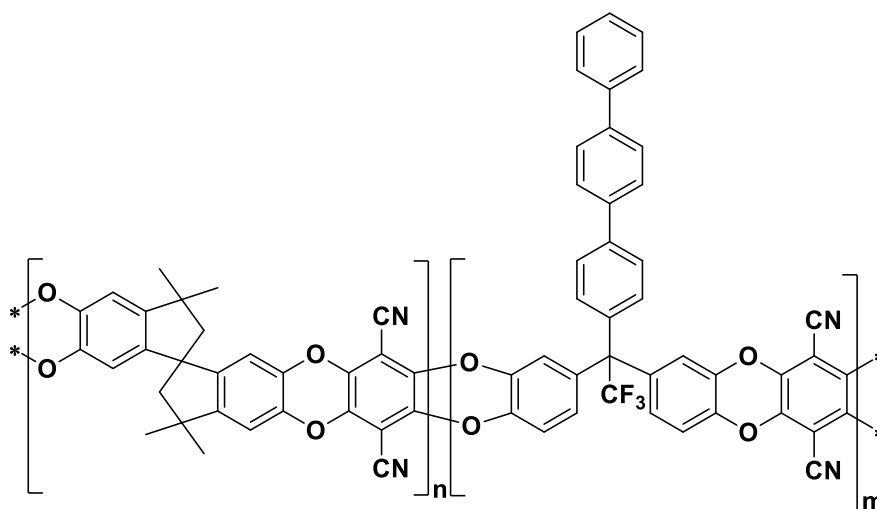
General procedure (X8) was followed using 1,1-bis(3,4-dihydroxyphenyl)-2,2,2-trifluoro-1-(4-trifluorotolyl)ethane (TF2) (**14**) (0.50 g, 1.11 mmol), 5,5',6,6'-tetrahydroxy-3,3,3',3'-tetramethyl-1,1'-spirobisindane (0.38 g, 1.11 mmol), tetrafluoroterephthalonitrile (0.45 g, 2.25 mmol), anhydrous DMF (20 ml) and anhydrous potassium carbonate (2.45 g, 17.76 mmol). The mixture was heated to 90 $^\circ C$ for 7 days to afford PIM-1-TF2 (1.00 g, 85%); FTIR (solid, cm^{-1}) ν = 2951, 2833, 2241, 1510, 1450, 1325, 1308, 1288, 1263, 1233, 1170, 1123, 1111, 1072, 1012, 980, 961, 817, 752; 1H NMR (500 MHz, $CDCl_3$) δ_H = 7.64 (br. s, 2H, ArH), 7.28 (br. s, 2H, ArH), 7.00 (br. s, 2H, ArH), 6.80 (br. m, 6H, ArH), 6.42 (br. s, 2H, ArH), 2.35 (br. s, 4H, CH_2), 1.35 (br., 12H, CH_3); ^{13}C NMR (126 MHz, $CDCl_3$) δ_C = 150.1, 147.3, 142.2, 139.9, 139.7, 139.5, 139.3, 138.7, 136.6, 130.1, 127.3, 125.9, 118.8, 117.1, 112.5, 94.4, 59.0, 57.3, 43.8, 31.5, 30.1; BET surface area = 505 m^2/g , total pore volume = 0.35 cm^3/g at (P/P_0 = 0.9814); GPC: M_n = 3340, M_w = 4270 g/mol; TGA analysis: Initial weight loss due to thermal degradation commences at ~ 452 $^\circ C$ with a 34% loss of mass below 800 $^\circ C$.

1.14: Synthesis of copolymers PIM-1-co-TF3



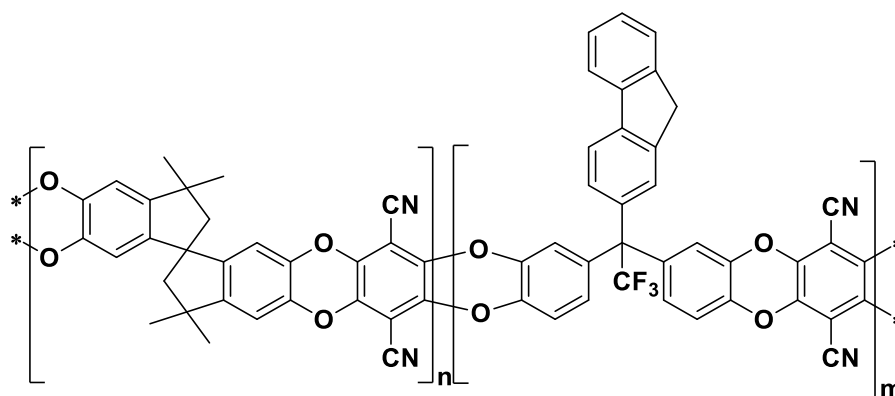
General procedure (X8) was followed using 1,1-bis(3,4-dihydroxyphenyl)-2,2,2-trifluoro-1-(4-biphenyl)ethane (TF3) (**15**) (0.50 g, 1.10 mmol), 5,5',6,6'-tetrahydroxy-3,3,3',3'-tetramethyl-1,1'-spirobisindane (0.37 g, 1.10 mmol), tetrafluoroterephthalonitrile (0.44 g, 2.21 mmol), anhydrous DMF (50 ml) and anhydrous potassium carbonate (2.24 g, 17.68 mmol). The mixture was heated to 65 °C for 56 h to afford PIM-1-TF3 (1.00 g, 92%); FTIR (solid, cm^{-1}) $\nu = 2955, 2864, 2241, 1604, 1508, 1447, 1263, 1211, 1168, 1152, 1009, 978, 959, 876, 814, 752$; ^1H NMR (500 MHz, CDCl_3) $\delta_{\text{H}} = 7.60$ (br. s, 2H, ArH), 7.40 (br. m, 4H, ArH), 7.18 (br. m, 2H, ArH), 6.95 (br. m, 4H, ArH), 6.81 (br. m, 5H, ArH), 6.42 (br. m, 2H, ArH), 1.54 (br. s, 4H, CH_2), 1.33 (br. s, 12H, CH_3); ^{13}C NMR (126 MHz, CDCl_3) $\delta_{\text{C}} = 150.0, 139.8, 139.7, 139.6, 139.5, 139.4, 139.3, 138.9, 137.4, 130.0, 129.0, 128.9, 128.0, 127.4, 127.3, 120.9, 118.9, 116.9, 112.5, 110.7, 109.3, 94.6, 59.0, 57.3, 43.8, 31.5, 30.1$; BET surface area $660 = \text{m}^2/\text{g}$, total pore volume = $0.51 \text{ cm}^3/\text{g}$ at ($P/P_0 = 0.98$); GPC: $M_n = 30000$, $M_w = 61000 \text{ g/mol}$; TGA analysis: Initial weight loss due to thermal degradation commences at ~ 427 °C with a 32% loss of mass below 1000 °C.

1.15: Synthesis of copolymers PIM-1-co-TF4



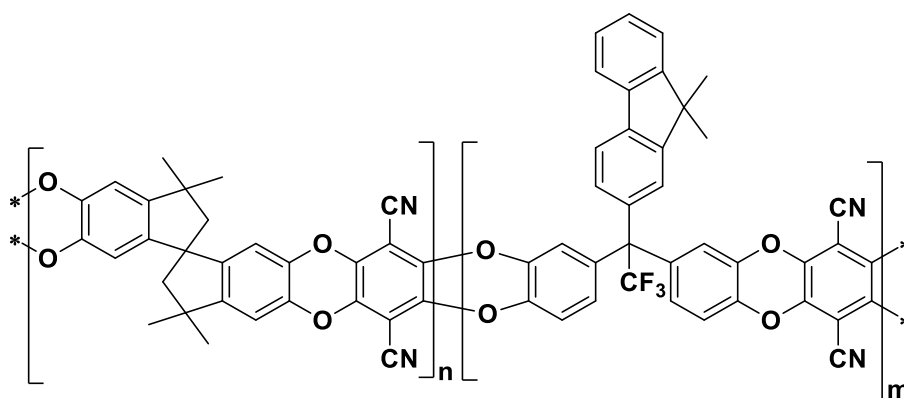
General procedure (X8) was followed using 1,1-bis(3,4-dihydroxyphenyl)-2,2,2-trifluoro-1-(4-terphenyl)ethane (TF4) (**16**) (0.50 g, 0.94 mmol), 5,5',6,6'-tetrahydroxy-3,3,3',3'-tetramethyl-1,1'-spirobisindane (0.32 g, 0.94 mmol), tetrafluoroterephthalonitrile (0.37 g, 1.89 mmol), anhydrous DMF (40 ml) and anhydrous potassium carbonate (2.09 g, 15.12 mmol). The mixture was heated to 100 °C for 7 days to afford PIM-1-TF4 (0.7 g, 67%); FTIR (solid, cm^{-1}) $\nu = 2957, 2868, 2241, 1604, 1504, 1447, 1308, 1263, 1166, 1152, 1013, 978, 875, 816, 752$; ^1H NMR (500 MHz, CDCl_3) $\delta_{\text{H}} = 7.66$ (br. m, 8H, ArH), 7.20 (br. m, 4H, ArH), 6.95 (br. m, 4H, ArH), 6.81 (br. s, 4H, ArH), 6.42 (br. m, 3H, ArH), 2.04 (br. s, 4H, CH_2), 1.31 (br. s, 12H, CH_3); ^{13}C NMR (126 MHz, CDCl_3) $\delta_{\text{C}} = 139.8, 139.6, 139.4, 138.8, 135.3, 131.2, 130.2, 130.1, 129.0, 127.7, 127.6, 127.3, 127.1, 126.9, 126.8, 126.2, 125.3, 124.7, 124.5, 123.8, 123.5, 122.5, 122.3, 118.9, 118.4, 59.0, 57.3, 43.8, 31.5, 30.1$; BET surface area = 460 m^2/g , total pore volume = 0.35 cm^3/g at ($P/P_0 = 0.98$); GPC: $M_n = 2800$, $M_w = 4800$ g/mol; TGA analysis: Initial weight loss due to thermal degradation commences at ~ 443 °C with a 28% loss of mass below 1000 °C.

1.16: Synthesis of copolymers PIM-1-co-TF5



General procedure (X8) was followed using 1,1-bis(3,4-dihydroxyphenyl)-2,2,2-trifluoro-1-(2-fluorenyl)ethane (TF5) (**17**) (0.70 g, 1.50 mmol), 5,5',6,6'-tetrahydroxy-3,3,3',3'-tetramethyl-1,1'-spirobisindane (0.51 g, 1.50 mmol), tetrafluoroterephthalonitrile (0.60 g, 3.01 mmol), anhydrous DMF (40 ml) and anhydrous potassium carbonate (3.32 g, 24.08 mmol). The mixture was heated to 65 °C for 72 h to afford insoluble polymer in all common solvents. PIM-1-TF5 (1.30 g, 86%); FTIR (solid, cm^{-1}) $\nu = 2957, 2864, 2239, 1605, 1506, 1447, 1265, 1211, 1163, 1109, 1013, 982, 876, 816, 752$; ^{13}C NMR (100.561 MHz, Solid) $\delta_{\text{C}} = 148.7, 139.8, 127.4, 120.1, 111.5, 94.8, 78.3, 64.9, 57.9, 43.7, 36.6, 31.0$; BET surface area = 700 m^2/g , total pore volume = 0.55 cm^3/g at (P/Po = 0.98); TGA analysis: A 5% loss of weight occurred at between 50-165 °C. Initial weight loss due to thermal degradation commences at ~ 450 °C with a 27% loss of mass below 1000 °C.

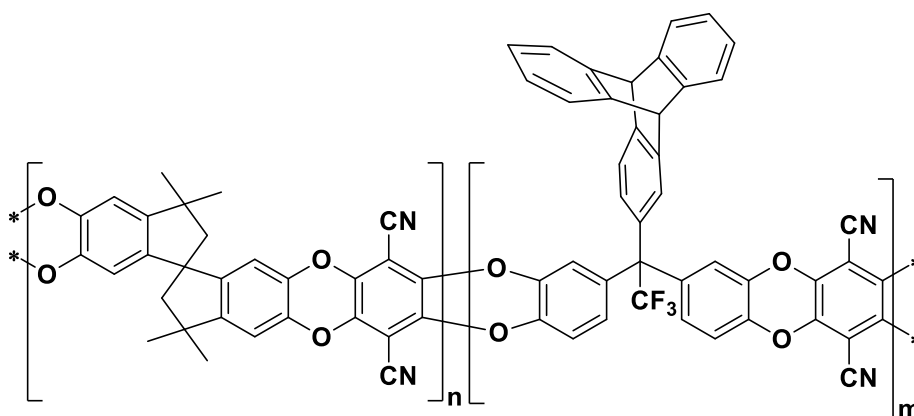
1.17: Synthesis of copolymers PIM-1-co-TF6



General procedure (X8) was followed using 1,1-bis(3,4-dihydroxyphenyl)-2,2,2-trifluoro-1-(9,9-dimethyl-2-fluorenyl)ethane (TF6) (**18**) (1.0 g, 2.03 mmol), 5,5',6,6'-tetrahydroxy-3,3,3',3'-tetramethyl-1,1'-spirobisindane (0.69 g, 2.03 mmol),

tetrafluoroterephthalonitrile (0.81 g, 4.06 mmol), anhydrous DMF (50 ml) and anhydrous potassium carbonate (4.48 g, 32.48 mmol). The mixture was heated to 100 °C for 72 h to afford PIM-1-TF6 (1.80 g, 80%); FTIR (solid, cm^{-1}) $\nu = 2957, 2862, 2241, 1508, 1449, 1364, 1306, 1263, 1168, 1151, 1109, 1013, 978, 876, 816, 738$; ^1H NMR (500 MHz, CDCl_3) $\delta_{\text{H}} = 7.68$ (br. d, $J = 26.4$ Hz, 1H, ArH), 7.37 (br. m, 3H, ArH), 7.23 (br. m, 3H, ArH), 6.88 (br. m, 8H, ArH), 6.42 (br. s, 2H, ArH), 2.17 (br. s, 4H, CH_2), 1.43 (br. s, 6H, CH_3), 1.33 (br. s, 12H, CH_3); ^{13}C NMR (126 MHz, CDCl_3) $\delta_{\text{C}} = 154.1, 149.9, 147.2, 147.1, 139.8, 139.6, 139.5, 139.4, 138.9, 138.1, 137.9, 137.8, 137.1, 128.1, 127.5, 127.3, 123.7, 122.8, 120.6, 118.9, 118.8, 112.5, 110.7, 109.3, 94.5, 58.9, 57.3, 47.2, 43.8, 31.5, 30.1, 27.1$; BET surface area = 500 m^2/g , total pore volume = 0.37 cm^3/g at (P/Po = 0.98); GPC: $M_{\text{n}} = 2000$, $M_{\text{w}} = 4000$ g/mol; TGA analysis: 4% loss of weight occurred at between 117-376 °C. Initial weight loss due to thermal degradation commences at ~ 433 °C with a 30% loss of mass below 1000 °C.

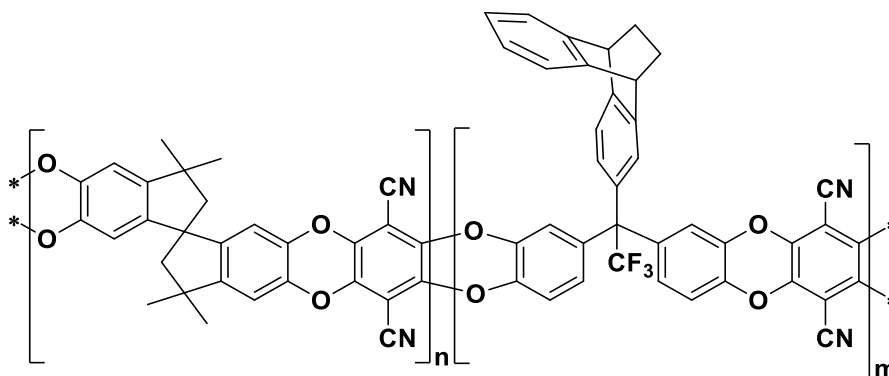
1.18: Synthesis of Copolymers of PIM-1-co-TF7



General procedure (X8) was followed using 1,1-bis(3,4-dihydroxyphenyl)-2,2,2-trifluoro-1-(2-triptyceny)ethane (TF7) (**19**) (0.8 g, 1.44 mmol), 5,5',6,6'-tetrahydroxy-3,3,3',3'-tetramethyl-1,1'-spirobisindane (0.49 g, 1.44 mmol), tetrafluoroterephthalonitrile (0.58 g, 2.89 mmol), anhydrous DMF (50 ml) and anhydrous potassium carbonate (3.19 g, 23.12 mmol). The mixture was heated to 65 °C for 72 h to afford PIM-1-TF7 (0.80 g, 55%); FTIR (solid, cm^{-1}) $\nu = 2955, 2864, 2241, 1506, 1449, 1308, 1288, 1265, 1211, 1169, 1109, 1012, 978, 876, 764$; ^1H NMR (500 MHz, CDCl_3) $\delta_{\text{H}} = 7.66$ (br. m, 6H, ArH), 7.39 (br. m, 2H, ArH), 6.97 (br. m, 7H, ArH), 6.41 (br. s, 6H, ArH), 2.34 (br. s, 1H, CH), 2.16 (br. s, 1H, CH), 1.65 (s, 4H, CH_2), 1.34 (br. s, 12H, CH_3); ^{13}C NMR (126 MHz, CDCl_3) $\delta_{\text{C}} = 149.9, 147.1, 140.6, 139.7, 139.4, 138.8, 137.4, 129.0, 127.7, 127.6, 127.3, 127.2, 127.1, 127.0, 126.7, 125.6, 118.9, 116.9, 112.5, 110.7, 109.3, 94.5, 59.0, 58.9, 57.3, 43.8, 31.5, 30.1$; BET surface area = 572 m^2/g , total pore

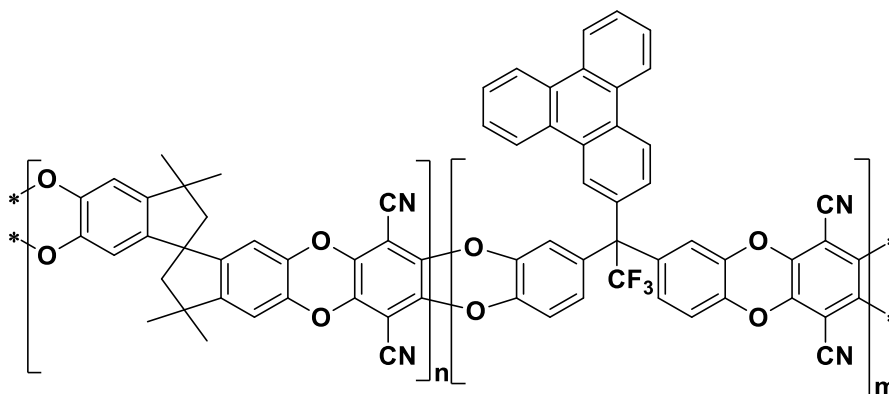
volume = 0.42 cm³/g at (P/Po = 0.98); GPC: M_n = 2100, M_w = 5000 g/mol; TGA analysis: Initial weight loss due to thermal degradation commences at ~ 370 °C with a 25% loss of mass below 1000 °C.

1.19: Synthesis of copolymers PIM-1-co-TF8



General procedure (X8) was followed using 1,1-bis(3,4-dihydroxyphenyl)-2,2,2-trifluoro-1-(2-ethanoanthracenyl)ethane (TF8) (**20**) (0.80 g, 1.58 mmol), 5,5',6,6'-tetrahydroxy-3,3,3',3'-tetramethyl-1,1'-spirobisindane (0.54 g, 1.58 mmol), tetrafluoroterephthalonitrile (0.63 g, 3.17 mmol), anhydrous DMF (50 ml) and anhydrous potassium carbonate (3.50 g, 25.36 mmol). The temperature gently risen to 65 °C for 72 h to afford PIM-1-TF8 (1.40 g, 86%) as a yellow powder; FTIR (solid, cm⁻¹) ν = 2955, 2868, 2241, 1604, 1506, 1447, 1263, 1213, 1165, 1109, 1010, 982, 959, 875, 752; ¹H NMR (500 MHz, CDCl₃) δ_H = 7.26 (br. m, 4H, ArH), 7.11 (br. s, 2H, ArH), 6.96 (br. m, 2H, ArH), 6.80 (br. m, 7H, ArH), 6.42 (br. s, 2H, ArH), 3.49 (br. s, 4H, CH₂), 2.17 (br. s, 2H, CH), 1.62 (br. s, 4H, CH₂), 1.34 (br. s, 12H, CH₃); ¹³C NMR (126 MHz, CDCl₃) δ_C = 150.0, 149.9, 147.2, 144.4, 143.4, 139.7, 139.5, 139.4, 138.9, 127.6, 127.1, 125.9, 124.3, 123.6, 123.5, 116.8, 112.5, 110.7, 109.3, 94.5, 59.0, 57.3, 44.4, 43.8, 31.5, 31.1, 30.1; BET surface area = 583 m²/g, total pore volume = 0.43 cm³/g at (P/Po = 0.9814); GPC: M_n = 12000, M_w = 20000 g/mol; TGA analysis: A 5% loss of weight occurred at between 50-170 °C. Initial weight loss due to thermal degradation commences at ~ 275 °C with a 2% loss of mass below 434 °C consistent with the loss of an ethylene fragment from the ethanoanthracene unit via a retro Diels-Alder reaction²⁰² and a further 35% loss of mass below 1000 °C.

1.20: Synthesis of copolymers PIM-1-co-TF9



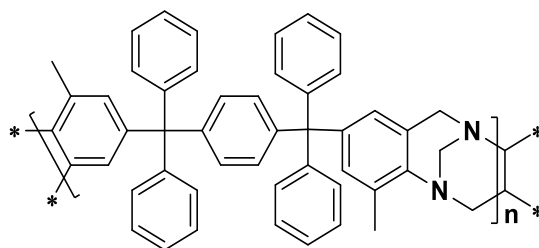
General procedure (X8) was followed using 1,1-bis(3,4-dihydroxyphenyl)-2,2,2-trifluoro-1-(4-terphenyl)ethane (TF9) (**21**) (0.5 g, 0.95 mmol), 5,5',6,6'-tetrahydroxy-3,3,3',3'-tetramethyl-1,1'-spirobisindane (0.32 g, 0.95 mmol), tetrafluoroterephthalonitrile (0.38 g, 1.90 mmol), anhydrous DMF (70 ml) and anhydrous potassium carbonate (2.10 g, 15.19 mmol). The mixture was heated to 65 °C for 72 h to afford insoluble polymer in common solvent PIM-1-TF9 (1.00 g, 95%); FTIR (solid, cm^{-1}) $\nu = 2957, 2864, 2239, 1607, 1506, 1447, 1263, 1211, 1169, 1150, 1109, 1013, 978, 876, 754$; ^{13}C NMR (100.561 MHz, Solid) $\delta_{\text{C}} = 149.2, 139.5, 129.4, 122.9, 109.7, 94.5, 64.9, 57.6, 43.4, 29.8$; BET surface area = 452 m^2/g , total pore volume = 0.35 cm^3/g at (P/Po = 0.98); TGA analysis: Initial weight loss due to thermal degradation commences at ~ 433 °C with a 32% loss of mass below 1000 °C.

8.3.2: Synthesis of Tröger Base Polymers (PIM-TB)

X9: General Procedure of PIM-TB

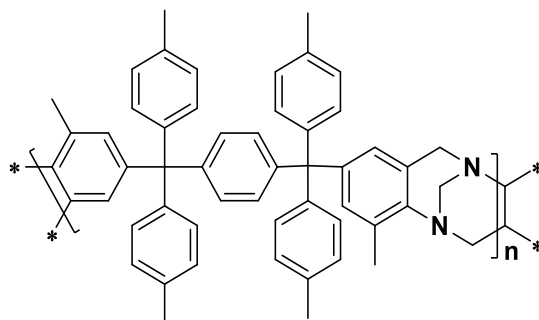
The diamino monomer was dissolved or suspended into dimethoxymethane and the mixture was cooled in an ice bath. TFA was added drop-wise and the mixture was allowed to stir at room temperature for an appropriate time. The viscous mixture was slowly poured into aqueous ammonium hydroxide solution and stirred vigorously for 2 h during which a solid was formed. The solid was collected by filtration, washed with water, methanol and then acetone until the washings were clear. The resulting powder was dissolved in chloroform and re-precipitated with methanol for three times then dissolved in chloroform and the solution added drop-wise into petroleum ether with vigorous stirring. The polymer as a fine powder was collected by filtration. The polymer was dried in a vacuum oven at 120 °C for 5 h.

2.1: Synthesis of PIM-BAB1-TB



General procedure (X9) was followed using *p*-bis(4-amino-3-methylphenyldiphenylmethyl)benzene (BAB1) (**24**) (3.00 g, 4.80 mmol), DMM (1.79 g, 23.48 mmol), DCM (5 ml) and TFA (30 ml). The mixture was stirred for 72 h to afford PIM-BAB1-TB (2.51 g, 79%) as an off-white powder; FTIR (solid, cm^{-1}) ν = 1680, 1597, 1489, 1477, 1442, 744, 700; ^1H NMR (500 MHz, CDCl_3) δ_{H} = 7.31 (br. m, 20H, ArH), 7.22 (br. d, $J_{\text{HH}} = 7.5$ Hz, 2H, ArH), 7.17 (br. d, $J_{\text{HH}} = 7.5$ Hz, 2H, ArH), 6.81 (br. s, 2H, ArH), 6.61 (br. s, 2H, ArH), 4.45 (br. s, 2H, N- CH_2 -Ar), 4.25 (br. s, 2H, N- CH_2 -N), 3.87 (br. s, 2H, N- CH_2 -Ar), 2.27 (br. s, 6H, CH_3); ^{13}C NMR (126 MHz, CDCl_3) δ_{C} = 147.0, 144.6, 144.3, 141.8, 132.6, 131.7, 131.4, 130.4, 128.0, 127.4, 126.7, 126.5, 126.0, 67.5, 64.3, 55.1, 17.5; BET surface area = 40 m^2/g , total pore volume = 0.09 cm^3/g at ($P/P_0 = 0.98$); GPC: $M_n = 11400$, $M_w = 19400$ g/mol; TGA analysis: Initial weight loss due to thermal degradation commences at ~ 390 $^\circ\text{C}$ with a 6% and a further 38% mass loss below 800 $^\circ\text{C}$.

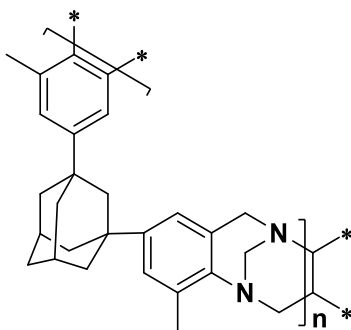
2.2: PIM-BAB3-TB



General procedure (X9) was followed using *p*-bis-(4-amino-3-methylphenyldiphenylmethyl) benzene (BAB3) (**26**) (2.00 g, 2.95 mmol), DMM (1.1 g, 14.8 mmol), DCM (5 ml) and TFA (20 ml). The mixture was stirred for 5 days to afford from PIM-BAB3-TB (1.80 g, 83%) as an off-white powder; FTIR (solid) ν = 1724, 1676, 1509, 1279, 1192, 1007, 1020, 810, 708; ^1H NMR (500 MHz, CDCl_3) δ_{H} = 6.96 (br. m, 24H, ArH), 4.41 (br. s, 4H, N- CH_2 -Ar), 3.83 (br. s, 2H, N- CH_2 -N), 2.29 (br. s, 12H, CH_3), 2.17 (br. s, 6H, CH_3);

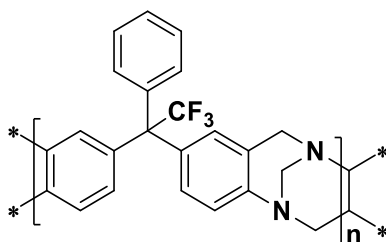
^{13}C NMR (126 MHz, CDCl_3) $\delta_{\text{C}} = 145.8, 144.3, 139.9, 138.7, 135.6, 133.7, 132.8, 132.6, 131.5, 130.4, 130.3, 128.4, 128.3, 67.0, 63.6, 55.1, 31.1, 21.0$; BET surface area = $22 \text{ m}^2/\text{g}$, total pore volume = $0.04 \text{ cm}^3/\text{g}$ at ($P/P_0 = 0.98$); GPC: $M_n = 3500, M_w = 5500 \text{ g/mol}$; TGA analysis: Initial weight loss due to thermal degradation commences at $\sim 325 \text{ }^\circ\text{C}$ with a 14% and a further 48% mass loss below $800 \text{ }^\circ\text{C}$.

2.3: Synthesis of PIM-AD2-TB



General procedure (X9) was followed using 1,3-bis(3-methyl-4-aminophenyl)adamantane (AD2) (**27**) (1.00 g, 2.89 mmol), DMM (1.50 g, 14.40 mmol), DCM (2ml) and TFA (25 ml). The mixture was stirred for 72 h to afford PIM-AD2-TB (0.8 g, 70%) as a pale yellow powder; FTIR (solid, cm^{-1}) $\nu = 2903, 2849, 1672, 1578, 1514, 14881, 1449, 1350, 1105, 951, 800, 737$; ^1H NMR (500 MHz, CDCl_3) $\delta_{\text{H}} = 7.02$ (br. d, $J_{\text{HH}} = 16.1 \text{ Hz}$, 2H, ArH), 6.72 (br. d, $J_{\text{HH}} = 16.1 \text{ Hz}$, 2H, ArH), 6.66 (br. s, 2H, ArH), 4.55 (br. s, 4H, N- CH_2 -Ar), 3.97 (br.s, 2H, N- CH_2 -N), 2.28 (br. m, 12H, CH_2 & CH), 1.90 (br. m, 6H, CH_3); ^{13}C NMR (126 MHz, CDCl_3) $\delta_{\text{C}} = 147.1, 131.9, 129.8, 129.1, 125.7, 121.0, 67.3, 56.3, 39.6, 37.1, 31.1, 29.9, 29.2, 17.7$; BET surface area = $30 \text{ m}^2/\text{g}$, total pore volume = $0.09 \text{ cm}^3/\text{g}$ at ($P/P_0 = 0.98$); GPC: $M_n = 1350, M_w = 2500 \text{ g/mol}$; TGA analysis: Initial weight loss due to thermal degradation commences at $\sim 360 \text{ }^\circ\text{C}$ with a 70% loss of mass below $800 \text{ }^\circ\text{C}$.

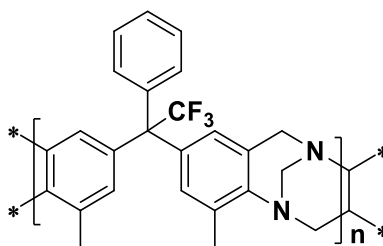
2.4: Synthesis of PIM-TFA1-TB



General procedure (X9) was followed using 1,1-bis(4-aminophenyl)-1-phenyl-2,2,2-trifluoroethane (TFA1) (**32**) (2.00 g, 5.84 mmol), DMM (1.33 g, 17.52 mmol) and TFA (15

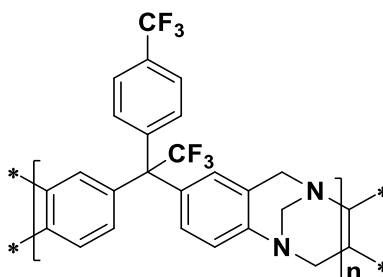
ml). The mixture was stirred for 1h to afford PIM-TFA1-TB (2.10 g, 91%) as a brown powder; FTIR (solid, cm^{-1}) $\nu = 1610, 1510, 1227, 1136, 815, 700$; ^1H NMR (500 MHz, CDCl_3) $\delta_{\text{H}} = 6.85$ (br. m, 11H, ArH), 3.77 (br. m, 6H, N- CH_2 -Ar & N- CH_2 -N); ^{13}C NMR (126 MHz, CDCl_3) $\delta_{\text{C}} = 143.0, 132.4, 132.1, 131.7, 131.4, 131.1, 131.0, 130.0, 128.4, 128.1, 63.7, 55.6, 51.0$; BET surface area = $38 \text{ m}^2/\text{g}$, total pore volume = $0.13 \text{ cm}^3/\text{g}$ at (P/Po = 0.98); the polymer was partial soluble in CHCl_3 ; TGA analysis: Initial weight loss due to thermal degradation commences at $\sim 325 \text{ }^\circ\text{C}$ with a 34% and a further 16% loss of mass below $1000 \text{ }^\circ\text{C}$.

2.5: Synthesis of PIM-TFA2-TB



General procedure (X9) was followed using 1,1-bis(3-methyl-4-aminophenyl)-1-phenyl-2,2,2-trifluoroethane (TFA2) (**33**) (4.00 g, 10.79 mmol), DMM (2.47 g, 32.40 mmol) and TFA (30 ml). The mixture was stirred for 72 h to afford PIM-TFA2-TB (3.52 g, 78%) as an off-white powder; FTIR (solid, cm^{-1}) $\nu = 2947, 2891, 2849, 1682, 1479, 1221, 1144, 1123, 719, 700$; ^1H NMR (500 MHz, CDCl_3) $\delta_{\text{H}} = 6.71$ (br. m, 9H, ArH), 4.46 (br. s, 2H, N- CH_2 -Ar), 4.27 (br. s, 2H, N- CH_2 -Ar), 3.87 (br. m, 2H, N- CH_2 -N), 2.96 (br. s, 6H, CH_3); ^{13}C NMR (126 MHz, CDCl_3) $\delta_{\text{C}} = 145.7, 140.5, 135.4, 132.8, 130.5, 130.0, 128.1, 127.7, 127.6, 126.0, 67.4, 64.5, 55.0, 17.5$; BET surface area = $220 \text{ m}^2/\text{g}$, total pore volume = $0.30 \text{ cm}^3/\text{g}$ at (P/Po = 0.98); GPC: $M_{\text{n}} = 16500$, $M_{\text{w}} = 30000 \text{ g/mol}$; TGA analysis: Initial weight loss due to thermal degradation commences at $\sim 353 \text{ }^\circ\text{C}$ with a 10% and a further 31% loss of mass below $1000 \text{ }^\circ\text{C}$.

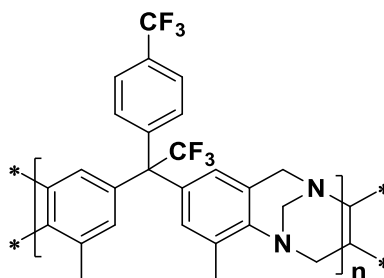
2.6: Synthesis of PIM-TFA4-TB



General procedure (X9) was followed using 1,1-bis(4-aminophenyl)-1-(4-trifluorotoluy)l)-2,2,2-trifluoroethane (TFA4) (**35**) (4.00 g, 9.75 mmol), DMM (2.23 g, 29.25

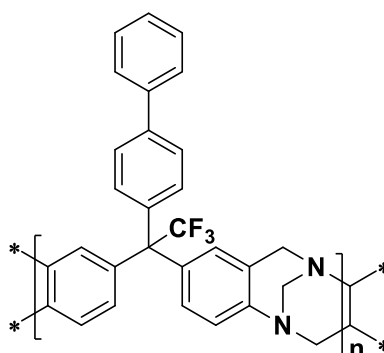
mmol) and TFA (30 ml). The mixture was stirred for 72 h to afford PIM-TFA4-TB (3.20 g, 71%) as a white powder; FTIR (solid, cm^{-1}) $\nu = 1618, 1493, 1412, 1325, 1233, 1209, 1120, 1072, 1018, 964, 931, 818, 610$; ^1H NMR (500 MHz, CDCl_3) $\delta_{\text{H}} = 7.53$ (br. m, 2H, ArH), 6.91 (br. m, 8H, ArH), 4.58 (br. s, 2H, N- CH_2 -Ar), 4.27 (br. s, 2H, N- CH_2 -Ar), 4.05 (br. s, 2H, N- CH_2 -N); ^{13}C NMR (126 MHz, CDCl_3) $\delta_{\text{C}} = 148.1, 134.9, 130.6, 130.4, 130.4, 129.2, 129.1, 125.4, 125.3, 125.2, 66.7, 58.5, 54.0$; BET surface area = $255 \text{ m}^2/\text{g}$, total pore volume = $0.31 \text{ cm}^3/\text{g}$ at (P/Po 0.98); GPC: $M_{\text{n}} = 2100, M_{\text{w}} = 5000 \text{ g/mol}$; TGA analysis: Initial weight loss due to thermal degradation commences at $\sim 362 \text{ }^\circ\text{C}$ with a 13% and a further 28% loss of mass below $1000 \text{ }^\circ\text{C}$.

2.7: Synthesis of PIM-TFA5-TB



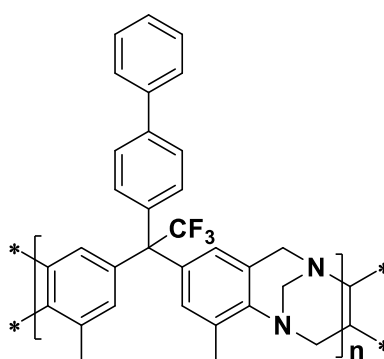
General procedure (X9) was followed using 1,1-bis(3-methyl-4-aminophenyl)-1-(4-trifluorotoluy)-2,2,2-trifluoroethane (TFA5) (**36**) (4.00 g, 9.12 mmol), DMM (2.08 g, 27.37 mmol) and TFA (30 ml). The mixture was stirred for 72 h to afford PIM-TFA5-TB (3.10 g, 69%) as an off-white powder; FTIR (solid, cm^{-1}) $\nu = 1620, 1481, 1325, 1121, 1072, 1018$; ^1H NMR (500 MHz, CDCl_3) $\delta_{\text{H}} = 7.57$ (br. m, 2H, ArH), 6.79 (br. m, 6H, ArH), 4.52 (br. s, 2H, N- CH_2 -Ar), 4.29 (br. s, 2H, N- CH_2 -Ar), 3.89 (br. s, 2H, N- CH_2 -N), 2.29 (br. s, 6H, CH_3); ^{13}C NMR (126 MHz, CDCl_3) $\delta_{\text{C}} = 148.8, 135.8, 132.1, 131.6, 130.8, 130.6, 130.5, 125.9, 125.4, 125.1, 64.3, 62.1, 54.8, 17.5$; BET surface area = $377 \text{ m}^2/\text{g}$, total pore volume = $0.24 \text{ cm}^3/\text{g}$; GPC: $M_{\text{n}} = 3000, M_{\text{w}} = 6300 \text{ g/mol}$; TGA analysis: Initial weight loss due to thermal degradation commences at $\sim 375 \text{ }^\circ\text{C}$ with a 13% and a further 23% loss of mass below $1000 \text{ }^\circ\text{C}$.

2.8: Synthesis of PIM-TFA7-TB



General procedure (X9) was followed using 1,1-bis(4-aminophenyl)-1-(4-biphenyl)-2,2,2-trifluoroethane (TFA7) (**38**) (4.00 g, 9.56 mmol), DMM (2.18 g, 28.68 mmol) and TFA (30 ml). The mixture was stirred for 72 h to afford PIM-TFA7-TB (2.75 g, 61%) as an off-white powder; FTIR (solid, cm^{-1}) $\nu = 1611, 1489, 1230, 1140, 1113, 819, 763, 696$; ^1H NMR (500 MHz, CDCl_3) $\delta_{\text{H}} = 7.44$ (br. m, 9H, ArH), 6.58 (br. m, 6H, ArH), 4.57 (br. s, 2H, N-CH₂-Ar), 4.27 (br. s, 2H, N-CH₂-Ar), 4.05 (br. s, 2H, N-CH₂-N); ^{13}C NMR (126 MHz, CDCl_3) $\delta_{\text{C}} = 140.4, 139.7, 130.7, 130.6, 130.5, 130.4, 129.4, 129.2, 129.1, 129.0, 127.5, 127.3, 127.2, 127.1, 64.8, 61.7, 55.1$; BET surface area = 70 m^2/g , total pore volume = 0.31 cm^3/g at (P/Po = 0.98); GPC: $M_{\text{n}} = 4050$, $M_{\text{w}} = 7000$ g/mol; TGA analysis: Initial weight loss due to thermal degradation commences at ~ 325 $^{\circ}\text{C}$ with a 18% and a further 18% loss of mass below 1000 $^{\circ}\text{C}$.

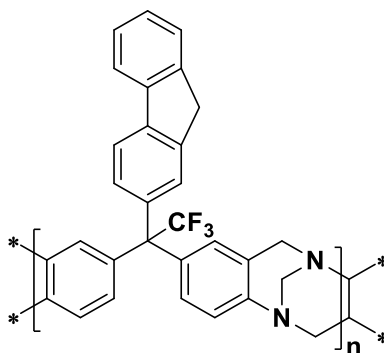
2.9: Synthesis of PIM-TFA8-TB



General procedure (X9) was followed using 1,1-bis(4-aminophenyl)-1-(4-biphenyl)-2,2,2-trifluoroethane (TFA8) (**39**) (5.0 g, 11.21 mmol), DMM (2.56 g, 33.60 mmol) and TFA (40 ml). The mixture was stirred for 72 h to afford PIM-TFA8-TB (3.5 g, 63%) as an off-white powder; FTIR (solid, cm^{-1}) $\nu = 1684, 1483, 1219, 1146, 1123, 762, 696$; ^1H NMR (500 MHz, CDCl_3) $\delta_{\text{H}} = 7.54$ (br. m, 5H, ArH), 6.8 (br. m, 8H, ArH), 4.60 (br. m, 2H, N-CH₂-Ar), 4.30

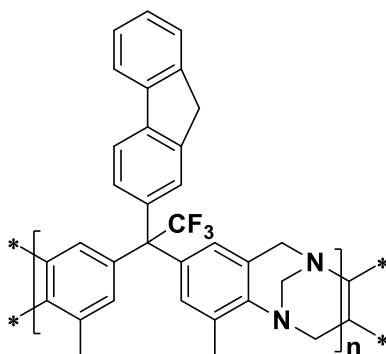
(br. s, 2H, N-CH₂-Ar), 3.92 (br. s, 2H, N-CH₂-N), 2.31 (br. s, 6H, CH₃); ¹³C NMR (126 MHz, CDCl₃) δ_C = 145.8, 140.2, 139.5, 135.4, 132.8, 130.7, 130.4, 129.0, 127.7, 127.6, 127.1, 126.6, 126.0, 125.8, 67.5, 64.2, 55.0, 17.6; BET surface area = 30 m²/g, total pore volume = 0.08 cm³/g at (P/Po = 0.98); GPC: M_n = 12600, M_w = 29000 g/mol; TGA analysis: Initial weight loss due to thermal degradation commences at ~ 387 °C with a 15% and a further 22% loss of mass below 1000 °C.

2.10: Synthesis of PIM-TFA10-TB



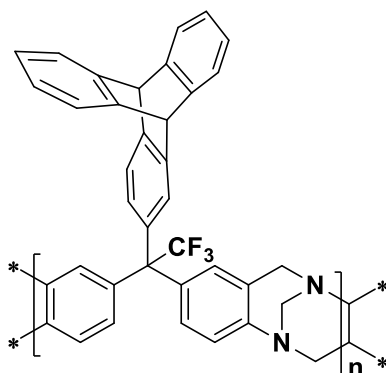
General procedure (X9) was followed using 1,1-bis(4-aminophenyl)-1-(2-fluorenyl)-2,2,2-trifluoroethane (TFA10) (**41**) (4.00 g, 9.29 mmol), DMM (2.12 g, 27.88 mmol) and TFA (30 ml). The mixture was stirred for 72 h to afford PIM-TFA10-TB (3.36 g, 75%) as an off-white powder; FTIR (solid, cm⁻¹) ν = 1682, 1610, 1493, 1229, 1138, 820, 767, 735; ¹H NMR (500 MHz, CDCl₃) δ_H = 7.56 (br. m, 2H, ArH), 6.97 (br. m, 11H, ArH), 4.51 (m, 8H, CH₂ & N-CH₂-N, Ar-CH₂-N); ¹³C NMR (126 MHz, CDCl₃) δ_C = 145.8, 145.4, 144.3, 143.8, 142.4, 142.1, 141.6, 136.4, 136.1, 135.3, 133.6, 132.6, 132.0, 131.1, 129.3, 129.2, 127.1, 116.9, 65.1, 63.1, 59.8, 29.1; BET surface area = 24 m²/g, total pore volume = 0.06 cm³/g at (P/Po = 0.98); the polymer was partial soluble in CHCl₃; TGA analysis: Initial weight loss due to thermal degradation commences at ~ 308 °C with a 16% and a further 23% loss of mass below 1000 °C.

2.11: Synthesis of PIM-TFA11-TB



General procedure (X9) was followed using 1,1-bis(3-methyl-4-aminophenyl)-1-(2-fluorenyl)-2,2,2-trifluoroethane (TFA11) (**42**) (2.00 g, 4.36 mmol), DMM (1.00 g, 13.09 mmol) and TFA (15 ml). The mixture was stirred for 30 h to afford PIM-TFA11-TB (1.35 g, 61%) as an off-white powder; FTIR (solid, cm⁻¹) ν = 1736, 1477, 1229, 1132, 1123, 935, 768, 735; ¹H NMR (500 MHz, CDCl₃) δ_{H} = 7.70 (br. m, 3H, ArH), 7.49 (br. s, 2H, ArH), 7.30 (br. s, 1H, ArH), 6.77 (br. m, 5H, ArH), 4.45 (br. s, 2H, N-CH₂-Ar), 4.28 (br. s, 2H, N-CH₂-Ar), 3.86 (br. m, 2H, N-CH₂-N), 2.27 (br. s, 2H, CH₂), 2.05 (br. s, 6H, CH₃); ¹³C NMR (126 MHz, CDCl₃) δ_{C} = 145.8, 143.8, 143.2, 141.5, 141.2, 137.5, 135.7, 133.0, 132.8, 129.5, 129.0, 127.6, 127.3, 127.0, 126.5, 125.3, 120.2, 119.4, 116.7, 68.1, 60.5, 55.0, 21.2, 14.4; BET surface area = 381 m²/g, total pore volume = 0.40 cm³/g at (P/Po = 0.98); GPC: M_{n} = 20000, M_{w} = 48000 g/mol; TGA analysis: Initial weight loss due to thermal degradation commences at ~ 369 °C with a 9% and a further 20% loss of mass below 1000 °C.

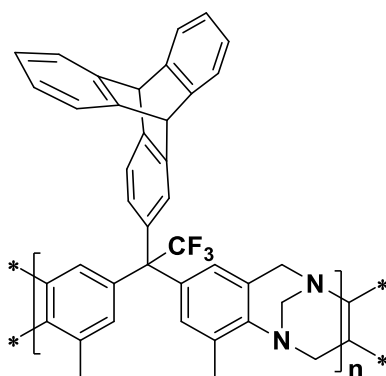
2.12: Synthesis of PIM-TFA13-TB



General procedure (X9) was followed using 1,1-bis(4-aminophenyl)-1-(2-tripcenyl)-2,2,2-trifluoroethane (TFA13) (**44**) (4.00 g, 7.71 mmol), DMM (1.77 g, 23.14 mmol) and TFA (30 ml). The mixture was stirred for 72 h to afford PIM-TFA13-TB (3.20 g, 73%) as an off-

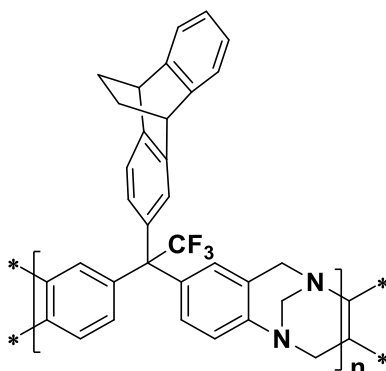
white powder; FTIR (solid, cm^{-1}) $\nu = 1609, 1476, 1458, 1209, 1148, 1103, 813, 748, 625$; ^1H NMR (500 MHz, CDCl_3) $\delta_{\text{H}} = 7.86$ (br. m, 6H, ArH), 6.93 (br. m, 13H, ArH & CH), 3.94 (br. s, 4H, N- CH_2 -Ar), 2.04 (br. s, 2H, N- CH_2 -N); ^{13}C NMR (126 MHz, CDCl_3) $\delta_{\text{C}} = 145.8, 145.5, 133.3, 131.4, 131.2, 130.2, 128.3, 127.9, 126.2, 125.8, 125.6, 125.4, 124.8, 67.3, 64.9, 60.7, 53.8, 53.7$; BET surface area = $70 \text{ m}^2/\text{g}$, total pore volume = $0.23 \text{ cm}^3/\text{g}$ at (P/Po = 0.98); the polymer was partial soluble in CHCl_3 ; TGA analysis: Initial weight loss due to thermal degradation commences at $\sim 348 \text{ }^\circ\text{C}$ with a 16% and a further 25% loss of mass below $1000 \text{ }^\circ\text{C}$.

2.13: Synthesis of PIM-TFA14-TB



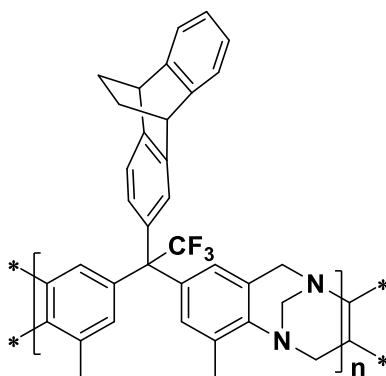
General procedure (X9) was followed using 1,1-bis(3-methyl-4-aminophenyl)-1-(2-tripicenyl)-2,2,2-trifluoroethane (TFA14) (**45**) (1.50 g, 2.74 mmol), DMM (0.66 g, 8.68 mmol) and TFA (10.0 ml). The mixture was stirred for 72 h to afford PIM-TFA14-TB (0.90 g, 55%) as a light brown powder; FTIR (solid, cm^{-1}) $\nu = 1780, 1610, 1489, 1456, 1358, 1231, 1163, 1111, 841, 733$; ^1H NMR (500 MHz, CDCl_3) $\delta_{\text{H}} = 7.36$ (br. m, 4H, ArH), 7.17 (br. m, 1H, ArH), 6.96 (br. m, 5H, ArH), 6.45 (br. m, 5H, ArH), 5.40 (br. s, 1H, CH), 5.27 (br. s, 1H, CH), 4.42 (br. s, 2H, N- CH_2 -Ar), 4.24 (br. s, 2H, N- CH_2 -Ar), 3.79 (br. s, 2H, N- CH_2 -N), 2.22 (br. s, 6H, CH_3); ^{13}C NMR (126 MHz, CDCl_3) $\delta_{\text{C}} = 145.6, 145.4, 145.3, 137.5, 135.5, 132.7, 130.7, 128.5, 127.5, 126.1, 125.5, 125.3, 123.9, 123.8, 123.1, 67.4, 64.3, 55.0, 54.3, 53.8, 17.5$; BET surface area = $510 \text{ m}^2/\text{g}$, total pore volume = $0.23 \text{ cm}^3/\text{g}$ at (P/Po = 0.98); GPC: $M_n = 2900$, $M_w = 5000 \text{ g/mol}$; TGA analysis: a 4% loss of weight of solvent between $65\text{--}140 \text{ }^\circ\text{C}$. Initial weight loss due to thermal degradation commences at $\sim 364 \text{ }^\circ\text{C}$ with a 7% and a further 22% loss of mass below $1000 \text{ }^\circ\text{C}$.

2.14: Synthesis of PIM-TFA16-TB



General procedure (X9) was followed using 1,1-bis[(4-aminophenyl)-1-(2-(9,10-dihydro-9,10-ethanoanthracenyl))]-2,2,2-trifluoroethane (TFA16) (**47**) (4.00 g, 8.50 mmol), DMM (1.94 g, 25.52 mmol) and TFA (32 ml). The mixture was stirred for 48 h to afford PIM-TFA16-TB (3.50 g, 78%) as an off-white powder; FTIR (solid, cm^{-1}) ν = 1610, 1493, 1211, 1138, 1113, 818, 750; ^1H NMR (500 MHz, CDCl_3) δ_{H} = 6.55 (br. m, 13H, ArH), 4.51 (br. s, 2H, N- CH_2 -Ar), 4.14 (br. m, 10H, N- CH_2 -Ar, N- CH_2 -N, CH_2 & CH); ^{13}C NMR (126 MHz, CDCl_3) δ_{C} = 143.6, 143.3, 141.5, 139.5, 135.3, 135.1, 133.1, 131.1, 130.3, 127.5, 127.5, 127.0, 125.5, 124.7, 124.4, 123.4, 123.4, 123.2, 121.0, 66.1, 63.2, 51.1, 43.9, 43.7, 31.1; BET surface area = 90 m^2/g , total pore volume = 0.23 at (P/Po = 0.98), cm^3/g ; GPC: M_{n} = 5000, M_{w} = 8500 g/mol; TGA analysis: Initial weight loss due to thermal degradation commences at ~ 280 $^{\circ}\text{C}$ with a 6% consistent with the loss of an ethylene fragment from the ethanoanthracene unit via a retro Diels-Alder reaction²⁰² then at ~ 376 $^{\circ}\text{C}$ loss of mass 14% and a further 18% loss of mass below 1000 $^{\circ}\text{C}$.

2.15: Synthesis of PIM-TFA17-TB



General procedure (X9) was followed using 1,1-bis[(3-methyl-4-aminophenyl)-1-(2-(9,10-dihydro-9,10-ethanoanthracenyl))]-2,2,2-trifluoroethane (TFA17) (**48**) (4.00 g, 8.02

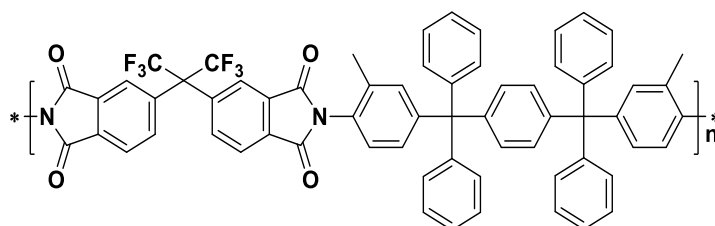
mmol), DMM (3.05 g, 40.11 mmol) and TFA (35 ml). The mixture was stirred for 72 h to afford PIM-TFA17-TB (3.51 g, 80%) as an off-white powder; FTIR (solid, cm^{-1}) $\nu = 2945, 2868, 1476, 1219, 1150, 1134, 1123, 936$; ^1H NMR (500 MHz, CDCl_3) $\delta_{\text{H}} = 7.00$ (br. m, 7H, ArH), 6.69 (br. m, 4H, ArH), 4.34 (br. m, 10H, N- CH_2 -Ar, CH_2), 3.83 (br. s, 2H, N- CH_2 -N), 2.21 (br. s, 6H, CH_3); ^{13}C NMR (126 MHz, CDCl_3) $\delta_{\text{C}} = 147.9, 146.3, 143.8, 143.5, 141.5, 139.0, 137.7, 136.6, 136.1, 133.0, 132.7, 130.9, 126.0, 125.8, 124.7, 67.7, 54.9, 54.4, 34.5, 26.8, 17.5$; BET surface area = $445 \text{ m}^2/\text{g}$, total pore volume = $0.59 \text{ cm}^3/\text{g}$ at ($P/P_0 = 0.98$); GPC: $M_n = 6500$, $M_w = 10000 \text{ g/mol}$; TGA analysis: Initial weight loss due to thermal degradation commences at $\sim 290 \text{ }^\circ\text{C}$ with a 5% consistent with the loss of an ethylene fragment from the ethanoanthracene unit via a retro Diels-Alder reaction²⁰² then at $\sim 380 \text{ }^\circ\text{C}$ loss of mass 10% and a further 21% loss of mass below $1000 \text{ }^\circ\text{C}$.

8.3.3: Polyimides Synthesis

X10: General Procedure of Polyimides Synthesis

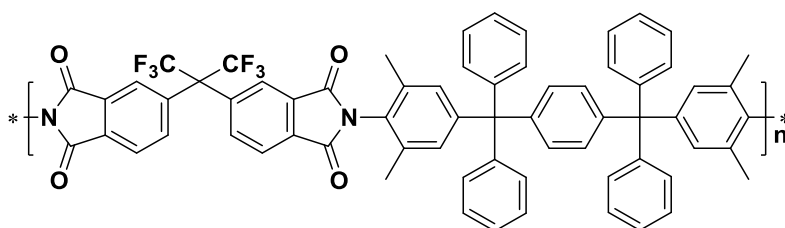
Under a nitrogen atmosphere, commercial dianhydride 6FDA was dissolved in ethanol in a two-necked flask equipped with a reflux condenser. Triethylamine was added and the mixture was refluxed for 1 h to form the ester-acid compound. The side arm was opened to remove the solvent to give a very highly viscous liquid. The corresponding diamine monomer was dissolved in NMP and was added to the ester-acid. The mixture was heated to $80 \text{ }^\circ\text{C}$ for 1 h. The side arm was opened occasionally to remove ethanol formed in the reaction. The mixture was gradually heated to $200 \text{ }^\circ\text{C}$ over 2 h and any water formed was removed by opening the side arm. The mixture was refluxed for an appropriate time then the mixture was cooled to $20 \text{ }^\circ\text{C}$ and CHCl_3 was added to dilute the reaction mixture and this mixture is poured slowly into MeOH to precipitate the crude polymer. The solid was collected by filtration, the resulting powder was dissolved in CHCl_3 and re-precipitated into methanol then dissolved with CHCl_3 and re-precipitated with petroleum ether. The polymer was dried under vacuum oven to afford the desired polymer.

3.1: Synthesis of PIM-BAB1-PI



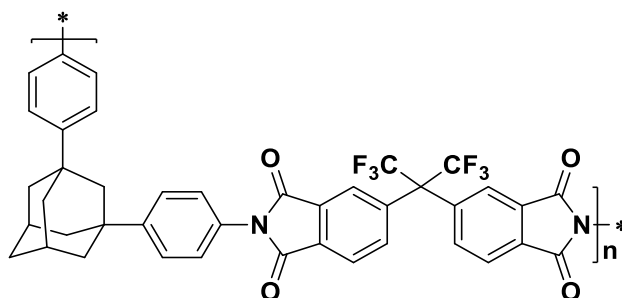
General procedure (X10) was followed using 6FDA (0.78 g, 1.70 mmol), ethanol (10 ml), triethylamine (0.89 g, 8.70 mmol), *p*-bis(4-amino-3-methylphenyldiphenylmethyl)benzene (BAB1) (**24**) (1.00 g, 1.70 mmol) and NMP (5 ml). The mixture was refluxed for 24 h to afford PIM-BAB1-PI (0.64 g, 37%) as a light brown powder; FTIR (solid, cm^{-1}) $\nu = 1786, 1724, 1499, 1369, 1256, 1192, 1192, 1105, 746, 733, 723$; ^1H NMR (500 MHz, CDCl_3) $\delta_{\text{H}} = 8.02$ (br. d, $J_{\text{HH}} = 8.0$ Hz, 2H, ArH), 7.95 (br. s, 2H, ArH), 7.87 (br. d, $J_{\text{HH}} = 8.0$ Hz, 2H, ArH), 7.16 (br. m, 30H, ArH), 2.12 (br. s, 6H, CH_3); ^{13}C NMR (126 MHz, CDCl_3) $\delta_{\text{C}} = 166.3, 166.1, 148.3, 146.4, 144.3, 139.2, 136.0, 135.3, 134.0, 133.1, 132.8, 131.9, 131.4, 130.6, 130.1, 128.2, 127.7, 127.5, 126.3, 125.5, 124.2, 64.7, 18.7$; BET surface area = $8 \text{ m}^2/\text{g}$, total pore volume = $0.30 \text{ cm}^3/\text{g}$ at (P/Po = 0.98); GPC: $M_{\text{n}} = 9000$, $M_{\text{w}} = 16700$ g/mol; TGA analysis: Initial weight loss due to thermal degradation commences at ~ 438 °C with a 19% loss of mass below 1000 °C.

3.2: Synthesis of PIM-BAB2-PI



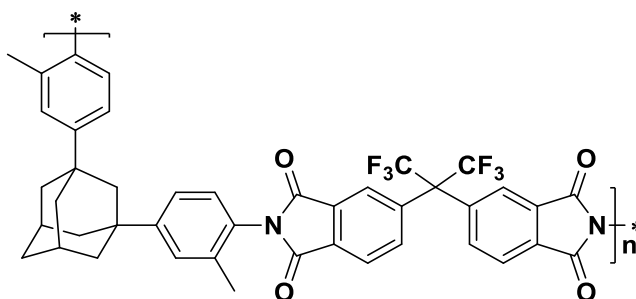
General procedure (X10) was followed using 6FDA (1.00 g, 2.25 mmol), ethanol (10 ml), triethylamine (1.14 g, 11.25 mmol), *p*-bis(4-amino-3,5-dimethylphenyldiphenylmethyl)benzene (BAB2) (**25**) (1.46 g, 2.25 mmol) and NMP (5 ml). The mixture was refluxed for 24 h to afford PIM-BAB2-PI (0.90 g, 38%) as a light brown powder; FTIR (solid, cm^{-1}) $\nu = 1786, 1724, 1489, 1368, 1254, 1209, 1192, 1142, 735, 702$; ^1H NMR (500 MHz, CDCl_3) $\delta_{\text{H}} = 8.03$ (br. d, $J_{\text{HH}} = 8.1$ Hz, 2H, ArH), 7.96 (br. s, 2H, ArH), 7.88 (br. d, $J_{\text{HH}} = 8.1$ Hz, 2H, ArH), 7.25 (br. m, 24H, ArH), 7.12 (br. s, 4H, ArH), 2.07 (br. s, 12H, CH_3); ^{13}C NMR (126 MHz, CDCl_3) $\delta_{\text{C}} = 166.2, 166.0, 148.2, 146.5, 144.3, 139.2, 135.5, 133.1, 132.7, 131.6, 131.4, 130.6, 127.6, 127.5, 126.3, 125.4, 124.2, 110.1, 64.6, 18.7$; BET surface area = $63 \text{ m}^2/\text{g}$, total pore volume = $0.30 \text{ cm}^3/\text{g}$ at (P/Po = 0.98); GPC: $M_{\text{n}} = 11000$, $M_{\text{w}} = 20200$ g/mol; TGA analysis: Initial weight loss due to thermal degradation commences at ~ 471 °C with a 21% loss of mass below 1000 °C.

3.3: Synthesis of PIM-AD1-PI²¹⁰



General procedure (X10) was followed using 6FDA (1.95 g, 4.39 mmol), ethanol (10 ml), triethylamine (2.22 g, 21.99 mmol), 1,3-bis(4-aminophenyl)adamantane (AD1) (1.39 g, 4.39 mmol) and NMP (5ml). The mixture was refluxed for 24 h to afford PIM-AD1-PI (1.10 g, 33%) as a light brown powder; FTIR (solid, cm^{-1}) $\nu = 2901, 2851, 1784, 1760, 1514, 1435, 1371, 1296, 1253, 1207, 1192, 1142, 1093, 964, 850, 817, 745, 721$; $^1\text{H NMR}$ (500 MHz, CDCl_3) $\delta_{\text{H}} = 8.02$ (br. s, 2H, ArH), 7.87 (br. m, 2H, ArH), 7.55 (br. m, 4H, ArH), 7.39 (br. m, 4H, ArH), 2.35 (br. s, 2H, CH_2), 1.88 (br. m, 12H, CH_2 & CH); $^{13}\text{C NMR}$ (126 MHz, CDCl_3) $\delta_{\text{C}} = 166.4, 166.3, 151.0, 139.2, 132.9, 132.6, 129.0, 126.5, 126.3, 126.1, 124.2, 123.7, 48.8, 42.3, 38.6, 37.5, 35.9, 29.6$; BET surface area = 175 m^2/g , total pore volume = 0.58 cm^3/g at (P/Po = 0.98); GPC: $M_{\text{n}} = 4000$, $M_{\text{w}} = 9900$ g/mol; TGA analysis: Initial weight loss due to thermal degradation commences at ~ 447 $^{\circ}\text{C}$ with a 45% loss of mass below 1000 $^{\circ}\text{C}$.

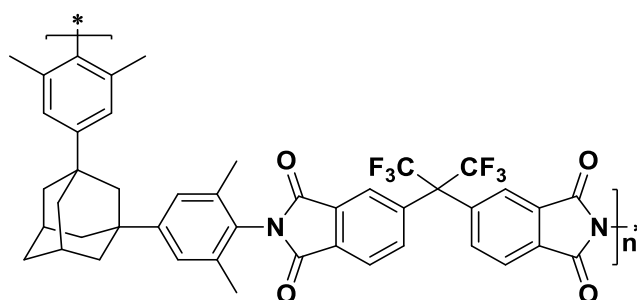
3.4: Synthesis of PIM-AD2-PI



General procedure (X10) was followed using 6FDA (1.30 g, 2.96 mmol), ethanol (10 ml), triethylamine (1.48 g, 14.63 mmol), 1,3-bis(3-methyl-4-aminophenyl)adamantane (AD2) (**27**) (1.01 g, 2.96 mmol) and NMP (5 ml). The mixture was refluxed for 24 h to afford PIM-AD2-PI (0.70 g, 32%) as a light brown powder; FTIR (solid, cm^{-1}) $\nu = 2902, 2851, 1786, 1725, 1508, 1414, 1366, 1296, 1253, 1209, 1192, 1142, 1107, 983, 848, 813, 748, 723$; $^1\text{H NMR}$ (500 MHz, CDCl_3) $\delta_{\text{H}} = 8.02$ (br. m, 1H, ArH), 7.92 (br. s, 1H, ArH), 7.89 (br. s, 1H, ArH), 7.43

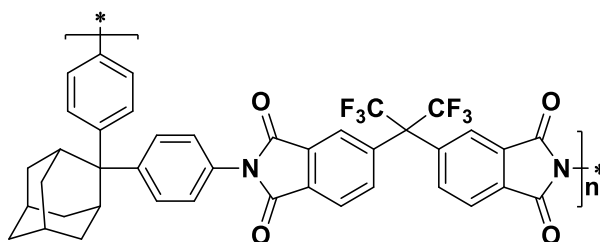
(br. m, 1H, ArH), 7.33 (br. m, 1H, ArH), 7.15 (br. m, 1H, ArH), 2.20 (br. s, 2H, CH₂), 2.18 (br. s, 6H, CH₃), 2.05 (br. m, 2H, CH₂), 1.86 (br. m, 10H, CH₂); ¹³C NMR (126 MHz, CDCl₃) δ_C = 161.6, 161.4, 161.3, 161.0, 160.7, 151.2, 133.3, 127.5 (q, J_{C-F} = 237.4 Hz), 126.7, 126.4, 119.8, 117.4, 115.1, 112.8, 46.0, 42.0, 40.9, 36.6, 35.6, 29.3, 28.9; BET surface area = 250 m²/g, total pore volume = 0.24 cm³/g at (P/Po = 0.98); GPC: M_n = 5600, M_w = 17600 g/mol; TGA analysis: Initial weight loss due to thermal degradation commences at ~ 466 °C with a 56% loss of mass below 1000 °C.

3.5: Synthesis of PIM-AD3-PI



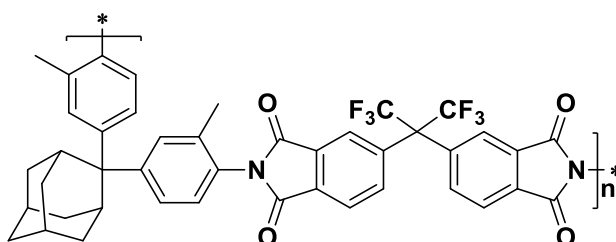
General procedure (X10) was followed using 6FDA (1.95 g, 4.39 mmol), ethanol (10 ml), triethylamine (2.22 g, 21.95 mmol), 1,3-bis(3,5-dimethyl-4-aminophenyl)adamantane (AD3) (**28**) (1.64 g, 4.39 mmol) and NMP (5 ml). The mixture was refluxed for 24 h to afford PIM-AD3-PI (1.10 g, 32%) as a light brown powder, FTIR (solid, cm⁻¹) ν = 2903, 2851, 1786, 1719, 1601, 1491, 1437, 1367, 1294, 1253, 1207, 1190, 1141, 1105, 983, 962, 868, 848, 750, 725, 705; ¹H NMR (500 MHz, CDCl₃) δ_H = 8.05 (br. d, J_{HH} = 8.1 Hz, 1H, ArH), 7.96 (br. s, 1H, ArH), 7.91 (br. d, J_{HH} = 8.1 Hz, 1H, ArH), 7.21 (br. s, 2H, ArH), 2.34 (br. s, 2H, CH₂), 2.17 (br. m, 20H, CH₃ & CH₂), 1.99 (br. m, 2H, CH), 1.79 (br. m, 2H, CH₂); ¹³C NMR (126 MHz, CDCl₃) δ_C = 166.4, 166.2, 152.0, 150.6, 139.2, 136.2, 133.1, 132.7, 127.0, 126.2 (q, J_{C-F} = 367.2 Hz), 125.6, 124.3, 48.9, 43.2, 42.3, 37.4, 29.7, 29.1, 18.7; BET surface area = 370 m²/g, total pore volume = 1.76 cm³/g at (P/Po = 0.98); GPC: M_n = 6000, M_w = 19300 g/mol; TGA analysis: Initial weight loss due to thermal degradation commences at ~ 390 °C with a 41% loss of mass below 1000 °C.

3.6: Synthesis of PIM-AD4-PI



General procedure (X10) was followed using 6FDA (1.40 g, 3.15 mmol), ethanol (10 ml), triethylamine (1.59 g, 15.75 mmol), 2,2-bis(4-aminophenyl)adamantane (AD4) (**29**) (1.00 g, 3.15 mmol) and NMP (5ml). The mixture was refluxed for 24 h to afford PIM-AD4-PI (1.10 g, 48%) as a light brown powder, FTIR (solid, cm^{-1}) $\nu = 2911, 2857, 1784, 1725, 1510, 1437, 1369, 1296, 1254, 1207, 1192, 1144, 1101, 1018, 981, 964, 850, 812, 744, 725$; ^1H NMR (500 MHz, CDCl_3) $\delta_{\text{H}} = 7.98$ (br. d, $J_{\text{HH}} = 8.1$ Hz, 1H, ArH), 7.93 (br. s, 2H, ArH), 7.80 (br. d, $J_{\text{HH}} = 8.1$ Hz, 1H, ArH), 7.57 (br. d, $J_{\text{HH}} = 8.2$ Hz, 3H, ArH), 7.34 (br. d, $J_{\text{HH}} = 8.2$ Hz, 3H, ArH), 3.29 (br. s, 2H, CH), 2.65 (br. m, 4H, CH_2), 1.80 (br. m, 8H, CH_2 & CH); ^{13}C NMR (126 MHz, CDCl_3) $\delta_{\text{C}} = 166.2, 166.1, 148.0, 139.2, 136.1, 132.8, 132.5, 128.4, 127.0, 126.4, 125.4, 124.2$ (q, $J_{\text{C-F}} = 292.3$ Hz), 77.37, 50.76, 38.03, 33.41, 32.40, 27.54; BET surface area = 370 m^2/g , total pore volume = 0.42 cm^3/g at (P/Po = 0.98); GPC: $M_{\text{n}} = 9300$, $M_{\text{w}} = 16000$ g/mol; TGA analysis: Initial weight loss due to thermal degradation commences at ~ 450 $^{\circ}\text{C}$ with a 49% loss of mass below 1000 $^{\circ}\text{C}$.

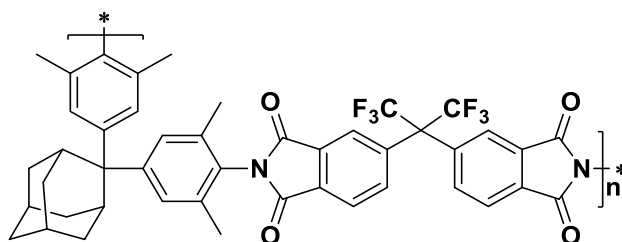
3.7: Synthesis of PIM-AD5-PI



General procedure (X10) was followed using 6FDA (3.50 g, 7.87 mmol), ethanol (15 ml), triethylamine (3.98 g, 39.35 mmol), 2,2-bis(3-methyl-4-aminophenyl)adamantane (AD5) (**30**) (2.73 g, 7.87 mmol) and NMP (10 ml). The mixture was refluxed for 72 h to afford PIM-AD5-PI (4.50 g, 76%) as a light brown powder; FTIR (solid, cm^{-1}) $\nu = 2913, 2857, 1786, 1725, 1504, 1437, 1371, 1296, 1257, 1209, 1192, 1170, 1141, 1101, 1038, 983, 849, 817, 748, 723, 713, 675$; ^1H NMR (500 MHz, CDCl_3) $\delta_{\text{H}} = 8.00$ (br. d, $J_{\text{HH}} = 8.0$ Hz, 1H, ArH), 7.93 (br. s,

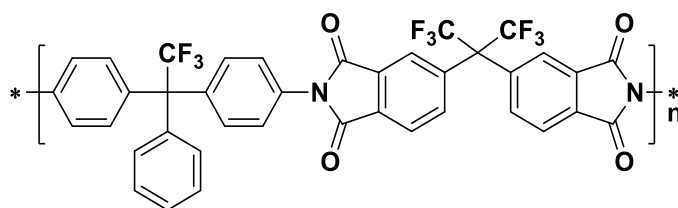
1H, ArH), 7.85 (br. d, $J_{HH} = 8.0$ Hz, 1H, ArH), 7.39 (br. m, 4H, ArH), 7.09 (br. s, 1H, ArH), 3.26 (br. s, 6H, CH_3), 2.23 (br. m, 10H, CH_2 & CH), 1.79 (br. m, 8H, CH_2 & CH); ^{13}C NMR (126 MHz, $CDCl_3$) $\delta_C = 166.3, 166.1, 149.1, 139.1, 136.2, 135.9, 133.1, 132.8, 129.1, 128.6, 127.3, 125.4, 124.9, 124.2, 123.3(q, J_{C-F} = 287.3$ Hz), 65.4, 50.5, 38.1, 33.4, 32.5, 27.5, 18.9; BET surface area = 430 m^2/g , total pore volume = 0.54 cm^3/g at (P/Po = 0.98); GPC: $M_n = 23600$, $M_w = 47300$ g/mol; TGA analysis: Initial weight loss due to thermal degradation commences at ~ 450 $^{\circ}C$ with a 51% loss of mass below 1000 $^{\circ}C$.

3.8: Synthesis of PIM-AD6-PI



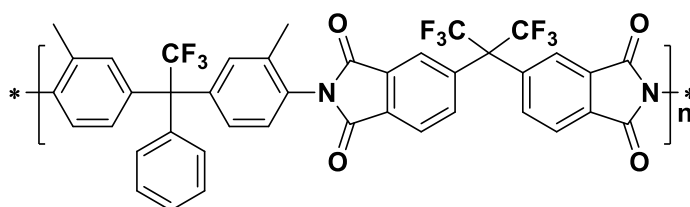
General procedure (X10) was followed using 6FDA (1.20 g, 2.70 mmol), ethanol (10 ml), triethylamine (1.36 g, 13.50 mmol), 2,2-bis(3,5-dimethyl-4-aminophenyl)adamantane (AD6) (**31**) (1.01 g, 2.70 mmol) and NMP (5ml). The mixture was refluxed for 24 h to afford PIM-AD6-PI (1.50 g, 71%) as a light brown powder; FTIR (solid, cm^{-1}) $\nu = 2909, 2857, 1786, 1725, 1597, 1498, 1439, 1367, 1294, 1254, 1207, 1192, 1142, 1103, 1033, 984, 964, 876, 845, 750, 723, 721, 712, 692$; 1H NMR (500 MHz, $CDCl_3$) $\delta_H = 8.01$ (br. d, $J_{HH} = 8.0$ Hz, 2H, ArH), 7.95 (br. s, 2H, ArH), 7.86 (br. d, $J_{HH} = 8.0$ Hz, 2H, ArH), 7.22 (br. s, 4H, ArH), 3.21 (br. s, 12H, CH_3), 2.70 (br. m, 8H, CH_2), 1.72 (br. m, 8H, CH_2 & CH); ^{13}C NMR (126 MHz, $CDCl_3$) $\delta_C = 166.2, 166.0, 148.9, 139.1, 136.5, 136.0, 133.1, 132.7, 126.5, 125.4, 124.2, 123.6$ (q, $J_{C-F} = 287.6$ Hz), 65.4, 50.3, 38.1, 33.5, 32.5, 27.5, 18.9; BET surface area = 560 m^2/g , total pore volume = 0.78 cm^3/g at (P/Po = 0.98); GPC: $M_n = 62500$, $M_w = 131000$ g/mol; TGA analysis: Initial weight loss due to thermal degradation commences at ~ 465 $^{\circ}C$ with a 51% loss of mass below 1000 $^{\circ}C$.

3.9: Synthesis of PIM-TFA1-PI



General procedure (X10) was followed using 6FDA (1.00 g, 2.25 mmol), ethanol (10 ml), triethylamine (1.13 g, 11.25 mmol), 1,1-bis(4-aminophenyl)-1-phenyl-2,2,2-trifluoroethane (TFA1) (**32**) (0.77 g, 2.25 mmol) and NMP (5 ml). The mixture was refluxed for 48 h to afford PIM-TFA1-PI (0.90 g, 53%) as an off-white powder; FTIR (solid, cm^{-1}) $\nu = 1786, 1722, 1609, 1512, 1368, 1254, 1240, 1209, 1192, 1192, 1144, 824, 714$; ^1H NMR (500 MHz, CDCl_3) $\delta_{\text{H}} = 8.05$ (br. d, $J_{\text{HH}} = 8.0$ Hz, 4H, ArH), 7.97 (br. s, 2H, ArH), 7.87 (br. d, $J_{\text{HH}} = 8.0$ Hz, 4H, ArH), 7.46 (br. m, 2H, ArH), 7.37 (br. m, 2H, ArH), 7.34 (br. m, 2H, ArH), 7.21 (br. m, 1H, ArH); ^{13}C NMR (126 MHz, CDCl_3) $\delta_{\text{C}} = 166.0, 165.9, 139.9, 136.2, 132.8, 132.5, 131.2, 131.0, 130.1, 128.6, 125.9, 125.5, 124.4, 65.2, 65.0$; BET surface area = 270 m^2/g , total pore volume = 0.46 cm^3/g at (P/Po = 0.98); GPC: $M_{\text{n}} = 42000$, $M_{\text{w}} = 68000$ g/mol; TGA analysis: Initial weight loss due to thermal degradation commences at $\sim 459^\circ\text{C}$ with a 41% loss of mass below 1000 $^\circ\text{C}$.

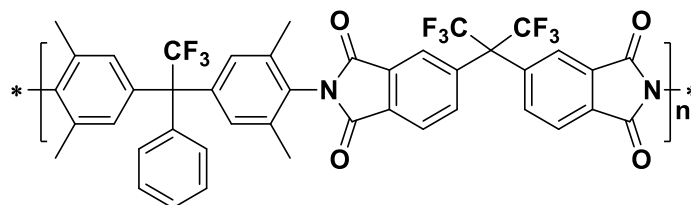
3.10: Synthesis of PIM-TFA2-PI



General procedure (X10) was followed using 6FDA (1.20 g, 2.70 mmol), ethanol (10 ml), triethylamine (1.36 g, 13.50 mmol), 1,1-bis(3-methyl-4-aminophenyl)-1-phenyl-2,2,2-trifluoroethane (TFA2) (**33**) (1.00 g, 2.70 mmol) and NMP (5 ml). The mixture was refluxed for 24 h to afford PIM-TFA2-PI (0.75 g, 36%) as an off-white powder; FTIR (solid, cm^{-1}) $\nu = 1788, 1724, 1608, 1506, 1369, 1255, 1240, 1209, 1192, 1141, 1005, 723, 708$; ^1H NMR (500 MHz, CDCl_3) $\delta_{\text{H}} = 8.05$ (br. d, $J_{\text{HH}} = 8.1$ Hz, 2H, ArH), 7.96 (br. s, 2H, ArH), 7.90 (br. d, $J_{\text{HH}} = 8.1$ Hz, 2H, ArH), 7.37 (br. s, 2H, ArH), 7.21 (br. m, 4H, ArH), 7.11 (br. m, 5H, ArH), 2.20 (br. s, 6H, CH_3); ^{13}C NMR (126 MHz, CDCl_3) $\delta_{\text{C}} = 166.1, 165.9, 141.3, 139.4, 139.3, 136.4, 136.1, 133.0, 132.8, 132.7, 130.1, 130.1, 128.9, 128.5, 128.4, 128.2, 125.6, 124.4, 65.2, 65.0$,

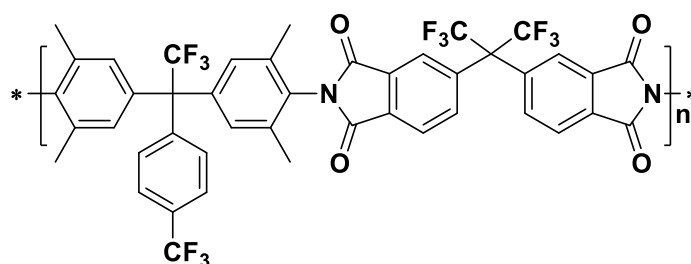
18.8; BET surface area = 375 m²/g, total pore volume = 0.84 cm³/g at (P/Po = 0.98); GPC: M_n = 28100, M_w = 48300 g/mol; TGA analysis: Initial weight loss due to thermal degradation commences at ~ 457 °C with a 43% loss of mass below 1000 °C.

3.11: Synthesis of PIM-TFA3-PI



General procedure (X10) was followed using 6FDA (1.00 g, 2.25 mmol), ethanol (10 ml), triethylamine (1.13 g, 11.25 mmol), 1,1-bis(3,5-dimethyl-4-aminophenyl)-1-phenyl-2,2,2-trifluoroethane (TFA3) (**34**) (0.89 g, 2.25 mmol) and NMP (5 ml). The mixture was refluxed for 72 h to afford PIM-TFA3-PI (1.20 g, 67%) as an off-white powder; FTIR (solid, cm⁻¹) ν = 2926, 1788, 1724, 1610, 1489, 1368, 1256, 1240, 1209, 1146, 1107, 851, 721, 708; ¹H NMR (500 MHz, CDCl₃) δ_H = 8.05 (br. d, J_{HH} = 8.4 Hz, 2H, ArH), 7.98 (br. s, 2H, ArH), 7.91 (br. d, J_{HH} = 8.4 Hz, 2H, ArH), 7.35 (br. m, 6H, ArH), 7.22 (br. m, 2H, ArH), 7.00 (br. m, 1H, ArH), 2.14 (br. s, 12H, CH₃); ¹³C NMR (126 MHz, CDCl₃) δ_C = 166.0, 165.8, 141.2, 139.6, 139.3, 136.7, 136.2, 133.0, 132.7, 130.4, 130.2, 129.3, 128.4, 128.1, 125.5, 124.3, 65.1, 64.9, 18.8; BET surface area = 460 m²/g, total pore volume = 0.56 cm³/g at (P/Po = 0.98); GPC: M_n = 81400, M_w = 103300 g/mol; TGA analysis: Initial weight loss due to thermal degradation commences at ~ 462 °C with a 41% loss of mass below 1000 °C.

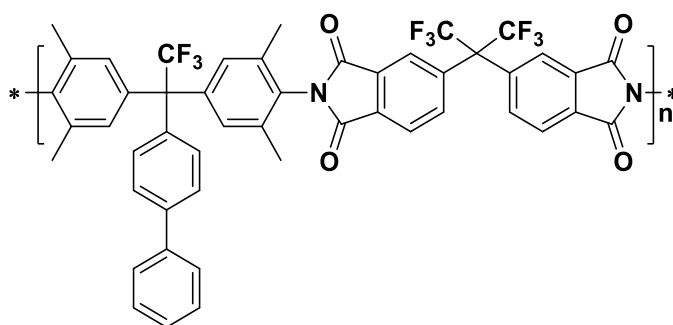
3.12: Synthesis of PIM-TFA6-PI



General procedure (X10) was followed using 6FDA (1.00 g, 2.25 mmol), ethanol (10 ml), triethylamine (1.1 g, 11.25 mmol), 1,1-bis(3,5-dimethyl-4-aminophenyl)-1-(4-trifluorotolyl)-2,2,2-trifluoroethane (TFA6) (**37**) (1.05 g, 2.25 mmol) and NMP (5 ml). The mixture was refluxed for 72 h to afford PIM-TFA6-PI (1.60 g, 83%) as an off-white powder; FTIR (solid, cm⁻¹) ν = 1788, 1724, 1622, 1489, 1368, 1327, 1256, 1242, 1209, 1192, 1152,

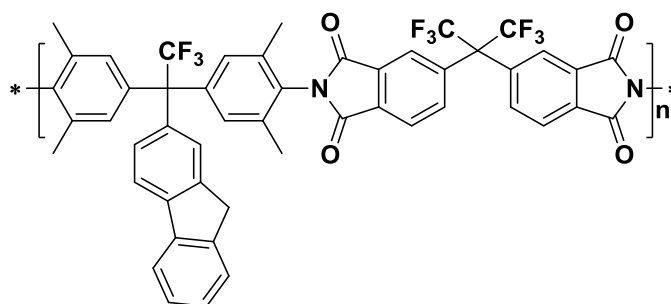
1009, 1073, 1018, 984, 851, 835, 723; ^1H NMR (500 MHz, CDCl_3) $\delta_{\text{H}} = 8.06$ (br. d, $J_{\text{HH}} = 8.1$ Hz, 2H, ArH), 7.98 (br. s, 2H, ArH), 7.92 (br. d, $J_{\text{HH}} = 8.1$ Hz, 2H, ArH), 7.65 (br. d, $J_{\text{HH}} = 8.4$ Hz, 2H, ArH), 7.38 (br. d, $J_{\text{HH}} = 8.4$ Hz, 2H, ArH), 6.98 (br. s, 4H, ArH), 2.15 (br. s, 12H, CH_3); ^{13}C NMR (126 MHz, CDCl_3) $\delta_{\text{C}} = 166.0, 165.7, 143.5, 140.4, 139.4, 137.1, 136.2, 133.0, 132.6, 130.7, 130.2, 129.7, 125.6, 125.4, 124.4, 123.0, 65.1, 64.8, 18.8$; BET surface area = $470 \text{ m}^2/\text{g}$, total pore volume = $0.49 \text{ cm}^3/\text{g}$ at ($\text{P}/\text{Po} = 0.98$); GPC: $M_{\text{n}} = 30000$, $M_{\text{w}} = 42500$ g/mol; TGA analysis: Initial weight loss due to thermal degradation commences at ~ 471 °C with a 46% loss of mass below 1000 °C.

3.13: Synthesis of PIM-TFA9-PI



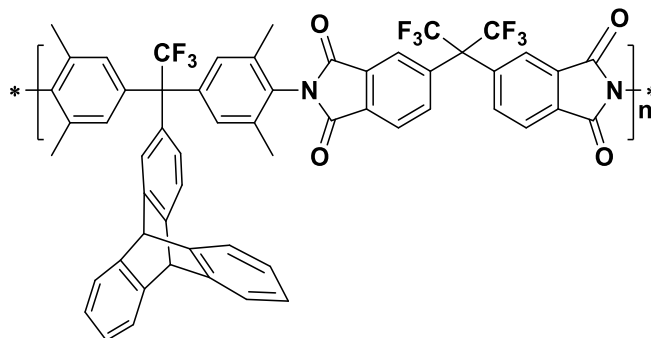
General procedure (X10) was followed using 6FDA (0.9 g, 2.02 mmol), ethanol (10 ml), triethylamine (1.02 g, 10.13 mmol), 1,1-bis(3,5-dimethyl-4-aminophenyl)-1-(4-biphenyl)-2,2,2-trifluoroethane (TFA9) (**40**) (0.95 g, 2.1 mmol) and NMP (5 ml). The mixture was refluxed for 48 h to afford PIM-TFA9-PI (1.70 g, 92%) as an off-white powder; FTIR (solid, cm^{-1}) $\nu = 1788, 1724, 1487, 1368, 1256, 1242, 1209, 1192, 1146, 1007, 750, 723$; ^1H NMR (500 MHz, CDCl_3) $\delta_{\text{H}} = 8.05$ (br. d, $J_{\text{HH}} = 8.1$ Hz, 2H, ArH), 7.99 (br. s, 2H, ArH), 7.90 (br. d, $J_{\text{HH}} = 8.1$ Hz, 2H, ArH), 7.63 (br. m, 4H, ArH), 7.46 (br. m, 2H, ArH), 7.35 (br. m, 1H, ArH), 7.30 (br. d, $J_{\text{HH}} = 8.5$ Hz, 2H, ArH), 7.04 (br. d, $J_{\text{HH}} = 8.5$ Hz, 4H, ArH), 2.15 (br. s, 12H, CH_3); ^{13}C NMR (126 MHz, CDCl_3) $\delta_{\text{C}} = 166.1, 165.8, 141.2, 140.7, 140.2, 139.4, 138.6, 136.8, 136.2, 133.0, 132.7, 130.7, 130.4, 129.4, 129.0, 127.8, 127.2, 125.5, 124.7, 124.4, 64.7, 52.3, 18.9$; BET surface area = $375 \text{ cm}^3/\text{g}$, total pore volume = $0.28 \text{ cm}^3/\text{g}$ at ($\text{P}/\text{Po} = 0.98$); GPC: $M_{\text{n}} = 46000$, $M_{\text{w}} = 77700$ g/mol; TGA analysis: Initial weight loss due to thermal degradation commences at ~ 453 °C with a 47% loss of mass below 1000 °C.

3.14: Synthesis of PIM-TFA12-PI



General procedure (X10) was followed using 6FDA (0.91 g, 2.05 mmol), ethanol (10 ml), triethylamine (1.03 g, 10.20 mmol), 1,1-bis(3,5-dimethyl-4-aminophenyl)-1-(2-fluorenyl)-2,2,2-trifluoroethane (TFA12) (**43**) (1.00 g, 2.05 mmol) and NMP (5 ml). The mixture was refluxed for 72 h to afford PIM-TFA12-PI (1.75 g, 95%) as an off-white powder; FTIR (solid, cm^{-1}) $\nu = 1788, 1726, 1489, 1439, 1368, 1256, 1209, 1192, 1157, 1033, 851, 735, 723$; ^1H NMR (500 MHz, CDCl_3) $\delta_{\text{H}} = 8.05$ (br. d, $J_{\text{HH}} = 8.1$ Hz, 2H, ArH), 7.99 (br. s, 2H, ArH), 7.90 (br. d, $J_{\text{HH}} = 8.1$ Hz, 2H, ArH), 7.80 (br. d, $J_{\text{HH}} = 7.5$ Hz, 1H, ArH), 7.76 (br. d, $J_{\text{HH}} = 8.3$ Hz, 1H, ArH), 7.55 (br. d, $J_{\text{HH}} = 7.5$ Hz, 1H, ArH), 7.45 (br. s, 4H, ArH), 7.35 (br. m, 2H, ArH), 7.20 (br. d, $J_{\text{HH}} = 8.3$ Hz, 1H, ArH), 7.04 (br. m, 2H, ArH), 3.92 (br. s, 2H, CH_2), 2.14 (br. s, 12H, CH_3); ^{13}C NMR (126 MHz, CDCl_3) $\delta_{\text{C}} = 166.1, 165.9, 157.7, 155.6, 153.5, 152.4, 149.2, 147.6, 145.9, 144.8, 143.9, 141.5, 139.4, 136.7, 133.0, 132.8, 132.7, 131.9, 130.5, 130.4, 129.4, 129.4, 129.2, 127.0, 125.5, 125.3, 124.7, 124.4, 66.5, 60.5, 35.4, 18.8$; BET surface area = $450 \text{ m}^2/\text{g}$, total pore volume = $0.46 \text{ cm}^3/\text{g}$ at ($P/P_0 = 0.98$); GPC: $M_n = 203000$, $M_w = 321000 \text{ g/mol}$; TGA analysis: Initial weight loss due to thermal degradation commences at $\sim 438^\circ\text{C}$ with a 39% loss of mass below 1000°C .

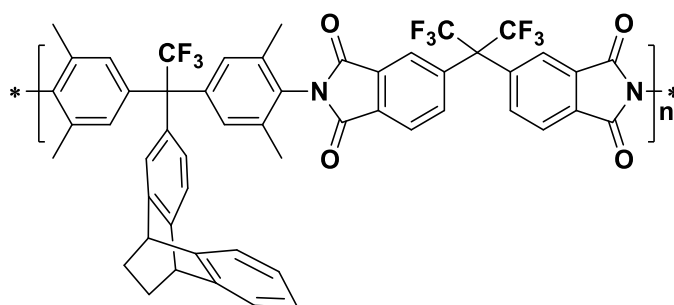
3.15: Synthesis of PIM-TFA15-PI



General procedure (X10) was followed using 6FDA (0.77 g, 1.74 mmol), ethanol (10 ml), triethylamine (0.88 g, 8.70 mmol), 1,1-bis(3,5-dimethyl-4-aminophenyl)-1-(2-tripcenyl)-

2,2,2-trifluoroethane (TFA15) (**46**) (1.00 g, 1.74 mmol) and NMP (5 ml). The mixture was refluxed for 72 h to afford PIM-TFA15-PI (1.60 g, 94%) as a light brown powder; FTIR (solid, cm^{-1}) $\nu = 1788, 1726, 1489, 1458, 1368, 1294, 1256, 1209, 1192, 1155, 1109, 984, 745, 723$; ^1H NMR (500 MHz, CDCl_3) $\delta_{\text{H}} = 8.03$ (br. d, $J_{\text{HH}} = 8.1$ Hz, 2H, ArH), 7.98 (br. s, 2H, ArH), 7.89 (br. d, $J_{\text{HH}} = 8.1$ Hz, 2H, ArH), 7.37 (br. m, 7H, ArH), 6.99 (br. m, 4H, ArH), 6.85 (br. m, 4H, ArH), 5.44 (br. s, 1H, CH), 5.41 (br. s, 1H, CH), 2.08 (br. s, 12H, CH_3); ^{13}C NMR (126 MHz, CDCl_3) $\delta_{\text{C}} = 166.1, 165.8, 145.7, 145.5, 145.4, 145.3, 141.4, 139.3, 136.6, 133.0, 132.7, 130.4, 130.4, 129.2, 126.9, 125.5, 125.8, 124.3, 124.0, 123.8, 120.1, 117.9, 54.2, 53.8, 27.2, 18.7$; BET surface area = $500 \text{ m}^2/\text{g}$, total pore volume = $0.37 \text{ cm}^3/\text{g}$ at ($P/P_0 = 0.98$); GPC: $M_n = 45000$, $M_w = 91400 \text{ g/mol}$; TGA analysis: Initial weight loss due to thermal degradation commences at $\sim 474 \text{ }^\circ\text{C}$ with a 37% loss of mass below $1000 \text{ }^\circ\text{C}$.

3.16: Synthesis of PIM-TFA18-PI



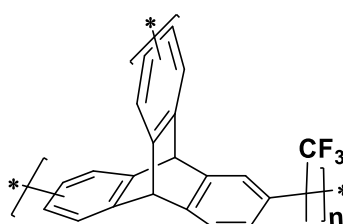
General procedure (X10) was followed using 6FDA (0.84 g, 1.89 mmol), ethanol (10 ml), triethylamine (0.95 g, 9.45 mmol), 1,1-bis[(3,5-dimethyl-4-aminophenyl)-1-(2-(9,10-dihydro-9,10-ethanoanthracenyl))] -2,2,2-trifluoroethane (TFA18) (**49**) (1.00 g, 1.89 mmol) and NMP (5 ml). The mixture was refluxed for 72 h to afford PIM-TFA18-PI (1.50 g, 82%) as a light brown powder; FTIR (solid, cm^{-1}) $\nu = 1786, 1728, 1624, 1487, 1439, 1367, 1296, 1256, 1209, 1192, 1142, 1109, 984, 750, 723$; ^1H NMR (500 MHz, CDCl_3) $\delta_{\text{H}} = 8.53$ (br. s, 2H, ArH), 7.98 (br. m, 4H, ArH), 7.05 (br. m, 11H, ArH), 3.91 (br. m, 6H, CH & CH_2), 2.84 (br. s, 12H, CH_3); ^{13}C NMR (126 MHz, CDCl_3) $\delta_{\text{C}} = 179.8, 175.2, 166.2, 165.7, 143.7, 143.6, 142.0, 139.1, 136.8, 136.4, 132.9, 132.5, 130.2, 129.3, 128.6, 127.6, 125.8, 125.6, 124.2, 123.5, 110.0, 49.5, 44.2, 30.7, 29.6, 17.7$; BET surface area = $490 \text{ m}^2/\text{g}$, total pore volume = $0.64 \text{ cm}^3/\text{g}$ at ($P/P_0 = 0.98$); GPC: $M_n = 3200$, $M_w = 4300 \text{ g/mol}$; TGA analysis: Initial weight loss due to thermal degradation commences at $\sim 275 \text{ }^\circ\text{C}$ with a 5% consistent with the loss of an ethylene fragment from the ethanoanthracene unit via a retro Diels-Alder reaction²⁰² then at $\sim 399 \text{ }^\circ\text{C}$ 28% loss of mass below $1000 \text{ }^\circ\text{C}$.

8.3.4: Aromatic Fluorinated Polymers

X11: General procedure of Aromatic Fluorinated Polymers

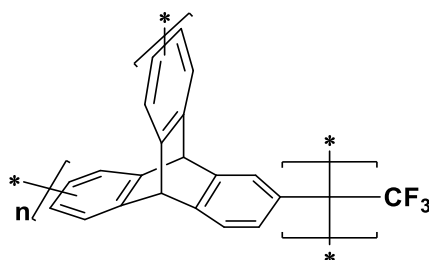
A mixture of an aromatic compound, trifluoroaryl ketone and DCM were cooled in an ice bath then TFSA was added to mixture with vigorous stirring, the mixture was allowed to warm to room temperature, the mixture was stirred at this temperature for an appropriate time. The resulting crude polymer was purified by reprecipitation from chloroform solution into methanol.

4.1: Poly[2-(2,6(7),13(14)-tritycenyyl)-1-trifluoro-2-propylene] (PIM-CF₃-A1)



General procedure (X11) was followed using triptycene (1.00 g, 3.9 mmol), 1,1,1-trifluoroacetone (0.44 g, 3.9 mmol), DCM (3 ml) and TFSA (3 ml). The mixture was stirred for 3 h to afford insoluble of PIM-CF₃-A1 (1.10 g, 80%) as an off-white powder; FTIR (solid, cm⁻¹) $\nu = 3071, 3017, 2957, 1477, 1464, 1140, 1123, 1074, 743$; ¹³C NMR (100.561 MHz, Solid) $\delta_c = 145.5, 135.9, 126.0, 114.6, 63.2, 50.1, 25.5$; BET surface area = 520 m²/g, total pore volume 0.45 cm³/g at (P/Po = 0.98); TGA analysis: Initial weight loss due to thermal degradation commences at ~ 497 °C with an 34% loss of mass below 1000 °C.

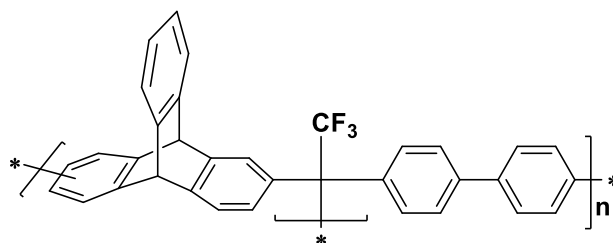
4.2: Poly[1-(2,6(7),13(14)-tritycenyyl)-2-trifluoroethylene] (PIM-CF₃-A2)



General procedure (X11) was followed using 2-tritycenyyltrifluoromethylketone (1.00 g, 2.85 mmol), DCM (10 ml) and TFSA (1 ml), the mixture was stirred for 2 h to afford insoluble of PIM-CF₃-A2 (0.82 g, 86%) as an off-white powder; FTIR (solid, cm⁻¹) $\nu = 1458, 1263, 1146, 1107, 741$; ¹³C NMR (100.561 MHz, Solid) $\delta_c = 145.4, 135.8, 124.1, 114.8,$

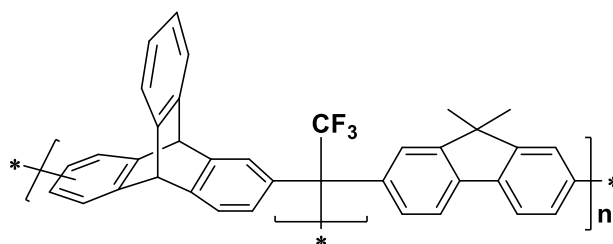
63.2 , 55.1; BET surface area = 790 m²/g, total pore volume 0.58 cm³/g at (P/Po = 0.98); TGA analysis: Initial weight loss due to thermal degradation commences at ~ 390 °C with a 21% loss of mass below 1000 °C.

4.3: Poly[2-(2,6(7)-tritypcenyl)-2-(4,4'-biphenyl)-1-trifluoroethylene] (PIM-CF₃-A3)



General procedure (X11) was followed using 2-tritypcenyl trifluoromethyl ketone (**10**) (1.00 g, 2.85 mmol), biphenyl (0.44 g, 2.85 mmol), DCM (10 ml) and TFSA (1 ml). The mixture was stirred for 24 h and purified with dissolved in CHCl₃ and re-precipitated into methanol three times to afford PIM-CF₃-A3 (0.75 g, 54%) as a light brown powder; FTIR (solid, cm⁻¹) ν = 1458, 1261, 1150, 1107 and 741 cm⁻¹; ¹H NMR (500 MHz, CDCl₃) δ _H = 7.47 (br. m, 13H, ArH), 6.98 (br. s, 4H, ArH), 5.37 (br. s, 2H, CH); ¹³C NMR (126 MHz, CDCl₃) δ _C = 145.1, 130.6, 130.6, 129.0, 127.2, 127.1, 125.3, 123.9, 123.7, 53.8, 31.0; BET surface area = 500 m²/g , total pore volume 0.28 ml/g at (P/Po = 0.98); GPC: M_n = 2600, M_w = 3500 g/mol; TGA analysis: Initial weight loss due to thermal degradation commences at ~ 407 °C with an 10% and an additional 12% loss of mass below 800 °C.

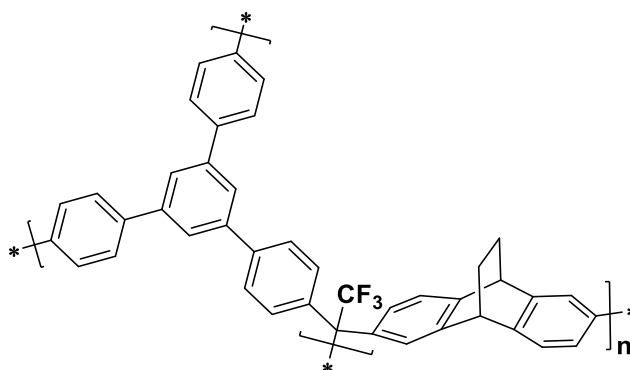
4.4: Poly[2-(2,6(7)-tritypcenyl)-2-(2,7-(9,9-dimethyl)fluorenyl)-1-trifluoroethylene] (PIM-CF₃-A4)



General procedure (X11) was followed using 2-tritypcenyl trifluoromethyl ketone (**10**) (1.00 g, 2.85 mmol), 9,9-dimethylfluorene (0.55 g, 2.85 mmol), DCM (5 ml) and TFSA (2.40 ml). The mixture was stirred for 24 h and purified with dissolved in CHCl₃ and re-precipitated into methanol three times to afford PIM-CF₃-A4 (0.87 g, 58%) as a light brown powder; FTIR (solid, cm⁻¹) ν = 1458, 1258, 1152, 1105, 739; ¹H NMR (500 MHz, CDCl₃) δ 7.3 (br. m , 11H,

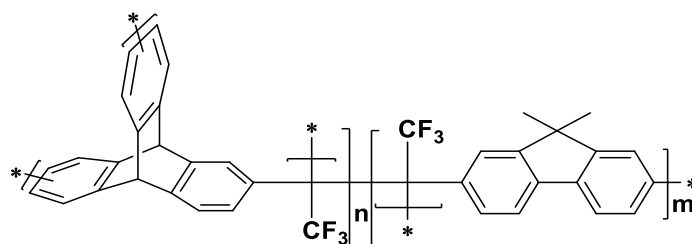
ArH), 6.98 (br. s, 4H, ArH), 5.41 (br. s, 2H, CH), 2.17 (br. s, 6H, CH₃); ¹³C NMR (126 MHz, CDCl₃) 145.2, 138.6, 128.1, 127.6, 127.2, 125.4, 123.9, 123.8, 122.7, 120.2, 115.4, 53.8, 47.1, 31.1, 27.2; BET surface area = 390 m²/g, total pore volume 0.35 cm³/g at (P/Po = 0.98); GPC: M_n = 3000, M_w = 7000 g/mol; TGA analysis: Initial weight loss due to thermal degradation commences at ~ 406 °C with a 6% and a further 21% loss of mass below 1000 °C.

4.5: Poly[2-(2,6(7)-ethanoanthracenyl)-2-(4,4',4''-(1,3,5-triphenylbenzene)-1-trifluoroethylene] (PIM-CF₃-A5)



General procedure (X11) was followed using 2-(9,10-dihydro-9,10-ethanoanthracenyl) trifluoromethyl ketone (3.00 g, 9.92 mmol), 1,3,5-triphenylbenzene (1.01 g, 3.31 mmol), DCM (10 ml) and TFSA (10 ml). The mixture was stirred for 3 h to afford insoluble of PIM-CF₃-A5 (3.1 g, 79%) as a light brown powder; FTIR (solid, cm⁻¹) ν = 2943, 1261, 1446, 1109, 818, 761; ¹³C NMR (100.561 MHz, Solid) δ_c = 142.8, 127.4, 64.9, 45.2, 26.2; BET surface area = 955 m²/g, total pore volume 0.74 cm³/g at (P/Po = 0.98); TGA analysis: Initial weight loss due to thermal degradation commences at ~ 256 °C with a 7% consistent with the loss of an ethylene fragment from the ethanoanthracene unit via a retro Diels-Alder reaction²⁰² then at ~ 425 °C with a 22% loss of mass below 1000 °C.

4.6: Poly[1-(2,6(7),13(14)-triptycenyl)-2-trifluoroethylene-co-2-(2,7-(9,9-dimethyl)fluorenyl)-1-trifluoroethylene] (PIM-CF₃-A6)



General procedure (X11) was followed using 2-triptycenyyl trifluoromethyl ketone (**10**) (1.11 g, 3.18 mmol), 2-(9,9-dimethyl)fluorenyl trifluoromethyl ketone (**9**) (0.62 g, 2.35 mmol), DCM (2.4 ml) and TFSA (2.4 ml). The mixture was stirred 2 h to afford insoluble of PIM-CF₃-A6 (1.25 g, 76%) as a light brown powder; FTIR (solid, cm⁻¹) ν = 2943, 1261, 1446, 1109, 818, 761; ¹³C NMR (100.561 MHz, Solid) δ_c = 154.0, 145.4, 139.3, 124.1, 65.1, 55.3, 46.7, 25.5; BET surface area = 735 m²/g, total pore volume 0.78 cm³/g at (P/Po = 0.98); TGA analysis: Initial weight loss due to thermal degradation commences at ~ 382 °C with a 23% loss of mass below 1000 °C.

Bibliography:

1. J. Rouquerol, D. Avnir, C. W. Fairbridge, D. H. Everett, J. H. Haynes, N. Pernicone, J. D. F. Ramsay, K. S. W. Sing and K. K. Unger, *Pure and Applied Chemistry*, 1994, 66, 1739-1758.
2. X. S. Zhao, *Journal of Materials Chemistry*, 2006, 16, 623-625.
3. Å. Oterhals, M. Solvang, R. Nortvedt and M. H. G. Berntssen, *European Journal of Lipid Science and Technology*, 2007, 109, 691-705.
4. H. Furukawa and O. M. Yaghi, *Journal of the American Chemical Society*, 2009, 131, 8875-8883.
5. Y. Wang, N. B. McKeown, K. J. Msayib, G. A. Turnbull and I. D. W. Samuel, *Sensors*, 2011, 11, 2478-2487.
6. J. Shailaja, P. H. Lakshminarasimhan, A. R. Pradhan, R. B. Sunoj, S. Jockusch, S. Karthikeyan, S. Uppili, J. Chandrasekhar, N. J. Turro and V. Ramamurthy, *The Journal of Physical Chemistry A*, 2002, 107, 3187-3198.
7. C. C. Freyhardt, M. Tsapatsis, R. F. Lobo, K. J. Balkus and M. E. Davis, *Nature*, 1996, 381, 295-298.
8. S. M. Csicsery, *Zeolites*, 1984, 4, 202-213
9. Y. Rong, R. Malpass-Evans M. Carta, N. B. McKeown, G. A. Attard and F. Marken, *Electroanalysis*, 2014, 26, 904-909.
10. S. V. Adymkanov, Y. P. Yampol'skii, A. M. Polyakov, P. M. Budd, K. J. Reynolds, N. B. McKeown and K. J. Msayib, *Polymer Science Series A*, 2008, 50, 444-450.
11. A. Dyer, T. Las and M. Zubair, *Journal of Radioanalytical and Nuclear Chemistry*, 2000, 243, 839-841.
12. Y. Rong, A. Kolodziej, E. Madrid, M. Carta, R. Malpass-Evans, N. B. McKeown and F. Marken, *Journal of Electroanalytical Chemistry*, 2015, *In Press*.
13. T. Masuda, E. Isobe, T. Higashimura and K. Takada, *Journal of the American Chemical Society*, 1983, 105, 7473-7474.
14. R. M. de Vos and H. Verweij, *Journal of Membrane Science*, 1998, 143, 37-51.
15. S. Sircar, *Separation and Purification Technology*, 1999, 17, 11-20.
16. D. Wang, W.K. Teo and K. Li, *Separation and Purification Technology*, 2004, 35, 125-131.
17. P. M. Budd, N. B. McKeown, B. S. Ghanem, K. J. Msayib, D. Fritsch, L. Starannikova, N. Belov, O. Sanfirova, Y. Yampolskii and V. Shantarovich, *Journal of Membrane Science*, 2008, 325, 851-860.

18. S. Sircar, W. E. Waldron, M. B. Rao and M. An, *Separation and Purification Technology*, 1999, 17, 11-20.
19. N. B. McKeown, B. Gahnem, K. J. Msayib, P. M. Budd, C. E. Tattershall, K. Mahmood, S. Tan, D. Book, H. W. Langmi and A. Walton, *Angewandte Chemie International Edition*, 2006, 45, 1804-1807.
20. C. D. Wood, B. Tan, A. Trewin, H. Niu, D. Bradshaw, M. J. Rosseinsky, Y. Z. Khimyak, N. L. Campbell, R. Kirk, E. Stöckel and A. I. Cooper, *Chemistry Materials*, 2007, 19, 2034-2048.
21. D. Zhao, D. Yuan and H. Zhou, *Energy & Environmental Science*, 2008, 1, 222-235.
22. L. J. Murray, M. Dincă, J. R. Long, *Chemical Society reviews*, 2009, 38, 1294-1314.
23. R. Dawson, E. Stöckel, J. R. Holst, D. J. Adams, A. I. Cooper, *Energy and Environmental Science*, 2011, 4, 4239-4245.
24. T. J. Barton, L. M. Bull, W. G. Klemperer, D. A. Loy, B. McEnaney, M. Misono, P. A. Monson, G. Pez, G. W. Scherer, J. C. Vartuli and O. M. Yaghi, *Chemistry Materials*, 1999, 11, 2633-2656
25. J. Parmentier, F. O. M. Gaslain, O. Ersen, T. A. Centeno and L. A. Solovyov, *Langmuir*, 2013, 30, 297-307.
26. B. H. Davis and K. S. W. Sing, in *Handbook of Porous Solids*, Wiley, Hoboken, New Jersey, 2008, ch.1, pp. 1-23.
27. A. F. Masters and T. Maschmeyer, *Microporous and Mesoporous Materials*, 2011, 142, 423-438.
28. H. van Bekkum, E. M. Flanigen, J. C. Jansen and P. A. Jacobs, *Introduction to Zeolite Science and Practice*, 2001, vol. 137.
29. A. K. Cheetham, G. Ferey and T. Loiseau, *Angew. Chemie-International Ed.*, 1999, 38, 3268-3292.
30. C. Baerlocher, L. McCusker and D. Olson, *Atlas of zeolite framework types*, 2007, vol. 12.
31. D. R. Corbin, L. Abrams, G. A. Jones, M. M. Eddy, W. T. A. Harrison, G. D. Stucky and D. E. Cox, *Journal of the American Chemical Society*, 1990, 112, 4821-4830.
32. A. Bieniok and K. D. Hammonds, *Microporous Mesoporous Materials*, 1998, 25, 193-200.
33. C. Quintelas, Z. Rocha, B. Silva, B. Fonseca, H. Figueiredo and T. Tavares, *Chemical Engineering Journal*, 2009, 152, 110.
34. D. J. C. Yates, *Canadian Journal of Chemistry*, 1968, 46, 1695-1701.
35. J. C. Van Der Waal and H. Van Bekkum, *Journal of Porous Materials*, 1998, 5, 289-303.
36. Y., Zheng, X., Li and P. K. Dutta, *Sensors (Basel)*, 2012, 12, 5170-5194.

37. S. Velu, X. Ma and C. Song, *Industrial and Engineering Chemical Research*, 2003, 42, 5293-5304.
38. W. Qiu and Y. Zheng, *Journal of Hazardous Materials*, 2007, 148, 721-726.
39. S. H. Hyun, J. K. Song, B. I. Kwak, J. H. Kim and S. A. Hong, *Journal of Materials Science*, 1999, 34, 3095-3103.
40. A. Zecchina, S. Bordiga, J. G. Vitillo, G. Ricchiardi, C. Lamberti, G. Spoto, M. Bjorgen and K. P. Lillerud, *Journal of the American Chemical Society*, 2005, 127, 6361-6366.
41. A. Corma, M. J. Diaz-Cabanas, J. Martinez-Triguero, F. Rey and J. Rius, *Nature*, 2002, 418, 514-517.
42. S. R. Batten, N. R. Champness, X. Chen, J. Garcia-Martinez, S. Kitagawa, L. Öhrström, M. O’Keeffe, M. P. Suh and J. Reedijk, *Pure Appl. Chem.*, 2013, vol. 85, No. 8, 1715-1724.
43. H. K. Chae, D. Y. Siberio-Pérez, J. Kim, Y. Go, M. Eddaoudi, A. J. Matzger, M. O’Keeffe and O. M. Yaghi, *Nature*, 2004, 427, 523-527.
44. O. K. Farha, I. Eryazici, N. C. Jeong, B. G. Hauser, C. E. Wilmer, A. A. Sarjeant, R. Q. Snurr, S. T. Nguyen, A. Ö. Yazaydın and J. T. Hupp, *Journal of the American Chemical Society*, 2012, 134, 15016-15021.
45. K. K. Tanabe and S. M. Cohen, *Chemical Society Reviews*, 2011, 40, 498-519.
46. J. Lee, O. K. Farha, J. Roberts, K. A. Scheidt, S. T. Nguyen and J. T. Hupp, *Chemical Society Reviews*, 2009, 38, 1450-1459.
47. B. V. Harbuzaru, A. Corma, F. Rey, P. Atienzar, J. L. Jorda, H. Garcia, D. Ananias, L. D. Carlos and J. Rocha, *Angewandte Chemie International Edition English*, 2008, 47, 1080-1083.
48. J. Li, R. J. Kuppler and H. Zhou, *Chemical Society Reviews*, 2009, 38, 1477-1504.
49. N. L. Rosi, J. Eckert, M. Eddaoudi, D. T. Vodak, J. Kim, M. O’Keeffe and O. M. Yaghi, *Science*, 2003, 1127-1129.
50. B. Liu, L. Pang, L. Hou, Y. Wang, Y. Zhang and Q. Shi, *CrystEngComm* 2012, 14, 6246-6251.
51. P. Horcajada, T. Chalati, C. Serre, B. Gillet, C. Sebrie, T. Baati, J. F. Eubank, D. Heurtaux, P. Clayette, C. Kreuz, J.-S. Chang, Y. K. Hwang, V. Marsaud, P.-N. Bories, L. Cynober, S. Gil, G. Ferey, P. Couvreur and R. Gref, *Nature Materials*, 2010, 9, 172-178.
52. P. Horcajada, C. Serre, M. Vallet-Regi, M. Sebban, F. Taulelle and G. Ferey, *Angewandte Chemie International Edition English*, 2006, 45, 5974-5978.
53. M. Mastalerz, *Angewandte Chemie International Edition*, 2008, 47, 445-447.
54. A. P. Côté, A. I. Benin, N. W. Ockwig, M. O’Keeffe, A. J. Matzger and O. M. Yaghi, *Science*, 2005, 310, 1166-1170.

55. L. Wang, L. Wang, J. Zhao and T. Yan, *Journal of Applied Physics*, 2012, 111, 112628.
56. M. Dogru and T. Bein, *Chemical Communications*, 2014, 50, 5531-5546.
57. J. L. Mendoza-Cortes, T. A. Pascal and W. A. Goddard, *The Journal of Physical Chemistry A*, 2011, 115, 13852-13857.
58. S. Ding, J. Gao, Q. Wang, Y. Zhang, W. Song, C. Su and W. Wang, *Journal of the American Chemical Society*, 2011, 133, 19816-19822.
59. S. Wan, J. Guo, J. Kim, H. Ihee and D. Jiang, *Angewandte Chemie International Edition English*, 2008, 47, 8826-8830.
60. R. W. Tilford, S. J. Mugavero III, P. J. Pellechia and J. J. Lavigne, *Advanced Materials*, 2008, 20, 2741-2746.
61. S. S. Han, H. Furukawa, O. M. Yaghi and W. A. Goddard. *Journal of the American Chemical Society*, 2008, 130, 11580-11581.
62. J. Lan, D. Cao, W. Wang and B. Smit, *ACS Nano*, 2010, 4, 7, 4225-4237.
63. N. B. McKeown and P. M. Budd, *Macromolecules*, 2010, 43, 5163-5176.
64. J. M. Dias, M. C. M. Alvim-Ferraz, M. F. Almeida, J. Rivera-Utrilla and M. Sánchez-Polo, *Journal of Environmental Management*, 2007, 85, 833-846.
65. A. Bhatnagar, W. Hogland, M. Marques and M. Sillanpää, *Chemical Engineering Journal*, 2013, 219, 499-511.
66. Y. Zhao, L. Zhao, K. X. Yao, Y. Yang, Q. Zhang and Y. Han, *Journal of Materials Chemistry*, 2012, 22, 19726-19731.
67. M. Sobiesiak, B. Gawdzik, A. M. Puziy and O. I. Poddubnaya, *Applied Surface Science*, 2010, 256, 5355-5360.
68. H. Jüntgen, *Fuel*, 1986, 65, 1436-1446.
69. N. Areerachakul, S. Vigneswaran, H. H. Ngo and J. Kandasamy, *Separation and Purification Technology*, 2007, 55, 206-211.
70. S. M. Manocha, *Sadhana*, 2003, 28, 335-348.
71. P. Ehrenfreund and B. H. Foing, *Science*, 2010, 329, 1159-1160.
72. T. Ben, H. Ren, S. Ma, D. Cao, J. Lan, X. Jing, W. Wang, J. Xu, F. Deng, J. M. Simmons, S. Qiu and G. Zhu, *Angewandte Chemie International Edition English*, 2009, 121, 9621-9624.
73. A. Trewin, A. I. Cooper, *Angewandte Chemie International Edition English*, 2010, 49, 1533-1535.
74. G. Zhu and H. Ren, *Porous Organic Frameworks: Design, Synthesis and Their Advanced Applications*, Springer, 2014, vol. 28.
75. T. Ben and S. Qiu, *CrystEngComm*, 2013, 15, 17-26.

76. J. R. Holst, E. Stöckel, D. J. Adams and A. I. Cooper, *Macromolecules*, 2010, 43, 8531-8538.
77. T. Ben, C. Pei, D. Zhang, J. Xu, F. Deng, X. Jing, and S. Qiu, *Energy & Environmental Science*, 2011, 4, 3991-3999.
78. D. Yuan, W. Lu, D. Zhao and H. Zhou, *Advanced Materials*, 2011, 23, 3723-3725.
79. R. Dawson, A. I. Cooper and D. J. Adams, *Progress in Polymer Science*, 2012, 37, 530-563.
80. M. P. Tsyurupa and V. A. Davankov, *Reactive & Functional Polymers*, 2002, 53, 193-203.
81. B. Li, R. Gong, Y. Luo and B. Tan, *Soft Matter*, 2011, 7, 10910-10916.
82. J. Ahn, J. Jang, C. Oh, S. Ihm, J. Cortez and D. C. Sherrington, *Macromolecules*, 2006, 39, 627-632.
83. J. Germain, J. Hradil, J. M. J. Fréchet and F. Svec, *Chemistry Materials*, 2006, 18, 4430-4435.
84. J. Lee, C. D. Wood, D. Bradshaw, M. J. Rosseinsky and A. I. Cooper, *Chemical Communications*, 2006, 2670-2672.
85. B. C. Pan, Y. Xiong, A. M. Li, J. L. Chen, Q. X. Zhang and X. Y. Jin, *Reactive and Functional Polymers*, 2002, 53, 63-72.
86. J. Germain, J. M. J. Fréchet and F. Svec, *Journal of Materials Chemistry*, 2007, 17, 4989-4997.
- 87.- Y. Luo, B. Li, W. Wang, K. Wu and B. Tan, *Advanced Materials*, 2012, 24, 5703-5707.
88. Q. Zhou, M. Wang, A. Li, C. Shuang, M. Zhang, X. Liu and L. Wu, *Frontiers of Environmental Science & Engineering*, 2013, 7, 3, 412-419.
89. M. Chen, Y. Liu, X. Xing, X. Zhou, Y. Feng and B. Yuan, *Chemistry A European Journal*, 2013, 19, 1035-1041.
90. N. B. McKeown and P. M. Budd, *Encyclopedia of Polymer Science and Technology*, John Wiley & Sons, Inc., 2009.
91. N. B. McKeown, P. M. Budd, K. J. Msayib, B. S. Ghanem, H. J. Kingston, C. E. Tattershall, S. Makhseed, K. J. Reynolds, D. Fritsch, *Chemistry A European Journal*, 2005, 11, 2610-2620.
92. P. M. Budd, N. B. McKeown and D. Fritsch, *Journal of Materials Chemistry*, 2005, 15, 1977-1986.
93. E. S. Finkelshtein, K. L. Makovetskii, M. L. Gringolts, Y. V. Rogan, T. G. Golenko, L. E. Starannikova, Y. P. Yampolskii, V. P. Shantarovich and T. Suzuki, *Macromolecules*, 2006, 39, 7022-7029.
94. H. Zhang, S. Wang and S. G. Weber, *Journal of Membrane Science*, 2013, 443, 115-123.
95. J. C. Jansen, F. Tasselli, E. Tocci and E. Drioli, *Desalination*, 2006, 192, 207-213.

96. Y. Hu, M. Shiotsuki, F. Sanda, B. D. Freeman and T. Masuda, *Macromolecules*, 2008, 41, 8525-8532.
97. B. S. Ghanem, N. B. McKeown, P. M. Budd, J. D. Selbie and D. Fritsch, *Advanced Materials*, 2008, 20, 2766-2771.
98. B. S. Ghanem, K. J. Msayib, N. B. McKeown, K. D. M. Harris, Z. Pan, P. M. Budd, A. Butler, J. Selbie, D. Book and A. Walton, *Chemical Communications*, 2007, 67-69.
99. P. M. Budd, E. S. Elabas, B. S. Ghanem, S. Makhseed, N. B. McKeown, K. J. Msayib, C. E. Tattershall and D. Wang, *Advanced Materials*, 2004, 16, 5, 456-459.
100. N. B. McKeown, S. Makhseed and P. M. Budd, *Chemical Communications*, 2002, 2780-2781.
101. B. S. Ghanem, M. Hashem, K. D. M. Harris, K. J. Msayib, M. Xu, P. M. Budd, N. Chaukura, D. Book, S. Tedds, A. Walton and N. B. McKeown, *Macromolecules*, 2010, 43, 5287-5294.
102. H. Izumikawa, T. Masuda and T. Higashimura, *Polymer Bulletin*, 1991, 27, 193-199.
103. V. S. Khotimsky, M. V. Tchirkova, E. G. Litvinova, A. I. Rebrov and G. N. Bondarenko, *Journal of Polymer Science Part A Polymer Chemistry*, 2003, 41, 2133-2155.
104. C. E. Sroog, *Progress in Polymer Science*, 1991, 16, 561-694.
105. C. E. Sroog, A. L. Endrey, S. V. Abramo, C. E. Berr, W. M. Edwards and K. L. Olivier, *Journal of Polymer Science Part A: General Papers*, 1965, 3, 1373-1390.
106. M. A. Meador, *Annual Review of Materials science*, 1998, 28, 599-630.
107. D. Liaw, K. Wang, Y. Huang, K. Lee, J. Lai and C. Ha, *Progress in Polymer Science*, 2012, 37, 907-974.
108. M. L. Cecopieri-Gómez, J. Palacios-Alquisira and J. M. Domínguez, *Journal of Membrane Science*, 2007, 293, 53-65.
109. S. Sridhar, R. S. Veerapur, M. B. Patil, K. B. Gudasi and T. M. Aminabhavi, *Journal of Applied Polymer Science*, 2007, 106, 1585-1594.
110. Y. Rogan, R. Malpass-Evans, M. Carta, M. Lee, J. C. Jansen, P. Clarizia, E. Tocci, K. Friess, M. Lanc and Neil B. Mckeown, *Journal of Materials Chemistry A*, 2014, 2, 4874-4877.
111. C. Nagel, K. Gunther-Schade, D. Fritsch, T. Strunskus and F. Fauupel, *Macromolecules*, 2002, 35, 2071-2077.
112. R. R. Tiwari, Z. P. Smith, H. Lin, B. D. Freeman and D. R. Paul, *Polymer*, 2014, 55, 5788-5800.
113. R. R. Tiwari, Z. P. Smith, H. Lin, B. D. Freeman and D. R. Paul, *Polymer*, 2015, 61, 1-14.

114. F. Alghunaimi, B. Ghanem, N. Alaslai, R. Swaidan, E. Litwiller and I. Pinnau, *Journal of Membrane Science*, 2015, 490, 321-327.
115. Y. J. Cho and H. B. Park, *Macromolecular Rapid Communications*, 2011, 32, 579-586.
116. Q. Zhang, G. Chen and S. Zhang, *Polymer*, 2007, 48, 2250-2256.
117. M. Heuchel, D. Fritsch, P. M. Budd, N. B. McKeown and D. Hofmann, *Journal of Membrane Science*, 2008, 318, 84-99.
118. Y. Rogan, L. Starannikova, V. Ryzhikh, Y. Yampolskii, P. Bernardo, F. Bazzarelli, J. C. Jansen and N. B. McKeown, *Polymer Chemistry*, 2013, 4, 3813-3820.
119. X. Ma, B. Ghanem, O. Salines, E. Litwiller and I. Pinnau, *ACS Macro Letters*, 2015, 4, 231-235.
120. R. Swaidan, M. Al-Saedi, B. Ghanem, E. Litwiller and I. Pinnau, *Macromolecules*, 2014, 47, 5104-5114.
121. B. S. Ghanem, R. Swaidan, E. Litwiller and I. Pinnau, *Advanced Materials*, 2014, 26, 3688-3692.
122. R. Swaidan, B. Ghanem, E. Litwiller and I. Pinnau, *Macromolecules*, 2015, 48, 18, 6553-6561.
123. R. J. Swaidan, B. Ghanem, R. Swaidan, E. Litwiller and I. Pinnau, *Journal of Membrane Science*, 2015, 492, 116-122.
124. N. B. McKeown and P. M. Budd, *Chemical Society Reviews*, 2006, 35, 675-683.
125. P. M. Budd, B. S. Ghanem, S. Makhseed, N. B. McKeown, K. J. Msayib and C. E. Tattershall, *Chem. Commun.*, 2004, 230-231.
126. A. Yushkin, A. Grekhov, S. Matson, M. Bermeshev, V. Khotimsky, E. Finkelstein, P. M. Budd, V. Volkov, T. J.H. Vlught, A. Volkov, *Reactive and Functional Polymers*, 2015, 86, 269-281.
127. N. Du, G. P. Robertson, J. Song, I. Pinnau and M. D. Guiver, *Macromolecules*, 2009, 42, 6038-6043.
128. J. Weber, N. Du and M. D. Guiver, *Macromolecules*, 2011, 44, 1763-1767.
129. N. Du, G. P. Robertson, M. M. Dal-Cin, L. Scoles and M. D. Guiver, *Polymer*, 2012, 53, 4367-4372.
130. W. F. Yong, F. Y. Li, Y. C. Xiao, P. Li, K. P. Pramoda, Y. W. Tong and T. S. Chung, *Journal of Membrane Science*, 2012, 407, 47-57.
131. N. Du, G. P. Robertson, J. Song, I. Pinnau, S. Thomas, and M. D. Guiver, *Macromolecules*, 2008, 41, 9656-9662.

132. B. S. Ghanem, N. B. McKeown, P. M. Budd and D. Fritsch, *Macromolecules*, 2008, 41, 1640-1646.
133. P. M. Budd, K. J. Msayib, C. E. Tattershall, B. S. Ghanem, K. J. Reynolds, N. B. McKeown and D. Fritsch, *Journal of Membrane Science*, 2005, 251, 263-269.
134. P. M. Budd, N. B. McKeown and D. Fritsch, *Macromolecular Symposia*, 2006, 245-246, 403-405.
135. C. G. Bezzu, M. Carta, A. Tonkins, J. C. Jansen, P. Bernardo, F. Bazzarelli and N. B. McKeown, *Advanced Materials*, 2012, 24, 5930-5933.
136. M. Carta, P. Bernardo, G. Clarizia, J. C. Jansen, and N. B. McKeown, *Macromolecules*, 2014, 47, 8320-8327.
137. J. Tröger, *Journal für Praktische Chemie*, 1887, 36, 225-245.
138. M. A. Spielman, *Journal of the American Chemical Society*, 1935, 57, 583-585.
139. S. B. Larson and C. S. Wilcox, *Acta Crystallographica Section C*, 1986, 42, 224-227.
140. S. Sergeev, *Helvetica Chimica Acta*, 2009, 92, 415-444.
141. D. Didier, B. Tylleman, N. Lambert, C. Velde, F. Blockhuys, A. Collas and S. Sergeev, *Tetrahedron*, 2008, 64, 6252-6262.
142. O. Trapp and V. Schurig, *Journal of the American Chemical Society*, 2000, 122, 1424-1430.
143. B. M. Wepster, *Recueil des Travaux Chimiques des Pays-Bas*, 1953, 72, 661-672.
144. E. Marquis, J. Graton, M. Berthelot, A. Planchat and C. Laurence, *Canadian Journal of Chemistry*, 2004, 82, 1413-1422.
145. Ö. V. Rúnarsson, J. Artacho and K. Wärnmark, *European Journal of Organic Chemistry*, 2012, 2012, 7015-7041.
146. M. Fukae and T. Inazu, *Journal of Inclusion Phenomena*, 1984, 2, 223-229.
147. R. A. Johnson, R. R. Gorman, R. J. Wnuk, N. J. Crittenden and J. W. Aiken, *Journal of Medicinal Chemistry*, 1993, 36, 3202-3206.
148. U. Maitra, B. G. Bag, P. Rao and D. Powell, *Journal of the Chemical Society, Perkin Transactions 1*, 1995, 2049-2056.
149. B. G. Bag and U. Maitra, *Synthetic Communications*, 1995, 25, 1849-1856.
150. M. Carta, M. Croad and N. B. McKeown, WO2012035328 A1, 2010.
151. M. Carta, R. Malpass-Evans, M. Croad, Y. Rogan, J. C. Jansen, P. Bernardo, F. Bazzarelli and N. B. McKeown, *Science*, 2013, 339, 303-307.
152. Y. Rong, R. Malpass-Evans, M. Carta, N. B. McKeown, G. A. Attard and F. Marken, *Electroanalysis*, 2014, 26, 904-909.

153. J. R. Cabrero-Antonino, T. García, P. Rubio-Marqués, J. A. Vidal-Moya, A. Leyva-Pérez, S. S. Al-Deyab, S. I. Al-Resayes, U. Díaz and A. Corma, *ACS Catalysis*, 2011, 1, 147-158.
154. E. Poli, E. Merino, U. Diaz, D. Brunel and A. Corma, *Journal Physical Chemistry C*, 2011, 115, 7573-7585.
155. L. Peters, A. Hussain, M. Follmann, T. Melin and M.-B. Hägg, *Chemical Engineering Journal*, 2011, 172, 952- 960.
156. J. Zhou, X. Zhu, J. Hu, H. Liu, Y. Hua and J. Jiang, *Physical Chemistry Chemical Physics*, 2014, 16, 6075-6083.
157. H. Marsh and F. R. Reinoso, *Activated Carbon*, Elsevier, 2006.
158. T. M. Long and T. M. Swager, *Advanced Materials*, 2001, 13, 601-604.
159. M. Carta, M. Croad, K. Bugler, K. J. Masyib and N. B. McKeown, *Polymer Chemistry*, 2014, 5, 5262-5266.
160. F. A. L. Dullien, *Porous Media: Fluid Transport and Pore Structure*, Academic Press, 1992.
161. G. S. Larsen, P. Lin, K. E. Hart and C. M. Colina, *Macromolecules*, 2011, 44, 6944-6951.
162. L. J. Abbott, A. G. McDermott, A. Del Regno, R. G. D. Taylor, C. G. Bezzu, K. J. Msayib, N. B. McKeown, F. R. Siperstein, J. Runt and C. M. Colina, *Journal Physical Chemistry B*, 2013, 117, 355-64.
163. J. Rouquerol, G. Baron, R. Denoyel, H. Giesche, J. Groen, P. Klobes, P. Levitz, A. V. Neimark, S. Rigby, R. Skudas, K. Sing, M. Thommes and K. Unger, *Pure and Applied Chemistry*, 2012, 84, 107-136.
164. S. Brunauer, P. H. Emmett and E. Teller, *Journal of the American Chemical Society*, 1938, 60, 309-319.
165. I. Langmuir, *Journal of the American Chemical Society*, 1917, 39, 1848-1906.
166. I. M. K. Ismail, *Carbon*, 1990, 28, 423-434.
167. K. Sing, *Pure and Applied Chemistry*, 1985, 57, 603-619.
168. D. R. Paul and Y. P. Yampol'skii, *Polymeric Gas Separation Membranes*, CRC Press, 1993.
169. R. W. Baker, *Membrane Technology and Applications*, 2012.
170. M. Mulder, *Basic Principles of Membrane Technology*, Springer Science & Business Media, 1996, vol. 384.
171. C. A. Scholes, S. E. Kentish and G. W. Stevens, *Recent Patents on Chemical Engineering*, 2008, 1, 52-66.

172. R. W. Baker, *Membrane Technology and Applications*, Wiley, Hoboken, New Jersey, 2004.
173. K. Kamide, S. Manabe, H. Makino, T. Nohmi, H. Narita and T. Kawai, *Polymer Journal*, 1983, 15, 179-193.
174. T. Graham, *Philosophical Magazine and Journal of Science*, 1866, 401-420.
175. B. Freeman and Y. Yampolskii, *Membrane Gas Separation*, Wiley, Hoboken, New Jersey, 2011.
176. B. Freeman, Y. Yampolskii and I. Pinnau, *Materials Science of Membranes for Gas and Vapor Separation*, Wiley, Hoboken, New Jersey, 2006.
177. H. L. Frisch, *Journal of Applied Polymer Science*, 1970, 14, 1657-1657.
178. W. R. Vieth, J. M. Howell and J. H. Hsieh, *Journal of Membrane Science*, 1976, 1, 177-220.
179. K. Nagai, A. Higuchi and T. Nakagawa, *Journal of Polymer Science Part B: Polymer Physics*, 1995, 33, 289-298.
180. K. D. Dorkenoo and P. H. Pfromm, *Macromolecules*, 2000, 33, 3747-3751.
181. D. W. Breck, *Zeolite molecular sieves: structure, chemistry, and use*, Wiley, Hoboken, New Jersey, 1973.
182. R. Baker and I. Blume, *Chemtech*, 1986, 16, 232-238.
183. K. Mohanty and M. K. Purkait, *Membrane Technologies and Applications*, CRC press, Boca Raton, Florida, 2011.
184. L. M. Robeson, *Journal of Membrane Science*, 1991, 62, 165-185.
185. L. M. Robeson, *Journal of Membrane Science*, 2008, 320, 390-400.
186. M. Carta, M. Croad, R. Malpass-Evans, J. C. Jansen, P. Bernardo, G. Clarizia, K. Friess, M. Lanċ and N. B. McKeown, *Advanced Materials*, 2014, 26, 3526-3531.
187. E. Weber, K. Skobridis, A. Wierig, L. R. Nassimbeni and L. Johnson, *Journal of the Chemical Society, Perkin Transactions 2*, 1992, 2123-2130.
188. X. Creary, *The Journal Organic Chemistry*, 1987, 52, 5026-5030.
189. G.K. S. Prakasha, J. Hua, M. M. Alauddinb, P. S. Contib, G. A. Olah, *Journal of Fluorine Chemistry*, 2003, 121, 239-243.
190. E. Martinelli, A. C. Vicini, M. Mancinelli, A. Mazzanti, P. Zani, L. Bernardi and M. Fochi, *Chemical Communications*, 2015, 51, 658-660.

191. J. Wang, J. Kubicki, T. L. Gustafson and M. S. Platz; *Journal of the American Chemical Society*, 2008, *130*, 2304-2313.
192. M. Bandini, A. Pietrangelo, R. Sinisi, A. Umami-Ronchi, and M. O. Wolf, *European Journal of Organic Chemistry*, 2009, *21*, 3554-3561.
193. L. A. Esposito, M. F. Hudson, T. Lake, C. Joel, W. Manfred and A. D. Snow; *USA Patent Application*, 20120035230, 2012.
194. L. Tao, H. Yang, J. Liu, L. Fan and S. Yang, *Synthetic Communications*, 2013, *43*, 2319-2325.
195. W. F. Burgoyne, Jr., M. Langsam, *USA Patent*, 4990667, 1991.
196. K. Choi, M. H. Yi, *Macromolecules Symposia*, 1999, *142*, 193.
197. C. Gao, S. Zhang, L. Gao, M. Ding, *Macromolecules*, 2003, *36*, 5559.
198. S. Yang, X. Zhao, L. Fan, J. Liu, *Chinese patent*, CN 101307004A, 2008.
199. J. E. True, T. D. Thomas, R. W. Winter and G. L. Gard, *Inorganic Chemistry*, 2003, *42*, 14, 4437-4441.
200. B. Ameduri and B. Boutevin, *Well-architected fluoropolymers synthesis, properties and applications*, 1st Ed., Elsevier, 2004, pp. 2-3.
201. K. S. W. Sing, D. H. Everett, R. A. W. Haul, L. Moscou, R. A. Perotti, J. Rouquerol and T. Siemieniewska, *Pure and Applied Chemistry*, 1985, *57*, 603.
202. Y. Chung, B. F. Duerr, T. A. McKelvey, P. Nanjappan and A. W. Czarnik, *The Journal of Organic Chemistry*, 1989, *54*, 1018-1032.
203. Y. Yampolskii and B. Freeman, *Membrane Gas Separation*, John Wiley & Sons, Ltd, 2010, pp. 30-31.
204. M. Crata, M. Croad, J. C. Jansen, P. Bernardo, G. Clarizia and N. B. McKeown, *Polymer Chemistry*, 2014, *5*, 5255-5261.
205. S. A. Stern, *Journal of Membrane Science*, 1994, *94*, 1-65.
206. M. R. Coleman, W. J. Koros, *Journal of Polymer Science Part B: Polymer Physics*, 1994, *32*, 1915-1926.

207. T. M. Moy, C. D. DePorter and J. E. McGrath, *Polymer*, 1993, 34, 819-824.
208. Y. Kung and S. Hsiao, *Journal of Materials Chemistry*, 2011, 21, 1746-1754.
209. L. B. Nohara, M. L. Costa, M. A. Alves, M. F. K. Takahashi, E. L. Nohara and M. C. Rezende, *Materials Research*, 2010, 13, 245-252.
210. Y. Chern and H. Shiue, *Macromolecular Chemistry and Physics*, 1998, 199, 963-969.
211. B. S. Ghanem, N. B. McKeown, P. M. Budd, N. M. Al-Harbi, D. Fritsch, K. Heinrich, L. Starannikova, A. Tokarev, and Y. Yampolskii, *Macromolecules* 2009, 42, 7881–7888.
212. L. I. Olvera, M. T. Guzmán-Gutiérrez, M. G. Zolotukhin, S. Fomine, J. Cárdenas, F. A. Ruiz-Trevino, D. Villers, T. A. Ezquerro, and E. Prokhorov, *Macromolecules*, 2013, 46, 7245-7256.
213. M.T. Guzmán-Gutiérrez, M. H. Rios-Dominguez, F. A. Ruiz-Trevino, M. G. Zolotukhin, J. Balmaseda, D. Fritsch and E. Prokhorov, *Journal of Membrane Science*, 385-386, 2011, 277-284.
214. N. T. Tsui, A. J. Paraskos, L. Torun, T. M. Swager and E. L. Thomas, *Macromolecules*, 2006, 39, 3350-3358.
215. J. R. Wiegand, Z. P. Smith, Q. Liu, C. T. Patterson, B. D. Freeman and R. Guo, *Journal of Materials Chemistry A*, 2, 2014, 13309-13320.
216. G. J. Sloan and W. R. Vaughan, *Journal of the American Chemical Society*, 1956, 22, 750-763.
217. H. Tanaka, M. Mouri, H. Takeuchi and S. Tokito, *Japanese patent*, JP 2001110572A, 2001.
218. A. P. Krapcho, D. S. Kashdan and G. E. Jahngen, Jr., *Journal of Organic Chemistry*, 1977, 42, 1186-1189.

Appendix:

Table 1 Polyimide of Adamantane Membrane Permeability Measurements							
Transport parameter	Membrane	N ₂	O ₂	CO ₂	CH ₄	H ₂	He
P_x [Barrer]	PIM-AD5-PI 168 μm As Cast	7.4	31.3	179.0	8.8	144.9	107.0
	PIM-AD6-PI 94 μm As Cast	39	133	722	44	486	281
	PIM-AD5-PI 166 μm MeOH	34.5	142.7	573.0	19.3	682.0	385.2
	PIM-AD6-PI 103 μm MeOH	143	451	2167	152	1582	776
$\alpha(P_x/PN_2)$	PIM-AD5-PI 168 μm As Cast	-	4.25	24.27	1.20	19.64	14.51
	PIM-AD6-PI 94 μm As Cast	-	3.39	18.35	1.12	12.35	7.13
	PIM-AD5-PI 166 μm MeOH	-	4.14	16.61	0.56	19.77	11.17
	PIM-AD6-PI 103 μm MeOH	-	3.16	15.18	1.06	11.08	5.44
D_x [10^{-12} m ² s ⁻¹]	PIM-AD5-PI 168 μm As Cast	7.6	23.7	7.2	2.0	733	1995
	PIM-AD6-PI 94 μm As Cast	21.6	60.9	18.7	6.1	1313.1	3232.4
	PIM-AD5-PI 166 μm MeOH	14.6	51.2	16.8	2.6	1514	3269
	PIM-AD6-PI 103 μm MeOH	47.1	132.5	40.7	13.6	2759.8	4956.0
$\alpha(D_x/DN_2)$	PIM-AD5-PI 168 μm As Cast	-	3.13	0.96	0.27	96.77	263
	PIM-AD6-PI 94 μm As Cast	-	2.8	0.9	0.3	60.7	149.3
	PIM-AD5-PI 166 μm MeOH	-	3.51	1.15	0.18	104	225
	PIM-AD6-PI 103 μm MeOH	-	2.81	0.86	0.29	58.63	105.28
S_x [cm ³ cm ⁻³ bar ⁻¹]	PIM-AD5-PI 168 μm As Cast	0.73	0.99	18.57	3.25	0.15	0.04
	PIM-AD6-PI 94 μm As Cast	1.363	1.644	28.876	5.373	0.277	0.065
	PIM-AD5-PI 166 μm MeOH	1.78	2.09	25.63	5.67	0.34	0.02
	PIM-AD6-PI 103 μm MeOH	2.27	2.55	40.7	8.38	0.43	0.12
$\alpha(S_x/SN_2)$	PIM-AD5-PI 168 μm As Cast	-	1.36	25.41	4.44	0.20	0.06
	PIM-AD6-PI 94 μm As Cast	-	1.2	21.2	3.9	0.2	0.0
	PIM-AD5-PI 166 μm MeOH	-	1.18	14.42	3.19	0.19	0.05
	PIM-AD6-PI 103 μm MeOH	-	1.12	17.56	3.68	0.19	0.05

Table 2 Polyimide of PIM-TFA Membrane Permeability Measurements

Transport parameter	Membrane & Thickness	N ₂	O ₂	CO ₂	CH ₄	H ₂	He
<i>P_x</i> [Barrer]	PIM-TFA1-PI 193.3µm As Cast	2.8	9.5	59.7	1.8	57.3	57.3
	PIM-TFA2-PI 91.5 µm As Cast	2.6	14.1	78.2	3.0	83.0	78.3
	PIM-TFA3-PI 107 µm As Cast	12.5	49.4	309.8	12.0	239.8	308.5
	PIM-TFA6-PI 93.6 µm As Cast	23.2	89.1	507.3	22.3	354.6	269.0
	PIM-TFA9-PI 88.8 µm As Cast	11	48	273	11	208	149
	PIM-TFA12-PI 60.71 µm As Cast	12.2	51.4	315	11.4	237	194
	PIM-TFA15-PI 121.1 µm As Cast	10.8	46.5	274.4	11.0	215.7	154.8
	PIM-TFA2-PI 93.8 µm MeOH	13	66	327	9	355	313
	PIM-TFA3-PI 112 µm MeOH	33.2	147.5	814.0	32.5	645.1	427.8
	PIM-TFA9-PI 114.4 µm MeOH	32	104	608	8	427	789
	PIM-TFA12-PI 62 µm MeOH	42.5	170.3	948.4	39.2	759.4	467.0
	PIM-TFA15-PI 115.7 µm MeOH	60.1	277	1215	55	946	537
<i>α(P_x/PN₂)</i>	PIM-TFA1-PI 139.3 µm As Cast	-	3.36	21.23	0.64	20.39	20.38
	PIM-TFA2-PI 91.5 µm As Cast	-	5.94	29.75	1.14	31.55	29.79
	PIM-TFA3-PI 107 µm As Cast	-	3.95	24.77	0.96	19.18	14.16
	PIM-TFA6-PI 93.6 µm As Cast	-	3.84	21.88	0.96	15.29	11.61
	PIM-TFA9-PI 88.8 µm As Cast	-	4.3	24.2	1.00	18.49	13.25

	PIM-TFA12-PI 60.71 μm As Cast	-	4.23	25.93	0.94	19.54	15.97
	PIM-TFA15-PI 121.1 μm As Cast	-	4.41	26.03	1.05	20.46	14.68
	PIM-TFA2-PI 93.8 μm MeOH	-	3.21	24.66	0.66	26.69	23.60
	PIM-TFA3-PI 112 μm MeOH	-	4.44	24.52	0.98	19.43	12.89
	PIM-TFA9-PI 114.4 μm MeOH	-	3.24	19.07	0.25	13.39	24.72
	PIM-TFA12-PI 62 μm MeOH	-	4.01	22.32	0.92	17.87	10.99
	PIM-TFA15-PI 115.7 μm MeOH	-	4.61	20.23	0.91	15.75	8.94
D_x [10^{-12} m^2s^{-1}]	PIM-TFA1-PI 139.3 μm As Cast	5.1	11.0	3.3	0.7	319	1278
	PIM-TFA2-PI 91.5 μm As Cast	3.0	12.0	3.8	0.6	436	1363
	PIM-TFA3-PI 107 μm As Cast	9.3	30.9	11.1	2.3	839.1	2203
	PIM-TFA6-PI 93.6 μm As Cast	17.2	50.2	18.9	4.4	1217.0	2925.1
	PIM-TFA9-PI 88.8 μm As Cast	8.0	26.6	10.0	2.0	763.4	2013.5
	PIM-TFA12-PI 60.71 μm As Cast	9.0	30.6	11.2	2.1	1152	2819
	PIM-TFA15-PI 121.1 μm As Cast	8.8	29.0	10.7	2.3	863.0	2319.1
	PIM-TFA2-PI 93.8 μm MeOH	6.5	20.9	6.9	1.1	813.3	2161.4
	PIM-TFA3-PI 112 μm MeOH	15.0	44.1	18.7	3.7	1423	8718
	PIM-TFA9-PI 114.4 μm MeOH	13.4	69.1	14.1	6.1	937.1	4203.9
	PIM-TFA12-PI 62 μm MeOH	18.3	64.5	23.2	4.4	1474	2239
	PIM-TFA15-PI 115.7 μm MeOH	25.2	101	30.7	6.1	2029	9215

$\alpha (D_x/DN_2)$	PIM-TFA1-PI 139.3 μm As Cast	-	2.16	0.65	0.14	63.0	252
	PIM-TFA2-PI 91.5 μm As Cast	-	4.05	1.28	0.19	147.6	461.6
	PIM-TFA3-PI 107 μm As Cast	-	3.34	1.2	0.25	90.67	238
	PIM-TFA6-PI 93.6 μm As Cast	-	2.92	1.10	0.26	70.71	169.95
	PIM-TFA9-PI 88.8 μm As Cast	-	3.34	1.26	0.25	95.77	252..58
	PIM-TFA12-PI 60.71 μm As Cast	-	3.41	1.25	0.24	128	314
	PIM-TFA15-PI 121.1 μm As Cast	-	3.29	1.22	0.26	98.07	263.54
	PIM-TFA2-PI 93.8 μm MeOH	-	3.21	1.05	0.17	125	331
	PIM-TFA3-PI 112 μm MeOH	-	2.93	1.24	0.25	94.57	579.41
	PIM-TFA9-PI 114.4 μm MeOH	-	5.17	1.06	0.46	70.18	314.82
	PIM-TFA12-PI 62 μm MeOH	-	3.53	1.27	0.24	80.69	123
	PIM-TFA15-PI 115.7 μm MeOH	-	4.01	1.22	0.24	80.47	365
$S_x [\text{cm}^3 \text{cm}^{-3} \text{bar}^{-1}]$	PIM-TFA1-PI 193.3 μm As Cast	0.42	0.65	13.5	1.91	0.13	0.03
	PIM-TFA2-PI 91.5 μm As Cast	0.67	0.88	15.57	3.99	0.14	0.04
	PIM-TFA3-PI 107 μm As Cast	1.01	1.20	20.96	3.90	0.21	0.06
	PIM-TFA6-PI 93.6 μm As Cast	1.01	1.33	20.18	3.76	0.22	0.07
	PIM-TFA9-PI 88.8 μm As Cast	1.06	1.36	20.37	4.21	0.20	0.06
	PIM-TFA12-PI 60.71 μm As Cast	1.02	1.26	21.06	4.02	0.15	0.05
	PIM-TFA15-PI 121.1 μm As Cast	0.91	1.20	19.25	3.64	0.19	0.05

	PIM-TFA2-PI 93.8 μm MeOH	1.53	2.36	35.71	6.09	0.33	0.11
	PIM-TFA3-PI 112 μm MeOH	1.65	2.51	32.70	6.54	0.34	0.04
	PIM-TFA9-PI 114.4 μm MeOH	1.79	1.12	32.26	0.99	0.34	0.14
	PIM-TFA12-PI 62 μm MeOH	1.74	1.98	30.71	6.66	0.39	0.16
	PIM-TFA15-PI 115.7 μm MeOH	1.79	2.05	29.68	6.71	0.35	0.04
$\alpha (S_x/SN_2)$	PIM-TFA1-PI 193.3 μm As Cast	-	1.55	32.46	4.59	0.32	0.08
	PIM-TFA2-PI 91.5 μm As Cast	-	1.32	23.30	5.97	0.06	0.21
	PIM-TFA3-PI 107 μm As Cast	-	1.18	20.69	3.84	0.21	0.06
	PIM-TFA6-PI 93.6 μm As Cast	-	1.32	19.98	3.72	0.22	0.07
	PIM-TFA9-PI 88.8 μm As Cast	-	1.29	19.21	3.97	0.19	0.05
	PIM-TFA12-PI 166 μm As Cast	-	1.24	20.74	3.96	0.15	0.05
	PIM-TFA15-PI 121.1 μm As Cast	-	1.34	21.42	4.05	0.21	0.06
	PIM-TFA2-PI 93.8 μm MeOH	-	1.55	23.41	3.99	0.21	0.07
	PIM-TFA3-PI 112 μm MeOH	-	1.52	19.76	3.95	0.21	0.02
	PIM-TFA9-PI 114.4 μm MeOH	-	0.63	18.00	0.55	0.19	0.08
	PIM-TFA12-PI 62 μm MeOH	-	1.14	17.60	3.82	0.22	0.09
	PIM-TFA15-PI 115.7 μm MeOH	-	1.15	16.61	3.76	0.20	0.02

Table 3 Polybenzodioxane Membrane Permeability Measurements							
Transport parameter	Membrane	N ₂	O ₂	CO ₂	CH ₄	H ₂	He
P_x [Barrer]	PIM-1-co-TF1 66µm As Cast	80.8	274	1879	122	781	412
	PIM-1-co-TF3 167 µm As cast	60.6	179	1350	108	412	224
	PIM-1-co-TF1 70 µm MeOH	261	871	5381	378	2363	1061
$\alpha(P_x/PN_2)$	PIM-1-co-TF1 66 µm As cast	-	3.4	23.26	1.5	9.67	5.1
	PIM-1-co-TF3 167 µm As cast	-	2.95	22.28	1.79	6.80	3.70
	PIM-1-co-TF1 70 µm MeOH	-	3.34	20.62	1.45	9.05	4.07
D_x [10^{-12} m ² s ⁻¹]	PIM-1-co-TF1 66 µm As cast	34.3	101	45.5	12.2	1653	2806
	PIM-1-co-TF3 167 µm As cast	45.7	99.2	47.9	17.8	1472	3247
	PIM-1-co-TF1 70 µm MeOH	63.2	199.1	82.7	22.5	3299	4772
$\alpha(D_x/DN_2)$	PIM-1-co-TF1 66 µm As cast	-	2.95	1.33	0.36	48.3	81.9
	PIM-1-co-TF3 167 µm As cast	-	2.17	1.05	0.39	32.21	71.03
	PIM-1-co-TF1 70 µm MeOH	-	3.15	1.31	0.36	52.2	75.5
S_x [cm ³ cm ⁻³ bar ⁻¹]	PIM-1-co-TF1 66µm As cast	1.77	2.03	30.9	7.51	0.35	0.11
	PIM-1-co-TF3 167 µm As cast	0.99	1.35	21.12	4.58	0.21	0.05
	PIM-1-co-TF1 70 µm MeOH	3.10	3.28	48.79	12.62	0.54	0.17
$\alpha(S_x/SN_2)$	PIM-1-co-TF1 66µm As cast	-	1.15	17.49	4.24	0.20	0.06
	PIM-1-co-TF3 167 µm As cast	-	1.36	21.25	4.61	0.21	0.05
	PIM-1-co-TF1 70 µm MeOH	-	1.06	15.75	4.08	0.17	0.05